UNIVERSITY OF CALIFORNIA SAN DIEGO

Responses of the Southern California Current System Zooplankton Community to El Niño Variability

A dissertation submitted in partial satisfaction for the requirements for the degree Doctor of Philosophy

in

Oceanography

by

Laura Elizabeth Lilly

Committee in charge:

Mark D. Ohman, Chair
Bruce D. Cornuelle
Peter J. S. Franks
Michael R. Landry
Daniel L. Rudnick
Jonathan B. Shurin

2021

The dissertation of Laura Elizabeth Lilly is approved, and it is acceptable in quality and form for publication on microfilm and electronically.

University of California San Diego

2021

DEDICATION

This work is dedicated to all contributors to the California Cooperative Oceanic Fisheries Investigations program (CalCOFI) throughout the seven decades since its inception: to the original designers for their wisdom and foresight in setting up a sampling system that has proven its worth innumerable times over, and to all seagoing personnel, ship crews, and land-based researchers and technicians who have maintained the high-quality, consistent, and unparalleled timeseries across so much time and space. Without their efforts, this thesis – and much of our understanding of the California Current System – would not exist.

EPIGRAPH

“Let yourself be silently drawn by the strange pull of what you really love. It will not lead you astray.” – Rumi

“Only that day dawns to which we are awake.” – Henry David Thoreau

TABLE OF CONTENTS

LIST OF FIGURES

LIST OF TABLES

LIST OF SUPPLEMENTAL ANIMATIONS

Lilly_Ch3_SuppAnms.zip

- Lilly_Ch3_SuppAnms_Eexim
- Lilly_Ch3_SuppAnms_Egibb
- Lilly_Ch3_SuppAnms_Epaci
- Lilly_Ch3_SuppAnms_Ndiff
- Lilly_Ch3_SuppAnms_Nsimp

ACKNOWLEDGEMENTS

This thesis is dedicated foremost to my parents, who helped me find my way again and again to the sea. Although I grew up in landlocked Sacramento, CA, my parents recognized early on my love for (obsession with) the beach and the vast blue expanses beyond. All I could explain was that I loved the ocean "because you can't see the other side", but they didn't ask questions. They just supported my call by sending me to sea to fulfill my dream of (safely) becoming a pirate by sailing and learning hands-on oceanography with the Sea Education Association (SEA) when I was 16. I sailed around Cape Cod, conducted CTD casts and plankton tows at 2 a.m., and affirmed my longstanding desire to pursue a lifetime of oceanography. I recognized even then that not everyone has such incredible opportunities, and I am forever grateful for my parents' assistance and belief in me. Mostly, they never told me what they thought I should do or become; they just listened and encouraged me to follow the pull of what interested me. I am also grateful to the lifelong guidance of my older brother, Charlie, who has been a steady presence and source of wisdom as I navigate growing up. I can't wait to teach Wyatt to surf!

My graduate school experience would have been much less rich and educational without the guidance of my advisor, Mark Ohman. Through many lengthy Friday afternoon chats, at-sea anomalous-plankton-encounter-fueled project ideas, and answers to my too many emails with "just one more question", Mark helped me hone my critical thinking skills and hypothesis-driven project framing – skills I truly struggled with before grad school. Although I stubbornly resisted Mark's insistences that I finish one project before attempting to start (ten) others, I always secretly listened and knew he had my best interests in mind (and in the end I usually agreed). Mark had a unique ability to offer me key scientific support and guidance while giving me

immense latitude to develop my interests and struggle sufficiently to grow. For that I am most grateful, because it helped me become the scientist I came to graduate school to be.

My committee members each contributed uniquely and indelibly to my scientific growth and life wisdom. Dan Rudnick taught me objective mapping and other data analysis techniques with way more patience than I deserved, and helped me gain confidence that it was ok (in fact best) to start new projects simply by looking at maps and visualizations and pondering what might be happening, before running a bunch of "fancy" quantitative analyses. Mike Landry provided useful questions and insights about zooplankton habitat use and was a calm and sage presence on our CCE-LTER cruises. Jon Shurin helped me puzzle through GAMs and contributed important perspectives from the larger ecological picture. Peter Franks was an invaluable sounding board and brought me back to the basics of biological oceanography when I tried to reach for abstract concepts. Peter also taught me that you cannot "logic away" things that are bothering you; you have to face them head-on. Hearing that lesson at a significant struggle-point transformed my life perspective. Bruce Cornuelle has been an essential and witty presence throughout Chs. 2 and 3 and suffered through too many phone and Zoom calls, but he never let me quit until I truly understood new concepts and methods, despite my frustrating obtuseness (if only I had been born a physical oceanographer!). I deeply enjoyed my conversations with each of my committee members and look forward to more, even as I move out into the world.

Thank you to the SIO Graduate Office for their tremendous behind-the-scenes work to make the graduate experience fun and fully supported. Thanks also to the Scripps Administration for allowing me to initiate many sustainability-related efforts around campus, and for their willingness to work with us to make changes. I am grateful to Allyson Long, my Scripps Sustainability co-leader and the true force behind most of our projects and efforts.

Thank you to the CCE-LTER graduate student/post-doc group for your camaraderie at sea and on land. You made all-night transects a blast and became a family for me. Thanks to the Send Lab for five great mooring cruises. You guys increased my knowledge of engineering and ocean instrumentation exponentially and made our trips memorably fun along the way. I owe a tremendous acknowledgement to my many past scientific mentors at various jobs and internships, including NOAA PIFSC, SCCOOS and CDIP, and the Block and Bonaventura Labs. You guided me through my first forays into coding and lab work and patiently weathered my cocky youthful certainty that I knew more than everyone else. I was humbled many times over by the depths of knowledge of those who came before me.

I would be nowhere without my friends, who supported me in every way imaginable and helped (sometimes pushed) me to grow. My Ohman Labmates have been the big family I always dreamt of. Jenni, Cat, and Jeff passed along many grad school tips from those who had come before. Emma and Sven brought wonderfully engaging energies to our lab and helped us bond outside of Scripps. I owe a big thanks to Ben for being an amazing shipmate on CCE Process Cruises and friend on land. Ben can fix anything and always pulls more than his share of the work with good humor (even after all-night MOCNESS tows), and he always checks to make sure his “labbies” are afloat. Valerie Bednarski is an honorary lab member after P1706, as well as a lifelong friend and backpacking buddy. Last, whether Stephanie wanted to or not, she became one of my closest friends, and I am forever grateful that she came to Scripps. During all-night Bongo and MOCNESS frenzies, ethanol flipping, bow chats, and hiking and camping trips, Stephanie has been there unendingly with wisdom and good humor to help me puzzle through all aspects of life. Thanks for always being willing to answer the phone and listen.

Linsey Sala is also a wonderful labmate but deserves special recognition for her incredible, detailed, labor-intensive CalCOFI identification work and deep knowledge of zooplankton in the California Current and beyond. I remember asking at the start of grad school why we didn't have zooplankton enumerations from all four CalCOFI cruises each year, and having Linsey and Mark roll their eyes at my ignorance. Now I understand why. I marveled at Linsey's unending ability to talk plankton life-histories and decades-old discoveries, and I enjoyed swapping stories of San Diego sea creature encounters from our surfboards and kayaks.

Thanks to my BO cohort (Ashlyn, Eadoh, Lindsey, and Sarah, plus our honorary member, Camille) for so much fun, especially our BO Departmental study parties. Bryce Inman deserves a shoutout as my officemate who put up with my neurotic study habits for 4.5 years and was still willing to talk waves. Nathalí, you were a phenomenal roommate, life/soul converser, and dancefloor partner at Blonde Bar. More soon! Tammy, thanks for so many birding hikes and life chats. Annie, we have been through so much since we first met 10 (!) years ago on B Watch, and I am grateful for our deep mutual connection, even when we go months without talking. To my surf guru, Raymond, I am still amazed at the irony of the universe that reconnected us, but you have been such a supportive friend these past few years. Thanks for always being up for a morning surf trek to San Miguel! To the San Diego polo community, thank you for every opportunity to play polo and ride horses on a grad student budget. The lessons I learned from polo about teamwork and quick decision-making under pressure have helped guide all aspects of my life. Last, to Jen, Gretchen, Jessica, and Grace: none of you know each other, but each of you has been an amazing role model for me as a self-confident, assertive, kind, graceful, and highly athletic woman (Gretchen, I'll never forget all our surf sessions, from Trestles to Morocco!). I draw strength from your examples and hope I can pass those principles on to others.

The last (but not least important) people I thank are the incredible crews of the *R/Vs Sally Ride, Sikuliaq, Atlantis, Revelle,* and all the NOAA and SEA ships I have sailed on. Despite having spent over 250 days at sea since I first sailed past the horizon at age 16, I find each trip back out to be a unique and profoundly transformative experience. Many of my most valuable lessons in human interaction and self-growth, and some of the best connections I have made, occurred on ships. Thanks to all of you, going to sea is always an incredibly positive and supportive experience. I look forward to many more MOCNESS tows, comet sightings, and chances to pay my lessons forward.

Last of all, I thank the ocean, without which we would have nothing (least of all Ph.D.s).

Chapter 1, in full, is a reprint of the material as it appears in Deep-Sea Research Part I: Oceanographic Research Papers, 2018. Lilly, Laura E.; Ohman, Mark D. The dissertation author was the primary investigator and author of this paper.

Chapter 2, in full, is a reprint of the material as it appears in Progress in Oceanography, 2021. Lilly, Laura E.; Ohman, Mark D. The dissertation author was the primary investigator and author of this paper.

Chapter 3, in full, is currently being prepared for submission for publication of the material. Lilly, Laura E.; Cornuelle, Bruce D.; Ohman, Mark D. The dissertation author was the primary investigator and author of this paper.

Chapter 4, in full, is a reprint of the material as it appears in Journal of Geophysical Research: Oceans, 2019. Lilly, Laura E.; Send, Uwe; Lankhorst, Matthias; Martz, Todd R.; Feely, Richard A.; Sutton, Adrienne J.; Ohman, Mark D. The dissertation author was the primary investigator and author of this paper.

VITA

2012 Bachelor of Science (Earth Systems – Oceanography), Stanford University

conferred with distinction, elected to Phi Beta Kappa

2013 Master of Science (Marine Ecosystem Conservation), Stanford University

2021 Doctor of Philosophy, University of California San Diego

RESEARCH CRUISE EXPERIENCE

(selected; 17 cruises total, 258 sea days)

2020 CalCOFI Summer Cruise 2007SR, *R/V Sally Ride,* CCS (15 d)

2019 CCE-LTER Process Cruise P1908, *R/V Atlantis*, CCS (32 d)

2019 CCE1/CCE2/Del Mar mooring turnaround, *R/V Sikuliaq*, CCS (7 d)

2018 CCE1 mooring turnaround, *R/V Bell Shimada,* CCS (6 d)

2018 CCE2 mooring turnaround, *R/V Sikuliaq*, CCS (6 d)

2017 CCE-LTER Process Cruise P1706, *R/V Roger Revelle*, CCS (32 d)

2017 CCE2 mooring turnaround, *R/V Sally Ride*, CCS (3 d)

2016 CCE1 mooring turnaround, *R/V Reuben Lasker*, CCS (8 d)

2016 CCE-LTER P1604 RAPID Response El Niño Cruise, *R/V Sikuliaq*, CCS (24 d)

2015 Stanford@SEA College Semester (Assistant Scientist), Sea Education Association, *SSV Robert C. Seamans*, Tahiti-Honolulu (35 d)

2011 Integrated Ecosystem Assessment, NOAA PIFSC, *R/V Oscar Elton Sette*, Kona, HI (14 d)

2011 Stanford@SEA College Semester, Sea Education Association, *SSV Robert C. Seamans*, Equatorial Pacific and Line Islands (35 d)

LEADERSHIP

2017-2020 CCE-LTER Program, *Graduate Student Representative*

2017-2021 Scripps Sustainability Group, *Leader (1/20-12/20), Co-Leader (2/17-12/19)*

TEACHING AND OUTREACH

2019 Scripps Institution of Oceanography, *Teaching Assistant*

2018 East Village High School, San Diego, CA, *Lesson development and teaching*

2017-2018 Calexico High School, Calexico, CA, *Lesson development and teaching*

PUBLICATIONS

Lilly, L. E., Cornuelle, B. D., and Ohman, M., D. (in prep). *Using a Lagrangian particle tracking model to evaluate impacts of El Niño-related anomalous advection on euphausiids in the southern California Current System.*

Lilly, L. E., and M.D. Ohman (2021). Euphausiid spatial displacements elucidate El Niño forcing mechanisms in the southern California Current System. *Progress in Oceanography*, 102554.

Lilly, L. E., Send, U., Lankhorst, M., Martz, T. R., Feely, R. A., Sutton, A. J., & Ohman, M. D. (2019). Biogeochemical Anomalies at Two Southern California Current System Moorings During the 2014–2016 Warm Anomaly-El Niño Sequence. *Journal of Geophysical Research: Oceans*, *124*(10), 6886-6903. https://doi.org/10.1029/2019JC015255.

Lilly, L. E., and M.D. Ohman (2018). ENSO-related zooplankton community shifts in the southern California Current System. *Deep Sea Research Part I: Oceanographic Research Papers, 140,* 36-51. https://doi.org/10.1016/j.dsr.2018.07.015.

Lilly, L. E., Bonaventura, J., Lipnick, M. S., & Block, B. A. (2015). Effect of temperature acclimation on hemoglobin-oxygen binding in Pacific bluefin tuna *(Thunnus orientalis)* and yellowfin tuna *(Thunnus albacares). Comparative Biochemistry and Physiology Part A: Molecular & Integrative Physiology, 181,* 36-44. https://doi.org/10.1016/j.cbpa.2014.11.014.

Lilly, L. E., Blinebry, S. K., Viscardi, C. M., Perez, L., Bonaventura, J., & McMahon, T. J. (2013). Parallel Assay of Oxygen Equilibria of Hemoglobin. *Analytical Biochemistry, 441,* 63-68. https://doi.org/10.1016/j.ab.2013.06.010.

ABSTRACT OF THE DISSERTATION

Responses of the Southern California Current System Zooplankton Community to El Niño Variability

by

Laura Elizabeth Lilly

Doctor of Philosophy in Oceanography

University of California San Diego, 2021

Professor Mark D. Ohman, Chair

The zooplankton community of the California Current System (CCS) can change substantially during El Niño events, but few studies have definitively identified the forcing mechanisms underlying these changes. Physical expressions of El Niño can vary in both the equatorial Pacific and CCS, producing different combinations of remote and local forcing on zooplankton. This thesis considers the relative impacts of two dominant mechanisms, anomalous advection and altered *in situ* population growth, on CCS zooplankton populations across multiple El Niños of the last seven decades.

This thesis uses the California Cooperative Oceanic Fisheries Investigations (CalCOFI) spring zooplankton timeseries (1951-2018) to analyze zooplankton community variability in the southern CCS during seven El Niño events and the 2014-15 Warm Anomaly. It first determines

whether the zooplankton community varies consistently during El Niño and further aligns with physical delineations into Eastern Pacific (EP) and Central Pacific (CP) Niño events. Second, it uses spatial, habitat, and reproductive variability to identify forcing mechanisms that impact ten dominant euphausiid (krill) species. A particle tracking model forced by the California State Estimate (CASE), the regional implementation of a general circulation model, investigates the influence of advection on euphausiids. Biogeochemical fluctuations at two CCS moorings during 2014-16 provide a high-resolution analysis of habitat changes for pelagic molluscs.

El Niño events primarily affect certain zooplankton taxa and species proportions rather than total zooplankton biomass. Within the euphausiids, dominant cool-water species undergo nearshore and poleward compression during major EP Niños; reduced larval abundances suggest dominant population forcing by decreased reproduction under unfavorable habitat conditions. In contrast, subtropical coastal and offshore species increase variably in the southern CCS with anomalous advection; prolonged warm conditions may support temporary *in situ* reproduction. The 2014-15 Warm Anomaly produced zooplankton community changes comparable to moderate CP Niños. The zooplankton community rapidly rebounds to pre-Niño composition within 1-2 years, indicating high resilience to short-term perturbations.

Projections of euphausiid distributional changes by Year 2100 suggest non-Niño and CP Niño conditions will enhance subtropical populations, including moderate poleward and onshore expansion. Future EP Niños will continue to induce shoreward compression and decreased abundances of cool-water species, with potentially significant impacts on marine mammals and seabirds that preferentially target those species. Identifying El Niño-related forcing mechanisms on zooplankton sectors will improve future predictions of changes in zooplankton biomass and distributions, with implication for fisheries management and carbon flux estimates.

INTRODUCTION

Mesozooplankton

Mesozooplankton are the small, passively drifting, animal component of the world's oceans, ranging from 0.2-20 mm in body length. Within marine ecosystems, mesozooplankton link primary production to higher trophic levels (forage fishes, marine mammals, seabirds; Ainley & Hyrenbach, 2010; Croll et al., 2005; Croll et al., 1998; Keiper et al., 2005) and contribute substantially to vertical fluxes and sequestration of atmospherically-derived carbon (Ducklow et al., 2001; Steinberg & Landry, 2017; Stukel et al., 2013). Not all mesozooplankton are created equal, however. Some taxa, and even species within taxa, serve disproportionately important roles in the above processes.

Dominant crustacean taxa (copepods, euphausiids, hyperiid amphipods) form large proportions of the diets of higher trophic levels, but baleen whales and some seabirds are known to selectively forage on certain highly nutritious crustacean species, even when other species of the same taxon are more abundant (Croll et al., 1998; Nickels et al., 2018, 2019; Thayer & Sydeman, 2007). Copepod and euphausiid species that inhabit colder waters tend to have higher lipid and wax ester contents than their subtropical congeners, making them more nutritious, and therefore desirable, prey items (Fisher et al., 2020; Fisher et al., 2015). Conversely, although some gelatinous tunicate taxa (e.g., salps, pyrosomes) have historically been considered less desirable food for higher trophic levels, these groups function as important carbon exporters, removing high quantities of small phytoplankton particles from the water column and producing dense, rapidly-sinking fecal pellets and carcasses that export carbon to the subsurface ocean (Henschke et al., 2016; Miller et al., 2019; O'Loughlin et al., 2020; Smith et al., 2014). Thus,

changes in abundances and relative proportions of different taxa within the mesozooplankton community, and even individual species within a taxon, can significantly alter higher trophic level foraging success and zooplankton-mediated carbon export.

Three main factors influence zooplankton community composition. First, ocean currents can advect populations into a region from external sources, either continuously, periodically, or sporadically in conjunction with an anomalous event (Brinton, 1960, 1981; Keister et al., 2011; Lavaniegos & Ambriz-Arreola, 2012; Marinovic et al., 2002). Second, changes to *in situ* habitat conditions (e.g., temperature, food availability, upwelling timing and strength) may enhance reproduction and proliferation of certain species and increase mortality of others (Blackburn, 1979; Chelton et al., 1982; Mackas et al., 2006; Pares-Escobar et al., 2018). Third, altered competition and predation, due to the above factors or other influences (e.g., removal of predators via fishing), can further favor dominance by certain species (Dalpadado & Skjoldal, 1996; Hanazato & Yasuno, 1989; Reid et al., 2000; Skjoldal & Rey, 1989). All three mechanisms serve important and interconnected roles in shaping zooplankton communities (Ohman et al., 2017), but due to data limitations this thesis does not consider the effects of altered competition and predation on zooplankton. This thesis addresses the relative influences of advection and *in situ* population growth in causing short-term changes in zooplankton communities in the southern California Current System (CCS).

Causes of physical ocean anomalies in the southern California Current System

Both advection (magnitude, dominant directions of flow) and *in situ* habitat conditions (temperature, oxygen, chlorophyll-*a*, predators) in the southern CCS can be altered by atmosphere and ocean perturbations, including: **i) decadal oscillations,** such as the Pacific

Decadal Oscillation (PDO, Mantua et al., 1997), whose positive phase produces warmer water temperatures and anomalous poleward advection in the CCS (Keister et al., 2011); and the North Pacific Gyre Oscillation (NPGO, Di Lorenzo et al., 2008), whose positive phase conversely enhances upwelling of cool, highly productive waters in the CCS; **ii) cyclical perturbations,** predominantly the El Niño-Southern Oscillation (ENSO) cycle, which emerges every 3-8 years in the equatorial Pacific and produces El Niño or La Niña events; the El Niño phase is associated with significant warming, reduced productivity, and altered circulation in the CCS (Jacox et al., 2016; Lynn, 1983; Lynn & Bograd, 2002; Ramp et al., 1997); **iii) sporadic anomalous events,** notably the 2014-15 Eastern North Pacific Warm Anomaly, a multiyear period of unprecedented anomalously warm temperatures (to +5^{o}C), upper ocean stratification, and anomalous onshore flow (Bond et al., 2015; Chao et al., 2017; Gentemann et al., 2017; Zaba & Rudnick, 2016); and **iv) long-term secular changes** in CCS temperature and chlorophyll-*a* patterns (Hazen et al., 2013), CCS coastal upwelling strength and timing (Bakun et al., 2015; Garcia-Reyes et al., 2015; Rykaczewski et al., 2015), and relative occurrences of different types of equatorial Pacific El Niño events (Newman et al., 2018; Timmermann et al., 2019; Yeh et al., 2009).

Although all of the above perturbations have important and likely interactive effects on the CCS physical system and zooplankton responses, this thesis focuses on impacts of El Niño events and one sporadic anomalous event (the 2014-15 Warm Anomaly) on zooplankton in the southern CCS during the period 1951-2018. The southern CCS is defined here as extending from Monterey Bay, California, south to northern Baja California, from the coast to 128^{o}W.

El Niño variability

An El Niño event is defined by the National Oceanic and Atmospheric Administration (NOAA) as three consecutive months of sea surface temperature (SST) anomalies ≥0.5°C in the Niño3.4 region (5°S to 5°N, 170°W to 120°W) of the equatorial Pacific (Larkin & Harrison, 2005). However, increased observations in recent decades have shown that individual El Niño events can vary significantly in their developmental mechanisms and physical expressions (Capotondi, 2013; Capotondi et al., 2015; L'Heureux et al., 2017; Timmermann et al., 2019). Such variability has led to attempts to categorize El Niño events, resulting in a generally accepted dichotomy of 'Eastern Pacific' (EP) and 'Central Pacific' (CP) El Niños (Kao & Yu, 2009; Kug et al., 2009; Yeh et al., 2014), although the validity of categorization is debated (Karnauskas, 2013) and at least some El Niño events have both EP and CP characteristics (Timmermann et al., 2019). The EP and CP Niño dichotomy is useful, however, as an initial classification of events. How well any individual El Niño holds up to one category or another, and the variability in zooplankton community changes during that event compared to other events of the same category, can emphasize its unique characteristics and forcing mechanisms.

Eastern Pacific El Niño events have several distinguishing features in the equatorial Pacific: they are initiated by strong subsurface eastward propagation of Kelvin waves from the Western Pacific Warm Pool toward South America; these Kelvin waves induce significant thermocline depression off South America and elevated temperature anomalies in the Niño1+2 region of the Eastern Equatorial Pacific; and the events produce significant heat discharge to the extra-tropics, primarily via oceanic propagation (i.e., coastally trapped waves, CTWs) (Cane, 1983; McPhaden, 1999b; Wyrtki, 1975). In contrast, Central Pacific Niños are generally characterized by: more moderate temperature anomalies centered around the International Dateline, predominantly in the upper 100 m; event forcing by local wind anomalies and zonal

advective feedback, although they can also produce Kelvin waves; and a lack of heat discharge to the extra-tropics (Ashok & Yamagata, 2009; Kao & Yu, 2009; Kim et al., 2011).

Both EP and CP El Niño signals can propagate to the CCS via combinations of three mechanisms: **1) Oceanic coastally trapped waves (CTWs)** – when Kelvin waves reach the coast of South America, they translate into poleward-propagating CTWs that move along the coast of Central America and eventually reach the CCS, where they induce anomalous poleward flow of the California Undercurrent (Lynn & Bograd, 2002; Ramp et al., 1997; Strub & James, 2002), the northward-flowing segment of the CCS (Rudnick et al., 2017); **2) Atmospheric teleconnections** – some El Niño events produce atmospheric 'bridges' to the Eastern North Pacific (Alexander et al., 2002; Ashok et al., 2007), shifting the position of the Aleutian Low pressure system and altering local wind-driven circulation off the West Coast (Simpson, 1984); **3) Shoreward intrusions of offshore, southern-origin waters** – warm, salty waters associated with the North Pacific Central Gyre can be advected shoreward into the Southern California Bight (SCB) due to altered atmospheric circulation (Jacox et al., 2016; Simpson, 1984).

Two of the three major EP Niños on record (1997-98, 2015-16) showed evidence for CTW propagation to the CCS and enhanced nearshore poleward flow along California (Lynn & Bograd, 2002; Rudnick et al., 2017; Strub & James, 2002), while the third EP Niño (1982-83) was characterized more clearly by strong onshore flow of southern offshore waters (Simpson, 1984). Of the CP Niño events identified for this thesis, one event (1991-93) showed clear evidence for CTW arrival to the CCS along with atmospherically-induced onshore flows (Ramp et al., 1997) and has since been categorized as a mixed CP-EP event (Timmermann et al., 2019). Another two-year CP Niño (1957-59) strengthened the Inshore Countercurrent of the CCS (Lynn, 1983; Wyllie, 1966), although Reid (1960) attributed this to altered wind-forced regional

circulation rather than CTWs. The 2002-03 CP Niño also characterized as mixed CP-EP (Timmermann et al., 2019) but only caused moderate *in situ* physical changes in the CCS (Lavaniegos, 2009; Lavaniegos & Ambriz-Arreola, 2012), while the 2009-10 CP Niño had a significant equatorial expression but atmosphere-only signal propagation to the CCS (Rudnick et al., 2017; Todd et al., 2011). Lilly and Ohman (submitted, Supplemental Information) provide in-depth descriptions of the physical forcing mechanisms and characterizations of each El Niño event analyzed in this thesis.

Thus, even within the EP and CP Niño designations, individual events can vary in both their equatorial Pacific and CCS signatures and forcing mechanisms, inducing different combinations of anomalous advection strength and direction and *in situ* habitat changes. This thesis draws upon previously described variability in the physical CCS expressions and propagation mechanisms of such El Niño events to examine how varying magnitudes and types of anomalous advection and non-advective habitat conditions differentially impact southern CCS zooplankton community composition. Because I focused on the direct effects of El Niño events on zooplankton in the CCS, far removed from the equator, for this thesis I defined a new metric of 'CCS El Niño events', which included only those events that expressed sufficiently strongly in both the equatorial Pacific and southern CCS (see Chapter 1, Section 1.2.3 for definition).

El Niño impacts on zooplankton

The southern CCS zooplankton community showed clear short-term rearrangements during most El Niño events of the past 70 years (Berner, 1960; Brinton, 1960, 1981; Lavaniegos & Ambriz-Arreola, 2012; Lavaniegos et al., 2002; Lavaniegos & Ohman, 2007; Lilly & Ohman, 2018; Pares-Escobar et al., 2018; Rebstock, 2001). Within specific taxa, resident cool-water

species (those with at least moderate consistent presence in the southern CCS) decreased in biomass (Lavaniegos & Ohman, 2007; Lilly & Ohman, 2018; Mullin, 1998; Rebstock, 2001) and adult body length (Robertson & Bjorkstedt, 2020), and retracted nearshore and poleward (Brinton, 1960, 1981; Brinton & Reid, 1986; Lilly & Ohman, submitted), to varying degrees during most El Niño events, although such changes rapidly reversed to near-normal levels post-Niño (Lilly & Ohman, 2018, submitted). Conversely, subtropical and tropical species increased substantially in the southern CCS during many El Niño events (Brinton, 1960, 1981; Lavaniegos & Ambriz-Arreola, 2012; Lavaniegos et al., 2002; Lavaniegos & Ohman, 2007; Lilly & Ohman, 2018; Pares-Escobar et al., 2018; Rebstock, 2001). Most subtropical-tropical incursions did not persist at elevated levels for more than 1-2 years following the end of an El Niño event (Lilly & Ohman, 2018, submitted), although some species are known to show quasi-cyclical changes in conjunction with PDO phase (Brinton & Townsend, 2003; Di Lorenzo & Ohman, 2013).

El Niño-related decreases of resident cool-water species are generally thought to occur in response to unfavorable habitat changes (anomalous warming, decreased food availability). In contrast, subtropical species appearances are attributed to initial population advection into the region, but post-Niño mortality and southward or offshore retractions are considered negative responses to the return of cooler upwelling conditions (Blackburn, 1979; Brinton, 1981; Lavaniegos & Ambriz-Arreola, 2012; Lilly & Ohman, submitted). However, the individual and interactive effects of advection and *in situ* habitat changes on specific components of the southern CCS zooplankton community, particularly differential mechanisms affecting subtropical and cool-water species, remain mostly undescribed.

Characterization and evaluation of possible alignment of zooplankton responses with physical EP and CP Niño designations, and hypotheses about causal mechanisms of zooplankton

changes using these distinctions, have never been attempted for the southern CCS zooplankton community. In addition, although past El Niño events have appeared to induce only short-term, "transient" changes to the zooplankton community, with rapid rebounds in primary and secondary production following the ends of events (Lindegren et al., 2018), the potential for longer-term ecosystem shifts with future El Niño events and long-term physical changes has not been well analyzed. Understanding the forcing mechanisms that impact zooplankton during El Niño events will provide greater insight into likely community responses to other short- and long-term perturbations.

Outline of the Dissertation

El Niño events provide a form of 'natural experimentation' in which the southern CCS experiences varying degrees of anomalous advection and *in situ* habitat conditions compared to its non-Niño state. This thesis first characterizes the variability of the southern CCS mesozooplankton community during El Niño events from 1951-2018, as well as the 2014-15 Warm Anomaly. Second, it analyzes and proposes the likely combinations of dominant forcing mechanisms (advection, *in situ* habitat change) that influence population sizes and distributions of several dominant euphausiid species and the pteropod (pelagic mollusc) community in the southern CCS. This work draws primarily upon the CalCOFI spring zooplankton timeseries, for which detailed enumerations are available for regionally-aggregated samples from most of the zooplankton community and spatially-resolved samples for each euphausiid species. Although zooplankton samples are collected on every quarterly CalCOFI cruise, samples from other seasons have only been enumerated sporadically; Chapter 2 of this thesis draws upon winter enumerations, where available, to provide some context for spring across El Niño and non-Niño

periods. I also incorporate physical datasets from CalCOFI, moorings, the California State Estimate (CASE) regionally-optimized component of the MIT general circulation model, and other sources. Understanding the underlying forcing mechanisms that influence different zooplankton groups will improve our predictions of zooplankton responses to future El Niño events and other short-and long-term anomalous conditions, with implications for improved predictions of fluctuations in higher trophic levels and carbon fluxes.

In Chapter 1, "El Niño-related zooplankton variability in the southern California Current System," I analyze variability of 15 dominant zooplankton taxa, and species within three major taxa (calanoid copepods, euphausiids, hyperiid amphipods), across seven El Niño events (1951-2016) and the 2014-15 Warm Anomaly, using Southern California regionwide aggregated samples. I test whether higher taxa and particular species groups show consistent El Niño-related changes across events and whether they logically categorize into either EP or CP Niños. I find that several dominant taxa and euphausiid and calanoid copepod species compositions are more sensitive to El Niño than total mesozooplankton biomass. Euphausiid species variability further demarcates into EP and CP Niño categories. All groups show rapid returns to pre-Niño community composition within one year, reflecting community resilience to major perturbations. This chapter was published in *Deep-Sea Research: Part I* (Lilly and Ohman, 2018).

Chapter 2, "Euphausiid spatial displacements and habitat shifts in the southern California Current System in response to El Niño variability," analyzes changes in spatially resolved distributions of 10 euphausiid species during the above El Niño events, in contrast to Chapter 1, which addresses only temporal changes in the community. I also develop generalized additive models (GAMs) of habitat conditions to identify species' habitat 'envelopes,' and analyze differences between larval and adult developmental stages in order to assess El Niño-related

reproductive variability. I then use the GAMs to predict species distributional changes under Year 2100 projected habitat conditions during non-Niño, EP, and CP Niño conditions. Drawing upon consistent spatial responses and habitat ranges across species, I define five 'El Niño response' groups and develop hypotheses for dominant forcing mechanisms affecting each group. This chapter is in review in *Progress in Oceanography* (Lilly and Ohman, 2021).

Chapter 3, "Using a Lagrangian particle tracking model to evaluate impacts of El Niño-related anomalous advection on euphausiids in the southern California Current System," compares modeled flow fields from the California State Estimate (CASE) with euphausiid species distributions (from 2008-2017) to test whether anomalous flow alone can explain zooplankton fluctuations. Comparison of total population and calyptopis stage responses suggests that resident cool-water species reduce reproduction during advection of unfavorable habitat, while subtropical-tropical species experience whole-population transport into the region. I then use a particle tracking model to hindcast spring euphausiid distributions during three anomalous periods (2009-10 CP Niño, 2014-15 Warm Anomaly, 2015-16 EP Niño) to determine winter source water origins. This chapter is in preparation for submission (Lilly, Cornuelle, and Ohman, in prep.).

Chapter 4, "Biogeochemical Anomalies at Two Southern California Current System Moorings During the 2014–2016 Warm Anomaly-El Niño Sequence," analyzes physical-biogeochemical variability at two moorings west of Point Conception, CA, during the 2014-16 anomalies, and corresponding changes in pteropods (pelagic molluscs). Anomalous warming and near-zero nitrate and chlorophyll-*a* emerged in June 2014 and persisted through spring 2016, interrupted only by upwelling in spring 2015, although there were two distinct events across that time interval that showed very different expressions at the mooring. The Warm Anomaly

induced regionwide shallow (< 75 m depth) temperature anomalies and persistent near-zero nitrate and Chl-*a* levels from summer 2014-late winter 2015, while the El Niño event expressed in both surface and deeper (75 m) waters and had periods of stronger temperature anomalies but shorter duration. I also demonstrate that pteropod biomass was significantly elevated in springs 2014 and 2016, likely due to combinations of anomalous poleward transport of subtropical populations and *in situ* reproduction under aragonite saturation levels that were more favorable to calcifying organisms. This chapter was published in *Journal of Geophysical Research: Oceans* (Lilly, L. E.; Send, U.; Lankhorst, M.; Martz, T. R.; Feely, R. A.; Sutton, A. J.; Ohman, M. D., 2019).

To conclude the dissertation, I reiterate my conclusions about the likely dominant forcing mechanisms that influence cool-water and subtropical euphausiid species and the pteropod community. I further use these conclusions to speculate on likely forcing mechanisms that affect other components of the zooplankton community and likely future changes to various zooplankton sectors given forecasts of future El Niño and background habitat changes. I also compare my El Niño findings to the La Niña analyses I conduct in Chapter 1. I note two data limitations: a lack of higher-temporal-resolution sampling and a paucity of species-level growth experiments that could improve models of in situ growth. These limitations could be grounds for future sampling and experimental efforts by CalCOFI and other research programs. Last, I discuss the impacts of zooplankton community changes for the broader CCS ecosystem, and specifically how improved zooplankton measurements and predictions can better inform foraging models for higher trophic levels.

REFERENCES

Ainley, D. G. & Hyrenbach, K. D. (2010). Top-down and bottom-up factors affecting seabird population trends in the California current system (1985-2006). *Progress in Oceanography, 84*(3-4), 242-254. doi:10.1016/j.pocean.2009.10.001

Alexander, M. A., Blade, I., Newman, M., Lanzante, J. R., Lau, N. C. & Scott, J. D. (2002). The atmospheric bridge: The influence of ENSO teleconnections on air-sea interaction over the global oceans. *Journal of Climate, 15*(16), 2205-2231.

Ashok, K., Behera, S. K., Rao, S. A., Weng, H. & Yamagata, T. (2007). El Niño Modoki and its possible teleconnection. *Journal of Geophysical Research: Oceans, 112*(C11).

Ashok, K. & Yamagata, T. (2009). The El Niño with a difference. *Nature, 461*(7263), 481-484.

Bakun, A., Black, B. A., Bograd, S. J., Garcia-Reyes, M., Miller, A. J., Rykaczewski, R. R. & Sydeman, W. J. (2015). Anticipated Effects of Climate Change on Coastal Upwelling Ecosystems. *Current Climate Change Reports, 1*(2), 85-93. doi:10.1007/s40641-015-0008-4

Berner, L. D. (1960). Unusual features in the distribution of pelagic tunicates in 1957 and 1958. *CalCOFI Rep., 9*, 247-253.

Blackburn, M. (1979). Thaliacea of the California Current region: relations to temperature, chlorophyll, currents and upwelling. *CalCOFI Rep., 20*, 184-214.

Bond, N. A., Cronin, M. F., Freeland, H. & Mantua, N. (2015). Causes and impacts of the 2014 warm anomaly in the NE Pacific. *Geophysical Research Letters, 42*(9), 3414-3420. doi:10.1002/2015gl063306

Brinton, E. (1960). Changes in the distribution of euphausiid crustaceans in the region of the California Current. *CalCOFI Rep., 7*, 137-146.

Brinton, E. (1981). Euphausiid distributions in the California Current during the warm winter-spring of 1977–78, in the context of a 1949–1966 time series. *California Cooperative Oceanic Fisheries Investigations Reports, 22*, 135-154.

Brinton, E. & Reid, J. L. (1986). On the effects of interannual variations in circulation and temperature upon euphausiids of the California Current. *UNESCO Tech. Pap. Mar. Sci, 49*(25-34).

Brinton, E. & Townsend, A. (2003). Decadal variability in abundances of the dominant euphausiid species in southern sectors of the California Current. *Deep-Sea Research Part Ii-Topical Studies in Oceanography, 50*(14-16), 2449-2472. doi:10.1016/S0967-0645(03)00126-7

Cane, M. A. (1983). Oceanographic Events during El-Nino. *Science, 222*(4629), 1189-1195. doi:DOI 10.1126/science.222.4629.1189

Capotondi, A. (2013). ENSO diversity in the NCAR CCSM4 climate model. *Journal of Geophysical Research-Oceans, 118*(10), 4755-4770. doi:10.1002/jgrc.20335

Capotondi, A., Wittenberg, A. T., Newman, M., Di Lorenzo, E., Yu, J. Y., Braconnot, P., et al. (2015). Understanding ENSO diversity. *Bulletin of the American Meteorological Society, 96*(6), 921-938.

Chao, Y., Farrara, J. D., Bjorkstedt, E., Chai, F., Chavez, F., Rudnick, D. L., et al. (2017). The origins of the anomalous warming in the California coastal ocean and San Francisco Bay during 2014-2016. *Journal of Geophysical Research-Oceans, 122*(9), 7537-7557. doi:10.1002/2017jc013120

Chelton, D. B., Bernal, P. A. & Mcgowan, J. A. (1982). Large-Scale Interannual Physical and Biological Interaction in the California Current. *Journal of Marine Research, 40*(4), 1095-1125.

Croll, D. A., Marinovic, B., Benson, S., Chavez, F. P., Black, N., Ternullo, R. & Tershy, B. R. (2005). From wind to whales: trophic links in a coastal upwelling system. *Marine Ecology Progress Series, 289*, 117-130. doi:DOI 10.3354/meps289117

Croll, D. A., Tershy, B. R., Hewitt, R. P., Demer, D. A., Fiedler, P. C., Smith, S. E., et al. (1998). An integrated approach to the foraging ecology of marine birds and mammals. *Deep-Sea Research Part Ii-Topical Studies in Oceanography, 45*(7), 1353-+. doi:Doi 10.1016/S0967-0645(98)00031-9

Dalpadado, P. & Skjoldal, H. R. (1996). Abundance, maturity and growth of the Krill species Thysanoessa inermis and T. longicaudata in the Barent Sea. *Marine Ecology Progress Series, 144*, 175-183.

Di Lorenzo, E. & Ohman, M. D. (2013). A double-integration hypothesis to explain ocean ecosystem response to climate forcing. *Proceedings of the National Academy of Sciences, 110*(7), 2496-2499.

Di Lorenzo, E., Schneider, N., Cobb, K. M., Franks, P. J. S., Chhak, K., Miller, A. J., et al. (2008). North Pacific Gyre Oscillation links ocean climate and ecosystem change. *Geophysical Research Letters, 35*(8).

Ducklow, H. W., Steinberg, D. K. & Buesseler, K. O. (2001). Upper ocean carbon export and the biological pump. *Oceanography, 14*(4), 50-58.

Fisher, J. L., Menkel, J., Copeman, L., Shaw, C. T., Feinberg, L. R. & Peterson, W. T. (2020). Comparison of condition metrics and lipid content between Euphausia pacifica and

Thysanoessa spinifera in the northern California Current, USA. *Progress in Oceanography, 188*. doi:ARTN 102417 10.1016/j.pocean.2020.102417

Fisher, J. L., Peterson, W. T. & Rykaczewski, R. R. (2015). The impact of El Niño events on the pelagic food chain in the northern California Current. *Global Change Biology, 21*(12), 4401-4414.

Garcia-Reyes, M., Sydeman, W. J., Schoeman, D. S., Rykaczewski, R. R., Black, B. A., Smit, A. J. & Bograd, S. J. (2015). Under Pressure: Climate Change, Upwelling, and Eastern Boundary Upwelling Ecosystems. *Frontiers in Marine Science, 2*. doi:ARTN 10910.3389/fmars.2015.00109

Gentemann, C. L., Fewings, M. R. & Garcia-Reyes, M. (2017). Satellite sea surface temperatures along the West Coast of the United States during the 2014-2016 northeast Pacific marine heat wave. *Geophysical Research Letters, 44*(1), 312-319. doi:10.1002/2016gl071039

Hanazato, T. & Yasuno, M. (1989). Zooplankton community structure driven by vertebrate and invertebrate predators. *Oecologia, 81*(4), 450-458.

Hazen, E. L., Jorgensen, S., Rykaczewski, R. R., Bograd, S. J., Foley, D. G., Jonsen, I. D., et al. (2013). Predicted habitat shifts of Pacific top predators in a changing climate. *Nature Climate Change, 3*(3), 234-238. doi:10.1038/Nclimate1686

Henschke, N., Everett, J. D., Richardson, A. J. & Suthers, I. M. (2016). Rethinking the Role of Salps in the Ocean. *Trends in Ecology & Evolution, 31*(9), 720-733. doi:10.1016/j.tree.2016.06.007

Jacox, M. G., Hazen, E. L., Zaba, K. D., Rudnick, D. L., Edwards, C. A., Moore, A. M. & Bograd, S. J. (2016). Impacts of the 2015-2016 El Nino on the California Current System: Early assessment and comparison to past events. *Geophysical Research Letters, 43*(13), 7072-7080. doi:10.1002/2016gl069716

Kao, H. Y. & Yu, J. Y. (2009). Contrasting Eastern-Pacific and Central-Pacific Types of ENSO. *Journal of Climate, 22*(3), 615-632. doi:10.1175/2008jcli2309.1

Karnauskas, K. B. (2013). Can we distinguish canonical El Nino from Modoki? *Geophysical Research Letters, 40*(19), 5246-5251. doi:10.1002/grl.51007

Keiper, C. A., Ainley, D. G., Allen, S. G. & Harvey, J. T. (2005). Marine mammal occurrence and ocean climate off central California, 1986 to 1994 and 1997 to 1999. *Marine Ecology Progress Series, 289*, 285-306. doi:DOI 10.3354/meps289285

Keister, J. E., Di Lorenzo, E., Morgan, C. A., Combes, V. & Peterson, W. T. (2011). Zooplankton species composition is linked to ocean transport in the Northern California Current. *Global Change Biology, 17*(7), 2498-2511.

Kim, W., Yeh, S. W., Kim, J. H., Kug, J. S. & Kwon, M. (2011). The unique 2009–2010 El Niño event: A fast phase transition of warm pool El Niño to La Niña. *Geophysical Research Letters, 38*(15).

Kug, J. S., Jin, F. F. & An, S. I. (2009). Two Types of El Nino Events: Cold Tongue El Nino and Warm Pool El Nino. *Journal of Climate, 22*(6), 1499-1515. doi:10.1175/2008jcli2624.1

L'Heureux, M. L., Takahashi, K., Watkins, A. B., Barnston, A. G., Becker, E. J., Di Liberto, T. E., et al. (2017). Observing and Predicting the 2015/16 El Nino. *Bulletin of the American Meteorological Society, 98*(7), 1363-1382. doi:10.1175/Bams-D-16-0009.1

Larkin, N. K. & Harrison, D. E. (2005). On the definition of El Niño and associated seasonal average US weather anomalies. *Geophysical Research Letters, 32*(12).

Lavaniegos, B. E. (2009). Influence of a multiyear event of low salinity on the zooplankton from Mexican eco-regions of the California Current. *Progress in Oceanography, 83*(1-4), 369-375.

Lavaniegos, B. E. & Ambriz-Arreola, I. (2012). Interannual variability in krill off Baja California in the period 1997-2005. *Progress in Oceanography, 97*, 164-173. doi:10.1016/j.pocean.2011.11.008

Lavaniegos, B. E., Jimenez-Perez, L. C. & Gaxiola-Castro, G. (2002). Plankton response to El Nino 1997-1998 and La Nina 1999 in the southern region of the California Current. *Progress in Oceanography, 54*(1-4), 33-58. doi:10.1016/S0079-6611(02)00042-3

Lavaniegos, B. E. & Ohman, M. D. (2007). Coherence of long-term variations of zooplankton in two sectors of the California Current System. *Progress in Oceanography, 75*(1), 42-69.

Lilly, L. E. & Ohman, M. D. (2018). CCE IV: El Niño-related zooplankton variability in the southern California Current System. *Deep-Sea Research Part I: Oceanographic Research Papers*.

Lilly, L. E. & Ohman, M. D. (submitted). Euphausiid spatial displacements elucidate El Niño forcing mechanisms in the southern California Current System.

Lindegren, M., Checkley, D. M., Koslow, J. A., Goericke, R. & Ohman, M. D. (2018). Climate-mediated changes in marine ecosystem regulation during El Nino. *Global Change Biology, 24*(2), 796-809. doi:10.1111/gcb.13993

Lynn, R. J. (1983). The 1982-83 warm episode in the California Current. *Geophysical Research Letters, 10*(11), 1093-1095.

Lynn, R. J. & Bograd, S. J. (2002). Dynamic evolution of the 1997-1999 El Nino-La Nina cycle in the southern California Current System. *Progress in Oceanography, 54*(1-4), 59-75. doi:Pii S0079-6611(02)00043-5

Mackas, D. L., Peterson, W. T., Ohman, M. D. & Lavaniegos, B. E. (2006). Zooplankton anomalies in the California Current system before and during the warm ocean conditions of 2005. *Geophysical Research Letters, 33*(22).

Mantua, N. J., Hare, S. R., Zhang, Y., Wallace, J. M. & Francis, R. C. (1997). A Pacific interdecadal climate oscillation with impacts on salmon production. *Bulletin of the American Meteorological Society, 78*(6), 1069-1079. doi:Doi 10.1175/1520-0477(1997)078<1069:Apicow>2.0.Co;2

Marinovic, B. B., Croll, D. A., Gong, N., Benson, S. R. & Chavez, F. P. (2002). Effects of the 1997-1999 El Nino and La Nina events on zooplankton abundance and euphausiid community composition within the Monterey Bay coastal upwelling system. *Progress in Oceanography, 54*(1-4), 265-277. doi:10.1016/S0079-6611(02)00053-8

McPhaden, M. J. (1999). Genesis and evolution of the 1997-98 El Nino. *Science, 283*(5404), 950-954. doi:DOI 10.1126/science.283.5404.950

Miller, R. R., Santora, J. A., Auth, T. D., Sakuma, K. M., Wells, B. K., Field, J. C. & Brodeur, R. D. (2019). Distribution of Pelagic Thaliaceans, Thetys vagina and Pyrosoma atlanticum, during a period of mass occurrence within the California Current. . *CalCOFI Rep., 60*, 94-108.

Mullin, M. M. (1998). Interannual and interdecadal variation in California Current zooplankton: Calanus in the late 1950s and early 1990s. *Global Change Biology, 4*(1), 115-119.

Newman, M., Wittenberg, A. T., Cheng, L. Y., Compo, G. P. & Smith, C. A. (2018). The Extreme 2015/16 El Nino, in the Context of Historical Climate Variability and Change. *Bulletin of the American Meteorological Society, 99*(1), S16-S20. doi:10.1175/Bams-D-17-0116.1

Nickels, C. F., Sala, L. M. & Ohman, M. D. (2018). The morphology of euphausiid mandibles used to assess selective predation by blue whales in the southern sector of the California Current System. *Journal of Crustacean Biology, 38*(5), 563-573.

Nickels, C. F., Sala, L. M. & Ohman, M. D. (2019). The euphausiid prey field for blue whales around a steep bathymetric feature in the southern California current system. *Limnology and Oceanography, 64*(1), 390-405. doi:10.1002/lno.11047

O'Loughlin, J. H., Bernard, K. S., Daly, E. A., Zeman, S., Fisher, J. L., Brodeur, R. D. & Hurst, T. P. (2020). Implications of Pyrosoma atlanticum range expansion on phytoplankton standing stocks in the Northern California Current. *Progress in Oceanography, 102424*.

Ohman, M. D., Mantua, N., Keister, J., Garcia-Reyes, M. & McClatchie, S. (2017). ENSO impacts on ecosystem indicators in the California Current System. *US Clivar Variations, 15*(1), 8-15.

Pares-Escobar, F., Lavaniegos, B. E. & Ambriz-Arreola, I. (2018). Interannual summer variability in oceanic euphausiid communities off the Baja California western coast during 1998-2008. *Progress in Oceanography, 160*, 53-67. doi:10.1016/j.pocean.2017.11.009

Ramp, S. R., McClean, J. L., Collins, C. A., Semtner, A. J. & Hays, K. A. S. (1997). Observations and modeling of the 1991-1992 El Nino signal off central California. *Journal of Geophysical Research-Oceans, 102*(C3), 5553-5582. doi:Doi 10.1029/96jc03050

Rebstock, G. A. (2001). Long-term stability of species composition in calanoid copepods off southern California. *Marine Ecology Progress Series, 215*, 213-224. doi:DOI 10.3354/meps215213

Reid, J. L. (1960). *Oceanography of the eastern North Pacific in the last 10 years*. Retrieved from

Reid, P. C., Battle, E. J. V. & Batten, S. D. B., K. M. (2000). Impacts of fisheries on plankton community structure. *ICES Journal of Marine Science, 57*(3), 495-502.

Robertson, R. R. & Bjorkstedt, E. P. (2020). Climate-driven variability in Euphausia pacifica size distributions off northern California. *Progress in Oceanography, 188*. doi:ARTN 10241210.1016/j.pocean.2020.102412

Rudnick, D. L., Zaba, K. D., Todd, R. E. & Davis, R. E. (2017). A climatology of the California Current System from a network of underwater gliders. *Progress in Oceanography, 154*, 64-106. doi:10.1016/j.pocean.2017.03.002

Rykaczewski, R. R., Dunne, J. P., Sydeman, W. J., Garcia-Reyes, M., Black, B. A. & Bograd, S. J. (2015). Poleward displacement of coastal upwelling-favorable winds in the ocean's eastern boundary currents through the 21st century. *Geophysical Research Letters, 42*(15), 6424-6431. doi:10.1002/2015gl064694

Simpson, J. J. (1984). El-Nino-Induced Onshore Transport in the California Current during 1982-1983. *Geophysical Research Letters, 11*(3), 241-242.

Skjoldal, H. R. & Rey, F. (1989). Pelagic production and variability of the Barents Sea ecosystem. In K. S. a. L. M. Alexander (Ed.), *Biomass yields and geography of large marine ecosystems* (pp. 241-286). Colorado, USA: Westview Press.

Smith, K. L., Sherman, A. D., Huffard, C. L., McGill, P. R., Henthorn, R., Von Thun, S., et al. (2014). Large salp bloom export from the upper ocean and benthic community response in the abyssal northeast Pacific: Day to week resolution. *Limnology and Oceanography, 59*(3), 745-757. doi:10.4319/lo.2014.59.3.0745

Steinberg, D. K. & Landry, M. R. (2017). Zooplankton and the Ocean Carbon Cycle. *Annual Review of Marine Science, Vol 9, 9*, 413-444. doi:10.1146/annurev-marine-010814-015924

Strub, P. T. & James, C. (2002). The 1997-1998 oceanic El Niño signal along the southeast and northeast Pacific boundaries - an altimetric view. *Progress in Oceanography, 54*(1-4), 439-458.

Stukel, M. R., Ohman, M. D., Benitez-Nelson, C. R. & Landry, M. R. (2013). Contributions of mesozooplankton to vertical carbon export in a coastal upwelling system. *Marine Ecology Progress Series, 491*, 47-+. doi:10.3354/meps10453

Thayer, J. A. & Sydeman, W. J. (2007). Spatio-temporal variability in prey harvest and reproductive ecology of a piscivorous seabird, Cerorhinca monocerata, in an upwelling system. *Marine Ecology Progress Series, 329*, 253-265. doi:DOI 10.3354/meps329253

Timmermann, A., An, S.-I., Kug, J. S., Jin, F. F., Cai, W., Capotondi, A., et al. (2019). El Niño-Southern Oscillation complexity. *Nature, 559*, 535-545.

Todd, R. E., Rudnick, D. L., Davis, R. E. & Ohman, M. D. (2011). Underwater gliders reveal rapid arrival of El Nino effects off California's coast. *Geophysical Research Letters, 38*. doi:10.1029/2010gl046376

Wyllie, J. G. (1966). Geostrophic flow of the California Current at the surface and at 200 m. In *CalCOFI Atlas* (Vol. 4). University of California, San Diego.

Wyrtki, K. (1975). El Nino - Dynamic-Response of Equatorial Pacific Ocean to Atmospheric Forcing. *Journal of Physical Oceanography, 5*(4), 572-584. doi:Doi 10.1175/1520-0485(1975)005<0572:Entdro>2.0.Co;2

Yeh, S. W., Kug, J. S. & An, S. I. (2014). Recent progress on two types of El Niño: Observations, dynamics, and future changes. *Asia-Pacific Journal of Atmospheric Sciences, 50*(1), 69-81.

Yeh, S. W., Kug, J. S., Dewitte, B., Kwon, M. H., Kirtman, B. P. & Jin, F. F. (2009). El Nino in a changing climate (vol 461, pg 511, 2009). *Nature, 462*(7273). doi:10.1038/nature08546

Zaba, K. D. & Rudnick, D. L. (2016). The 2014-2015 warming anomaly in the Southern California Current System observed by underwater gliders. *Geophysical Research Letters, 43*(3), 1241-1248. doi:10.1002/2015gl067550

Chapter 1

CCE IV: El Niño-related zooplankton variability in the southern California Current System

Abstract

We analyzed seven El Niño events (springs 1958-59, 1983, 1992-93, 1998, 2003, 2010, and 2016) and the 2014-15 Pacific Warm Anomaly (spring 2015) for their impacts on zooplankton biomass and community composition in the southern sector of the California Current System (CCS). Although total mesozooplankton carbon biomass was only modestly affected during El Niño springs, community composition changed substantially. Five major zooplankton taxa correlated negatively with San Diego sea level anomaly (SDSLA), a regional metric of El Niño physical impacts in the CCS. Additional taxa were negatively related to SDSLA via a time-lagged response reflected in an autoregressive-1 (AR-1) model. All five SDSLA-correlated taxa decreased in carbon biomass during most El Niño years compared to the surrounding years; the exception was the mild event of 2003. Principal Component Analysis revealed coherent species-level responses to El Niño within the euphausiids, copepods, and hyperiid amphipods. Percent similarity index (PSI) comparisons showed pronounced changes in the compositions of euphausiid and, to a lesser extent, calanoid copepod communities during El Niño. By grouping El Niños into Eastern Pacific (EP) versus Central Pacific (CP) events based on their expressions along the equator, we found that CCS zooplankton assemblages showed a tendency toward greater changes in species composition during EP than CP El Niños, although we had low statistical power for these comparisons. Several species showed consistent biomass changes across La Niña events as well, generally opposite in sign to El Niño responses, but

overall community composition showed minimal change during La Niña. Carbon biomass and community composition returned to pre-Niño levels within 1-2 years following almost every event, suggesting high resilience of southern CCS zooplankton to El Niño perturbations to date.

1.1. Introduction

El Niño is a coupled atmosphere-ocean phenomenon that develops in the equatorial Pacific, with global impacts (Liu & Alexander, 2007). El Niño occurs when the equatorial Pacific trade winds weaken or reverse, and westerly wind bursts induce eastward propagation of Western Pacific Warm Pool waters via subsurface Kelvin Waves (Cane, 1983; McPhaden, 1999b; Wyrtki, 1975). El Niño can significantly alter the highly productive ecosystems in the equatorial Pacific, particularly off South America. Studies have observed decreased magnitude and spatial extent of primary production (Barber et al., 1996; Chavez et al., 1998; Cowles & Barber, 1977; Foley et al., 1997) and reduced biomass of commercial fish stocks and guano-producing seabird populations (Arcos et al., 2001; Barber & Chavez, 1983, 1986; Chavez et al., 2003; Schreiber & Schreiber, 1984) associated with El Niño.

El Niño events vary widely in their physical expressions and biological impacts. ENSO variability has gained significant attention in recent years due in part to NOAA's 2003 official designation of the phenomenon as a sustained three-month period of SST anomalies in the central equatorial Pacific (Larkin & Harrison, 2005). This definition identified several central Pacific warm events that had not been previously detected off South America. Subsequent studies have investigated whether El Niño events dichotomize into Eastern Pacific (EP or 'canonical') versus Central Pacific (CP, also 'Dateline' or 'Modoki') events or span a continuum of expressions and forcing mechanisms. One view posits that EP events are caused by strong

Kelvin Wave propagation from the Warm Pool to the eastern equatorial Pacific, while CP events are caused by local atmospheric forcing at the International Dateline (Ashok et al., 2007; Kao & Yu, 2009; Yu & Kao, 2007). A contrasting view suggests that all El Niño events are mixtures of these two types of forcing, and that variations in expression are due to the strength and timing of westerly wind bursts (Capotondi et al., 2015; Chavez et al., 1999; Karnauskas, 2013). El Niño can affect higher latitudes via three mechanisms: 1) coastally-trapped waves (CTWs, known as remote forcing) (Alexander et al., 2002; Schwing et al., 2002); 2) atmospheric teleconnections from the equator (Frischknecht et al., 2015; Simpson, 1984; Strub & James, 2002); or 3) anomalous advection of warm, saline water of southern or western origin into the CCS (Bograd & Lynn, 2001; Jacox et al., 2016; Lynn & Bograd, 2002; Simpson, 1984). Strong Kelvin Wave propagation associated with EP El Niños is thought to induce poleward-migrating CTWs, while CP-focused El Niños tend to show stronger evidence for atmospheric teleconnections to mid-latitudes (Ashok et al., 2007; Chavez, 1996; Frischknecht et al., 2015). The question of El Niño variability in the equatorial Pacific, and connective mechanisms to higher latitudes, is essential for our understanding of how El Niño affects mid-latitude ecosystems.

The California Current System (CCS) is a mid-latitude eastern boundary upwelling system home to a range of large pelagic species and commercially-valuable fisheries (Chelton et al., 1982; Hickey, 1979). A typical CCS El Niño response includes elevated ocean temperatures and sea surface height (SSH), depressed thermocline and nutricline, and increased poleward flow of the Inshore Countercurrent (Chavez, 1996; Hayward, 1993; Lynn & Bograd, 2002). El Niño-related physical perturbations can significantly alter biological production in the CCS. Primary production generally decreases and contracts nearshore (Chavez, 1996; Chavez et al., 2002; Fiedler, 1984; Hayward, 1993; Kahru & Mitchell, 2000), and the phytoplankton community can

switch from diatom to picoplankton dominance due to reduced nutrient inputs (Chavez, 1996). Mesozooplankton have shown decreased biomass and reduced dominance by resident cool species during El Niño (Mullin, 1998; Smith, 1985), as well as low community similarity to other years (Rebstock, 2001). Non-resident offshore and southerly euphausiid species generally associate with El Niño-related warm water intrusions into the southern CCS (Brinton, 1960, 1981; Brinton & Townsend, 2003). However, individual El Niño event responses can vary widely. Some recent El Niños lacked evidence for CTWs and increased poleward flow (Simpson, 1984; Todd et al., 2011), suggesting variability in forcing mechanisms underlying individual events. Although some El Niño years show increases in subtropical euphausiid species off Southern and Baja California, and corresponding decreases in resident cool-water species (Brinton, 1981; Lavaniegos et al., 2002; Marinovic et al., 2002), other events do not have major associated influxes of subtropical species (Todd et al., 2011). Fisher et al. (2015) found that the magnitude of copepod community anomalies in the northern CCS correlated positively with both the magnitude and duration of El Niño events, and that years tended to group into EP versus CP responses. Similarly, Pares-Escobar et al. (2018) found significant variability in summer euphausiid communities off Baja California between 1998-2008, a period encompassing two EP and two CP El Niños, suggesting that zooplankton may respond differently depending on the type of equatorial El Niño.

CCS El Niños generally correlate with equatorial events, but several El Niños have also persisted in the CCS for 1-2 years beyond the initial equatorial perturbation, and some years show anomalous CCS conditions without associated equatorial changes (Fiedler & Mantua, 2017). Recently, the 2014-15 Pacific Warm Anomaly occurred in the Eastern North Pacific with no corresponding significant equatorial El Niño signal (Chao et al., 2017; Di Lorenzo & Mantua,

2016). The combination of perturbations from the 2014-15 Warm Anomaly and 2015-16 El Niño produced a 2-3 year period of positive temperature and negative nutrient anomalies in the CCS (Bond et al., 2015; Di Lorenzo & Mantua, 2016; Frischknecht et al., 2017), only partially interrupted by spring upwelling in 2015 (Jacox et al., 2016; Kahru et al., 2018). The 2014-15 Warm Anomaly was notable because 1) it produced much greater temperature anomalies than any previous CCS warm event (Zaba & Rudnick, 2016), and 2) it preceded, rather than followed, an equatorial El Niño (Fiedler & Mantua, 2017). The Warm Anomaly may provide a glimpse into potential future ocean conditions of a warmer background state against which El Niño events occur.

The mechanisms by which El Niño influences CCS mesozooplankton are still not well understood. Quantifying variability in mesozooplankton community structure in response to individual events will help identify dominant forcing mechanisms of change, which can then be used to predict future El Niño-related mesozooplankton shifts and associated impacts on higher trophic levels. Toward this goal, the present paper addresses the following questions:

1. At what taxonomic level are CCS mesozooplankton responses to El Niño most pronounced?
2. Do CCS mesozooplankton respond consistently across all El Niños of the past 66 years?
3. Do responses vary between Eastern Pacific and Central Pacific El Niños?
4. How do the 2014-15 Warm Anomaly and 2015-16 El Niño compare to each other and to past El Niño events with respect to mesozooplankton shifts?
5. How resilient are CCS mesozooplankton to El Niño?

This study provides an initial analysis and categorization of El Niño-related mesozooplankton shifts in the southern CCS. We recognize the importance of spatial variations

within the larger region, and of decadal-scale changes in background Eastern North Pacific conditions, but we focus here explicitly on the variability between individual El Niño events.

1.2. Methods

1.2.1. Study region

Our study focused on the southern region of the California Current System (CCS), defined as California Cooperative Oceanic Fisheries Investigations (CalCOFI) lines 80-93.3, stations 26.7-70 (SC region, cf., Lavaniegos and Ohman (2007); see that publication for a map of the region). The region extends from just north of Pt. Conception, CA, south to the U.S.-Mexico border, and encompasses the southward-flowing core California Current and the northward-flowing Inshore Countercurrent and California Undercurrent.

1.2.2. El Niño indices

We used a combination of two equatorial Pacific El Niño indices and two local California Current System (CCS) indices to define El Niño occurrences that had an expression in the CCS. The Niño 3.4 (5^{o}S-5^{o}N, 170^{o}W-120^{o}W) and Niño 1+2 (0-10^{o}S, 90^{o}W-80^{o}W) indices measure sea surface temperature (SST) at two different regions in the equatorial Pacific Ocean (Climate Prediction Center, 2017). The two local CCS indices are: San Diego detrended sea level anomaly (SDSLA) and the depth of the 26.0 kg/m^3 density isopycnal in the nearshore 50 km along CalCOFI Line 90 ($Z_{26.0}$). The SDSLA timeseries is maintained by the University of Hawaii Sea Level Center (University of Hawaii Sea Level Center, 2017). The SDSLA data used here are monthly average anomalies, from which the seasonal cycle and long-term trend (1906-2016) were removed (data processed specifically using this method are available at:

http://oceaninformatics.ucsd.edu/datazoo/catalogs/ccelter/datasets/153). Our $Z_{26.0}$ index was constructed using data from the CalCOFI program, which samples four times per year. CalCOFI density measurements are obtained from hydrocast bottle samples at discrete depths; for our index, the data were then interpolated between bottle depths to resolve the depth of the 26.0 kg/m^3 isopycnal. Data for the index are only from CalCOFI Line 90, Stations 26.7-37, encompassing the nearshore 50 km, based on a similar $Z_{26.0}$ timeseries from Jacox et al. (2016) computed from merged Regional Ocean Modeling System (ROMS) and *Spray* glider *in situ* measurements, encompassing the time period 1981-2016. Our CalCOFI $Z_{26.0}$ index had a highly significant correlation with the ROMS-*Spray* index ($r = 0.89$, $p < 0.01$), confirming the suitability of using either index. We chose to utilize only the CalCOFI-based index here because it extends back to 1951, corresponding to the beginning of our zooplankton timeseries. The purpose of using both the SDSLA and $Z_{26.0}$ indices in our analyses is to capture different aspects of El Niño expression in the CCS: sea level anomaly can change due to changes in horizontal advection or local heating of water masses, while $Z_{26.0}$ is closely related to nutricline depths and primary production and can also be affected by local upwelling and wind changes (Jacox et al., 2016).

For each of the four El Niño indices, we calculated one average value per year based on wintertime monthly values (equatorial indices – November, December, and January (NDJ) average; CCS indices – December, January, and February (DJF) average). Each El Niño year refers to January of the average (e.g., '1958' means Nov 1957-Jan 1958 for equatorial indices and Dec 1957-Feb 1958 for CCS indices). We chose to average these months because: 1) previous studies have shown that El Niño peak anomalies occur along the equator in November-December and in the CCS in January-February (Jacox et al., 2015); and 2) CCS zooplankton

taxonomic analyses are only available in spring (sampled in March, April, or May) of each year, and we expect a two-three month time lag between CCS physical disturbances and zooplankton responses.

1.2.3. CCS El Niño classification

For this study, we defined El Niño perturbations in the CCS (hereafter: CCS El Niños) as three-month winter averages (see above) in which at least one Equatorial Index (Niño 3.4 or Niño 1+2) and at least one CCS index (SDSLA or $Z_{26.0}$) were both ≥ 1 S.D. above their respective long-term means. The following years fulfill these criteria: 1958, 1973, 1983, 1992, 1998, 2003, 2010, and 2016. CalCOFI did not sample zooplankton during spring 1973, so we removed that year from our analyses. We included 1959 and 1993 as El Niño Years 2 although they did not classify at the equator, because they were continuations of prior-year CCS El Niño events and were ≥ 1 S.D. in at least one CCS index. The equatorial signal during the 2014-15 Warm Anomaly was negligible (only > 0.5 S.D. in the Niño 3.4 Index) and the event was not considered an equatorial El Niño by NOAA standards, but we include 2015 in our analyses because of its extreme and unusual signals in the CCS. Therefore, our list of CCS El Niño Springs (indicating the spring period at the end of the fall-to-spring CCS El Niño cycle) is: 1958, 1959, 1983, 1992, 1993, 1998, 2003, 2010, and 2016, and the 2015 Warm Anomaly.

The Niño 1+2 index only reached ≥ 1 S.D. for years already classified by Niño 3.4, but we retained Niño 1+2 for use as a secondary means to categorize El Niño variability. Eastern equatorial Pacific-focused El Niño events (EP) are defined here as years when both the Niño 3.4

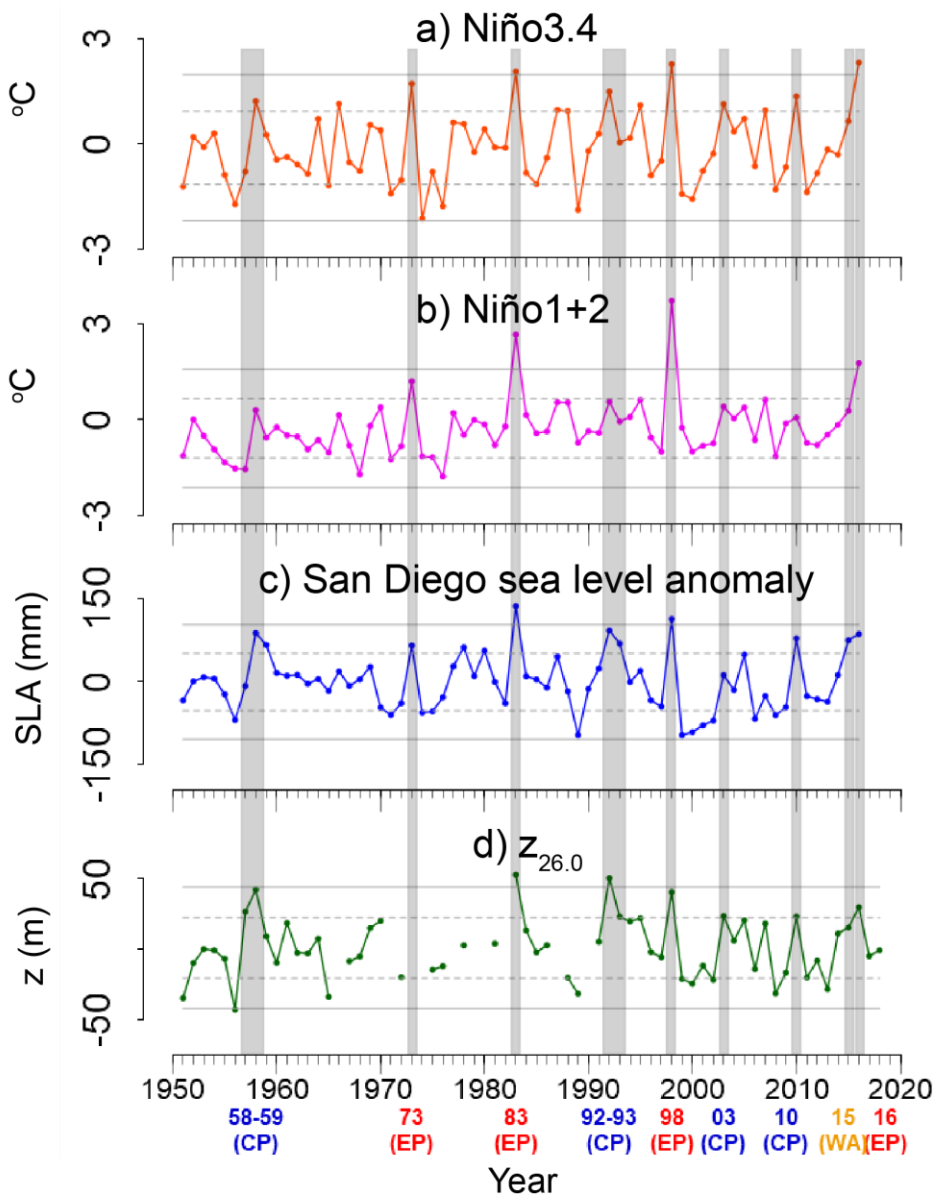

Figure 1.1. El Niño indices. Equatorial: a) Niño 3.4, b) Niño 1+2; and California Current System-specific: c) San Diego sea level anomaly (SDSLA), d) $Z_{26.0}$ CalCOFI. Anomalies from long-term mean; single three-month average per year. Horizontal grey lines indicate ± 1 S.D. (dashed) and ± 2 S.D. (solid). Vertical grey bars denote CCS El Niño years identified for this study. Labels are Eastern Pacific (EP) and Central Pacific (CP) El Niños and the 2014-15 Warm Anomaly (WA).

and Niño 1+2 indices exceed ≥ 1 S.D. (with corresponding ≥ 1 S.D. in at least one CCS index).

Using this secondary classification, the CCS El Niño events classify as follows: EP– 1983, 1998,

Table 1.1. Correlation coefficients between El Niño environmental indices. ** = $p < 0.01$.

	Niño 1+2	**SDSLA**	**$Z_{26.0}$**
Niño 3.4	$r = 0.81$ ($p < 0.01$)**	$r = 0.76$ ($p < 0.01$)**	$r = 0.77$ ($p < 0.01$)**
Niño 1+2	----	$r = 0.62$ ($p < 0.01$)**	$r = 0.65$ ($p < 0.01$)**
SDSLA	----	----	$r = 0.79$ ($p < 0.01$)**

2016; CP – 1958-59, 1992-93, 2003, and 2010. We did not classify the 2015 Warm Anomaly as either type of event.

We also defined a set of La Niña years for the CCS using the above metrics, where La Niña events are ≤ 1 S.D. below the mean. Under these criteria, the following are CCS La Niña Years: 1951, 1956, 1965, 1971, 1989, 1999, 2000, and 2008. CalCOFI zooplankton were not collected in 1971, so we excluded that year from our analyses. The same inter-year comparative analyses were performed on La Niña as on El Niño years. We considered 1999 and 2000 to be separate La Niña events because both years expressed significantly at the equator and the CCS.

1.2.4. Zooplankton data

1.2.4.1. Data collection and processing

Zooplankton samples were taken on quarterly CalCOFI cruises from 1951-2016 (reduced sampling years during the 1970s). Sampling net specifications changed during that period: from 1951-1968, a 1-m ring net with 550 μm mesh was towed obliquely from 0-140 m depth; from 1969-1977, 1-m ring net with 505 μm mesh was towed obliquely from 0-210 m; and since 1978 a twin-opening 0.71-m diameter bongo net with 505 μm mesh net has been towed obliquely from 0-210 m (Ohman & Smith, 1995). The effects of these changes on mesozooplankton have been discussed by Brinton and Townsend (1981), Ohman and Smith (1995), Ohman and Lavaniegos (2002), and Rebstock (2002), and do not influence the results presented here. Volumes filtered

were based on calibrated flowmeter readings. Samples were preserved in sodium borate-buffered formaldehyde and archived in the Pelagic Invertebrate Collection at Scripps Institution of Oceanography.

CalCOFI spring zooplankton samples were enumerated by microscopy to species level where possible, otherwise to higher taxa. The carbon content of each organism was obtained from taxon-specific length-carbon regressions (Lavaniegos & Ohman, 2007), and summed to calculate total carbon biomass. Samples were pooled for all nighttime stations within the sampling domain described above, except for 14 years when samples were enumerated by individual station (unpooled samples) to assess long-term changes in spatial variability (see Lavaniegos and Ohman (2007)). Unpooled samples were then averaged across all stations in the sampling domain to create a consistent timeseries across pooled and unpooled samples. Our purpose was to analyze the temporal variability within a standardized region, not to analyze within-region sampling variability. This approach has been successfully adopted for our sampling region by previous studies (Lavaniegos & Ohman, 2007; Mackas et al., 2006; Ohman et al., 2009; Rau et al., 2003; Rebstock, 2001).

Biomass was standardized to mg C m^{-2} to correct for changes in sampling depth, which could influence volumetric measurements. Salp abundances (used to calculate biomass) were multiplied by a net-correction factor of 2.68 for samples prior to 1978, to account for more accurate collection by the bongo net. See Lavaniegos and Ohman (2007) for full sampling details.

1.2.4.2. Copepod and euphausiid species

Our analyses involved two categories of copepod enumerations. The total copepods category includes length measurements for every copepod in a subsample, regardless of

taxonomic order or life history stage. These copepods were not identified to species. A separate category, calanoid copepods, was enumerated to calanoid species. The calanoid community is a subset of the total copepods, but because animals are enumerated from separate subsamples, we cannot subtract the calanoid component from the total copepods. Therefore, for our analyses, we analyzed both categories (total copepods, calanoid copepods) for taxon-level biomass shifts, but only one category (calanoid copepods) for species-level assemblage shifts. Only adult female calanoid copepods were identified, except for *Neocalanus cristatus* and *N. plumchrus*, which only occur as copepodid stage 5 (C5) in the SC region. For three species (*Calanus pacificus, Eucalanus californicus, Rhincalanus nasutus*), adult males and C5s were also enumerated, but for consistency we used only the adult females in our analyses.

Euphausiids were enumerated to species and life history phase and/or length class (cf., Brinton and Townsend (2003)), from all individual nighttime samples within the region described above, then converted to carbon content from length-carbon relationships from Ross (1982).

1.2.4.3. Community-level analyses

Three taxa (euphausiids, calanoid copepods, hyperiid amphipods) showed significant correlation with at least one CCS El Niño index (SDSLA or $Z_{26.0}$) and had sufficient species-level enumerations for more detailed taxonomic analyses. These three taxa were analyzed for species-level community (assemblage) shifts, where the community contained the consistently-enumerated species throughout the whole period (1951-2016). For this purpose, the euphausiid community includes 24 species, the calanoid copepods 40 species (a few enumerations could only be made to genus level, but were made consistently and are therefore included), and the hyperiid amphipods 13 species. Many additional rarer species are known from the region.

The hyperiid amphipod total biomass category includes all hyperiid amphipods and is therefore greater than the sum of the 13 individually enumerated species. Numerous hyperiids could only be identified to genus or family level, so we used only the 13 consistently identified species in order to understand species-level assemblage changes. For analyses involving taxon-level biomass, however, we used total hyperiid amphipod biomass.

Within the above three taxa, we also analyzed individual species that showed significant El Niño-related loadings in our principal component analysis (PCA). We used the SDSLA-correlated principal component to determine El Niño-responsive species within that taxon. Each taxon-specific threshold was determined visually based on a loading value surpassed by 6-9 species (generally several each of positive and negative correlations). For euphausiids, the loading threshold of PC1 was |0.25|; for calanoids, the PC2 threshold was |0.20|; for hyperiids, the PC1 threshold was |0.30|. Based on the sign of each species' loading on the PC, species were categorized as warm versus cool, where warm species are those with a positive correlation of PC loading with SDSLA, suggesting elevation during El Niño events.

1.2.5. Data analysis and statistical treatments

All statistical computations and plots were run in R version 1.0.136 (R-core-team, 2015).

1.2.5.1. Log-transformations

Nearly half of the higher taxa and species analyzed here had non-normal distributions for untransformed biomass data, so we analyzed all data in $\log_{10}$-transformed form unless otherwise noted. Data are plotted with 95% confidence intervals (C.I.) calculated from the t-distribution. Euphausiid biomass has C.I.s for every year because data were always enumerated by individual station and then combined into a southern California (SC) regional average. We make no attempt

to correct for temporal autocorrelation in timeseries because our sampling points are annual, a longer time-interval than the lifespan of most zooplankton.

1.2.5.2. El Niño vs. surrounding average biomass

For comparisons of biomass between El Niño and surrounding years, we calculated 'surrounding' as the average of the two years immediately preceding El Niño Year 1, and the second and third year following El Niño Year 1 or Year 2 (where applicable). For example, for the 1958-59 El Niño, surrounding biomass = mean(1956,1957,1961,1962), whereas for the 1983 El Niño, surrounding biomass = mean(1981,1982,1985,1986). We implemented the one-year lag to account for lagged biological responses due to reproduction. We used a Wilcoxon signed-rank matched pairs test to detect directional changes in biomass across El Niño years compared to surrounding average biomass.

1.2.5.3. Magnitude of zooplankton responses vs. magnitude of physical changes

The magnitude of the difference for each index (SDSLA, $Z_{26.0}$, zooplankton biomass; hereafter: mag(Δindex)) was calculated for each El Niño year minus its respective four-year surrounding average using the same method described in Section 1.2.5.2. The 2015 and 2016 events had only a two-year surrounding average (2013-14), because data were not yet available after 2016.

1.2.5.4. Principal Component Analysis (PCA)

Prior to performing PCA, we standardized log-transformed biomass data for each taxon or species within a group using species mean and standard deviation. Standardized biomass = (individual yearly biomass-mean biomass)/SD(all biomass).

1.2.5.5. Percent Similarity Indices

Percent Similarity Indices (PSI) were calculated from Whittaker (1952):

$$PSI = 100 - 0.5\Sigma|A_i - B_i| = \Sigma\min(A_i,B_i),$$

where A_i and B_i represent the percentages of species i in samples A and B, respectively. Untransformed biomass data were used for these calculations in order to assess proportions of each taxon within the community. PSIs were calculated for the total mesozooplankton (at the level of 15 taxa, hereafter referred to as "higher taxa"), and for species-level analyses of the euphausiid, calanoid copepod, and hyperiid amphipod communities. PSI calculations for each El Niño year were performed for two comparisons: 1) El Niño versus every other El Niño year, and 2) El Niño versus every non-El Niño year, using a Mann-Whitney U test.

1.3. Results

1.3.1. Physical indicators of El Niño in the CCS

California Current System El Niño events (CCS El Niños), as defined by our classifications, are indicated by vertical gray bands in figure 1.1. Each event is labeled by the year-spring of the latter portion of the event. Equatorial and CCS El Niño indices correlated significantly with each other, although Niño 3.4 had higher correlation values with CCS metrics than did Niño 1+2 (Table 1.1). Only three of the El Niño years (1983, 1998, 2016) for which we also had zooplankton data were classified as Eastern Pacific (EP) El Niños, although 1992 was just below the Niño 1+2 threshold. All other El Niños, including 1992-93, were classified as Central Pacific (CP) events (Fig. 1.1).

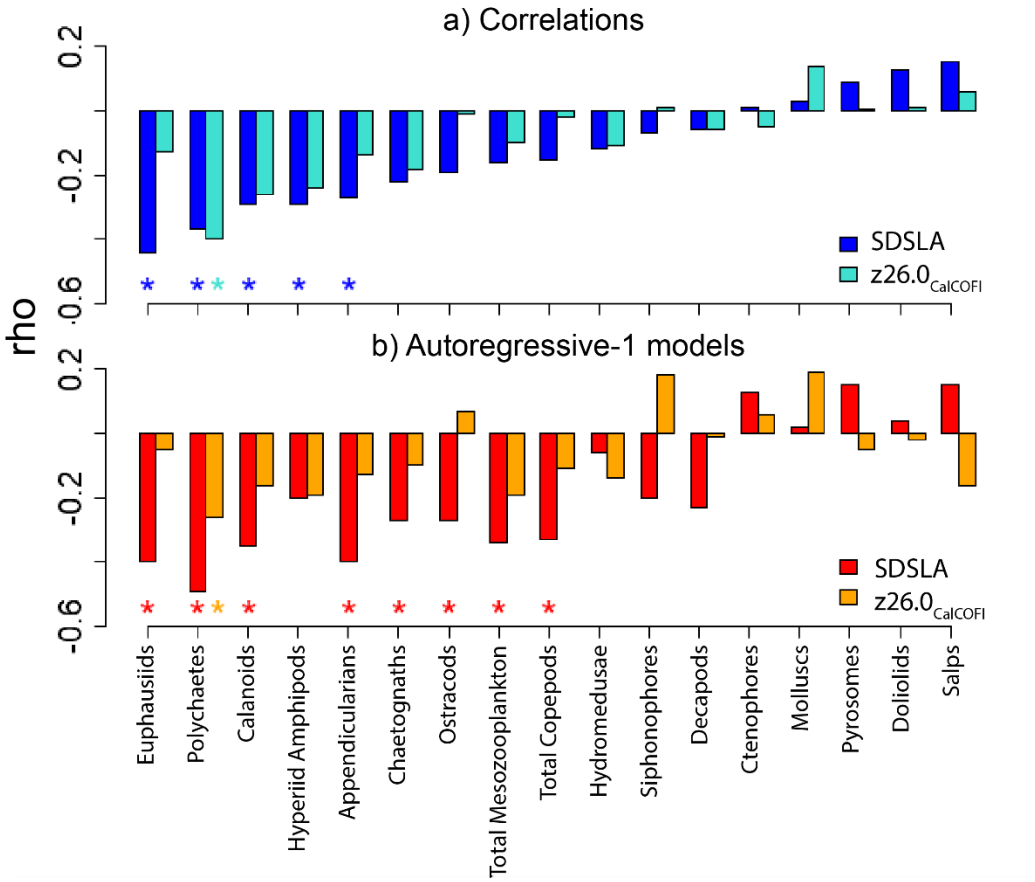

Figure 1.2. Correlation coefficients for a) measured log C biomass versus SDSLA and $Z_{26.0,}$ and b) AR-1-modeled C biomass (forced by SDSLA or $Z_{26.0}$) versus measured log C biomass for each major taxon. AR-1 models used damping scale of τ=3 months. Asterisk (*) = $p < 0.05$, color-coded by physical index.

1.3.2. Total mesozooplankton- and taxon-level shifts

1.3.2.1. Biomass changes during El Niño

1.3.2.1.1. Responses to physical changes

Total mesozooplankton carbon biomass showed a weak but non-significant ($p > 0.25$) relationship with both CCS El Niño indices (Fig. 1.2a). However, five taxa correlated significantly ($p < 0.05$) with at least one CCS index, in all cases declining during El Niño: euphausiids, polychaetes, calanoid copepods, hyperiid amphipods, and appendicularians.

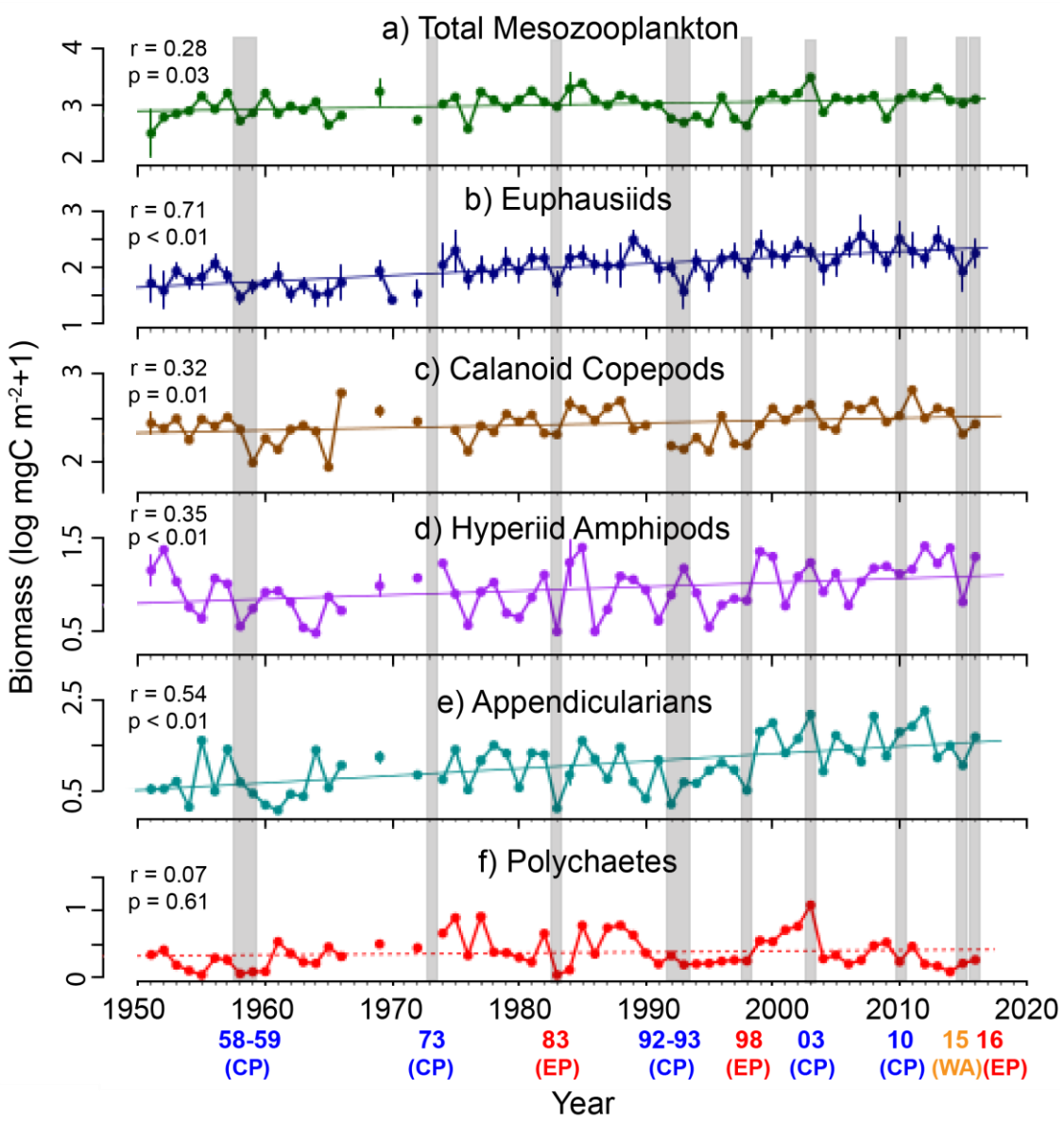

Figure 1.3. Timeseries of log C biomass for a) total zooplankton, and the five taxa that correlated significantly with SDSLA: b) euphausiids, c) calanoid copepods, d) hyperiid amphipods, e) appendicularians, f) polychaetes. Linear trends and associated correlation coefficients are shown. The purpose of the linear trendline is to indicate the overall non-stationarity of the timeseries, not to attempt to apply a descriptive model to the timeseries changes. Vertical grey bars indicate El Niño years (labels as in Fig. 1). Error bars indicate ±95% confidence interval.

Although thaliaceans (salps, doliolids, pyrosomes) and pelagic molluscs (pteropods and heteropods) showed small positive associations with the CCS El Niño indices, they were not

significant ($p > 0.20$). We further analyzed the carbon biomass timeseries with first-order autoregressive-modeled biomass timeseries (AR-1-models, damping time scale $\tau = 3$ months, cf., Di Lorenzo and Ohman (2013)) forced by SDSLA and $Z_{26.0}$ (Fig. 1.2b). Unlike measured carbon biomass, total mesozooplankton AR-1-modeled biomass correlated negatively with SDSLA ($p < 0.01$). All of the above El Niño-correlated taxa except hyperiid amphipods also correlated negatively with AR-1-modeled biomass, as did several additional taxa: chaetognaths, ostracods, and total copepods ($p < 0.05$).

Total mesozooplankton carbon biomass, as well as four of the five taxa that covaried with SDSLA, showed significant long-term upward trends (Fig. 1.3, $p < 0.05$). In order to avoid comparisons confounded by such long-term secular trends and other changes in background ocean state (e.g., due to the Pacific Decadal Oscillation, Mantua et al. (1997)), we have chosen to compare individual El Niño events only to their four immediately surrounding years. We also found that SDSLA yielded stronger correlations that $Z_{26.0}$ for all analyses, so we do not further report $Z_{26.0}$ results.

1.3.2.1.2. Consistency of biomass changes across El Niño events

Figure 1.4 compares biomass of each El Niño year with its four-year surrounding average, for total mesozooplankton and the five El Niño-responsive taxa. Only total calanoid copepod biomass showed a significant directional change across all El Niño events (Fig. 1.4c; Wilcoxon signed rank = 32, $p = 0.05$). Total mesozooplankton and all five taxa increased in biomass during the weak El Niño of 2003, and euphausiid biomass also increased in 2010 (Fig. 1.4b). All four taxa except polychaetes had larger biomass decreases during the 2015 Warm Anomaly than during the 2016 El Niño, when all biomasses returned to average or slightly

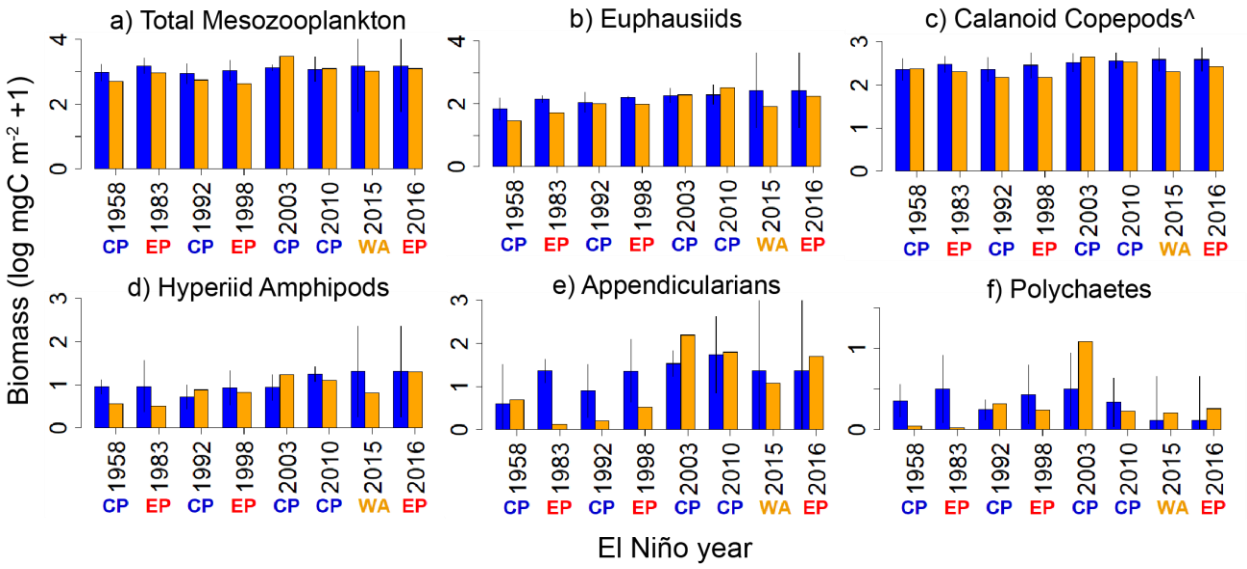

Figure 1.4. Comparisons of log C biomass during El Niño years (orange bars) and average log C biomass of the 4 surrounding years (blue bars). Error bars are 95% confidence interval. Year labels indicate El Niño year. Only El Niño Years 1 are shown (1959 and 1993 of two-year events excluded). ^ = p=0.05 (Wilcoxon matched pairs signed-rank test).

elevated levels. We further consider responses to individual events, including possible differential responses to EP versus CP events, below.

1.3.2.1.3. Magnitude of biomass change in relation to physical forcing

Only polychaetes and chaetognaths had weak negative correlations ($p < 0.10$) of the magnitude of change in biomass between El Niño and the surrounding four years with the corresponding magnitude of change in SDSLA. This suggests that the magnitude of change in biomass of higher taxa during an El Niño event is not determined by event magnitude.

1.3.2.1.4. Biomass resilience to El Niño

Total mesozooplankton and the four El Niño-related taxa besides appendicularians returned to pre-El Niño biomass levels within one year following each event except 1992-93 and 2003 (Fig. 1.3; see Fig. S1.1 for changes in additional taxa). Biomass of the above taxa

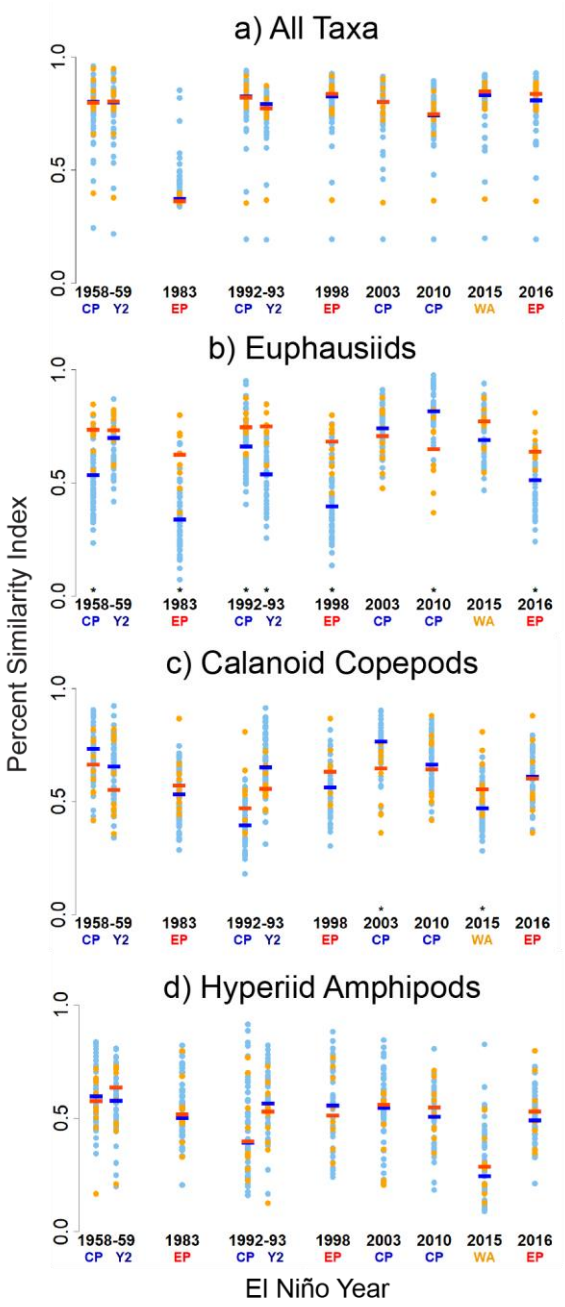

Figure 1.5. Percent Similarity Index (PSI) comparing each El Niño with every other year in the timeseries. Dots represent the individual similarities between that El Niño year and each other El Niño year (orange dots; red bars = median) or each non-El Niño year (blue dots; blue bars = median). a) all taxa, b) euphausiids, c) calanoid copepods, d) hyperiid amphipods. Year-labels indicate El Niño type: Eastern Pacific (EP), Central Pacific (CP), or Year 2 (Y2) El Niño, or the Warm Anomaly (WA). Asterisks above El Niño year labels indicate significant difference between median inter-El Niño comparison and median El Niño/non-El Niño comparison, using a Mann-Whitney U test.

remained at low levels after 1992-93, while biomass for all taxa declined substantially in the 1-3 years after 2003 from elevated levels during the event.

1.3.2.2. Community compositional changes during El Niño

1.3.2.2.1. Consistency of community composition across El Niño events

We used the percent similarity index (PSI) as a measure of how similar zooplankton communities (assemblages) were between individual El Niño events (Fig. 1.5). The total mesozooplankton community, differentiated into 15 higher taxa, did not show a consistently higher similarity of El Niño years to other El Niño years than similarity between El Niño years and non-El Niño years (Fig. 1.5a; orange dots indicate PSI values comparing a given El Niño year to each other individual El Niño; blue dots indicate PSI between that El Niño year and each individual non-El Niño year. Bars are the color-coded median values for the two types of comparisons. See figure caption for details). Both types of comparisons had similar ranges of values, and no El Niño year yielded a significant difference between medians for the two types of comparisons (Fig. 1.5a; $p > 0.30$ for all, using Mann-Whitney U test). Median PSIs were overall high (~0.80), except for 1983 (PSI < 0.40), which had a substantially lower PSI because of extremely high proportions of salps compared to all other years. When salps were removed, all PSI values and both median comparison values for 1983 were ~0.80.

Species-level compositional changes within individual higher taxa were often much greater than changes in the total community analyzed at the level of higher taxa. The euphausiid community had significantly higher median PSIs for community comparisons between El Niño years (Fig. 1.5b, orange symbols) than for El Niño versus non-El Niño comparisons (blue symbols; * = $p < 0.01$). The only non-significant comparisons were 1959, 2003 (identical median PSIs), and 2015. These results imply that the community of euphausiid species generally

shifts to a relatively consistent “El Niño” composition that differs significantly from non-El Niño years. Additionally, the 1983 and 1998 El Niños showed largest differences in median euphausiid community composition from all other years, suggesting that these events may have produced greater community impacts or had different forcing mechanisms than other El Niño events.

In contrast, the calanoid copepod community did not show consistently higher inter-El Niño similarities than El Niño versus non-El Niño, suggesting that the species composition of the calanoid community does not shift to one consistent composition during El Niño, but that individual events can produce quite different community compositions. Only two years had significant differences between inter-El Niño and El Niño versus non-El Niño median values: 2003 (higher El Niño/non-El Niño comparison) and 2015 (higher inter-El Niño comparison; Fig. 1.5c). Three El Niño years (1983, 1992, 1998) showed somewhat higher inter-El Niño median comparison values but no significant difference between the two types of medians ($p > 0.05$).

In contrast to both of the above taxa, the hyperiid amphipod assemblage showed no significant difference between median values between the two types of comparisons during any El Niño event (Fig. 1.5d). Additionally, median similarity values were the lowest (~0.40-0.60) of the four taxa analyzed, and the 2015 medians were notably low (PSI < 0.30). This finding of overall low similarity suggests that the hyperiid amphipod assemblage varies more between any given individual years than specifically in response to El Niño perturbations.

1.3.2.2.2. Magnitude of community change in relation to physical forcing

Only the calanoid copepod species-level community showed a significant correlation between the magnitude of change of community composition during El Niño and the corresponding magnitude of change of SDSLA across El Niño years relative to their four-year

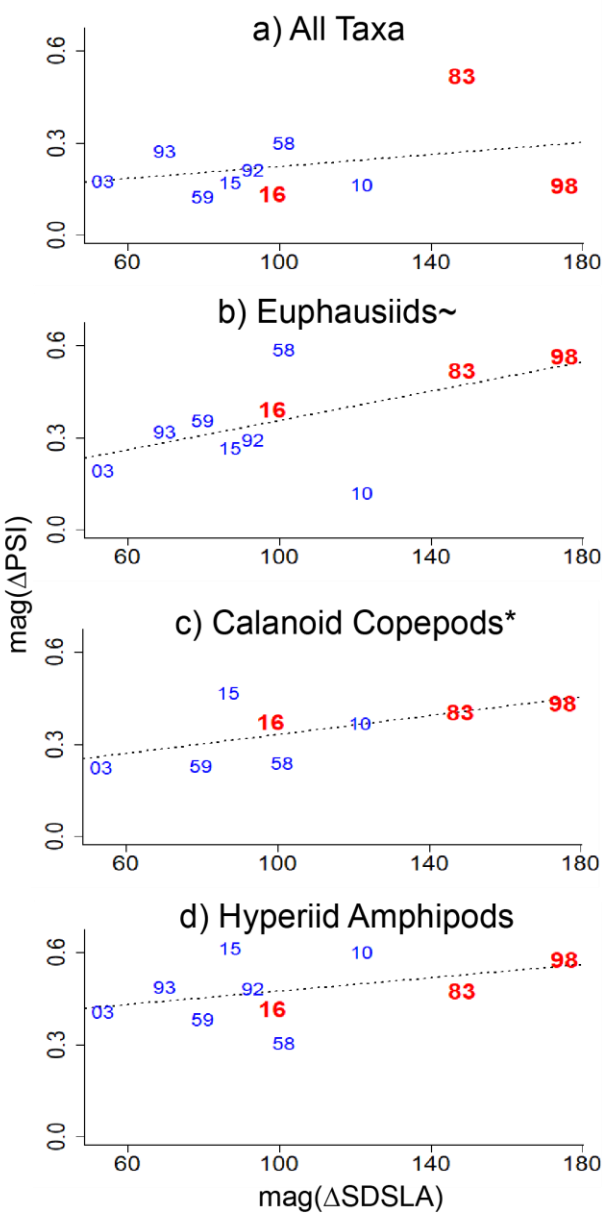

Figure 1.6. Magnitude of change in PSI compared to corresponding magnitude of change in SDSLA. Magnitude of change is calculated as: El Niño-average of 4 surrounding year. EP El Niño years are shown in red, CP years in blue. Dotted line indicates linear regression.

surrounding averages (Fig. 1.6, $r = 0.67$, $p < 0.05$). The euphausiid community showed a significant correlation when the 2010 El Niño was excluded ($r = 0.82$, $p = 0.01$).

1.3.2.2.3. Community composition resilience to El Niño

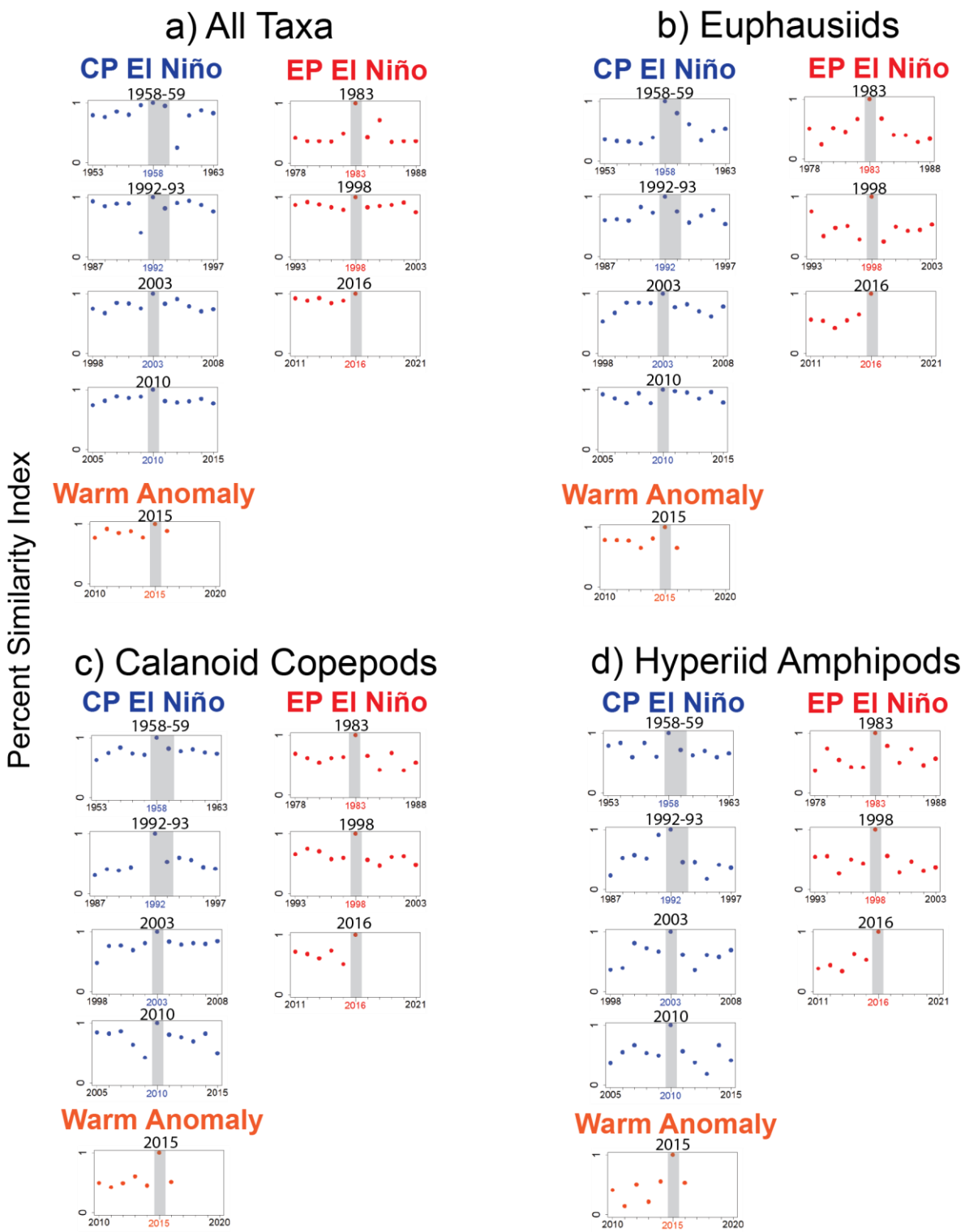

Figure 1.7. Percent Similarity Index (PSI) comparing each El Niño with the preceding five and following five years, for a) all taxa, b) euphausiids, c) calanoid copepods, and d) hyperiid amphipods. El Niño years are divided into (left) EP and (right) CP events, and (bottom) the Warm Anomaly. For two-year El Niños, only the first year was used in PSI calculations. Vertical dashed lines denote El Niño years. Gaps/lack of dots indicate years of no data.

To test for mesozooplankton community resilience to El Niño, we analyzed the total mesozooplankton community and the three species-enumerated taxa for PSI of each El Niño compared to its preceding five and following five years (Fig. 1.7). In nearly all cases, communities returned to pre-El Niño similarity by the following year. One exception was the euphausiid community in 1958-59, which gradually returned to pre-El Niño levels over the following three years. The calanoid copepod community showed decreased similarity in the two years before the 2010 El Niño, but the event itself was similar to other surrounding years (PSI ≥ 0.80).

1.3.3. Species-level changes during El Niño

1.3.3.1. Biomass responses to physical changes

We used PCA to test for coherent species-level El Niño responses within euphausiids, calanoid copepods, and hyperiid amphipods. The first two principal components of the euphausiid species-level community recovered 19.8% and 14.5% of variance, respectively (Fig. 1.8a,b). The euphausiid PC1 timeseries (Fig. 1.8c) correlated positively with SDSLA ($p < 0.01$), while PC2 did not ($p > 0.60$). We further used the PC1 loadings to identify individual species that showed consistent responses to El Niño events (Fig. 1.8a). We chose loading thresholds to determine El Niño-responsiveness based on values that identified approximately 6-9 species as 'El Niño responsive' (see Methods for full details). We used a loading threshold of |0.25| for euphausiid PC1: the dominant CCS euphausiid, *Euphausia pacifica* showed a 'cool-water species' response, while six warm-water species showed 'warm-water' responses.

The first two principal components of the calanoid copepod community recovered 14.5% and 13.2% of variance, respectively (Fig. 1.9a,b). In contrast to the other assemblages, calanoid

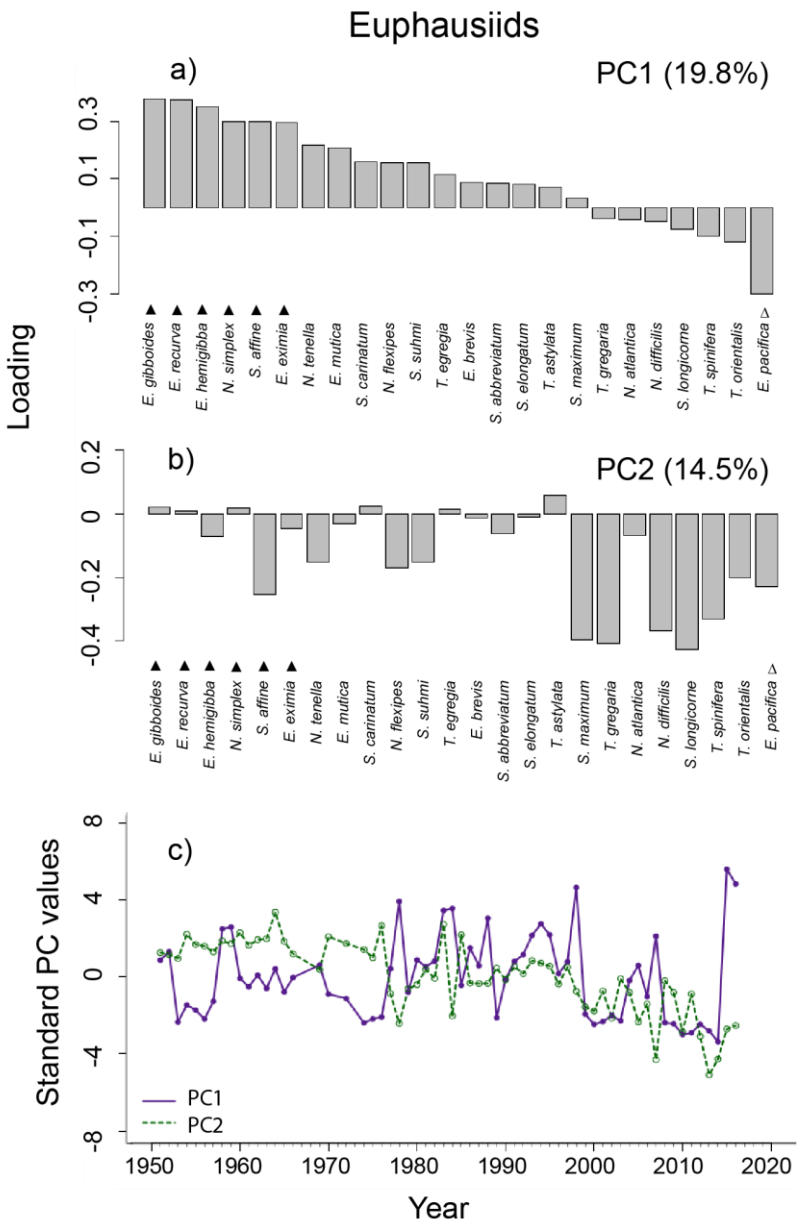

Figure 1.8. Principal component analysis of the euphausiid species-level community. Shown are loadings by species on a) PC1 and b) PC2, with corresponding % variance. c) Timeseries of PC1 (purple) and PC2 (orange). Triangles in a) and b) denote the cool-water (open) and warm-water (filled) species. PC1 is correlated with SDSLA ($r = 0.58$, $p<0.01$), but PC2 is not ($r = -0.01$, $p=0.92$). Species names are as follows: *Euphausia gibboides, Euphausia recurva, Euphausia hemigibba, Nyctiphanes simplex, Stylocheiron affine, Euphausia eximia, Nematoscelis tenella, Euphausia mutica, Stylocheiron carinatum, Nematobrachion flexipes, Stylocheiron suhmi, Thysanopoda egregia, Euphausia brevis, Stylocheiron abbreviatum, Stylocheiron elongatum, Thysanopoda astylata, Stylocheiron maximum, Thysanoessa gregaria, Nematoscelis atlantica, Nematoscelis difficilis, Stylocheiron longicorne, Thysanoessa spinifera Thysanopoda orientalis, Euphausia pacifica.*

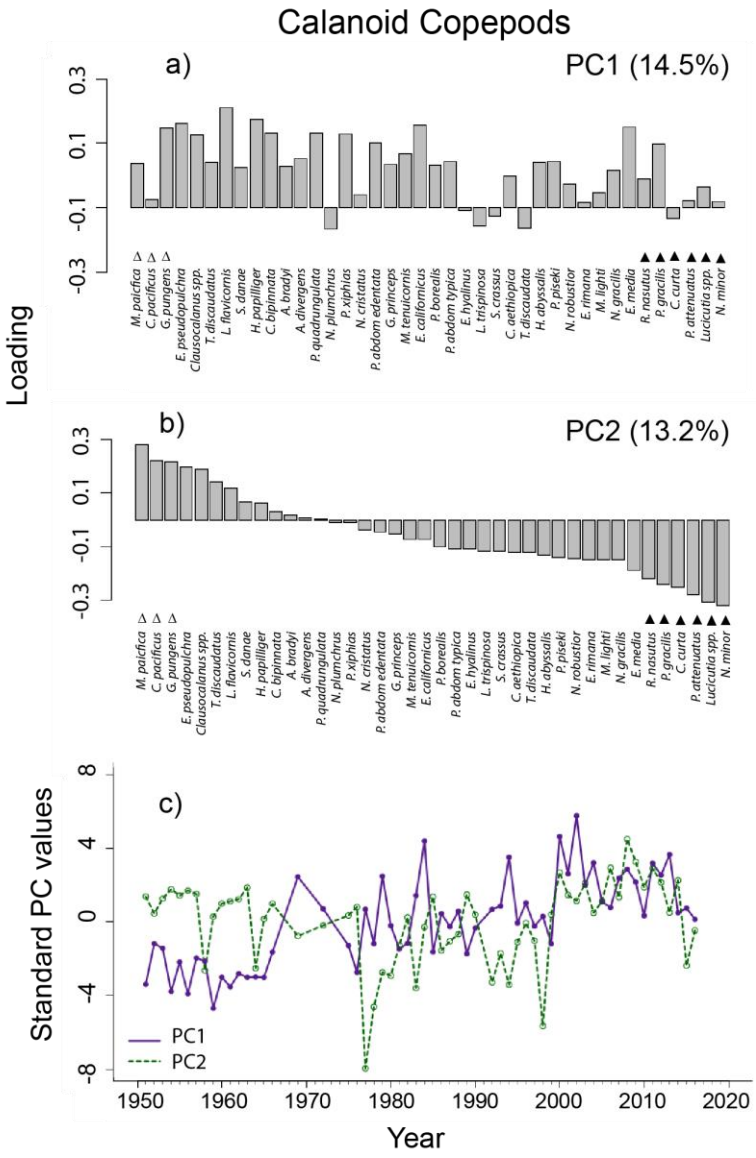

Figure 1.9. As in Fig. 1.8, but for calanoid copepod species. Triangles in a) and b) indicate cool-water (open) and warm-water (filled) species. Both PC loading plots are ordered by PC2 loadings. PC1 is not correlated with SDSLA (r = -0.13, p=0.33), but PC2 is (r= -0.53, p<0.01). Species names are as follows: *Metridia pacifica, Calanus pacificus, Gaidius pungens, Euchirella pseudopulchra, Clausocalanus spp., Tortanus discaudatus, Lucicutia flavicornis, Scolecithrix danae, Heterorhabdus papilliger, Candacia bipinnata, Aetideus bradyi, Aetideus divergens, Pleuromamma quadrungulata, Neocalanus plumchrus, Pleuromamma xiphias, Neocalanus cristatus, Pleuromamma abdominalis edentata, Gaussia princeps, Mesocalanus tenuicornis, Eucalanus californicus, Pleuromamma borealis, Pleuromamma abdominalis typica, Eucalanus hyalinus, Labidocera trispinosa, Subeucalanus crassus, Candacia aethiopica, Temora discaudata, Heterorhabdus abyssalis, Pleuromamma piseki, Neocalanus robustior, Euchaeta rimana, Mesocalanus lighti, Neocalanus gracilis, Euchaeta media, Rhincalanus nasutus, Pleuromamma gracilis, Candacia curta, Pareucalanus attenuatus, Lucicutia spp., Nannocalanus minor.*

PC1 did not correlate with SDSLA, but did show a long-term upward trend (Fig. 1.9c; $r = 0.73$, $p < 0.01$). PC2 correlated significantly negatively with SDSLA, so we used that to identify El Niño-responsive species (Fig. 1.9b). We used a loading threshold of |0.20| for calanoid PC2: three calanoid species showed a 'warm-water' and six species a 'cool-water' response (see Fig. 1.9 legend).

The first two principal components of the hyperiid amphipod species assemblage recovered 19.7% and 14.3% of variance, respectively (Fig. 1.10a,b). In contrast to the total mesozooplankton and euphausiid assemblages, hyperiid amphipod PC1 correlated negatively with SDSLA (Fig. 1.10c, $r = -0.28$, $p = 0.03$). All species except *Paraphronima crassipes* loaded positively on PC1. We used a threshold of > 0.30 for El Niño responses; six species loaded above that mark (Fig. 1.10a). The euphausiid PC1 and calanoid PC2 timeseries correlated with each other (Fig. 1.11, $r = 0.74$, $p < 0.01$) and showed corresponding dips during nearly all CCS El Niño events. Two different years were the 1977-78 CCS warm period (not classified as an El Niño in our analyses but identified in previous studies as a PDO sign change) and the 2015 Warm Anomaly. In 1977-78, calanoid PC2 decreased twice as much as euphausiid PC1, whereas in 2015 euphausiid PC1 decreased more than twice as much as calanoid PC2. These differences suggest that, while the two assemblages experience overall similarity in El Niño responses, they have differing additional sensitivities that cause year-specific variability.

Based the PC loading thresholds described above, we further analyzed the El Niño-responsive species for inter-event variability in biomass. The six warm-water El Niño-responsive euphausiid species correlated positively with SDSLA, while the dominant cool species correlated negatively ($p < 0.05$). The nine calanoid copepod species showed similar directional correlations, although only two cool species (negative) and four warm species (positive) correlated

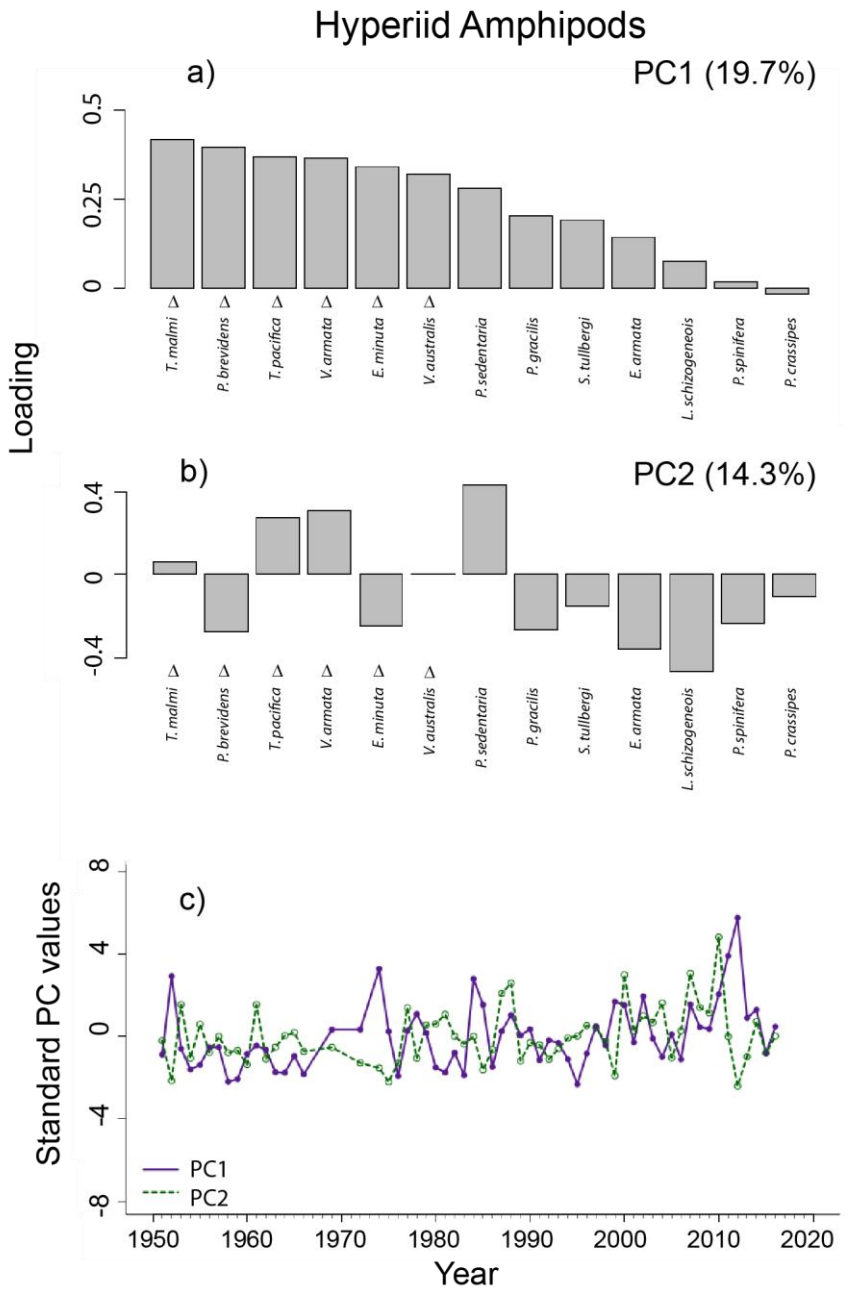

Figure 1.10. As in Fig. 1.8, but for hyperiid amphipod species. Triangles in a) and b) indicate cool-water (open) species (no warm species identified). PC1 is correlated with SDSLA (r = -0.28, p=0.03), but PC2 is not (r = 0.02, p=0.89). Species names are as follows: *Tryphana malmi, Primno brevidens, Themisto pacifica, Vibilia armata, Eupronoe minuta, Vibilia australis, Phronima sedentaria, Paraphronima gracilis, Scina tullbergi, Eupronoe armata, Lestrigonus schizogeneios, Phronimopsis spinifera, Paraphronima crassipes.*

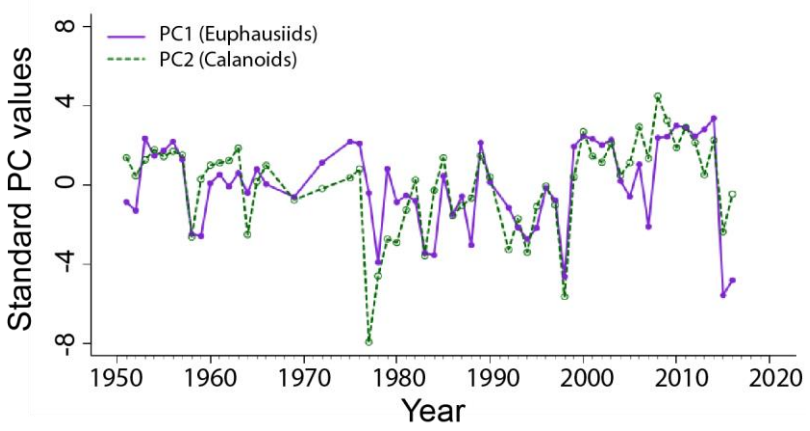

Figure 1.11. Timeseries of euphausiid PC1 (purple) and calanoid copepod PC2 (orange). The two timeseries are highly correlated ($r = 0.74$, $p<0.01$). Note that the euphausiid PC1 timeseries is flipped to align with calanoid copepod PC2.

significantly with SDSLA ($p < 0.05$). The six hyperiid amphipod species all classified as cool, and only two correlated significantly with SDSLA ($p < 0.01$). Species-level AR-1 model correlations generally matched correlation patterns of measured biomass with physical indices, although with fewer significant results for euphausiid and calanoid species. Only three calanoid and two hyperiid amphipod species showed significant long-term trends ($p < 0.01$), all upward except *Candacia curta.*

1.3.3.2. Consistency of biomass changes across El Niño events

Biomass fluctuations of individual species during El Niño revealed more consistent directional trends than for higher taxa. Two warm euphausiid species (*Euphausia eximia, E. gibboides*) increased and the cool euphausiid species (*E. pacifica)* decreased (Fig. 1.12a); one warm calanoid species (*Pleuromamma gracilis*) increased and two cool species (*Metridia pacifica, Gaidius pungens*) decreased (Fig. 1.12b); and two cool hyperiid amphipod species (*Primno brevidens, Themisto pacifica*) decreased (Fig. 1.12c) during almost all El Niños (Wilcoxon signed rank, $p \leq 0.05$ for all species mentioned). The six warm euphausiid species differed in their responses in 2015 and 2016: three species reached higher biomass levels in 2015

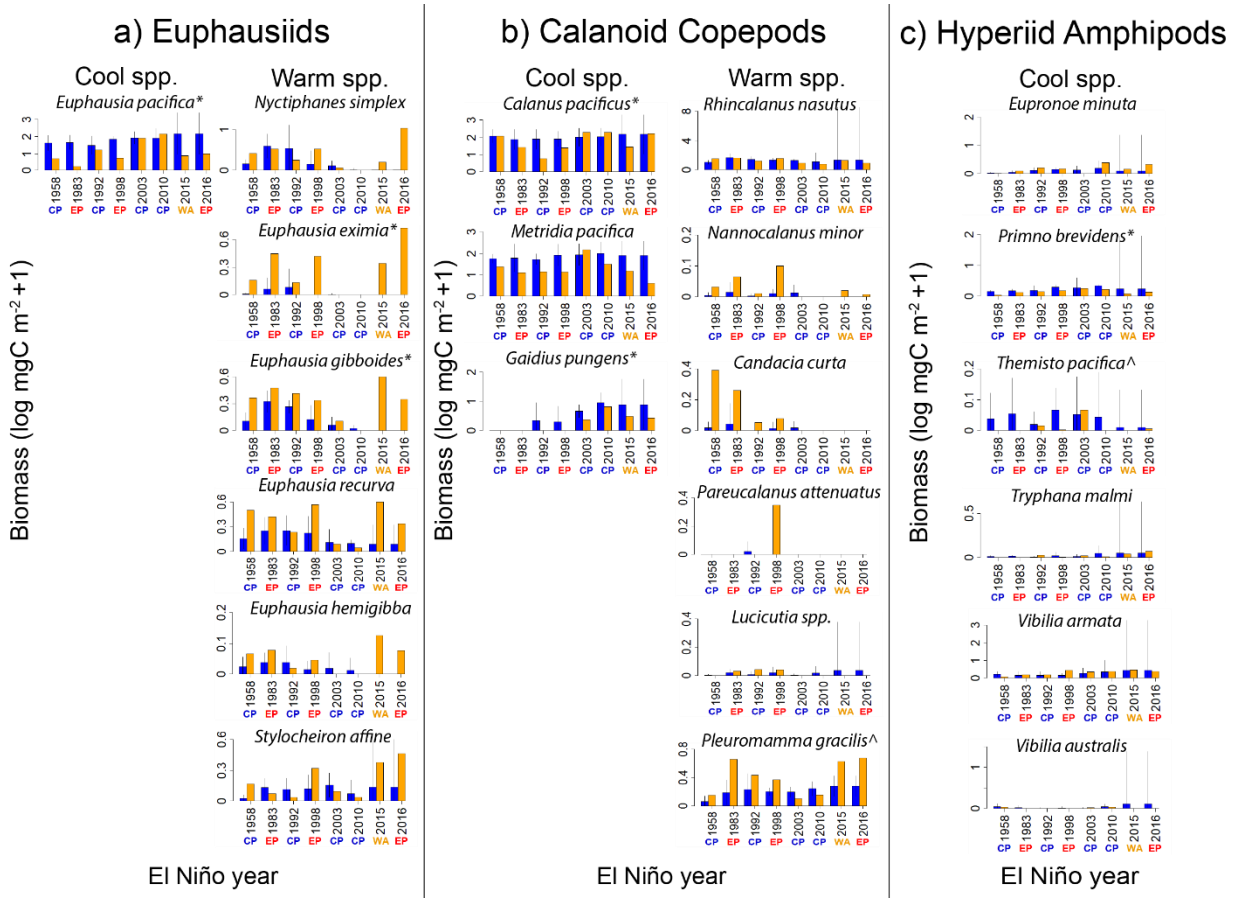

Figure 1.12. As in Fig. 1.4, but for El Niño-responsive cool-water (*left*) and warm-water (*right)* species for a) euphausiids, b) calanoid copepods, and c) hyperiid amphipods. ^ = p=0.05, * = p<0.05 (Wilcoxon matched pairs signed-rank test).

and then decreased in 2016, while the other three had higher biomass in 2016. In contrast, only two warm calanoid species increased in 2015 and 2016 compared to surrounding years, while three species were completely absent. Only one hyperiid amphipod species (*Eupronoe minuta*) increased substantially, while another (*Vibilia australis*) was completely absent in both 2015 and 2016. One hyperiid amphipod species also had a significant negative correlation ($p < 0.05$) between the magnitude of change in biomass during El Niño and the corresponding magnitude of change in SDSLA. These results corroborate our findings that El Niño responses are more strongly expressed at the species, rather than higher taxon, level.

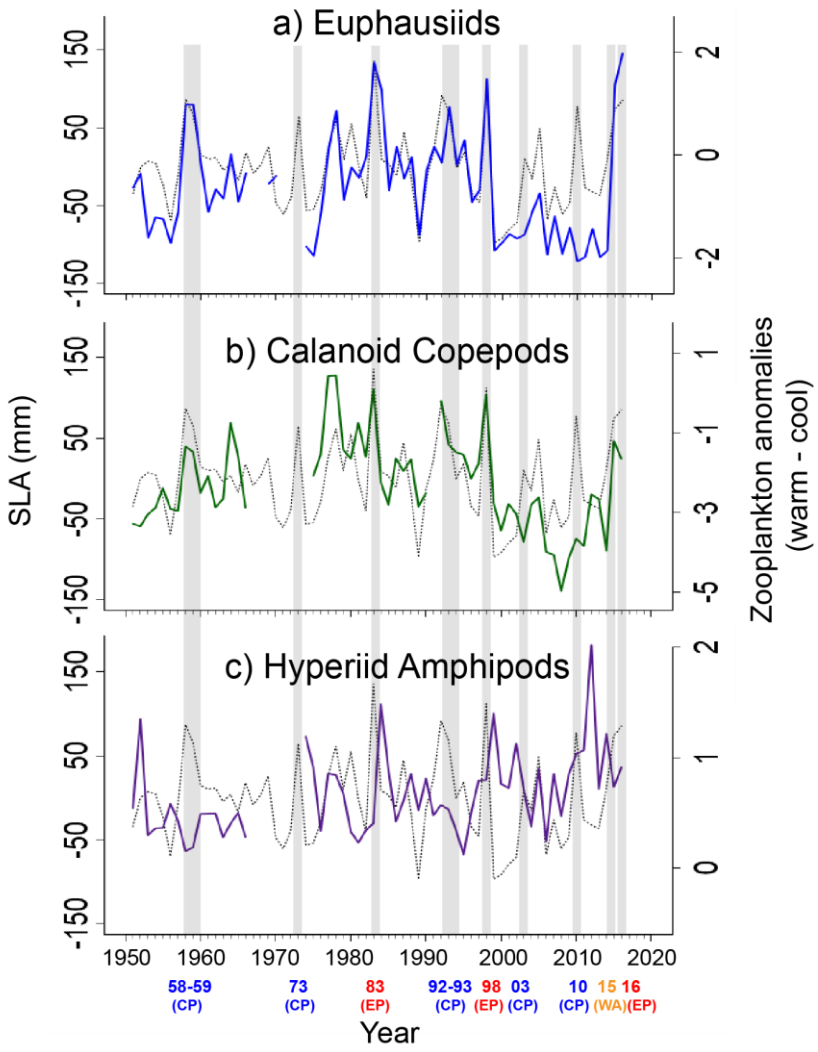

Figure 1.13. Indices of the difference between dominant warm species biomass minus cool species biomass. a) euphausiids, b) calanoid copepods, c) hyperiid amphipods. Black line is SDSLA timeseries. The hyperiid amphipod index is shown in reverse (cool-warm species).

1.3.3.3. Warm-water species indices

As a metric of the extent to which warm species dominate over cool species during El Niño, we calculated composite warm-water species indices for euphausiids, calanoid copepods, and hyperiid amphipods by subtracting the sum of dominant warm minus cool species. The euphausiid ($r = 0.63$) and calanoid ($r = 0.50$) indices correlated with SDSLA (Fig. 1.13a-b, $p < 0.01$). Both indices showed peaks in 1983 and 1998, corresponding to highest peaks in SDSLA,

but the overall highest peaks for the warm-water indices were 2015-16 (euphausiids) and 1977-78 (calanoids). The indices showed fourth highest peaks in 1958-59 (euphausiids) and 1992 (calanoids). These indices corroborate the euphausiid PC1 and calanoid PC2 timeseries comparison, which showed similar overall correlation of the two taxa but differences between individual events. The hyperiid amphipod index, which was comprised only of cool species (hence the reversed index sign in Fig. 1.13c), did not correlate with SDSLA, which corroborates our findings that hyperiid amphipods did not vary principally on El Niño timescales.

1.3.4. EP versus CP El Niños

We compared Eastern Pacific (EP) versus Central Pacific (CP) El Niño responses as i) taxonomic similarity (PSI) and ii) carbon biomass. The taxonomic comparisons (for 15 higher taxa and the euphausiid, calanoid copepod, and hyperiid amphipod species) all showed larger changes in percent similarity index during EP relative to CP events, but no comparison was significant at $p < 0.05$ (Fig. 1.14a-d; red dots are individual EP events and blue dots are individual CP events for all plots). The calanoid and euphausiid declines in PSI were greater for EP El Niños than for nearly every CP El Niño (Wilcoxon rank sum test; calanoids: $W = 0$, $p = 0.06$; euphausiids: $W = 0.01$, $p = 0.011$). Considering the small number of El Niños in each category (3 EP, 6 CP), our statistical power is low. In contrast, mean percentage changes in biomass were nearly identical between EP and CP events for three of four groups, and the fourth (hyperiid amphipods) had large ranges in values for both EP and CP events (Fig. 1.14e-h). Separating warm and cool species within the euphausiids, calanoid copepods, and hyperiid amphipods (Fig. 1.14i-m), the dominant cool euphausiid species had a greater depression of

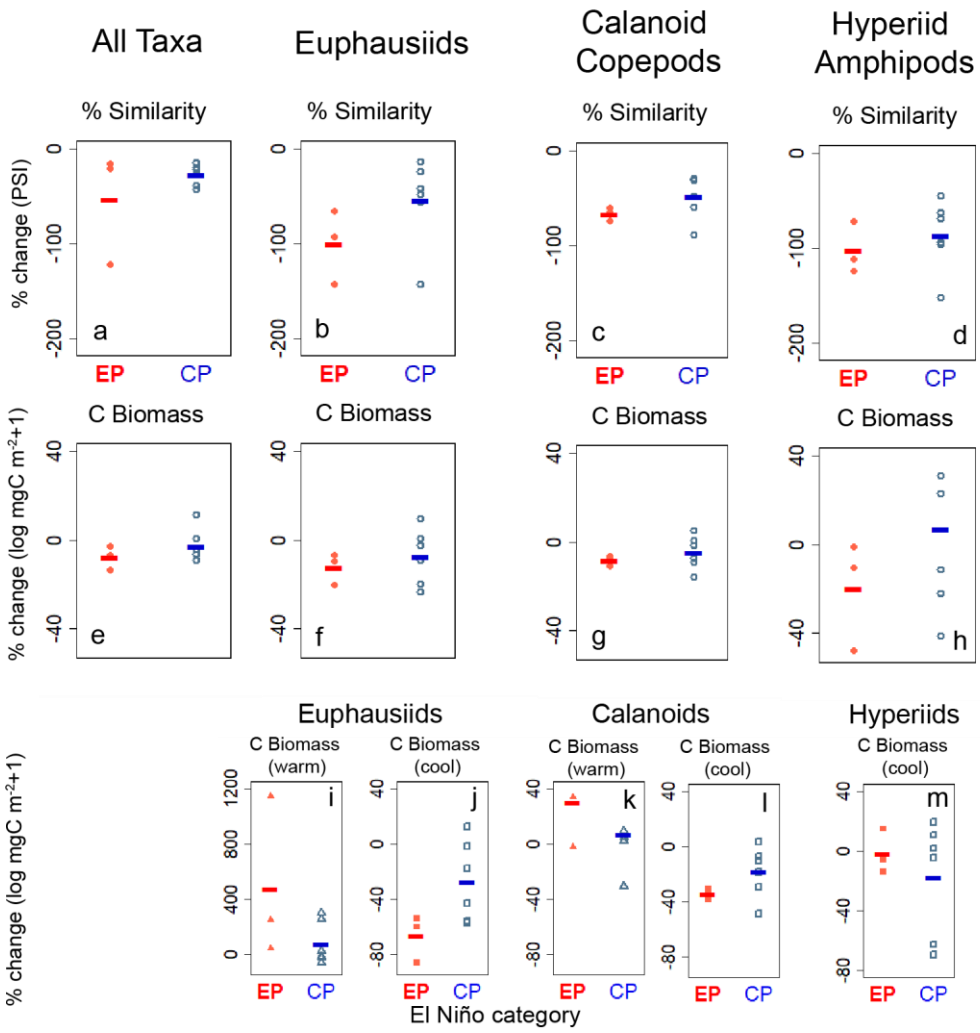

Figure 1.14. El Niño-related changed in (upper row) Percent Similarity Index and (middle-lower rows) biomass for (a,e) all taxa, (b,f,I,j) euphausiids, (c,g,k,l) calanoid copepods, and (d,h,m) hyperiid amphipods. El Niño years are categorized as EP or CP. Dots indicate values for each individual El Niño year; bars indicate means for EP (red) or CP (blue) categories. C biomass was further subdivided into total biomass (e-h; EP – red, CP – blue), and warm-water (i,k; EP – red triangles, CP – blue triangles) and cool-water species (j,l,m; EP – red squares, CP – blue squares). Biomass of warm-water euphausiids is shown on different a y-scale.

biomass in EP than CP events, though the difference was not significant (Fig. 1.14j; W = 2, p = 0.10). The warm euphausiid species showed the greatest percentage increase during El Niño events, but also had large ranges across individual events, and therefore no significant difference in magnitude of increase between EP and CP events (Fig. 1.14i).

1.3.5. La Niña events

1.3.5.1. Biomass fluctuations

Only the total hyperiid amphipod community (increase), three warm euphausiid species (decrease), and two warm calanoid species (decrease) showed significant directional changes in biomass during La Niña compared to surrounding years (Figs. S1.2-S1.3). The euphausiid *Euphausia eximia* was completely absent during all La Niña years, and *E. gibboides* was nearly zero during the 1989-2008 events. Testing for proportional changes in biomass relative to change in SDSLA yielded a significant relationship for only one hyperiid amphipod species, although euphausiids, chaetognaths, and pyrosomes suggested weak relationships in the direction of greater biomass increase during stronger La Niña events ($p < 0.10$).

1.3.5.2. Community composition

Comparisons of community similarity across La Niña years (using PSI, described above) showed significantly different mean inter-La Niña similarity (purple symbols) compared to La Niña/non-La Niña similarity in five years (blue symbols; Fig. S1.4) for both the euphausiids and calanoid copepods, though the significant years differed. The total mesozooplankton community had significant differences between medians in 1951 and 1999. Unlike El Niño years, the magnitude of change in community similarity across La Niña did not correlate with change in SDSLA for any assemblage (Fig. S1.5), although in all cases there was a tendency toward a negative relationship. In terms of resilience to La Niña, similarity generally returned to pre-Niña levels within 1-2 years after each event, although surrounding years sometimes showed higher variability in percent similarity to La Niña events compared to El Niño surrounding years (Fig. S1.6).

1.4. Discussion

1.4.1. Taxonomic levels of resolution that respond to El Niño

Our findings suggest that El Niño signals in the southern California Current System (CCS) express most strongly at the levels of species and individual taxonomic groups, while total mesozooplankton biomass and composition of higher taxa are not consistently affected. Differential responses of taxonomic levels suggest that species in the southern CCS can undergo rearrangements in dominance without substantially impacting total mesozooplankton biomass. Species rearrangements during El Niño can have important implications for foraging success and survival of higher trophic levels, as well as for carbon export. Many species of seabirds, fishes, and marine mammals are known to selectively target specific zooplankton taxa for foraging (Lee et al., 2007; Nickels et al., submitted). Zooplankton also vary in nutritional value: cool-water calanoid copepods tend to have higher lipid reserves than subtropical species (Hooff & Peterson, 2006; Lee et al., 1971), which can affect the net energy gain by higher trophic levels. The 1992-93 and 1997-98 El Niños caused significant reductions in survival and breeding success of Cassin's auklets (Lee et al., 2007) and altered distributions of marine mammal off California (Keiper et al., 2005). Both changes were attributed in part to reduced prey zooplankton availability, particularly certain species of euphausiids, which our results corroborate.

Zooplankton taxonomic composition can also significantly alter carbon export. Lavaniegos and Ohman (2007) noted that communities dominated by gelatinous tunicates such as salps tend to be less palatable and nutritious to higher trophic levels, although salps promote rapid carbon export (Lavaniegos & Ohman, 2007; Michaels & Silver, 1988; Smith et al., 2014). The 1983 El Niño was notable for exceptionally high proportions of salps relative to all other

years in our timeseries. Such changes in zooplankton community composition, and the subsequent effects on higher ecosystem levels, make it essential for us to understand the underlying mechanisms causing zooplankton changes, and their variability between individual events.

1.4.2. Consistency of responses across individual El Niño events

Only the euphausiid species-level community composition showed a consistent change during most El Niños compared to non-El Niño years. This change appears to be due in part to increased proportions of subtropical species during almost every event. Brinton (1981) and Brinton (1960) found that non-resident southerly and offshore euphausiid species intruded into the southern and central CCS during the 1958-59 El Niño and 1977-78 CCS warm period, in some locations even displacing resident cool-water species. These past studies and our findings suggest that most El Niño events are associated with some level of subtropical euphausiid intrusion into the SC region, although we note exceptions to this pattern below. The lack of a consistent El Niño-related change in the calanoid copepod community, and greatest species-level reordering during different years than for euphausiids, suggests that specific biological characteristics and life-histories cause calanoids to respond differently than euphausiids to a given perturbation. Brinton (1960) noted that euphausiids are long-lived (on the order of one year) compared to other zooplankton and are thus ‘conservative’ in terms of reflecting inter-seasonal and interannual, rather than shorter-term, changes in ocean conditions. Such time-lagged responses underly the double-integration mechanism previously proposed by Di Lorenzo and Ohman (2013). Euphausiid species also strongly associate with specific physical ocean environments on a biogeographic scale (Brinton, 1960, 1981). In contrast, calanoid copepods

have shorter life-spans, and several dominant CCS species undergo wintertime dormancy (Ohman et al., 1998). Our findings here of greatest euphausiid responses to 1958-59 and 2016 versus greater calanoid copepod responses to 1977-78 further suggest differential responses of the two taxa to the same forcing mechanisms. In contrast to both euphausiids and calanoid copepods, hyperiid amphipod community variability is likely determined more by variability in their gelatinous hosts than in direct response to El Niño, which likely explains why they show stronger year-to-year variability than consistent El Niño-related patterns (Lavaniegos, 2014; Lavaniegos & Hereu, 2009; Lavaniegos & Ohman, 1999).

The weak El Niños of 2003 and 2010 present unusual cases of anomalously elevated biomass and high compositional similarity to non-El Niño years. Both events occurred during the relatively cool 2000s, which experienced a sequence of back-to-back weak El Niño and La Niña events (Pares-Escobar et al., 2018). The 2003 event has been associated with southward-flowing subarctic water intrusions into the CCS, in contrast to increased poleward flow usually observed during El Niño (Lavaniegos, 2009; Murphree et al., 2003; Pares-Escobar et al., 2018). Subarctic-origin flows may have increased nutrient inputs to the southern CCS, enhancing growth of the existing community. Southward flows may have also delivered more subarctic-origin organisms to the southern CCS and reduced introduction of warm species from the south and offshore. Fisher et al. (2015) noted that chlorophyll concentrations were moderately higher than average off Oregon during the 2002-03 El Niño, supporting suggestions of increased high-nutrient flows and favorable conditions for resident species. Those authors also measured elevated biomass of southerly copepod species (e.g., *Calanus pacificus*, the dominant calanoid copepod in the southern CCS) off Oregon during the event. Our finding of increased biomass of *C. pacificus* in the southern CCS suggests that this species may have expanded its range in response to favorable

habitat throughout the CCS, perhaps aided by submesoscale water movements in opposition to the larger southward flow. The 2010 El Niño, in contrast, showed evidence for atmospherically-forced El Niño perturbations in the CCS, but no anomalous oceanic poleward advection (Todd et al., 2011). The complete absence of subtropical euphausiids in the southern CCS during 2010 corroborates this lack of influx by subtropical- and offshore-origin flows.

The anomalous responses of zooplankton during the relatively weak 2003 and 2010 events suggest that our classification of CCS El Niños may benefit from further refinement incorporating additional physical metrics and zooplankton responses to various events. Although the 2003 and 2010 events both classified as CCS El Niños based on our physical index thresholds, their anomalous zooplankton responses suggest that these events likely had different forcing mechanisms or factors compared to other El Niños. We also note past findings of the importance of multi-decadal variations in the background ocean state of the CCS (e.g., PDO, North Pacific Gyre Oscillation (NPGO)) in perturbing mesozooplankton communities (Brinton & Townsend, 2003; Di Lorenzo & Ohman, 2013; Keister et al., 2011; Lavaniegos & Ohman, 2003, 2007), and acknowledge that background state may have confounding effects on zooplankton responses. However, we had too few El Niño events within any given multi-decadal state to systematically analyze the possible interactions of those sources of variation.

1.4.3. EP vs. CP El Niño events

Both the euphausiid and calanoid copepod communities show differentiation of El Niño responses into EP versus CP categories, highlighting the apparent sensitivity of these taxa to event magnitude or event-specific forcing mechanisms. EP events, which tend to be oceanically-forced and stronger than CP events, appear to induce corresponding greater community changes

in both taxa. Two of three EP El Niños (1998, 2016) show evidence for coastally-trapped wave (CTW) propagation and increased poleward flow in the CCS (Frischknecht et al., 2017; Jacox et al., 2016; Lynn & Bograd, 2002). Assuming a direct link between increased subtropical-origin waters and subtropical euphausiid species, we would expect such proportional changes in euphausiid community composition. The 1983 EP El Niño presents a different case: Simpson (1984) suggested that it showed evidence for onshore flow of gyre waters rather than CTWs. We found that the percent change in the euphausiid community during 1983 was substantially higher than during the other two EP years, perhaps due to higher proportions of offshore species in 1983. *Euphausia eximia* and *E. hemigibba* were the two subtropical euphausiid species with the largest increases during 1983; these species tend to associate with Baja California and Central Pacific Gyre waters, so their presence corroborates onshore flow.

The southern CCS has been previously shown to experience rearrangement of dominant calanoid copepod species during El Niño (Rebstock, 2001). Our results, notably the significantly different percent change in community composition for EP versus CP years, and the significant correlation of magnitude of community change with SDSLA, further suggest that calanoid responses to El Niño vary depending on event strength. These findings align with findings from the northern CCS during the 1997-98 El Niño, which displaced boreal copepods with the more southerly *Calanus pacificus* (Peterson et al., 2002) and even caused influxes of subtropical and offshore euphausiid species off Oregon (Keister et al., 2005), possibly due to horizontal advection of surface waters (Keister et al., 2011). Similarly, Fisher et al. (2015) found that the magnitude of northern CCS copepod community change was strongly correlated with both the magnitude and duration of El Niño events, and that community composition was generally

different during EP versus CP events. Our results suggest that such proportional shifts may occur across multiple parts of the CCS.

Equatorial EP versus CP classifications do not always align with southern CCS zooplankton responses to El Niño, however. The 1958-59 El Niño was classified here as a CP event but produced changes in euphausiid biomass and community composition comparable to EP events, while the 1992-93 El Niño was just below our EP threshold but showed only moderate changes in taxon compositions. The 1958-59 event occurred during a cool PDO phase, in contrast to 1983 and 1998 (warm phase) but may have still experienced EP-like forcing mechanisms, resulting in higher-magnitude assemblage change from surrounding years. Brinton (1981) noted that subtropical euphausiid intrusions did not occur in the southern CCS at any point from 1949-1979 except during 1957-59, supporting our findings of substantial community change. Euphausiid community recovery after 1958-59 was also slower than after other events, suggesting lingering effects of the prolonged warm period. In contrast, the 1992-93 El Niño showed evidence for CTW forcing into the CCS (Chavez, 1996), so it is surprising that 1992 did not resemble EP zooplankton responses. Spring 1993 had prolonged warm anomalies in the CCS after the 1991-92 equatorial signal but showed greater differences in subtropical species biomass and composition from non-El Niño years than did 1992. These unusual changes might have been due to later arrival of perturbations into the CCS, or perhaps a year-lag response by zooplankton to the initial perturbation. Regardless, multi-year El Niño events present complications to EP versus CP classification and warrant further investigation to elucidate event-specific mechanisms. Some evidence suggests that CP El Niño events have doubled in intensity over the past three decades (McPhaden et al., 2011) and may be increasing in frequency (Yeh et al., 2011), although the evidence is not definitive (Newman et al., 2011). Understanding

mesozooplankton responses to CP events, as well as differences between individual CP years, may be especially important for predicting future community changes.

1.4.4. The 2014-15 Warm Anomaly and 2015-16 El Niño

The 2014-15 Warm Anomaly was caused by atmospheric changes in the Eastern North Pacific, with no associated equatorial signal, but it induced El Niño-like conditions in the southern CCS. These included near-surface temperatures of +5^{o}C, thermocline depression >20 m, and near-zero nitrate and chlorophyll levels for the entire period (Frischknecht et al., 2017; Lilly, 2016; Zaba & Rudnick, 2016). The Warm Anomaly differed from most El Niños, however, in its lack of enhanced poleward advection and dominance by near-surface temperature anomalies (Zaba & Rudnick, 2016). In contrast, the 2015-16 El Niño resembled 1997-98 in its early equatorial and CCS development and evidence for oceanic CTWs, although they were weaker than in previous El Niños (Frischknecht et al., 2017).

Our zooplankton findings roughly corroborate these differences. Euphausiid assemblage responses aligned with past EP and CP distinctions, in terms of a moderate 2015 response most similar to 1992 and a stronger change in 2016 but still less than past EP events. The presence of subtropical euphausiids in 2015 is somewhat surprising given the apparent lack of increased poleward flow during the Warm Anomaly. However, Zaba and Rudnick (2016) noted that, although alongshore velocities were not anomalous, nearshore salinity was anomalously fresh and corresponded to reduced coastal upwelling, indicating onshore flow of fresh offshore core California Current waters. Offshore subtropical euphausiids had higher-magnitude changes than coastal subtropical species and were perhaps transported onshore in conjunction with these flows or with small-scale changes in circulation. Alternately or in conjunction, the extreme temperature

anomalies during 2014-15 may have produced a more favorable inshore environment for offshore species or caused northward contraction of cool species out of the southern CCS. Peterson et al. (2017) found that the arrival of the Warm Anomaly brought previously unrecorded copepods to the very nearshore environment of the northern CCS, although these species are well known to occur farther offshore. This finding suggests onshore transport of a water mass with different origins than those typically brought by El Niño events.

The moderate changes in the 2016 zooplankton composition compared to past EP El Niños may have been due to upwelling winds in fall 2015 countering the effects of CTW arrival to the CCS (Frischknecht et al., 2017). Corresponding nitrate and chlorophyll anomalies during fall 2015 were slightly negative to neutral, but higher than in 1983 and 1998, suggesting more favorable ocean conditions for resident cool-water species. The significant change in the calanoid community in 2015 but neutral response in 2016 may also suggest responses to local temperature anomalies rather than to changes in ocean circulation.

1.4.5. Mesozooplankton resilience to El Niño

Mesozooplankton biomass and community composition in the southern CCS appear generally resilient to El Niño. We found that the total mesozooplankton community and the three species-enumerated assemblages (euphausiids, calanoid copepods, hyperiid amphipods) return to pre-El Niño composition within one year after almost every event. Even if subtropical species appear in the southern CCS in high proportions during El Niño, they do not appear to proliferate and maintain their presence following the perturbation. This pattern of rapid increase and subsequent decrease suggests either direct El Niño-related advective influxes or short-term favorable habitat changes without a sustained ability to reproduce and establish substantial

populations post-El Niño. One exception is the subtropical euphausiid *Nyctiphanes simplex*, which remained elevated for 10 years during the 1980s-90s. This may have been due to confounding PDO influences (Brinton & Townsend, 2003; Di Lorenzo & Ohman, 2013). Although the dominant cool-water euphausiid (*Euphausia pacifica*) and calanoid copepod (*Calanus pacificus, Metridia pacifica*) species generally decrease during El Niño, their rapid recovery within 1-2 years suggests either they have developed the ability to rapidly repopulate after short-term perturbations or they receive renewed population seeding with the return of pre-El Niño flow patterns. *Metridia pacifica* does not undergo deep water column wintertime dormancy like other dominant CCS calanoids (Ohman et al., 1998), and may be more susceptible to the winter-focused physical effects and changes in horizontal advection associated with El Niño.

It is also notable that the species with strongest El Niño responses are not necessarily the dominant biomass contributors within their taxa. Several numerically dominant cool-water euphausiid species (*Nematoscelis difficilis, Thysanoessa gregaria, T. spinifera*) in the southern CCS did not show any correlation with our El Niño indices. Pares-Escobar et al. (2018) found that, off Baja California, *N. difficilis* and *T. gregaria* did not covary with temperature or other physical variables during a multi-El Niño/La Niña period from 1998-2008, suggesting that dominant CCS species may have adapted to withstand the effects of short-term perturbations such as El Niño. Additionally, these species are known to live below the thermocline (at average depths of 400 m) and may be less susceptible to El Niño-related changes in advection strength and circulation of the upper 200 m. Mackas et al. (2007) reasoned that zooplankton species in the northern CCS have evolved to withstand seasonal fluctuations in temperature and stratification,

and that these adaptations can be effective against environmental perturbations of similar magnitude. The southern CCS is a dynamic region influenced by water masses ranging from tropical to subarctic origin (Checkley & Barth, 2009). High variability in physical conditions has likely selected for resident zooplankton species with characteristics that allow them to withstand physical perturbations associated with El Niño without major reductions in fitness.

We observed almost no significant long-term trends in El Niño-correlated species. In contrast, many species that were not El Niño-correlated showed significant upward trends (data not shown). It appears that El Niño responses and long-term trends tend not to co-occur in individual species but can co-occur at the taxon level. This difference suggests functional complementarity and compensatory changes among related species within a taxon (Lindegren et al., 2016).

1.4.6. Conclusions

Our goal in quantifying mesozooplankton variability during El Niño was to identify patterns of change that could suggest possible mechanisms affecting biomass and community composition. El Niño may affect mesozooplankton in several ways: changes in advection can produce species influxes from different regions; oceanic and atmospheric forcing can alter in situ physical and biological conditions, including temperature, thermocline and nutricline depths, and food sources (phytoplankton and microzooplankton); and altered species interactions may occur via predation, parasitism or competition for food (Ohman et al., 2017). Evidence for increased poleward and onshore advection during past El Niño events suggests that this is frequently an important forcing mechanism of species transport. In our study of the southern CCS, presence of offshore and southern euphausiid species suggest some component of advective forcing: their

high-magnitude but transient increases during El Niño events, with no time-lag to indicate local population growth or reproduction, suggests a direct physical forcing mechanism such as advection. The near-absence of subtropical species off Southern California during the 2003 and 2010 El Niños, in conjunction with a lack of enhanced poleward or onshore flow, further supports this interpretation.

The stronger associations of mesozooplankton higher taxa and species with SDSLA than with $Z_{26.0}$ may further highlight dominant forcing mechanisms underlying El Niño-related zooplankton variability. Increases in sea level can be caused by thermal expansion or by relaxation of upwelling and associated onshore flow, indicating water mass intrusion. Thermocline depth can be influenced by local wind-driven changes in upwelling and can convey signals related to reduced nutrient availability for primary production. Our evidence for species-level changes within communities suggests at least partial forcing by altered flow, but changes to in situ temperature and productivity likely interact to produce the responses to each individual event. Our CCS El Niño classifications may benefit from adding another physical metric such as the magnitude of alongshore flow in the core California Current.

The 2014-15 Pacific Warm Anomaly, although forced differently than El Niño, induced zooplankton community shifts similar to some past El Niños, particularly the moderate and prolonged 1992-93 event. The Warm Anomaly did not, however, clearly modify subsequent zooplankton responses to the 2015-16 El Niño, which most closely resembled 1997-98. Although individual El Niño events vary in their zooplankton responses, evidence for some consistency across El Niños, particularly in the euphausiid community, suggests that certain species and higher taxa may serve as useful tracers of physical and biological forcing mechanisms.

Understanding the specific mechanisms that cause responses to each event will be the topic of future study.

Acknowledgements

We thank the CalCOFI program, and particularly the at-sea operations crews, for long-term, consistent, and high-quality data collection, and E. Brinton, A. Townsend, L. Sala, and past managers of the Pelagic Invertebrate Collection for their detailed enumerations of CalCOFI zooplankton samples. None of this work would have been possible without them. We thank R. Goericke and M. Jacox for providing various $Z_{26.0}$ indices, and M. Jacox for thoughtful commentary on methods and analysis. We thank P. Franks for ideas and discussion. This work was supported by an NSF Graduate Research Fellowship to L. Lilly and by NSF OCE-1614359 and OCE-1637632 to the CCE-LTER site.

Chapter 1, in full, is a reprint of the material as it appears in Deep-Sea Research Part I: Oceanographic Research Papers, 2018. Lilly, Laura E.; Ohman, Mark D., 2018. The dissertation author was the primary investigator and author of this paper.

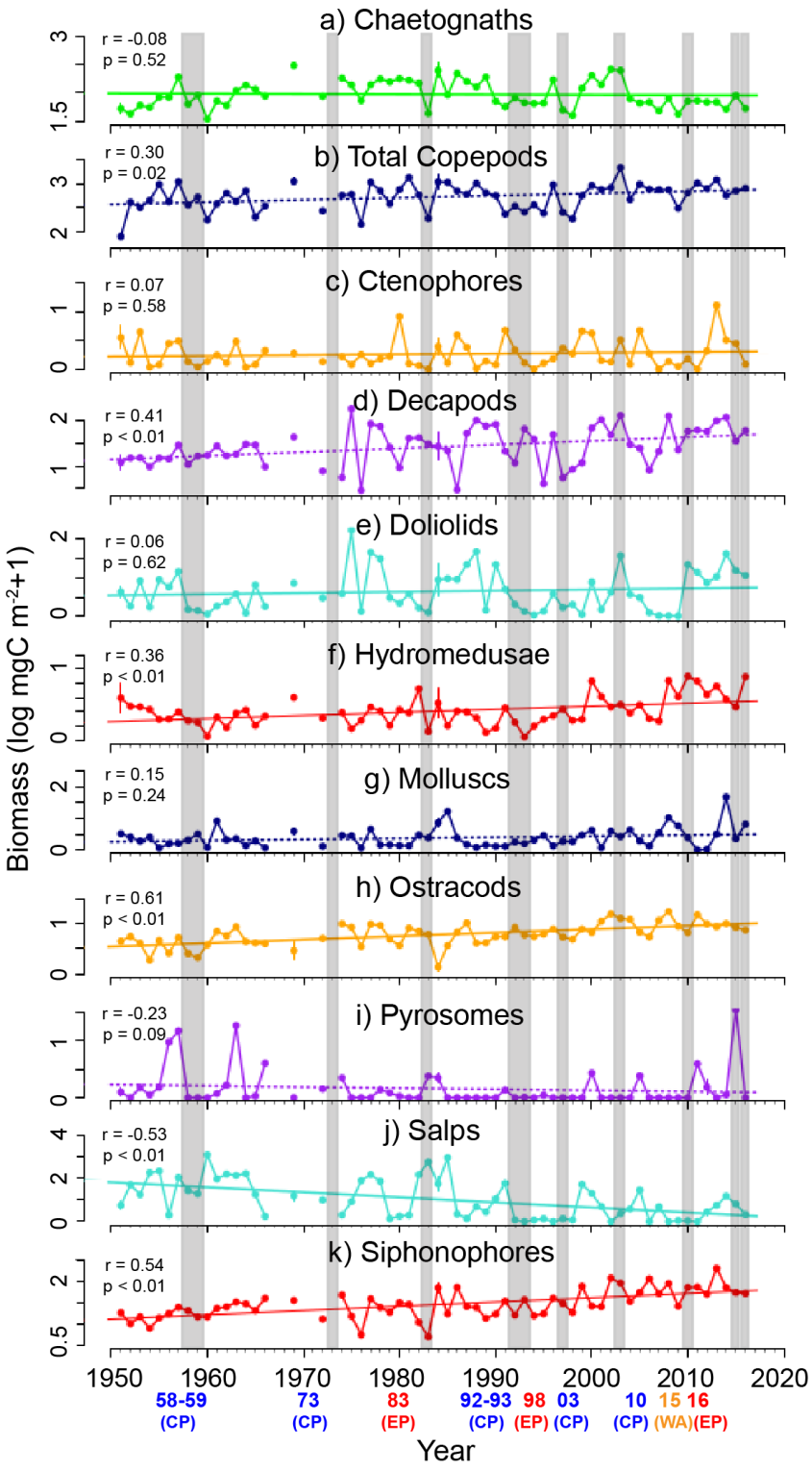

Figure S1.1. Timeseries of log C biomass for enumerated taxa not already shown in figure 1.3. Linear trends and associated correlation coefficients are shown. Vertical grey bars indicate El Niño years (labels as in figure 1.1).

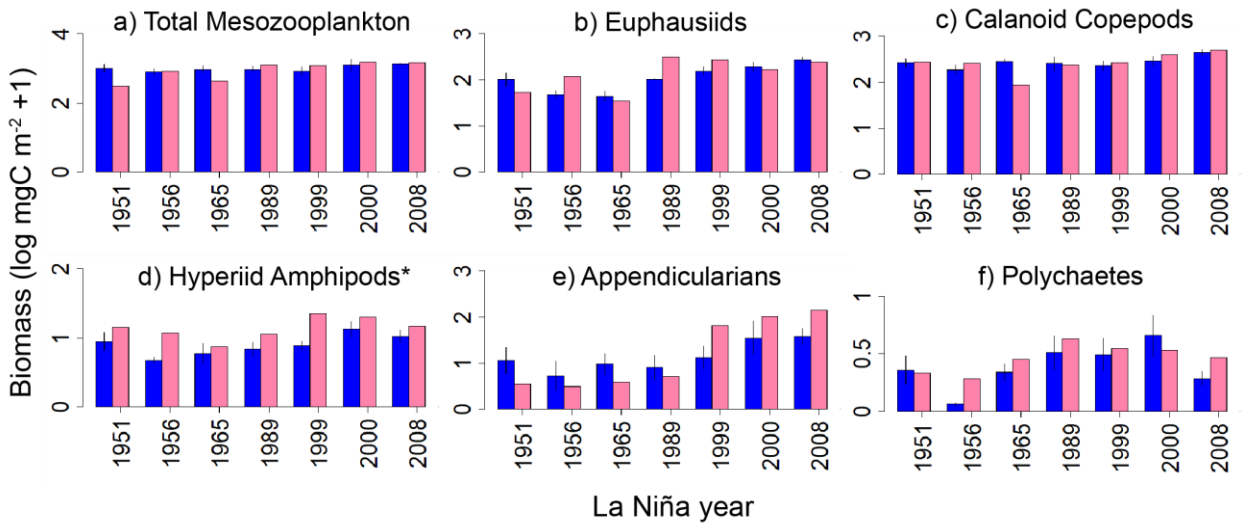

Figure S1.2. As in figure 1.4, but for La Niña years (purple bars) versus average of the 4 surrounding years (blue bars). *significant Wilcoxon signed-rank value.

Figure S1.3. As figure S1.2, but for La Niña-responsive cool-water (*left*) and warm-water (*right*) species for a) euphausiids, b) calanoid copepods, and c) hyperiid amphipods. *significant Wilcoxon signed-rank value.

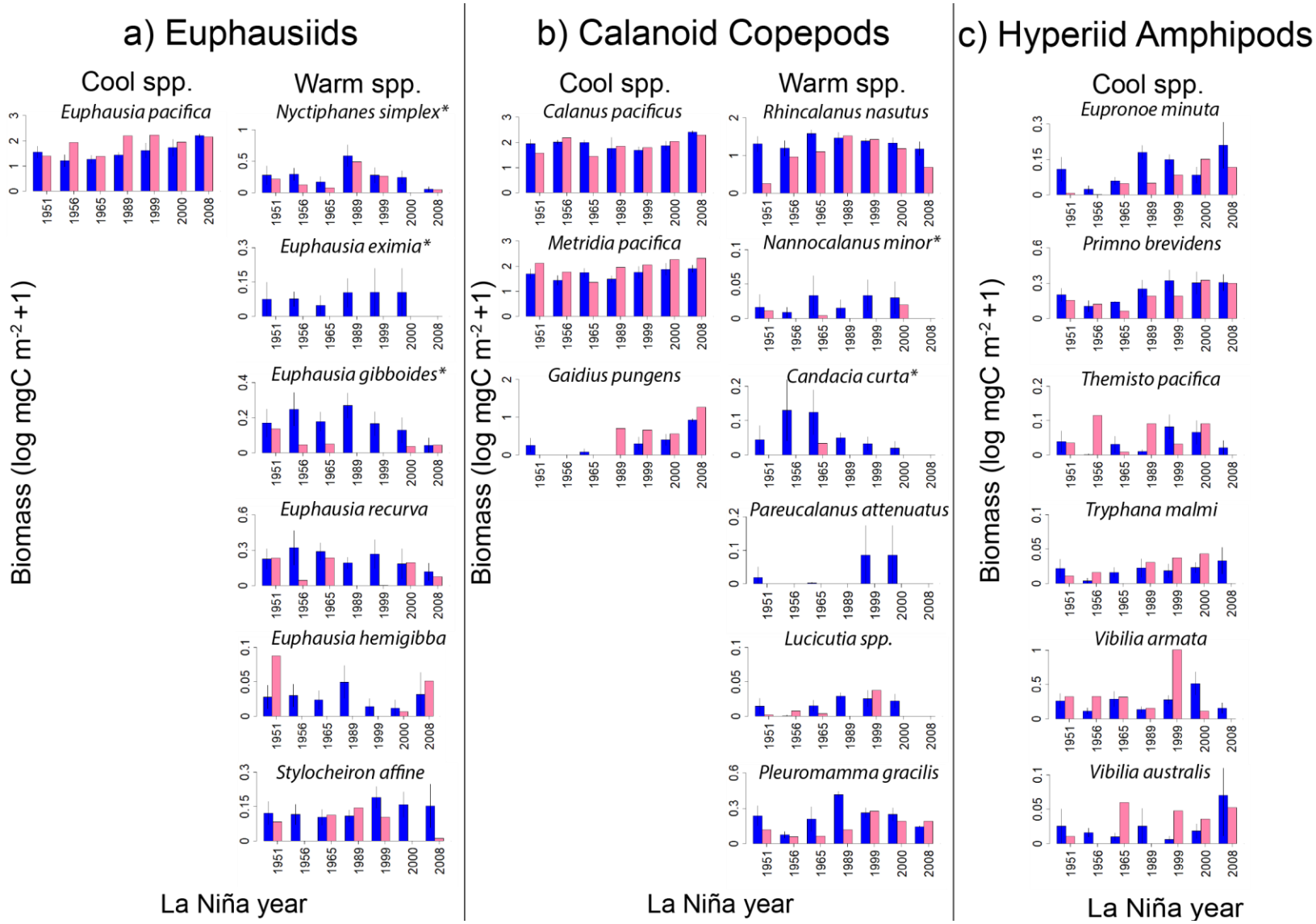
a) Euphausiids
Cool spp.
Warm spp.
Euphausia pacifica
Nyctiphanes simplex*
Euphausia eximia*
Euphausia gibboides*
Euphausia recurva
Euphausia hemigibba
Stylocheiron affine
b) Calanoid Copepods
Cool spp.
Warm spp.
Calanus pacificus
Rhincalanus nasutus
Metridia pacifica
Nannocalanus minor*
Gaidius pungens
Candacia curta*
Pareucalanus attenuatus
Lucicutia spp.
Pleuromamma gracilis
c) Hyperiid Amphipods
Cool spp.
Eupronoe minuta
Primno brevidens
Themisto pacifica
Tryphana malmi
Vibilia armata
Vibilia australis
Biomass (log mgC m-2 +1)
La Niña year
1951
1956
1965
1989
1999
2000
2008

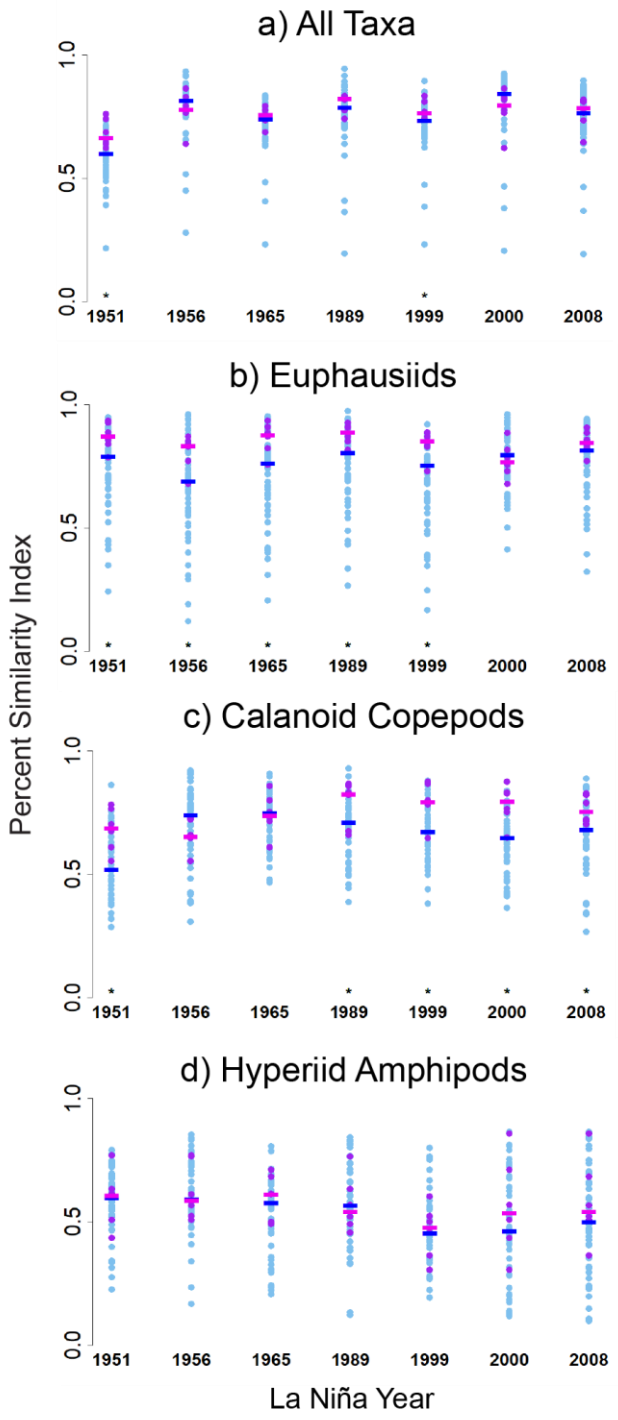

Figure S1.4. As in figure 1.5 using the Percent Similarity Index, but for La Niña-La Niña comparisons (purple symbols) and La Niña-non-La Niña comparisons (blue symbols). a) All taxa, b) euphausiids, c) calanoid copepods, d) hyperiid amphipods.

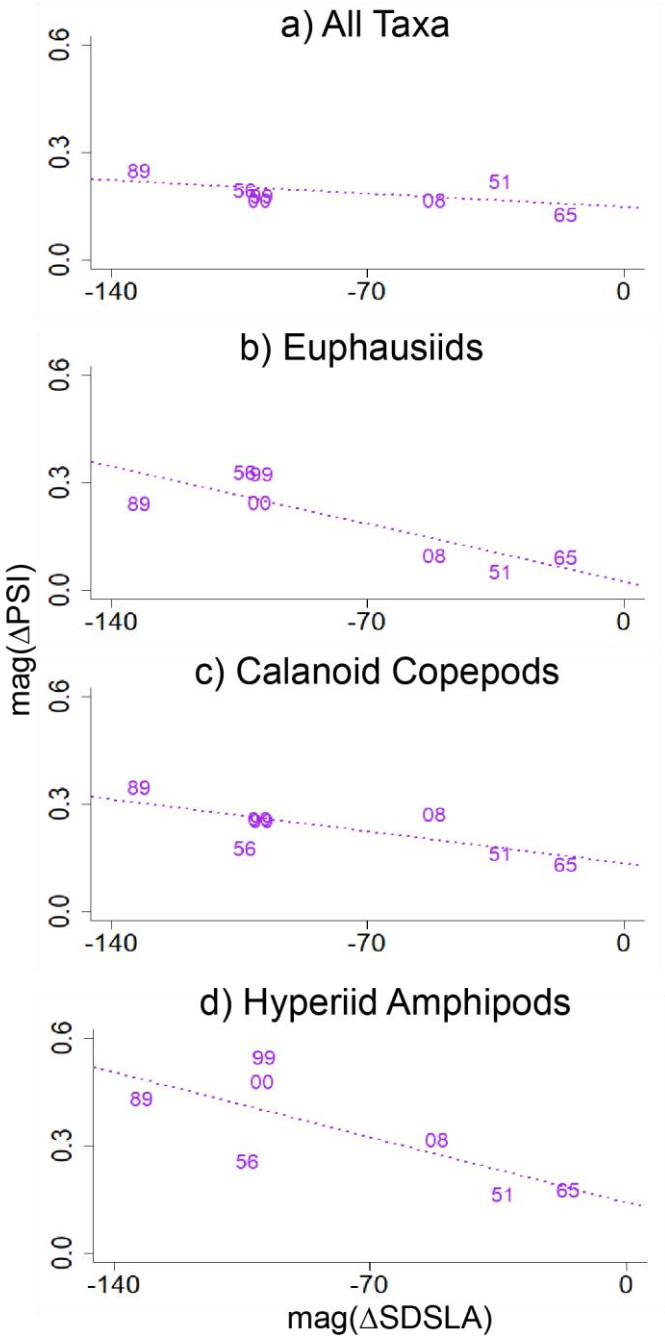

Figure S1.5. As in figure 1.6, but for La Niña correlations of mag(ΔPSI) vs. mag(ΔSDSLA). Dotted line indicates linear regression.

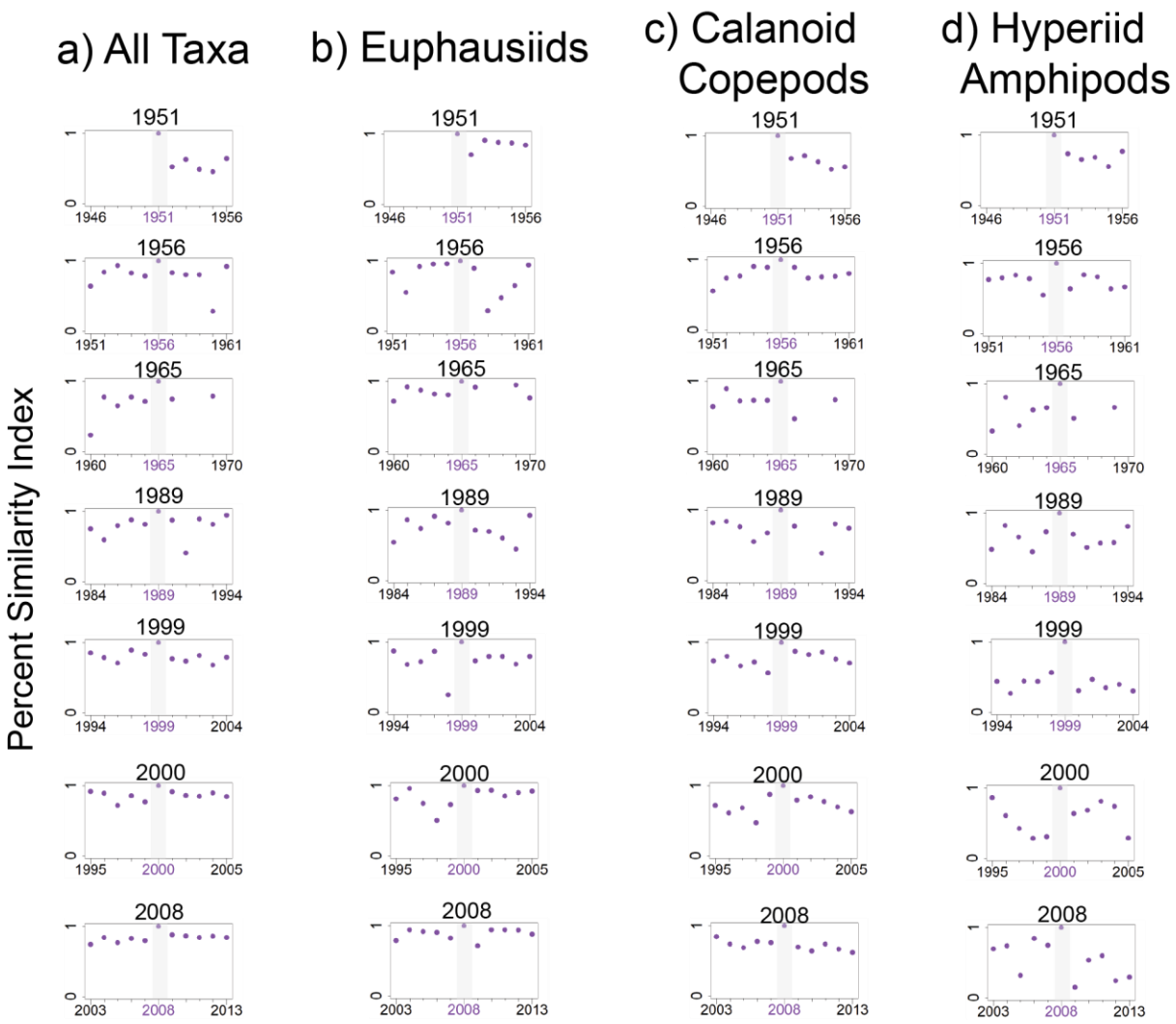

Figure S1.6. As in figure 1.7, but Percent Similarity Index (PSI) comparisons of each La Niña with the preceding five and following five years. Lack of a dot indicates year of no data.

References

Alexander, M. A., Blade, I., Newman, M., Lanzante, J. R., Lau, N. C. & Scott, J. D. (2002). The atmospheric bridge: The influence of ENSO teleconnections on air-sea interaction over the global oceans. *Journal of Climate, 15*(16), 2205-2231.

Arcos, D. F., Cubillos, L. A. & Núnez, S. P. (2001). The jack mackerel fishery and El Niño 1997–98 effects off Chile. *Progress in Oceanography, 49*(1), 597-617.

Ashok, K., Behera, S. K., Rao, S. A., Weng, H. Y. & Yamagata, T. (2007). El Nino Modoki and its possible teleconnection. *Journal of Geophysical Research-Oceans, 112*(C11). doi:Artn C1100710.1029/2006jc003798

Barber, R. T. & Chavez, F. P. (1983). Biological Consequences of El-Nino. *Science, 222*(4629), 1203-1210. doi:DOI 10.1126/science.222.4629.1203

Barber, R. T. & Chavez, F. P. (1986). Ocean Variability in Relation to Living Resources during the 1982-83 El-Nino. *Nature, 319*(6051), 279-285. doi:DOI 10.1038/319279a0

Barber, R. T., Sanderson, M. P., Lindley, S. T., Chai, F., Newton, J., Trees, C. C., et al. (1996). Primary productivity and its regulation in the equatorial Pacific during and following the 1991-1992 El Nino. *Deep-Sea Research Part Ii-Topical Studies in Oceanography, 43*(4-6), 933-969. doi:Doi 10.1016/0967-0645(96)00035-5

Bograd, S. J. & Lynn, R. J. (2001). Physical-biological coupling in the California Current during the 1997-99 El Niño-La Niña cycle. *Geophysical Research Letters, 28*(2), 275-278.

Bond, N. A., Cronin, M. F., Freeland, H. & Mantua, N. (2015). Causes and Impacts of the 2014 Warm Anomaly in the NE Pacific. *Geophysical Research Letters, 42*.

Brinton, E. (1960). Changes in the distribution of euphausiid crustaceans in the region of the California Current. *CalCOFI Reports, 7*, 137-146.

Brinton, E. (1981). Euphausiid distributions in the California Current during the warm winter-spring of 1977–78, in the context of a 1949–1966 time series. *Calif. Coop. Oceanic Fish. Invest. Rep,, 22*, 135-154.

Brinton, E. & Townsend, A. (2003). Decadal variability in abundances of the dominant euphausiid species in southern sectors of the California Current. *Deep-Sea Research Part Ii-Topical Studies in Oceanography, 50*(14-16), 2449-2472. doi:10.1016/S0967-0645(03)00126-7

Brinton, E. & Townsend, A. W. (1981). A comparison of euphausiid abundances from bongo and 1-m CalCOFI nets. . *California Cooperative Oceanic Fisheries Investigations Reports, 22*, 111-125.

Cane, M. A. (1983). Oceanographic Events during El-Nino. *Science, 222*(4629), 1189-1195. doi:DOI 10.1126/science.222.4629.1189

Capotondi, A., Wittenberg, A. T., Newman, M., Di Lorenzo, E., Yu, J. Y., Braconnot, P., et al. (2015). Understanding ENSO Diversity. *Bull. Amer. Meteor. Soc.*(96), 921–938.

Chao, Y., Farrara, J. D., Bjorkstedt, E., Chai, F., Chavez, F., Rudnick, D. L., et al. (2017). The origins of the anomalous warming in the California coastal ocean and San Francisco Bay during 2014–2016. *Journal of Geophysical Research: Oceans*.

Chavez, F. P. (1996). Forcing and biological impact of onset of the 1992 El Niño in central California. *Geophysical Research Letters, 23*(3), 265-268.

Chavez, F. P., Pennington, J. T., Castro, C. G., Ryan, J. P., Michisaki, R. P., Schlining, B., et al. (2002). Biological and chemical consequences of the 1997-1998 El Nino in central California waters. *Progress in Oceanography, 54*(1-4), 205-232. doi:Pii S0079-6611(02)00050-2. Doi 10.1016/S0079-6611(02)00050-2

Chavez, F. P., Ryan, J., Lluch-Cota, S. E. & Ñiquen, M. (2003). From anchovies to sardines and back: multidecadal change in the Pacific Ocean. *Science, 299*(5604), 217-221.

Chavez, F. P., Strutton, P. G., Friederich, C. E., Feely, R. A., Feldman, G. C., Foley, D. C. & McPhaden, M. J. (1999). Biological and chemical response of the equatorial Pacific Ocean to the 1997-98 El Nino. *Science, 286*(5447), 2126-2131. doi:DOI 10.1126/science.286.5447.2126

Chavez, F. P., Strutton, P. G. & McPhaden, M. J. (1998). Biological-physical coupling in the central equatorial Pacific during the onset of the 1997-98 El Nino. *Geophysical Research Letters, 25*(19), 3543-3546. doi:Doi 10.1029/98gl02729

Checkley, D. M. & Barth, J. A. (2009). Patterns and processes in the California Current System. *Progress in Oceanography, 83*(1-4), 49-64. doi:10.1016/j.pocean.2009.07.028

Chelton, D. B., Bernal, P. A. & Mcgowan, J. A. (1982). Large-Scale Interannual Physical and Biological Interaction in the California Current. *Journal of Marine Research, 40*(4), 1095-1125.

Climate Prediction Center, N. (2017, 17 Jan 2017). Oceanic Nino Index. Retrieved from https://catalog.data.gov/dataset/climate-prediction-center-cpcoceanic-nino-index

Cowles, T. J. & Barber, R. T. (1977). Biological Consequences of 1975 El Nino. *Science, 195*(4275), 285-287. doi:DOI 10.1126/science.195.4275.285

Di Lorenzo, E. & Mantua, N. (2016). Multi-year persistence of the 2014/15 North Pacific marine heatwave. *Nature Climate Change, 6*(11), 1042-1047.

Di Lorenzo, E. & Ohman, M. D. (2013). A double-integration hypothesis to explain ocean ecosystem response to climate forcing. *Proceedings of the National Academy of Sciences, 110*(7), 2496-2499.

Fiedler, P. C. (1984). Satellite observations of the 1982-1983 El Niño along the US Pacific coast. *Science, 224*(4654), 1251-1254.

Fiedler, P. C. & Mantua, N. J. (2017). How are warm and cool years in the California Current related to ENSO? *Journal of Geophysical Research-Oceans, 122*(7), 5936-5951. doi:10.1002/2017jc013094

Fisher, J. L., Peterson, W. T. & Rykaczewski, R. R. (2015). The impact of El Nino events on the pelagic food chain in the northern California Current. *Global Change Biology, 21*(12), 4401-4414. doi:10.1111/gcb.13054

Foley, D. G., Dickey, T. D., McPhaden, M. J., Bidigare, R. R., Lewis, M. R., Barber, R. T., et al. (1997). Longwaves and primary productivity variations in the equatorial pacific at 0°, 140dgW. *Deep Sea Research Part II: Topical Studies in Oceanography, 44*(9), 1801-1826.

Frischknecht, M., Munnich, M. & Gruber, N. (2015). Remote versus local influence of ENSO on the California Current System. *Journal of Geophysical Research-Oceans, 120*(2), 1353-1374. doi:10.1002/2014JC010531

Frischknecht, M., Münnich, M. & Gruber, N. (2017). Local atmospheric forcing driving an unexpected California Current System response during the 2015–2016 El Niño. *Geophysical Research Letters, 44*(1), 304-311.

Hayward, T. L. (1993). Preliminary-Observations of the 1991-1992 El-Nino in the California Current. *California Cooperative Oceanic Fisheries Investigations Reports, 34*, 21-29.

Hickey, B. M. (1979). The California Current system—hypotheses and facts. *Progress in Oceanography, 8*(4), 191-279.

Hooff, R. C. & Peterson, W. T. (2006). Copepod biodiversity as an indicator of changes in ocean and climate conditions of the northern California current ecosystem. *Limnology and Oceanography, 51*(6), 2607-2620. doi:DOI 10.4319/lo.2006.51.6.2607

Jacox, M. G., Fiechter, J., Moore, A. M. & Edwards, C. A. (2015). ENSO and the California Current coastal upwelling response. *Journal of Geophysical Research-Oceans, 120*(3), 1691-1702. doi:10.1002/2014jc010650

Jacox, M. G., Hazen, E. L., Zaba, K. D., Rudnick, D. L., Edwards, C. A., Moore, A. M. & Bograd, S. J. (2016). Impacts of the 2015-2016 El Nino on the California Current System: Early assessment and comparison to past events. *Geophysical Research Letters, 43*(13), 7072-7080. doi:10.1002/2016gl069716

Kahru, M., Jacox, M. G. & Ohman, M. D. (2018). The effect of the 2014-2016 northeast Pacific warm anomalies on the frequency of oceanic fronts and surface chlorophyll concentration in the California Current System. *Deep-Sea Research Part I*.

Kahru, M. & Mitchell, B. G. (2000). Influence of the 1997–98 El Niño on the surface chlorophyll in the California Current. *Geophysical Research Letters*(27), 2937–2940.

Kao, H. Y. & Yu, J. Y. (2009). Contrasting Eastern-Pacific and Central-Pacific Types of ENSO. *Journal of Climate, 22*(3), 615-632. doi:10.1175/2008jcli2309.1

Karnauskas, K. B. (2013). Can we distinguish canonical El Nino from Modoki? *Geophysical Research Letters, 40*(19), 5246-5251. doi:10.1002/grl.51007

Keiper, C. A., Ainley, D. G., Allen, S. G. & Harvey, J. T. (2005). Marine mammal occurrence and ocean climate off central California, 1986 to 1994 and 1997 to 1999. *Marine Ecology Progress Series, 289*, 285-306. doi:DOI 10.3354/meps289285

Keister, J. E., Di Lorenzo, E., Morgan, C. A., Combes, V. & Peterson, W. T. (2011). Zooplankton species composition is linked to ocean transport in the Northern California Current. *Global Change Biology, 17*, 2498-2511.

Keister, J. E., Johnson, T. B., Morgan, C. A. & Peterson, W. T. (2005). Biological indicators of the timing and direction of warm-water advection during the 1997/1998 El Nino off the central Oregon coast, USA. *Marine Ecology Progress Series, 295*, 43-48. doi:DOI 10.3354/meps295043

Larkin, N. K. & Harrison, D. E. (2005). On the definition of El Nino and associated seasonal average US weather anomalies. *Geophysical Research Letters, 32*(13). doi:Artn L13705 10.1029/2005gl022738

Lavaniegos, B. E. (2009). Influence of a multiyear event of low salinity on the zooplankton from Mexican eco-regions of the California Current. *Progress in Oceanography, 83*(1-4), 369-375.

Lavaniegos, B. E. (2014). Pelagic amphipod assemblage associated with subarctic water off the West Coast of the Baja California peninsula. *Journal of Marine Systems, 132*, 1-12.

Lavaniegos, B. E. & Hereu, C. M. (2009). Seasonal variation in hyperiid amphipods and influence of mesoscale structures off Baja California. *Marine Ecology Progress Series, 394*, 137-152.

Lavaniegos, B. E., Jiménez-Pérez, L. C. & Castro, G. (2002). Plankton response to El Niño 1997–98 and La Niña 1999 in the southern region of the California Current. *Progress in Oceanography, 54*, 33-58.

Lavaniegos, B. E. & Ohman, M. D. (1999). Hyperiid amphipods as indicators of climate change in the California Current. In F. R. Schram, von Vaupel Klein, J.C. (Eds.) (Ed.), (pp. 489-509). Leiden: Publisher.

Lavaniegos, B. E. & Ohman, M. D. (2003). Long-term changes in pelagic tunicates of the California Current. *Deep-Sea Research Part Ii-Topical Studies in Oceanography, 50*(14-16), 2473-2498. doi:10.1016/S0967-0645(03)00132-2

Lavaniegos, B. E. & Ohman, M. D. (2007). Coherence of long-term variations of zooplankton in two sectors of the California Current System. *Progress in Oceanography, 75*(1), 42-69.

Lee, D. E., Nur, N. & Sydeman, W. J. (2007). Climate and demography of the planktivorous Cassin's auklet Ptychoramphus aleuticus off northern California: implications for population change. *Journal of Animal Ecology, 76*(2), 337-347. doi:10.1111/j.1365-2656.2007.01198.x

Lee, R. F., Barnett, A. M. & Hirota, J. (1971). Distribution and Importance of Wax Esters in Marine Copepods and Other Zooplankton. *Deep-Sea Research, 18*(12), 1147-+. doi:Doi 10.1016/0011-7471(71)90023-4

Lilly, L. E. (2016). *Timing and effects of the 2014-15 Warm Anomaly and 2015-16 El Niño in the southern California Current System: Observations from a CCE-LTER Mooring.* Scripps Institution of Oceanography, La Jolla, CA. SIO/AORI Symposium.

Lindegren, M., Checkley, D. M., Ohman, M. D., Koslow, J. A. & Goericke, R. (2016). Resilience and stability of a pelagic marine ecosystem. *Proceedings of the Royal Society B-Biological Sciences, 283*(1822). doi:ARTN 20151931 10.1098/rspb.2015.1931

Liu, Z. Y. & Alexander, M. (2007). Atmospheric bridge, oceanic tunnel, and global climatic teleconnections. *Reviews of Geophysics, 45*(2).

Lynn, R. J. & Bograd, S. J. (2002). Dynamic evolution of the 1997-1999 El Nino-La Nina cycle in the southern California Current System. *Progress in Oceanography, 54*(1-4), 59-75. doi:Pii S0079-6611(02)00043-5

Mackas, D. L., Batten, S. & Trudel, M. (2007). Effects on zooplankton of a warmer ocean: Recent evidence from the Northeast Pacific. *Progress in Oceanography, 75*(2), 223-252. doi:10.1016/j.pocean.2007.08.010

Mackas, D. L., Peterson, W. T., Ohman, M. D. & Lavaniegos, B. E. (2006). Zooplankton anomalies in the California Current system before and during the warm ocean conditions of 2005. *Geophysical Research Letters, 33*(22).

Mantua, N. J., Hare, S. R., Zhang, Y., Wallace, J. M. & Francis, R. C. (1997). A Pacific interdecadal climate oscillation with impacts on salmon production. *Bulletin of the American Meteorological Society, 78*(6), 1069-1079.

Marinovic, B. B., Croll, D. A., Gong, N., Benson, S. R. & Chavez, F. P. (2002). Effects of the 1997-1999 El Nino and La Nina events on zooplankton abundance and euphausiid community composition within the Monterey Bay coastal upwelling system. *Progress in Oceanography, 54*(1-4), 265-277. doi:10.1016/S0079-6611(02)00053-8

McPhaden, M. J. (1999). Genesis and evolution of the 1997-98 El Nino. *Science, 283*(5404), 950-954. doi:DOI 10.1126/science.283.5404.950

McPhaden, M. J., Lee, T. & McClurg, D. (2011). El Nino and its relationship to changing background conditions in the tropical Pacific Ocean. *Geophysical Research Letters, 38*. doi:Artn L15709 10.1029/2011gl048275

Michaels, A. F. & Silver, M. W. (1988). Primary Production, Sinking Fluxes and the Microbial Food Web. *Deep-Sea Research Part a-Oceanographic Research Papers, 35*(4), 473-490. doi:Doi 10.1016/0198-0149(88)90126-4

Mullin, M. M. (1998). Interannual and interdecadal variation in California Current zooplankton: Calanus in the late 1950s and early 1990s. *Global Change Biology, 4*(1), 115-119.

Murphree, T., Bograd, S. J., Schwing, F. B. & Ford, B. (2003). Large scale atmosphere-ocean anomalies in the northeast Pacific during 2002. *Geophysical Research Letters, 30*(15). doi:Artn 8026 10.1029/2003gl017303

Newman, M., Shin, S. I. & Alexander, M. A. (2011). Natural variation in ENSO flavors. *Geophysical Research Letters, 38*(14).

Nickels, C. F., Sala, L. M. & Ohman, M. D. (submitted). Euphausiid mandible morphology used to assess selective predation by blue whales in the southern sector of the California Current System.

Ohman, M. D., Drits, A. V., Clarke, M. E. & Plourde, S. (1998). Differential dormancy of co-occurring copepods. *Deep-Sea Research Part Ii-Topical Studies in Oceanography, 45*(8-9), 1709-1740. doi:Doi 10.1016/S0967-0645(98)80014-3

Ohman, M. D. & Lavaniegos, B. E. (2002). Comparative zooplankton sampling efficiency of a ring net and bongo net with comments on pooling of subsamples. *California Cooperative Oceanic Fisheries Investigations Reports, 43*, 162-173.

Ohman, M. D., Lavaniegos, B. E. & Townsend, A. W. (2009). Multi-decadal variations in calcareous holozooplankton in the California Current System: Thecosome pteropods, heteropods, and foraminifera. *Geophysical Research Letters, 36*. doi:Artn L18608 10.1029/2009gl039901

Ohman, M. D., Mantua, N., Keister, J. E., Garcia-Reyes, M. & McClatchie, S. (2017). ENSO impacts on ecosystem indicators in the California Current System. *Variations (CLIVAR and OCB Newsletter)*(15), 8-15.

Ohman, M. D. & Smith, P. E. (1995). A comparison of zooplankton sampling methods in the CalCOFI time series. *California Cooperative Oceanic Fisheries Investigations Reports, 36*, 153-158.

Pares-Escobar, F., Lavaniegos, B. E. & Ambriz-Arreola, I. (2018). Interannual summer variability in oceanic euphausiid communities off the Baja California western coast during 1998–2008. *Progress in Oceanography, 160*, 53-67.

Peterson, W. T., Fisher, J. L., Strub, P. T., Du, X. N., Risien, C., Peterson, J. & Shaw, C. T. (2017). The pelagic ecosystem in the Northern California Current off Oregon during the 2014-2016 warm anomalies within the context of the past 20 years. *Journal of Geophysical Research-Oceans, 122*(9), 7267-7290. doi:10.1002/2017JC012952

Peterson, W. T., Keister, J. E. & Feinberg, L. R. (2002). The effects of the 1997-99 El Nino/La Nina events on hydrography and zooplankton off the central Oregon coast. *Progress in Oceanography, 54*(1-4), 381-398. doi:Doi 10.1016/S0079-6611(02)00059-9

R-core-team. (2015). A language and environment for statistical computing: R Foundation for Statistical Computing, Vienna, Austria. Retrieved from https://www.R-project.org/

Rau, G. H., Ohman, M. D. & Pierrot-Bults, A. (2003). Linking nitrogen dynamics to climate variability off central California: a 51 year record based on 15N/14N in CalCOFI zooplankton. . *Deep Sea Research Part II: Topical Studies in Oceanography, 50*(14-16), 2431-2447.

Rebstock, G. A. (2001). Long-term stability of species composition in calanoid copepods off southern California. *Marine Ecology Progress Series, 215*, 213-224.

Rebstock, G. A. (2002). Climatic regime shifts and decadal-scale variability in calanoid copepod populations off southern California. *Global Change Biology, 8*(1), 71-89.

Ross, R. M. (1982). Energetics of Euphausia-Pacifica .1. Effects of Body Carbon and Nitrogen and Temperature on Measured and Predicted Production. *Marine Biology, 68*(1), 1-13. doi:10.1007/Bf00393135

Schreiber, R. W. & Schreiber, E. A. (1984). Central Pacific seabirds and the El Niño southern oscillation: 1982 to 1983 perspectives. *Science, 225*, 713-716.

Schwing, F. B., Murphree, T. & Green, P. M. (2002). The evolution of oceanic and atmospheric anomalies in the northeast Pacific during the El Niño and La Niña events of 1995–2001. *Progress in Oceanography, 54*(1), 459-491.

Simpson, J. J. (1984). El-Nino-Induced Onshore Transport in the California Current during 1982-1983. *Geophysical Research Letters, 11*(3), 241-242.

Smith, K. L., Sherman, A. D., Huffard, C. L., McGill, P. R., Henthorn, R., Von Thun, S., et al. (2014). Large salp bloom export from the upper ocean and benthic community response in the abyssal northeast Pacific: Day to week resolution. *Limnology and Oceanography, 59*(3), 745-757. doi:10.4319/lo.2014.59.3.0745

Smith, P. E. (1985). A case history of an anti-El Nino to El Nino transition on plankton and nekton distribution and abundances. In W. S. Wooster, Fluharty, D.L. (Ed.), *El NinoNorth: Nino effects in the eastern subarctic Pacific Ocean.* (pp. 121-142). Seattle: Washington Sea Grant Program.

Strub, P. T. & James, C. (2002). The 1997-1998 oceanic El Niño signal along the southeast and northeast Pacific boundaries - an altimetric view. *Progress in Oceanography, 54*(1-4), 439-458.

Todd, R. E., Rudnick, D. L., Davis, R. E. & Ohman, M. D. (2011). Underwater gliders reveal rapid arrival of El Nino effects off California's coast. *Geophysical Research Letters, 38*. doi:10.1029/2010gl046376

University of Hawaii Sea Level Center, C. C. E. L. (2017). *University of Hawaii Sea Level Center, California Current Ecosystem LTER.* Retrieved from http://dx.doi.org/10.6073/pasta/b88324bad507a400095981d10ae33563

Whittaker, R. H. (1952). A Study of Summer Foliage Insect Communities in the Great Smoky Mountains. *Ecological Monographs, 22*(1), 1-44. doi:Doi 10.2307/1948527

Wyrtki, K. (1975). El Nino - Dynamic-Response of Equatorial Pacific Ocean to Atmospheric Forcing. *Journal of Physical Oceanography, 5*(4), 572-584. doi:Doi 10.1175/1520-0485(1975)005<0572:Entdro>2.0.Co;2

Yeh, S. W., Kirtman, B. P., Kug, J. S., Park, W. & Latif, M. (2011). Natural variability of the central Pacific El Nino event on multi-centennial timescales. *Geophysical Research Letters, 38*. doi:Artn L02704 10.1029/2010gl045886

Yu, J. Y. & Kao, H. Y. (2007). Decadal changes of ENSO persistence barrier in SST and ocean heat content indices: 1958-2001. *Journal of Geophysical Research-Atmospheres, 112*(D13).

Zaba, K. & Rudnick, D. (2016). The 2014–2015 warming anomaly in the Southern California Current System observed by underwater gliders. *Geophysical Research Letters, 43*(3), 1241-1248.

Chapter 2

Euphausiid spatial displacements and habitat shifts in the southern California Current System in response to El Niño variability

Abstract

We analyzed spatial distributions of 10 euphausiid species in the southern California Current System across seven El Niño events (1951-2018) and the 2014-15 Warm Anomaly to determine variations in habitat utilization and reproduction during Eastern Pacific (EP) and Central Pacific (CP) Niños. Our goal was to characterize the main forcing mechanisms by which El Niño events influence these dominant species. Our findings suggest cool-water euphausiids respond predominantly to changing *in situ* habitat conditions during El Niño, while subtropical species require initial advection to increase in the southern CCS. Cool-water coastally-associated species (*Euphausia pacifica, Thysanoessa spinifera*) compress shoreward and retract poleward to upwelling waters during EP Niños, likely in response to offshore warming. A subtropical coastal species (*Nyctiphanes simplex*) extends poleward nearshore during EP Niños, suggesting anomalous advection, but increases only moderately and variably off southern California during CP Niños. A Tropical Pacific-Baja California species (*Euphausia eximia*) only appears off southern California in spring during El Niño years (EP, some CP), suggesting direct advection and low tolerance for cooler, fresher conditions. Subtropical offshore species (*Euphausia gibboides, Euphausia recurva, Stylocheiron affine, Euphausia hemigibba*) expand shoreward during most Niños (strongest during 2014-15 Warm Anomaly) and show moderate *in situ* post-event persistence, suggesting combined influence of advection and temporarily favorable habitat nearshore. Regionwide temperate species (*Nematoscelis difficilis, Thysanoessa gregaria*)

contract only moderately shoreward during some Niños. Predictions of Year 2100 distributions using generalized additive models suggest future non-Niño conditions and CP Niños will produce regionwide *in situ* increases in subtropical species and moderate poleward and onshore expansions, while EP Niños will produce continued nearshore habitat compression and reduced abundance of coastal species. Understanding zooplankton spatial responses to El Niño can help predict community compositional shifts under other ocean changes (e.g., long-term trends, basin-wide warm anomalies).

2.1. Introduction

Euphausiids (krill) are shrimp-like crustacean zooplankton that comprise one of the dominant mesozooplankton taxa in the California Current System (CCS) and form an important link in energy transfer from primary production to higher trophic levels (Croll et al., 2005; Dorman et al., 2011a; Tanasichuk, 1998). Euphausiids show high species diversity in the southern CCS, to 39 species, 24 of which have been observed consistently since the California Cooperative Oceanic Fisheries Investigations program (CalCOFI) began zooplankton sampling in 1949 (Brinton, 1962; Brinton et al., 2000). Brinton (1962, 1967, 1981) characterized biogeographic affinities of common CCS euphausiid species into four regions: 1) Northern CCS/North Pacific Drift (*Euphausia pacifica, Nematoscelis difficilis*), 2) Intermediate/Subtropical Offshore (*E. gibboides, E. recurva, Thysanoessa gregaria*), 3) Baja California/Subtropical (*E. eximia, E. hemigibba, Stylocheiron affine*), and 4) Coastal: northern CCS (*T. spinifera*) and Baja California (*Nyctiphanes simplex*). Departures from these affinities, particularly increases of subtropical species in the southern and central CCS, have been used as indicators of Eastern North Pacific anomalous ocean conditions such as El Niño events and

Pacific Decadal Oscillation phase changes (Brinton, 1960, 1979, 1981; Brinton & Townsend, 2003; Di Lorenzo & Ohman, 2013; Lavaniegos et al., 2019; Lavaniegos et al., 2002; Lilly & Ohman, 2018; Marinovic et al., 2002; Pares-Escobar et al., 2018).

The dominant physical perturbation in the Pacific Ocean is the El Niño-Southern Oscillation (ENSO) cycle, which originates in the equatorial region. El Niño, the ENSO warm phase, develops every 3-8 years due to weakening equatorial trade winds (Cane, 1986; McPhaden, 1999b; Wyrtki, 1975). El Niño events can vary substantially in physical expression and biological impacts in the equatorial Pacific and in extratropical latitudes such as the CCS (Ashok et al., 2007; Capotondi et al., 2015; Kao & Yu, 2009; Larkin & Harrison, 2005). Whether this variability in El Niño characteristics has a clear typology is an ongoing debate (Karnauskas, 2013), but one proposed categorization is into Eastern Pacific (EP) and Central Pacific (CP) events (Capotondi et al., 2015; Kao & Yu, 2009; Ren & Jin, 2011; Timmermann et al., 2019; Yeh et al., 2009). Eastern Pacific El Niños are initiated, in part, by significant Kelvin wave propagation eastward along the Equator and characterized by anomalously warm temperatures and a deep thermocline off South America, with heat discharge to the extra-tropics via oceanic propagation (principally coastally trapped waves, CTWs; Capotondi et al., 2015; Kao & Yu, 2009; Kug et al., 2009). Central Pacific El Niños generally have more moderate temperature anomalies that are expressed most strongly near the International Dateline; are usually forced by local winds and zonal advective feedback, although they can sometimes induce Kelvin waves; and rarely show off-Equator heat discharge (Ashok et al., 2007; Ashok & Yamagata, 2009; Capotondi, 2013; Kao & Yu, 2009; Kim et al., 2011).

El Niño signals can travel to extra-tropical latitudes such as the CCS via a combination of oceanic and atmospheric pathways (Jacox et al., 2015): 1) CTWs can strengthen poleward

advection and transport subtropical waters from Baja California (Lynn & Bograd, 2002; Ramp et al., 1997; Schwing et al., 2002; Strub & James, 2002); 2) atmospheric teleconnections from the equatorial Pacific can alter the Aleutian Low pressure system, affecting local wind-driven circulation (Alexander et al., 2002; Simpson, 1984); and 3) warm, salty waters of southern offshore origin can be advected into the CCS due to altered atmospheric circulation (Bograd & Lynn, 2001; Jacox et al., 2016; Simpson, 1984). El Niño propagation mechanisms and CCS expressions can vary substantially, even for events of similar equatorial forms (see Supplemental Information to this manuscript for detailed physical characteristics and propagation mechanisms of each El Niño event analyzed in this study).

Maximum lifespans of CCS euphausiids range from approximately 8 months for *N. simplex* (Lavaniegos, 1992) to 1-1.5 years for *E. pacifica* (Brinton, 1976; Smiles & Pearcy, 1971) and possibly 1.5 years for *E. eximia* (Gomez, 1995), although lifespans for most species have not been well quantified. However, lifespans on the order of one year make euphausiids optimal organisms to track interannual perturbations such as El Niño (Brinton, 1960) and lower-frequency variations such as the Pacific Decadal Oscillation (Di Lorenzo & Ohman, 2013). Southern CCS total euphausiid biomass has generally decreased, and subtropical species presence increased, during and immediately following most El Niño events of the past seventy years (Brinton, 1981; Brinton & Townsend, 2003; Lavaniegos et al., 2019; Lavaniegos et al., 2002; Lavaniegos & Ohman, 2007; Lilly & Ohman, 2018; Mackas et al., 2006; Pares-Escobar et al., 2018). Baja California species (*N. simplex, E. eximia)* have been collected as far north as Oregon (Keister et al., 2005), Washington (Brodeur, 1986), and Vancouver Island, British Columbia (Mackas & Galbraith, 2002), during past El Niños, indicating significant short-term range extensions of subtropical species (Brinton, 1960; Marinovic et al., 2002). In contrast,

dominant cool-water CCS species (*E. pacifica, T. spinifera*) have decreased and shown evidence for northward retraction (Brinton, 1960; Brinton & Townsend, 2003). Such species-specific responses highlight that aggregated euphausiid bulk biomass, whether assessed by direct sampling or bioacoustics, is unlikely to be a sensitive indicator of either the true impact of El Niño or the underlying causal mechanisms.

Past studies have often attributed El Niño-related zooplankton shifts to advection of organisms into or out of a region, with only secondary consideration of *in situ* effects (Brinton, 1979, 1981; Wickett, 1967). However, the specific impacts of an El Niño event on a given euphausiid species depend upon the physical characteristics of the event; the biogeographic origin and inherent habitat tolerances of the species (i.e., mortality, growth, reproduction thresholds); and El Niño-induced alterations in *in situ* prey, predator, and physical-chemical characteristics of the ambient environment (Lavaniegos & Ambriz-Arreola, 2012; Ohman et al., 2017; Pares-Escobar et al., 2018). Analyzing species- and life history-specific spatial changes can provide insight beyond aggregated biomass metrics into the relative contributions of direct advection and *in situ* population growth or mortality during El Niño events. Clarifying these contributions will improve our understanding of the underlying mechanisms that influence community variability under anomalous ocean conditions, thus enabling better predictions of zooplankton responses to future El Niño events and longer-term ocean changes. Improving our understanding of euphausiid population spatial changes can also improve predictions of habitat use by higher trophic levels, particularly whales, seabirds, and mobulids that selectively forage on certain euphausiid species (Lee et al., 2007; Nickels et al., 2018; Notarbartolo-di-Sciara, 1988; Stewart et al., 2017; Sydeman et al., 2006; Szesciorka et al., 2020).

Previously we presented temporal changes in regionally-aggregated total zooplankton community composition during CCS El Niños (Lilly & Ohman, 2018). Here we analyze variability in spatial distributions, habitat conditions, and population stage structure of ten euphausiid species across seven decades of EP and CP Niño events to address the following questions:

1) Do spatial distributions of euphausiid species change in a consistent manner during El Niño events relative to non-Niño years?
2) Do spatial distributional changes differ between Eastern Pacific and Central Pacific El Niños?
3) Do species occupy different ranges of habitat conditions (temperature, salinity, O_2, Chl-*a*) during El Niño and non-Niño years?
4) Does the population structure (i.e., developmental stage composition) of any species change during El Niño, suggesting altered rates of population growth?
5) How will euphausiid spatial distributions likely change during future El Niño events?

Our overarching goals are to i) characterize 'typical' EP and CP Niño responses to assess whether distributional shifts provide insight into the relative impacts of physical (advection) and biological (*in situ* growth and mortality) forcing mechanisms in altering species abundances and distributions, and ii) to use the above mechanistic insights to inform predictions of euphausiid changes during future El Niño events.

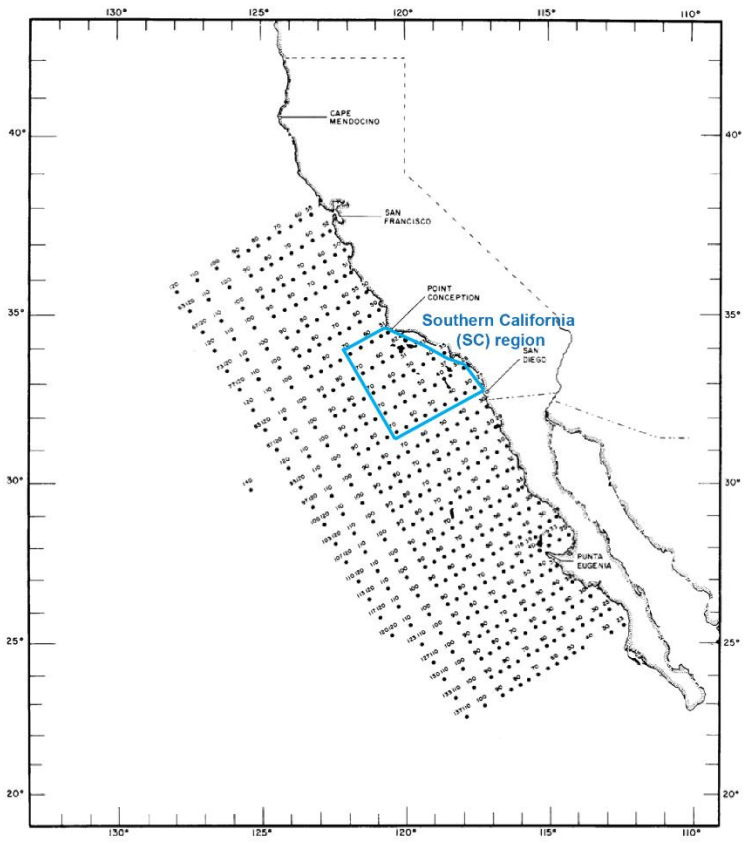

Figure 2.1. Locations of all California Cooperative Oceanic Fisheries Investigations (CalCOFI) sampling stations used in this study. The region shown here is a subset of the fullest sampling extent; see https://calcofi.org/. The sampling pattern within this region varies by year. See Fig. S2.10 for year-specific coverages. Blue box depicts Southern California ('SC') region. See Methods for more information.

2.2. Methods

2.2.1. Study region

All data are from the California Cooperative Oceanic Fisheries Investigations sampling program (CalCOFI, Bograd et al., 2003). The full CalCOFI sampling region extends from the northern border of California (Line 40: 42^{o}N, 125^{o}W at coast to 39^{o}N, 131^{o}W offshore) to the southern tip of Baja California (Line 157: 23.5^{o}N, 109^{o}W to 20^{o}N, 114.5^{o}W). However, not every station was sampled or enumerated for zooplankton every year in the timeseries. We thus show in figure 1 the maximum region that was available for our analyses, which includes stations

from Lines 60 (north)-130 (south) and from the coast out to Station 120 (Station 140 on Line 90), from 1951-2018. Even within this region, the sampling pattern for each year has varied, so our objective maps (see Section 2.2.4) include different coverage for each year (see figure S2.10). We refer here to the 'full CalCOFI region', which includes all available samples and variable coverage between years (Fig. 2.1, full grid), and the 'Southern California (SC) region', which is only the region consistently sampled across all years (Fig. 2.1, blue box). The SC region is defined as CalCOFI Lines 80-93.3, from the coast out to Station 70 (ranging from 180 km to 350 km offshore, due to the coastline curve) and excluding stations in < 200 m water depth (see https://calcofi.org/ for additional sampling information). Zooplankton samples are collected four times per year but only enumerated consistently for spring cruises, which occur between 15 Feb-31 May (exact dates vary by year). Where available, winter data are presented in Supplemental material. Euphausiid data are not available for 1967, 1968, 1971, or 1973 due to a temporary switch to triannual sampling. CalCOFI stations have occasionally been sampled multiple times within one spring period. If a station has multiple samples from one spring, we averaged replicate samples to a single value per station per year to maintain equal contribution of all stations (see Appendix 2A).

2.2.2. Euphausiid samples

CalCOFI zooplankton sampling procedures have changed during the timeseries. In all instances, at each station a net is lowered obliquely from the surface to depth, towed for 30 seconds, and recovered obliquely. Net types and depths are as follows: from 1951-1968, a 1-m ring net with 550 µm mesh was towed from 0-140 m; from 1969-1977, a 1-m ring net with 505 µm mesh was towed from 0-210 m; and from 1978-present a 0.71-m twin-opening bongo net

with 505 µm mesh has been towed from 0-210 m (Ohman & Smith, 1995). These sampling changes have been discussed elsewhere (Brinton & Townsend, 1981; Ohman & Lavaniegos, 2002) and do not affect the results presented here. Following net recovery, each zooplankton sample is preserved in sodium tetraborate-buffered formaldehyde and archived in the Pelagic Invertebrate Collection at Scripps Institution of Oceanography (Lavaniegos & Ohman, 2007; Lilly & Ohman, 2018). For euphausiids, an aliquot from each station on spring cruises is sorted and enumerated by species and length. Body lengths are converted to carbon biomass using known species length-carbon relationships (Lavaniegos & Ohman, 2007; Ross, 1982). We include only nighttime samples in this study to remove variance from day/night double-sampling, diel vertical migration, and daytime net avoidance. Data are available at https://oceaninformatics.ucsd.edu/euphausiid/. Twenty-four euphausiid species have been consistently observed and enumerated for the SC region since 1951. Here we examined ten euphausiid species: seven (*Euphausia pacifica, Nyctiphanes simplex, E. eximia, E. gibboides, E. recurva, E. hemigibba, Stylocheiron affine*) that we previously identified as having consistent regionwide biomass changes associated with El Niño (Lilly & Ohman, 2018), and three (*Nematoscelis difficilis, Thysanoessa gregaria, T. spinifera*) that did not show consistent El Niño changes but are numerically dominant in the southern CCS (Brinton & Townsend, 2003).

2.2.3. El Niño delineations

We defined El Niño events based on previous delineation of 'California Current System El Niños' (Lilly & Ohman, 2018). A 'CCS El Niño' refers to an El Niño event that reaches ≥ 1 standard deviation above the corresponding 1951-2016 mean for at least one Equatorial Pacific Niño index (Niño3.4 or Niño1+2: Nov-Dec-Jan average) and one CCS Niño index (San Diego

Harbor detrended sea level anomaly (SDSLA) or depth of the 26.0 kg/m^3 density isopycnal averaged along CalCOFI Line 90, Stations 26.7-37 ($z_{26.0}$): Dec-Jan-Feb averages). We refer to El Niño 'springs' as the spring CalCOFI cruise following the determinate winter physical average (e.g., spring 1983 for the 1982-83 El Niño). Since all our CCS El Niño events reached ≥ 1 S.D. in the Niño3.4 index, EP Niño events were defined using the additional criterion of also reaching ≥ 1 S.D. in the Niño1+2 region. CP Niño events met the Niño3.4 but not Niño1+2 criterion. We examined nine El Niño springs (EP: 1983, 1998, 2016; CP: 1958, 1959, 1992, 1993, 2003, 2010) and the 2014-15 Warm Anomaly (spring 2015), which was not significant in equatorial El Niño indices but produced unprecedented positive temperature anomalies in the CCS. Spring 1973 was categorized as an EP Niño, but we do not have zooplankton samples for that year. For analyses involving comparisons of non-Niño, EP Niño, and CP Niño years, we did not include spring 2015 in any group because it was characterized by different physical forcing mechanisms than El Niño events but was also significantly different from non-Niño years (Di Lorenzo & Mantua, 2016; Jacox et al., 2016; Lilly et al., 2019).

2.2.4. Objective maps

We used objective mapping to project euphausiid abundances measured at individual CalCOFI stations onto a uniform x/y grid and interpolate between points to produce regionwide spatial estimates. Objective mapping produces a minimum mean-square error estimate of a continuous function across a region based on discrete sampling points (i.e., CalCOFI stations; see Bretherton et al., 1976; Davis, 1985). We applied a rotation angle of -60^o (negative indicates clockwise rotation) to the CalCOFI grid to align the cross-shore and alongshore grid axes with x and y, respectively. Our mapping grid has evenly spaced resolutions of 14 km and 15 km in the x

and y directions, respectively. We selected decorrelation length-scales of 160 km in the x and 190 km in the y directions for all species based on optimal fits of Gaussian curves to autocovariance matrices, with the goal of smoothing small-scale variability resulting from discrete sampling of patchily distributed organisms, in order to depict the regionwide distribution of each species. We assumed an uncorrelated observation error variance of 0.1 of the signal variance (see Appendix 2B and figure 2.B1 for objective mapping process). We set a mean-square error threshold of 0.3 across all years to standardize all maps to a uniform interpolation error limit (Fig. 2.B2).

We used $\log_{10}$(abundance+1) euphausiid abundances for map calculations to avoid dominance by extreme untransformed abundance spikes. For mean interannual distribution maps, we averaged all yearly values for each station and objectively mapped the averaged grid using the same mapping parameters as for individual years. As noted in Section 2.2.1, sampling spatial coverage varies by year, so average maps (all years, e.g., figure 2.2b; or non, EP, and CP Niño categories; e.g., figure 2.2d) include different numbers of years for each station average within a map (see figure 2.B1 for total number of samples at each station and figure S2.10 for sampling coverage by year). We used the ETOPO1 global relief model (available from NOAA National Centers for Environmental Information, Amante & Eakins, 2009), subsetted for the CCS region and interpolated to our x/y mapping grid, to mask land projections. Coastline was compiled from shapefiles available through the UC Berkeley GeoData Library (https://geodata.lib.berkeley.edu/catalog). To quantitatively examine interannual species variability, we calculated yearly mean regionwide abundances for each species (e.g., figure 2.2c) and centers of gravity (COG) in the cross-shore (x) and alongshore (y) directions for both the SC

and full CalCOFI regions (see figure S2.1 and Appendix 2C). We calculated least squares linear regressions of abundance timeseries to evaluate significance of long-term trends (Fig. 2.2c).

2.2.5. Habitat conditions

2.2.5.1. Habitat range distributions

To determine the habitat range of each euphausiid species, we analyzed spring and winter (separate) abundance distributions in relation to four variables: temperature (50 m depth), salinity (50 m), oxygen (100 m), and chlorophyll-*a* (10 m). We include data from 1951-2017 (Chl-*a* available only from 1984-2017). Habitat data are from CalCOFI hydrocasts conducted concurrently by station with zooplankton sampling. Post-collection processing is described on the CalCOFI website (https://calcofi.org/field-work/bottle-sampling.html). We chose habitat variable depths that best represent upper water column conditions that impact the species we examined, several of which vertically migrate to the upper 50-100 m at night (Brinton, 1960; Matthews et al., 2020), and because El Niño events tend to have strongest influence in the upper 150 m (Ramp et al., 1997). Our initial temperature-abundance comparisons showed strongest El Niño responses above 100 m. Similarly, salinity is most strongly influenced by the California Current, which is freshest at 50-100 m (Rudnick et al., 2017). We therefore selected temperature and salinity at 50 m to represent upper ocean habitat conditions. We evaluated oxygen at 100 m because we expect these somewhat deeper waters to more closely approach oxygen undersaturation and hypoxia that may have detrimental effects on euphausiids. We included Chl-*a* at 10 m to represent both potential feeding and predator encounter; we expect near-surface Chl-*a* to reflect spatial variability in the subsurface Chl-*a* maximum layer while also correlating strongly with light attenuation, which can determine visual risk of predation on zooplankton

(Aksnes & Ohman, 2009; Ohman & Romagnan, 2016). We applied a natural log transformation to chlorophyll-*a* data to reduce skewness. We calculated separate euphausiid range distributions for non-Niño, EP Niño, and CP Niño categories of years, and calculated a weighted mean for each category using station-by-station product vectors: [value of habitat variable]*[euphausiid abundance at variable value]. The weighted mean accounts for varying abundances at different values of a habitat variable by multiplying each habitat value by its corresponding abundance before calculating the mean. We compared distributions of the three Niño conditions using a Kruskal-Wallis test ('kruskalwallis') and the 'multcompare' function in Matlab for post-hoc pairwise comparisons (Matlab 2018b; see Tables S2.1-S2.2 for spring and S2.3-S2.4 for winter mean values and inter-Niño differences, respectively). We did not include spring 2015 in any Niño group (see Section 2.2.3).

2.2.5.2. Euphausiid-water mass associations

To assess euphausiid species associations with specific water masses, we analyzed species distributions across previously calculated spring proportions of three dominant water masses that comprise the southern CCS (defined and calculated by Bograd et al., 2019). Pacific Subarctic Upper Water (PSUW) flows southward from the North Pacific Current via the core California Current, and is characterized as relatively cool, fresh, and high-O_2; Pacific Equatorial Water (PEW) flows northward coastally from the North Equatorial Countercurrent along Mexico, and is warm, salty, high-nutrient, and subsurface, representing the California Undercurrent; Eastern North Pacific Central Gyre Water (ENPCW) occurs offshore of the California Current and is warm, moderately salty, low-nutrient, and near-surface. Each water mass was defined from a 'source' box upstream of the SC region and characterized by measurements of temperature, salinity, oxygen, phosphate, nitrate, and silicic acid from the

World Ocean Database (Bograd et al., 2019). Each water mass was first characterized by upper and lower temperature and salinity limits based on its T-S diagram; optimum multiparameter analysis was then applied to the six upper and lower characterizations and the above six physical and nutrient variables to calculate the proportion of each water mass at each CalCOFI station in the SC region. Water mass proportions were only calculated from 1985-2017 due to prior lack of nutrient data (see Bograd et al., 2019 for methods and maps)**.** We considered each water mass at the depth of its strongest interannual expression in the CCS: PSUW at 150 m, PEW at 200 m, and ENPCW at 100 m. We calculated species' mean abundances using weighted means (Tables S2.5-S2.6; see Section 2.2.5.1). We also calculated the regionwide timeseries mean proportion of each water mass for each Niño group (i.e., the average proportion of PSUW across the SC region and 1985-2017; see arrows below x-axes in figure 2.11).

2.2.6. Adult and calyptopis abundance proportions

We quantified the relative proportions of adult and calyptopis abundances of each euphausiid species, averaged across the SC region, during each El Niño year and the three years before and after. Proportions are the abundance of each phase divided by the sum of the two phases (e.g., [adult]/[calyptopis+adult]). We calculated proportions individually for each station in the SC region and then averaged the proportions from all stations to obtain a region-averaged value. Years of no abundances of either adults or calyptopes (indicated by a missing bar in figures 2.12, S2.6) may still have species presence as furcilia and juvenile phases.

2.2.7. Generalized Additive Models

We developed spring species niche models based on generalized additive models (GAMs, Hastie & Tibshirani, 1987) to estimate individual and combined effects of habitat conditions on species abundances. We developed models from only SC region spring data, 1984-2017, because this region was consistently sampled across all years. Models were constructed from optimal combinations of individual and interactive terms: Temperature, O_2, ln(Chl-*a*), Lat, Lon, (Lat,Lon), (Temp,O_2), (Temp,lnChla), and (O_2,lnChla). Early model runs determined that salinity was nonsignificant for all species, so we removed it from further analyses. We applied default spline basis smoothers ('s') to individual terms and tensor-product smooth functions ('te') to interactive terms, and initialized each model with 5 knots per term, a Gaussian distribution, and method = 'REML'. We used log-transformed species abundances ($\log_{10}$(abund+1)) to reduce skew. We included 'Year' as a categorical variable to account for interannual variability in species abundances. We selected the top 3 models for each species from all term combinations, based on Akaike Information Criterion (AIC) and percent (%) deviance explained, and further adjusted k-values of those models to find the optimal model. We selected the optimal model for each species using a combination of lowest AIC, highest %deviance explained, and significance of all model terms ($p < 0.05$; see figures 2.13 and S2.8 for equations and Table S2.9 for values). We calculated and plotted GAMs using the 'mgcv' (v1.8-31) and 'mgcViz' (v0.1.6) packages in R (Fasiolo et al., 2019; Wood et al., 2017). We further tested the efficacy of each optimal model by cross-validation, i.e., omitting one year and using all other years to predict its abundances.

We next used each species' optimal GAM to predict potential spatial distributions during the three Niño categories (non, EP, CP) in Year 2100, given forecasted *in situ* conditions. We first calculated baseline (1951-2017) average habitat conditions for each Niño type by averaging each input habitat variable station-by-station across all years in that Niño group. We then added

expected habitat changes to each average to produce 'Year 2100 conditions': +1°C temperature, -0.63 ml/L oxygen, and +0.10 µg/L chlorophyll-*a* (untransformed scale), based on current trends and estimated projections for the SC region (Bograd et al., 2008; Hazen et al., 2013; Rykaczewski & Dunne, 2010). Although we calculated baseline conditions from the full (1951-2017) datasets for temperature and O_2, the Year 2100 distributions only include coverage based on the distributions from 1984-present because Chl-*a* data were not sampled prior to 1984. No CalCOFI samples exist south of San Diego for the EP and CP Niño years from 1984-present, so the EP and CP Niño predictions do not extend to Baja California (some non-Niño years from 1984-present did include sampling off Baja California).

To avoid negative abundance predictions arising from inclusion of station coordinates south and west of the SC region for which the GAMs were developed, we removed lat/lon terms from each GAM and only used habitat terms for Year 2100 predictions. To assess GAM accuracy without geographic terms, we evaluated the original GAM fits (SC region, 1984-2017) with and without lat/lon terms for four species. Non-lat/lon model fits and remaining term significance were similar to the original models for all terms (see Table S2.9 for comparisons for first four species). For calculations of total positive or negative distributional area in the difference maps (e.g., figure 2.2e: [average EP or CP]-[average non-Niño]; figure 2.14: [2100 prediction]-[current average]), we counted the total number of stations with a positive (or negative) difference and multiplied that count by the average 'station area of influence' (2100 km^2, see Appendix 2C).

2.3. Results

2.3.1. Spatial variability during El Niño events

We categorize five groups of southern CCS euphausiid species responses to El Niño: 1) Cool-Water Coastally-Associated (*Euphausia pacifica, Thysanoessa spinifera),* 2) Subtropical Coastal *(Nyctiphanes simplex*), 3) Tropical Pacific-Baja California (*Euphausia eximia*), 4) Subtropical Offshore (*Euphausia gibboides, Euphausia recurva, Stylocheiron affine, Euphausia hemigibba*), and 5) Regionwide Temperate (*Nematoscelis difficilis, Thysanoessa gregaria*). While these groupings partially align with the biogeographic affinities of Brinton (1962, 1981), they are a new set of categorizations based specifically on euphausiid responses to El Niño events. Our multiple groupings indicate that coastal or offshore origins are important considerations beyond 'warm' and 'cool' designations. To assess patterns of distributional change within each El Niño category, we calculated average non-Niño, Eastern Pacific (EP) Niño, and Central Pacific (CP) Niño distributions for each species from the entire 1951-2018 timeseries, although we note that these averages include variable sampling coverage by year (Figs. 2.2d-2.9d, S2.2d-S2.3d). We also present the individual El Niño events and their preceding and following years (Figs. S2.10-S2.19).

2.3.1.1. Cool-Water, Coastally-Associated Species

Euphausia pacifica is the dominant euphausiid species in the central and southern CCS and associates with cool waters (<15^{o}C) extending from the Subarctic Pacific to northern Baja California (Fig. 2.2a; see Brinton, 1962). The 1951-2018 CalCOFI mean spring distribution of *E. pacifica* indicates consistent presence from Monterey, CA, to the U.S.-Mexico border and out to 300 km offshore, with low abundance off northern Baja California (Fig. 2.2b). Total abundance of *E. pacifica* in both the Southern California (SC; light pink box on maps, blue line in Fig. 2.2c)

and full CalCOFI (pink line in Fig. 2.2c) regions decreased during every El Niño event except 2002-03 and 2009-10 (Figs. 2.2c, S2.10). The average EP Niño distribution of *E. pacifica* shows clear shoreward compression, poleward retraction, and regionwide population decreases relative to non-Niño years (Fig. 2.2d-e). The 1982-83 EP Niño induced the most significant reduction in regionwide abundance of *E. pacifica* of the entire timeseries, as well as nearshore compression and poleward retraction to well north of Point Conception, CA (Fig. 2.2c, S2.10). Center of gravity metrics reflect substantial shoreward compression and poleward retraction in 1983 (Fig. S2.1a). The 1997-98 EP Niño also caused substantial shoreward compression and decreased overall abundance of *E. pacifica*, although less severe than in 1983 (Fig. 2.2c, S2.1a, S2.10). In contrast, the 2015-16 EP Niño produced only moderate shoreward compression. High abundance in coastal regions suggests only moderate physical impacts and persistent nearshore upwelling during the event.

The average *E. pacifica* distribution during CP Niños shows only moderate poleward retraction compared to the non-Niño average (Fig. 2.2d-e). These changes are reflected in population decreases in the southern half of the distribution but localized nearshore increases in the northern third (Fig. 2.2d-e). However, *E. pacifica* distributional shifts vary substantially across individual CP Niños: 1957-59 (springs 1958, 1959) produced only moderately decreased abundance and poleward retraction, while 1991-93 (springs 1992, 1993) reduced abundance on par with EP Niños (Figs. S2.1a, S2.10). The 2002-03 and 2009-10 CP Niños, characterized as anomalously cool (spring 2003; Bograd & Lynn, 2003) or without enhanced poleward advection (spring 2010; Todd et al., 2011), showed average or elevated *E. pacifica* abundances and were part of a high-abundance period throughout the 2000s. The 2014-15 Warm Anomaly (spring 2015) produced greater poleward retraction and coastal compression than the 2015-16 El Niño

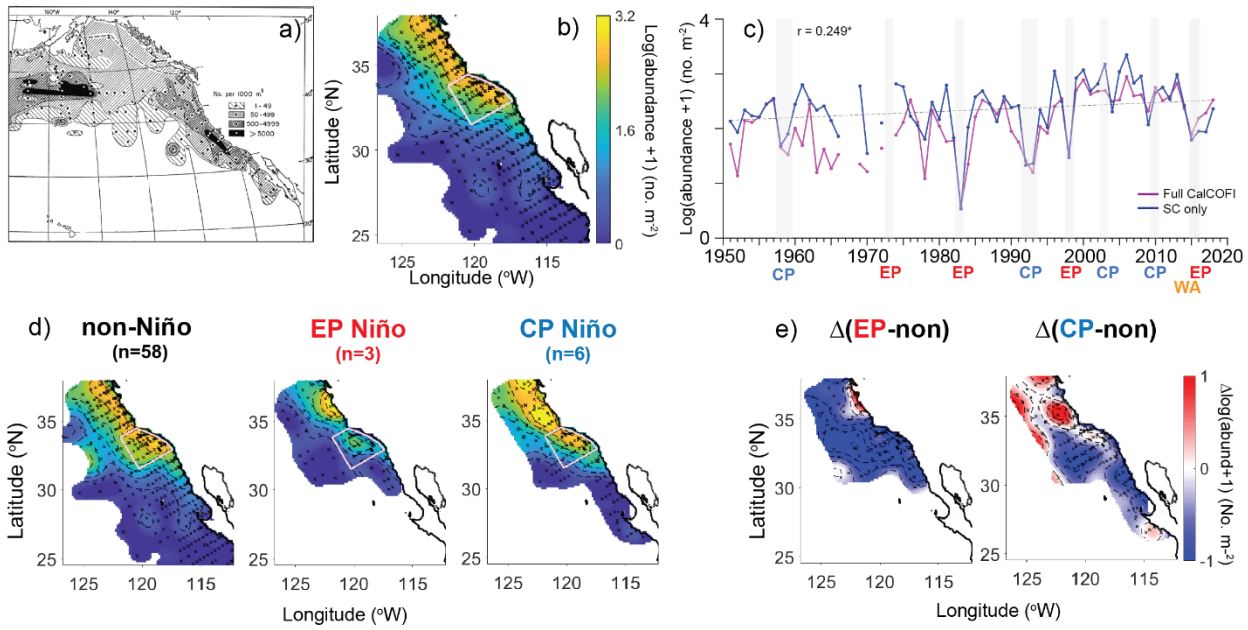

Figure 2.2. *Euphausia pacifica* a) biogeographic affinity from Brinton (1962), b) average spring distribution across full CalCOFI region, c) timeseries of region-averaged spring abundance for full CalCOFI (pink) and SC region only (blue), d) average spring abundance distributions for non-Niño years, EP Niños, and CP Niños, and e) differences between EP or CP and non-Niño averages. 'n' indicates number of years in average. The sampling pattern varies by year, so average maps are calculated from different numbers of stations in different regions (see figure S10 for individual year samples and figure B1 for total number of samples by station). Grey dashed linear fit in 'c' indicates significant long-term SC region trend; Spearman rank significance is shown at top (*p<0.05). Vertical grey bars denote El Niño years (EP – Eastern Pacific; CP – Central Pacific). 1973 was an EP Niño, but zooplankton were not sampled. Black crosses on maps show actual CalCOFI stations sampled. Light pink boxes denote SC region. Maps are objectively mapped representations of CalCOFI data (see Methods and Appendix 2A).

(Fig. S2.10), likely due to the Warm Anomaly's more expansive and persistently warm, low-productivity conditions.

Thysanoessa spinifera is another dominant cool-water species of the central CCS, although it inhabits only neritic upwelling waters with limited offshore extent (Fig. 2.3a-b; see Brinton, 1962). Previous analyses of *T. spinifera* did not detect consistent El Niño variability in regionwide total abundance (Lilly & Ohman, 2018), but the species shows El Niño-related spatial change (Fig. 2.3d). Both the EP and CP average Niño distributions show slight offshore

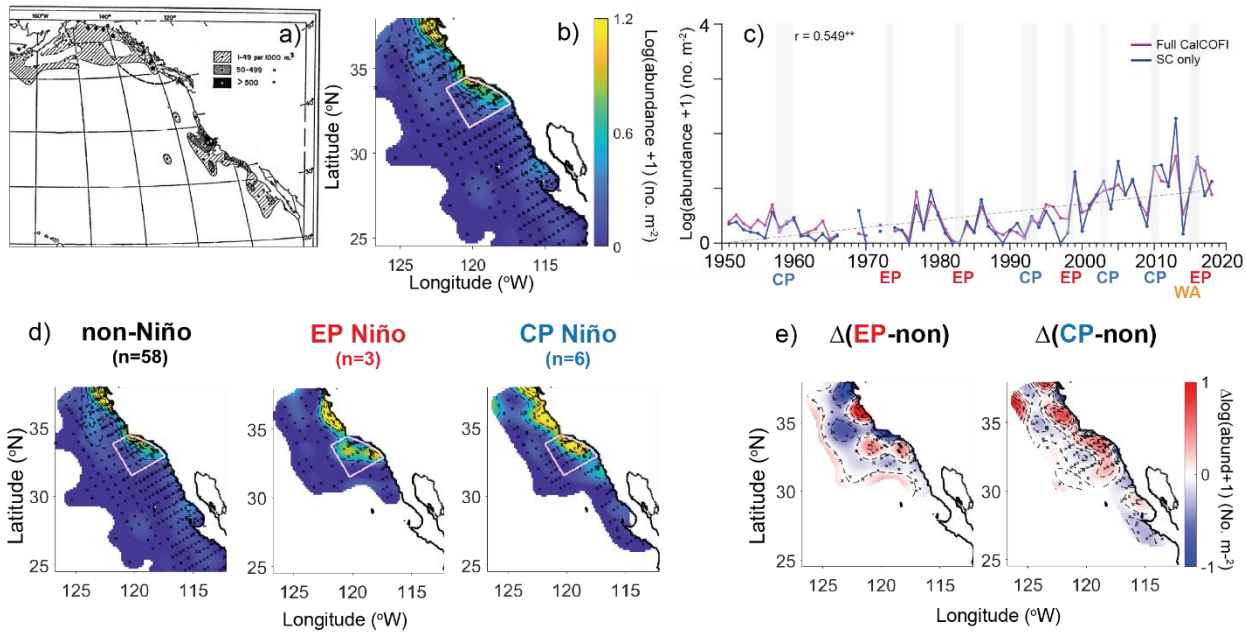

Figure 2.3. As in figure 2.2, but for *Thysanoessa spinifera*. Grey dashed linear fit indicates significant long-term trend; Spearman rank significance shown (**p<0.001).

expansion relative to the non-Niño average, and the '[CP]-[non-Niño]' difference plot shows a slight nearshore increase (Fig. 2.3e), although these patterns are likely dominated by single Niño extreme population increases (EP: 2016, CP: 2010; Fig. S2.11). *Thysanoessa spinifera* was present only at very low abundances in nearshore northern regions in springs 1958-59, 1992-93, and 1998, and completely absent from the CalCOFI region in spring 1983 (Fig. S2.11), likely due to significant reductions in upwelling habitat. These findings are corroborated by shoreward (1993, 2015, 2016) and poleward (1958-59, 1983, 1998) shifts in COG (Fig. S2.1b). As with *E. pacifica*, *T. spinifera* increased in abundance in springs 2003 and 2010 and was notably elevated off Point Conception in spring 2016, likely reflecting the return of upwelling at the end of the 2015-16 El Niño. Regionwide abundance of *T. spinifera* was also high in springs 1999 and 2017, suggesting rapid recovery following El Niño events. Both *E. pacifica* and *T. spinifera* show significant long- term increases in Southern California region average abundance across the

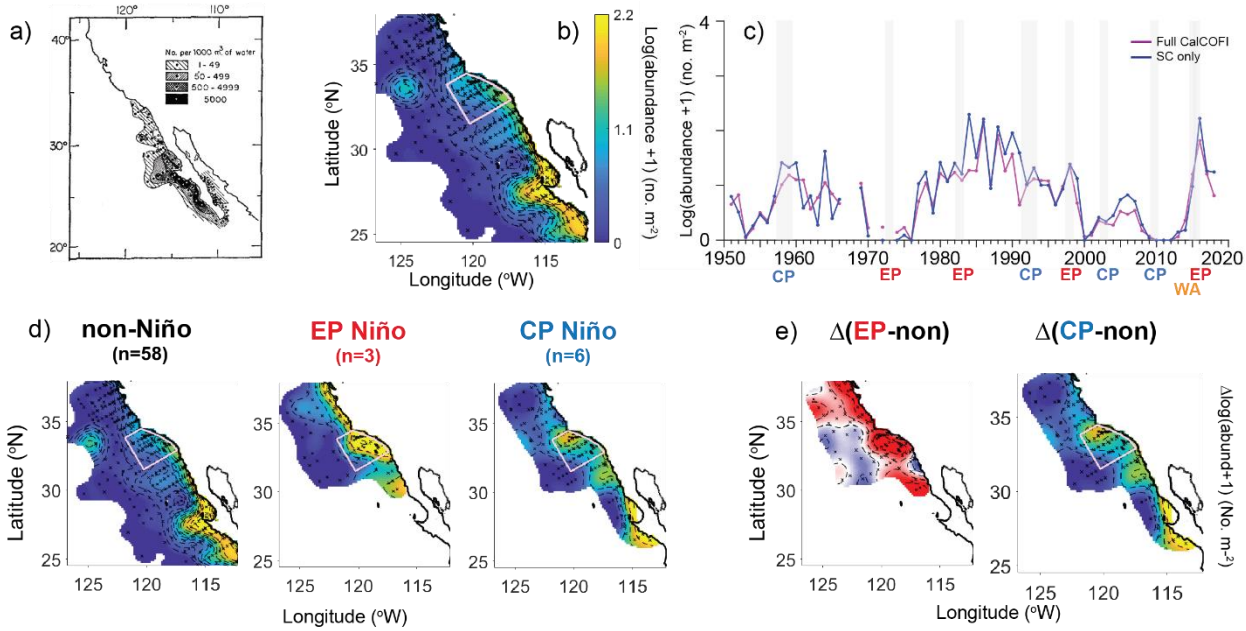

Figure 2.4. As in figure 2.2, but for *Nyctiphanes simplex.* Lack of linear trendline in 'c' indicates no significant long-term trend ($p > 0.05$).

1951-2018 period ($p < 0.05$ and 0.001, respectively; Figs. 2.2c and 2.3c).

2.3.1.2. Subtropical Coastal Species

Nyctiphanes simplex inhabits coastal waters off southern and Baja California and has a similar, though more southerly-centered, distribution to *T. spinifera* (Fig. 2.4a-b; see Brinton, 1962). The mean CalCOFI distribution of *N. simplex* shows a narrow nearshore band of moderate abundance up to Point Conception, CA. Regionwide mean abundance undergoes decadal variability associated with the Pacific Decadal Oscillation (Brinton & Townsend, 2003; Di Lorenzo & Ohman, 2013) but also varies significantly with El Niño events (Fig. 2.4c; Lilly & Ohman, 2018). Average EP and CP Niño distributions of *N. simplex* show clear but different poleward extensions: EP Niños show high abundance in a narrow coastal band, while CP Niños show more spatially diffuse poleward extension and low presence north of Point Conception

(Fig. 2.4d). Average distributions of both Niño categories show significant increases in the nearshore California region compared to the non-Niño average. All El Niño springs except 2003 and 2010, as well as the Warm Anomaly (spring 2015), showed regionwide increases in *N. simplex* abundance (Fig. S2.12). Spring 2016 had the highest *N. simplex* abundance of the timeseries aside from 1984, while the 1983 and 1998 EP Niño springs had the farthest poleward population extensions of any El Niño year, in narrow coastal bands (Figs. S2.1c, S2.12). Such extreme northward extension suggests that these El Niño events likely had a different dominant forcing mechanism (i.e., enhanced poleward advection) than other Niños. In contrast, the 2016 EP Niño spring produced significant offshore expansion in the SC region, similar to two-year CP Niños (springs 1958-59, 1992-93) and the Warm Anomaly (spring 2015) (Figs. S2.1c, S2.12). *Nyctiphanes simplex* was only present in spring 2003 in a low-abundance pocket off Monterey Bay, and completely absent in spring 2010.

2.3.1.3. Tropical Pacific-Baja California Species

Euphausia eximia has a mean distribution centered farther south and offshore than *N. simplex*, extending to the margins of tropical equatorial Pacific waters and mostly absent off California in spring except during El Niño events and the late 1970s (Fig. 2.5; see Brinton, 1962, 1981). *Euphausia eximia* expands shoreward to coastal Baja California during both EP and CP Niños, although only EP events and the Warm Anomaly show spring poleward extension north to the SC region (Fig. 2.5d). Highest *E. eximia* abundance in the SC region occurred during the Warm Anomaly (spring 2015), characterized by COG shifts poleward and onshore, while the 2016 EP Niño distribution was centered farther south (Figs. S2.1d, S2.13). In contrast, *E. eximia* was scarcely or not at all present off California during CP Niño springs except 1992-93. As mentioned for *N. simplex*, EP Niños likely have physical characteristics that induce more

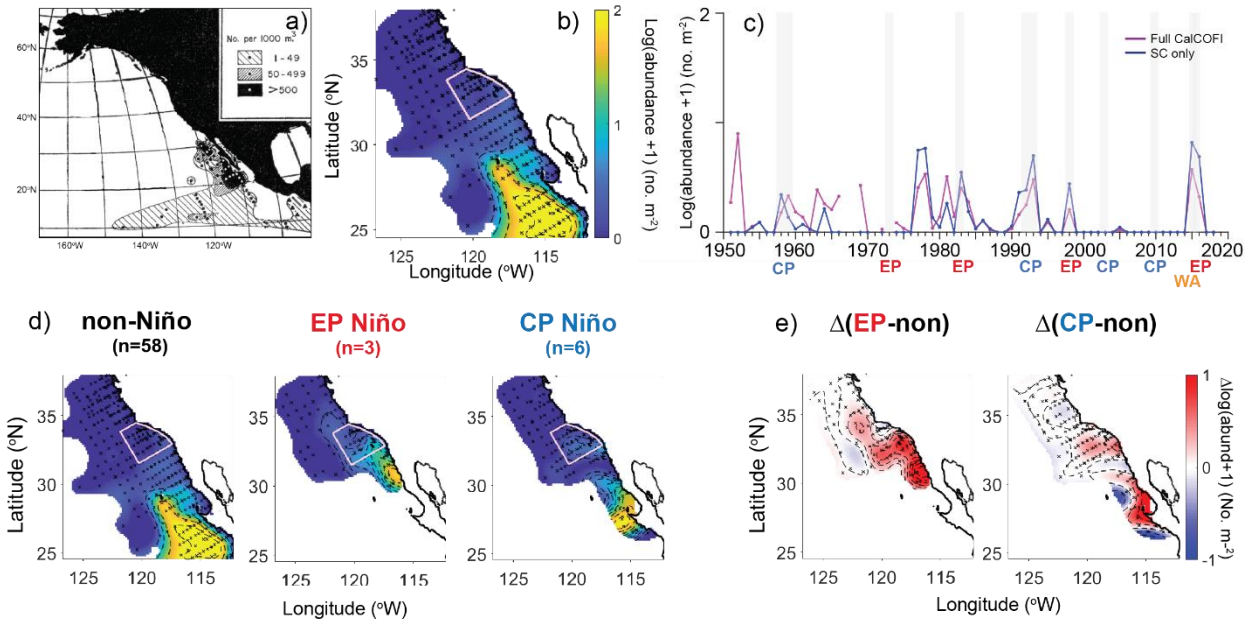

Figure 2.5. As in figure 2.2, but for *Euphausia eximia*. Lack of linear trendline in 'c' indicates no significant long-term trend ($p > 0.05$).

onshore expansion and poleward extension of tropical species than do CP events, explaining the SC region presence of *E. eximia* predominantly during EP Niños.

2.3.1.4. Subtropical Offshore Species

Euphausia gibboides and *E. recurva* classify as subtropical offshore species that inhabit North Pacific Subtropical (Central) Gyre waters, extending eastward to within 100 km of Baja California. Brinton (1962) classified *Stylocheiron affine* as a Baja California/Subtropical species along with *E. eximia*. However, the CalCOFI distribution and El Niño responses of *S. affine* align more closely with those of *E. gibboides* and *E. recurva*, so we categorize it as a Subtropical Offshore response. The three species show very similar El Niño responses, so we focus here on *E. gibboides* (Fig. 2.6, S2.1e, S2.14; see Figs. S2.1f, S2.2, S2.15 for *E. recurva*, and S2.1g, S2.3, S2.16 for *S. affine*). On average, during EP Niños *E. gibboides* expands poleward and shoreward

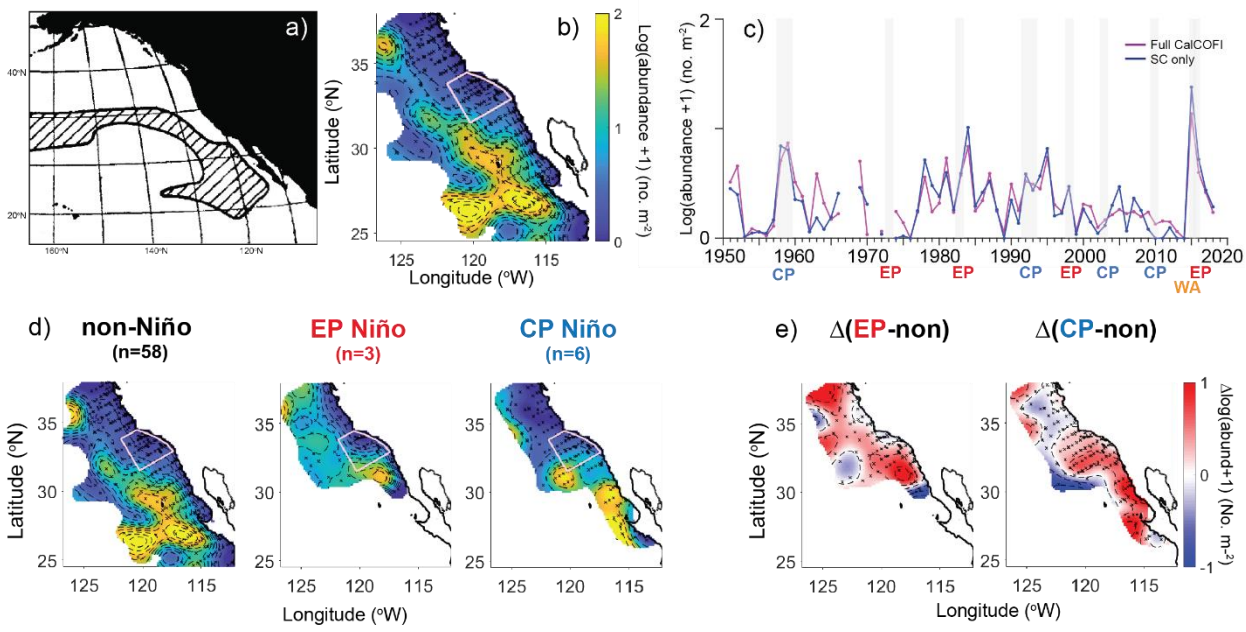

Figure 2.6. As in figure 2.2, but for *Euphausia gibboides*. Lack of linear trendline in 'c' indicates no significant long-term trend ($p > 0.05$).

regionwide except for a narrow coastal band (Fig. 2.6d). In contrast, the average CP Niño distribution shows *E. gibboides* expansion all the way to shore off southern and Baja California, perhaps transported by stronger onshore flows, although it does not extend as far poleward as during EP events. The total area of increase (Fig. 2.6e, sum of all red patches) during EP Niños compared to the non-Niño average is three times greater than the area of no change or decrease (sum of white and blue patches; values not shown), while the area of increase during CP Niños is only moderately greater than the corresponding area of decrease or no change.

However, *E. gibboides* shows variability between El Niño events of a given category (Fig. S2.14): the 1958-59 CP, 1992-93 CP, and 1983 EP Niño springs showed substantial population expansions into the nearshore SC region, though at only moderate abundances, while the 1998 and 2016 EP Niño springs produced elevated abundances offshore. During the 2003 and 2010 CP Niño springs, *E. gibboides* extended poleward offshore. Highest SC abundance and

farthest shoreward expansion of *E. gibboides* occurred during the 2015 Warm Anomaly (Figs. 2.6c, S2.1e). Lack of full shoreward expansion of *E. gibboides* during two EP Niños suggests that offshore species may be inhibited from onshore movement by the strongly anomalous coastal poleward flows of those events. In contrast, anomalous onshore advection and a lack of anomalously strong alongshore flow during other events (e.g., 1983 EP Niño, Simpson (1984); 1992-93 CP Niño, Ramp et al. (1997); 2015 Warm Anomaly, Zaba and Rudnick (2016)) corresponded to farther shoreward population expansions. *Euphausia recurva* and *S. affine* show similar average distributions to *E. gibboides* across Niño categories, although both species extend farther north and *S. affine* extends farther south and has a patchier El Niño distribution (Figs. S2.2-S2.3, S2.15-S2.16).

Euphausia hemigibba has a subtropical-tropical offshore distribution that lies between *E. eximia* and *E. gibboides* (Fig. 2.7a-b; Brinton, 1962; Brinton & Townsend, 2003). Its El Niño responses likewise show characteristics of both *E. eximia* and *E. gibboides*: it has the lowest SC average abundance of all 10 species but a more consistent presence than *E. eximia* (Fig. 2.7c). However, *E. hemigibba* population centers do not extend nearly as far poleward or onshore as *E. gibboides* during either Niño category, remaining mostly off Baja and southernmost California. Total areas of increase of *E. hemigibba* during average EP and CP Niños are slightly greater than areas of decrease (Fig. 2.7e, total red patches [increase] or blue patches [decrease]). As with *E. gibboides*, *E. hemigibba* had highest SC abundance and positive (poleward) COGy shifts during the 2015 Warm Anomaly, elevated offshore abundance and poleward extension in springs 1993 and 1998, and moderate offshore elevated populations in 1958-59, 1983, and 2016 (Figs. S2.1h, S2.17).

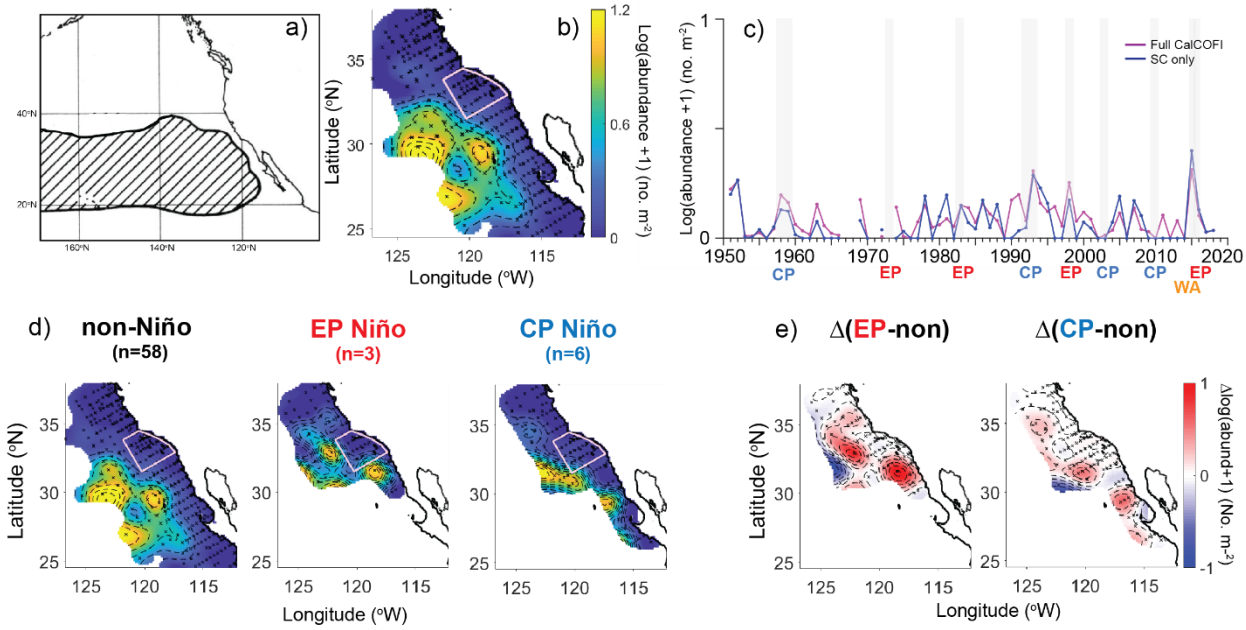

Figure 2.7. As in figure 2.2, but for *Euphausia hemigibba.* Lack of linear trendline in 'c' indicates no significant long-term trend ($p > 0.05$).

2.3.1.5. Regionwide Temperate Species

Nematoscelis difficilis and *Thysanoessa gregaria* are temperate-to-cool species that extend from the North Pacific Current (~40°N) to southern Baja California and to 300 km offshore (Figs. 2.8a-b, 2.9a-b; see Brinton, 1962, 1981). *T. gregaria* is displaced slightly offshore from *N. difficilis* and was classified by Brinton (1981) as an Intermediate Subtropical species. *Nematoscelis difficilis* is the second most abundant species in the CCS after *E. pacifica* (Fig. 2.8c; see Brinton & Townsend, 2003). Regionwide abundance of *N. difficilis* is relatively consistent across Niño and non-Niño years, with dips in 1983, 1992-93, and 2003 (Fig. 2.8c). *Thysanoessa gregaria* shows similar, though greater and more prolonged, decreases in abundance during the same events and 1958-59 (Fig. 2.9c). Average EP and CP distributions for both species are similar to non-Niño years, although with minor increases in the northern coastal California region during EP Niños and substantial decreases in the southern region during both

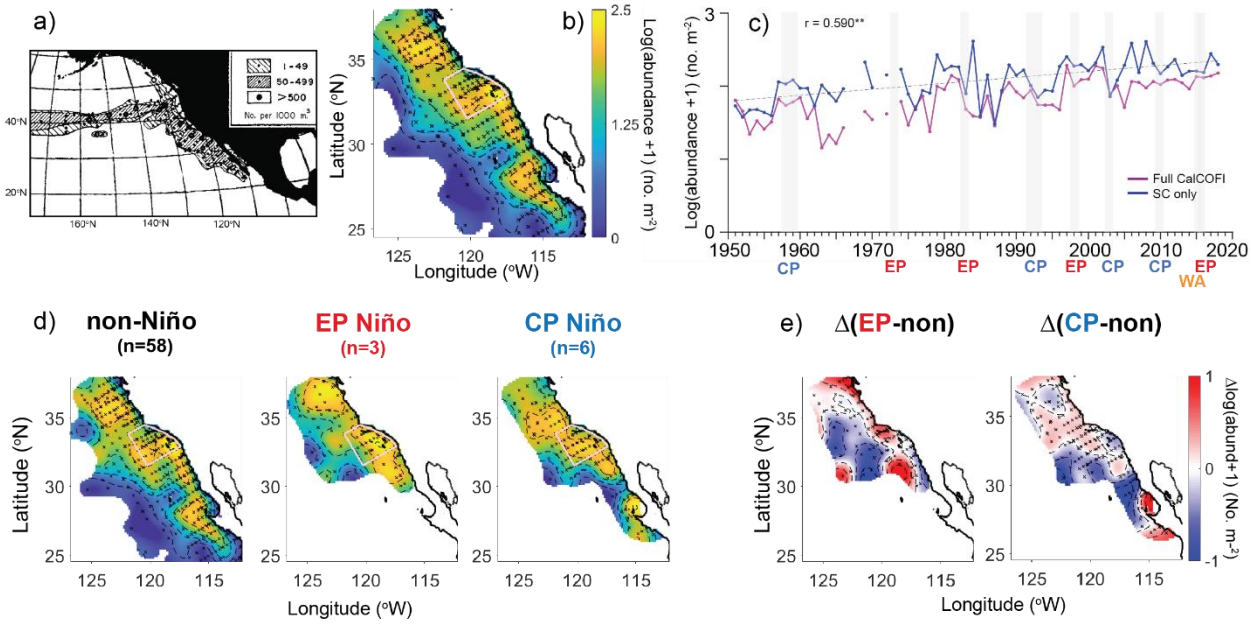

Figure 2.8. As in figure 2.2, but for *Nematoscelis difficilis.* Grey dashed linear fit indicates significant long-term trend; Spearman rank significance shown (**p<0.001).

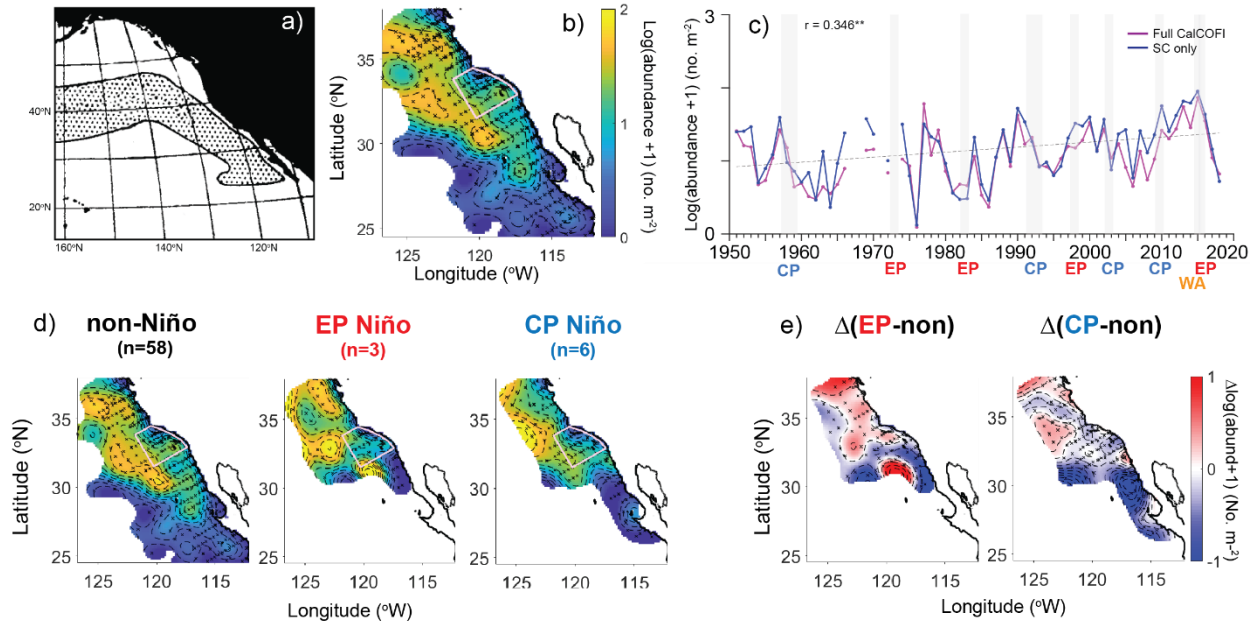

Figure 2.9. As in figure 2.2, but for *Thysanoessa gregaria.* Grey dashed linear fit indicates significant long-term trend; Spearman rank significance shown (**p<0.01).

EP and CP Niños (Figs. 2.8d-e, 2.9d-e). Centers of gravity were generally insensitive to population shifts because both species have consistent regionwide distributions (Fig. S2.1i-j). As with other cool-water species, *N. difficilis* and *T. gregaria* show significant long-term abundance increases in the SC region ($p < 0.001$ and 0.01, respectively).

2.3.2. El Niño-related habitat variability

2.3.2.1. Spring habitat distributions and source water masses

To determine El Niño-related variability in euphausiid habitats, we analyzed species abundances in comparison to four habitat variables measured at each CalCOFI station (Figs. 2.10, S2.4; see Tables S2.1 for mean distribution values and S2.2 for Kruskal-Wallis values of similarity comparisons across Niño types for a given variable). We focus on spring distributions but also analyzed habitat variables in winter (Section 2.3.2.2.: DJF, 1951-2002; Fig. S2.4, Tables S2.3-S2.4). To determine species associations with certain water masses, we further analyzed euphausiid abundance distributions in relation to proportions of three dominant water masses that comprise the SC region (Figs. 2.11, S2.5, Tables S2.5-S2.6). Pacific Subarctic Upper Water (PSUW) is southward-flowing, cool, high-oxygen, and indicative of the core CA Current; Pacific Equatorial Water (PEW) is warm, salty, subsurface, nearshore poleward-flowing, and indicative of the CA Undercurrent; and Eastern North Pacific Central Gyre Water (ENPCW) is warm, moderately salty, near-surface, and of southwestern offshore origin (see Methods Section 2.2.5.2 and Bograd et al. (2019) figures 1 and 2 for complete information). We present species abundance distributions across proportions of each water mass, where proportion is the contribution of that water mass to the total regional water makeup (sum of all water masses). We also show the mean proportion of each water mass averaged across the SC region and all years

within each Niño category (see arrows below x-axes in figures 2.11 and S2.5; colors correspond to Niño category).

2.3.2.1.1. Cool-Water, Coastally-Associated species

Consistent with their spatial distributions, *Euphausia pacifica* and *Thysanoessa spinifera* inhabit upwelling-characteristic waters (cool, salty, low O_2, higher Chl-*a*) (Fig. 2.10a-h). During EP Niños, the *E. pacifica* distribution shifts even farther into these conditions, reflecting spatial compression to only nearshore waters. In contrast, *T. spinifera* habitat remains consistent across non, EP, and CP Niños. Water mass associations indicate that during EP Niños, *E. pacifica* associates with higher proportions of PSUW and lower PEW than the mean regional proportions of each water mass, reflecting northward population compression into PSUW waters (Fig. 2.11a-b, Table S2.5; vertical arrows below x-axes indicate mean regionwide water mass proportions for each Niño category). Association of *E. pacifica* during CP Niños with lower PSUW and higher PEW reflects the species' elevated coastal presence in 2003 and 2010. *Thysanoessa spinifera* has similar water mass associations to *E. pacifica* across non-Niño and CP Niño types but much lower association with PSUW and higher associations with PEW and ENPCW during EP Niños (Fig. 2.11d-f). These differences likely reflect a combination of the more neritic distribution of *T. spinifera*, stronger shoreward compression during EP Niños, and population extension farther south into the SCB (ENPCW waters) in spring 2016 (Figs. 2.3d, S2.11).

2.3.2.1.2. Subtropical Coastal species

Nyctiphanes simplex shows habitat characteristics between cool-water coastal species and subtropical offshore-tropical species (Fig. 2.10i-l), reflecting its intermediate distribution as a subtropical but coastal species that regularly inhabits the nearshore Southern California Bight. Although *N. simplex* extends significantly poleward during EP Niños, it does not show dramatic

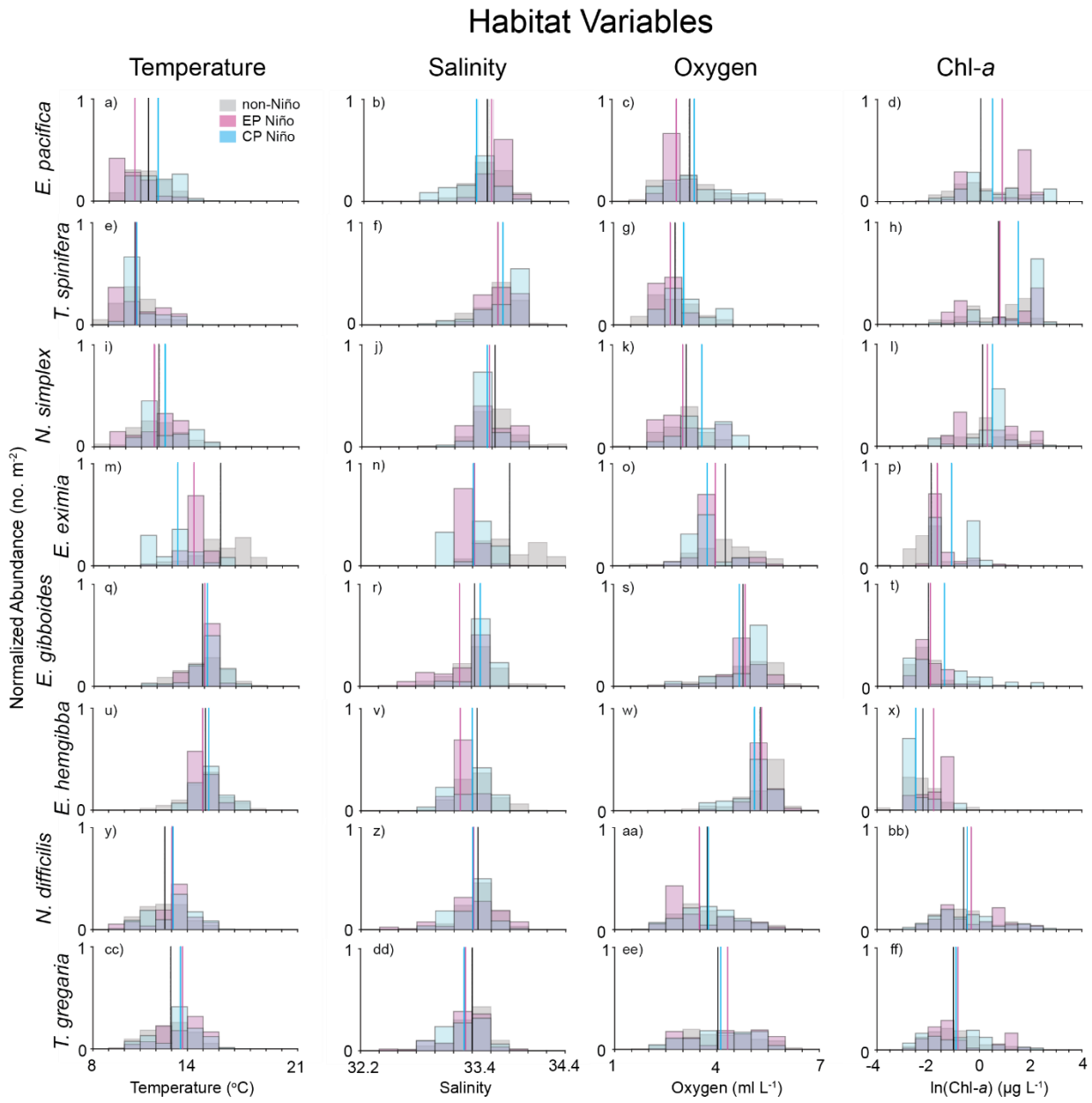

Figure 2.10. Spring abundance-weighted species distributions across four habitat variables: temperature at 50 m depth, salinity at 50 m, oxygen at 100 m, ln(chlorophyll-a) at 10 m. Vertical bars indicate means for each Niño type (grey bars and black line – non-Niño; pink bars and line – EP Niño; blue bars and line – CP Niño). See figure S2.4 for the remaining two species.

habitat shifts, suggesting that the population may initially be advected in conjunction with parent water masses. Elevated oxygen habitat during CP Niños could reflect outward population

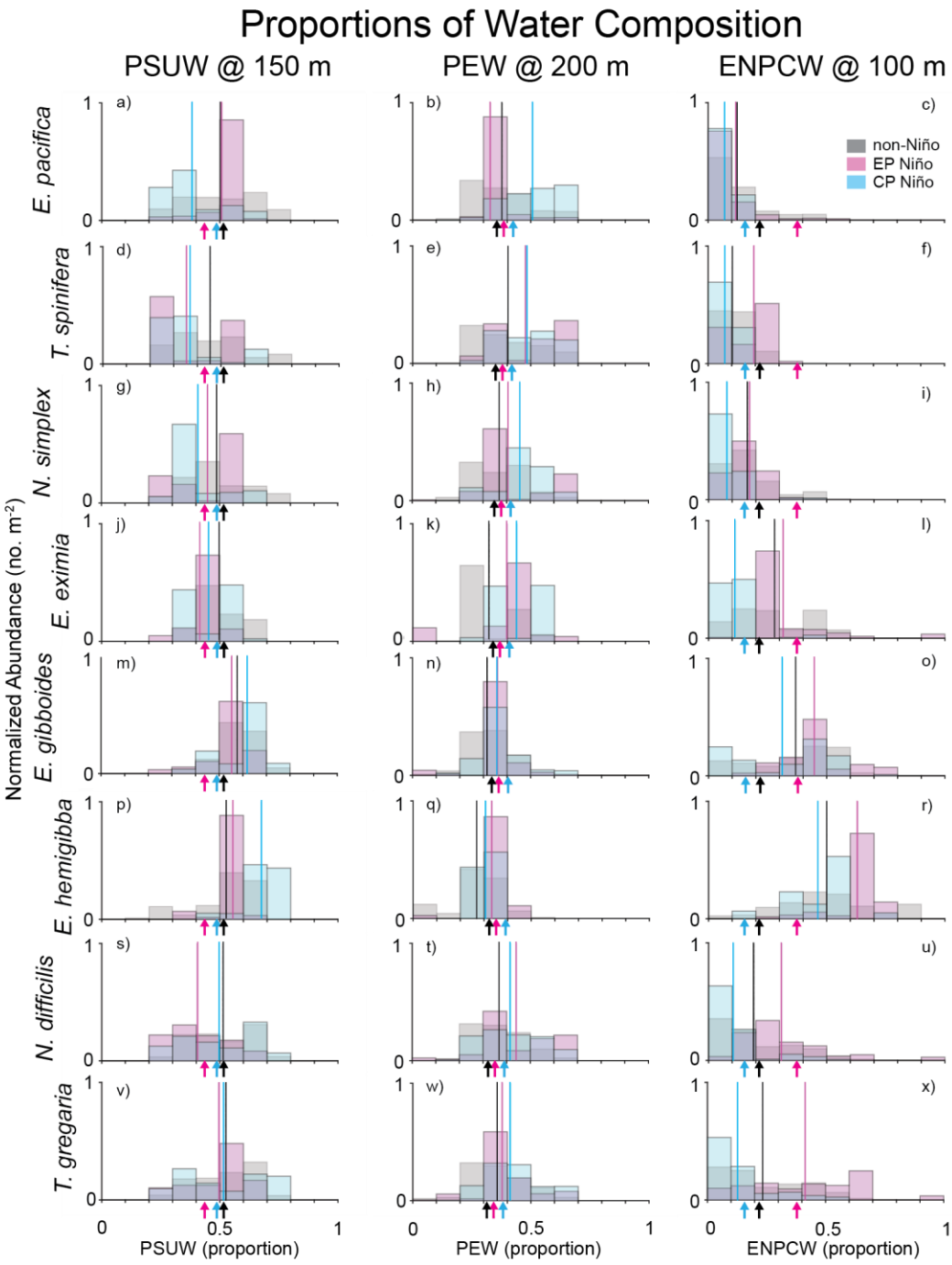

Figure 2.11. Spring species abundance distributions for proportions of three water masses (Pacific Subarctic Upper Water, PSUW; Pacific Equatorial Water, PEW; Eastern North Pacific Central Gyre Water, ENPCW) at given depths. Data are from the SC region only, 1985-2017. Arrows below x-axes indicate mean water mass proportions across the entire SC region and time period.

expansion toward the core California Current, while slightly warmer temperatures could reflect its center in more southerly and somewhat offshore waters off Baja California compared to its nearshore poleward transits during EP Niños (Fig. 2.10k). As with habitat characteristics, *N. simplex* shows similar water mass associations to *E. pacifica*, though lower PSUW and higher PEW during EP Niños and higher ENPCW across all years, reflecting its southerly and nearshore distribution (Fig. 2.11g-i).

2.3.2.1.3. Tropical Pacific-Baja California species

Euphausia eximia inhabits a significantly different habitat during EP and CP Niños compared to non-Niño years (Fig. 2.10m-p). During non-Niño years, *E. eximia* inhabits the warmest, saltiest waters of all our species. During El Niños it shifts to cooler, fresher, lower-O_2, higher-Chl-*a* waters, with greatest shifts during CP Niños. These changes corroborate the hypothesis of El Niño advection of *E. eximia* into cooler, fresher waters off southern California from its normal southern warm, salty, tropical habitat. *Highest E. eximia* abundances occur at the mean proportions of PSUW and PEW across all Niño categories, again suggesting Niño-related population advection into the SC region with certain water masses (Fig. 2.11j-l). Low associations of *E. eximia* with ENPCW during EP and CP Niños suggest that it moves into the SC region via coastal PEW rather than offshore ENPCW.

2.3.2.1.4. Subtropical Offshore species

Euphausia gibboides inhabits a narrow temperature range with mean values similar to *E. eximia*, but lowest salinity and Chl-*a* and highest O_2 ranges of all species analyzed, reflecting offshore, subtropical, Central Gyre-associated habitat (Fig. 2.10q-t). Consistent habitat distributions across Niño categories suggest advection with parent water masses (i.e., enhanced onshore flow during some Niños) rather than species movement into dramatically new

environments. The low-salinity distribution may come from the portion of the *E. gibboides* population that overlaps the fresh core California Current, and appears to be strongest during EP Niños, perhaps due to shoreward expansion (Fig. 2.10r). *Euphausia recurva* and *S. affine* have similar habitat distributions to *E. gibboides*, although slightly lower oxygen (both species) and higher Chl-*a* (*S. affine*), reflecting farther shoreward intrusions (Fig. S2.4, rows f-g). *Euphausia hemigibba* has similar habitat ranges to *E. gibboides*, although the highest O_2 and lowest Chl-*a* of the ten species (Fig. 2.10u-x).

Water mass associations indicate that *E. gibboides* inhabits high proportions of PSUW and ENPCW and low PEW across all Niño categories, reflecting its offshore distribution (Fig. 2.11m-o). Associations with decreased ENPCW and increased PSUW during CP Niños may reflect offshore northward population expansion, while opposite associations during EP Niños indicate onshore expansion into the southern SC region. Both *E. recurva* and *S. affine* have similar water mass associations to *E. gibboides*, although stronger PEW (*S. affine*) and ENPCW (both species) during EP Niños, likely due to shoreward population incursions into the SCB (Fig. S2.5). *Euphausia hemigibba* associates with all three water masses similarly to *E. gibboides* but with lower PSUW and PEW and the highest ENPCW association of any species, reflecting its presence predominantly in the southern offshore CCS (Fig. 2.11p-r).

2.3.2.1.5. Regionwide Temperate Species

Nematoscelis difficilis and *T. gregaria* have comparable habitat ranges and habitat consistency across Niño categories. The habitat ranges of *T. gregaria* are slightly higher-O_2 and lower-Chl-*a* than for *N. difficilis*, reflecting the *T. gregaria* center farther offshore (Fig. 2.10y-ff). Water mass associations of both species are comparable to *E. pacifica* for PSUW and PEW across most Niño categories, and align with the mean proportions of each water mass for the

region (Figs. 2.11s-w). Both species are positively associated with ENPCW across all Niño categories, reflecting their elevated presence in the offshore SCB (Figs. 2.11u,x).

2.3.2.2. Winter-Spring habitat shifts (all species)

Winter habitat conditions of cool and warm coastally-associated species (*E. pacifica, T. spinifera, N. simplex*) are warmer, fresher, higher-O_2, and lower-Chl-*a* than their corresponding spring distributions across all Niño categories, reflecting the usual winter-to-spring transition to upwelling conditions (Fig. S2.4, rows a-c; spring plots are reproduced from figure 2.10). Habitat distributions of coastal species during EP Niño winters show significantly higher temperatures and lower oxygen than during non-Niños, emphasizing winter onset of El Niño conditions. Winter initiation of extreme EP Niño conditions likely induces population die-off and reduced reproduction of cool-water coastal species that cannot tolerate such extremes, explaining spring shoreward compressions and poleward retractions (Figs. 2.2d, 2.3d).

In contrast, winter distributions of *E. eximia* are largely consistent across Niño categories, and generally align with the species' spring non-Niño distributions (Fig. S2.4, row d). Only during El Niño springs does *E. eximia* shift into significantly altered waters with characteristics of the core California Current, suggesting late winter-spring population poleward advection during EP events. In contrast, winter distributions of *E. gibboides* align with its spring habitat, further corroborating the idea of population movement with parent water masses; the exception is elevated winter temperatures during EP Niños, likely due to regionwide warming (Fig. S2.4, row e). This interpretation is corroborated by similar winter/spring distributions and EP Niño shifts of *E. recurva* and *S. affine*, since all three species inhabit the same waters (Fig. S2.4, rows f-g). *Euphausia hemigibba* has higher overall temperature and oxygen ranges than the above

three species but also shows consistency between winter and spring distributions (Fig. S2.4, row h). As with cool-water coastal species, regionwide temperate species (*N. difficilis, T. gregaria*) inhabit significantly warmer waters during EP Niño winters relative to non-Niño years (Fig. S2.4, rows i-j), which may instigate subsequent spring population die-off and reduced growth in offshore waters. However, the overall temperature and salinity ranges of *N. difficilis* and *T. gregaria* during both EP and CP Niño groups are the same as for non-Niño years, perhaps reflecting the sub-thermocline ranges of these species and therefore their lower susceptibility to El Niño.

2.3.3. Population structure during El Niño

To determine whether euphausiid population stage structure, as an index of potential population growth, is impacted by El Niño, we first examined SC region-averaged spring proportions of adult and calyptopis stages for each species across each El Niño event and surrounding years (Figs. 2.12, S2.6). We then examined spring habitat ranges for the calyptopis phase only, to determine whether reproduction occurs across a species' habitat range or only in a subset of conditions (Fig. S2.7, Tables S2.7-S2.8).

2.3.3.1. Cool-water, Coastally-associated species

Euphausia pacifica spring adult and calyptopis proportions did not change appreciably during CP Niños from surrounding years, while responses to EP Niños differed by event (Fig. 2.12a). The adult phase dominated *E. pacifica* during the 1983 event, suggesting reduced reproduction and calyptopis production or survival, while both 1998 and 2015-2016 had elevated calyptopis proportions, suggesting return of population reproduction in those El Niño/Warm Anomaly springs. Brinton (1962) noted relatively equal adult and larval calyptopis proportions in

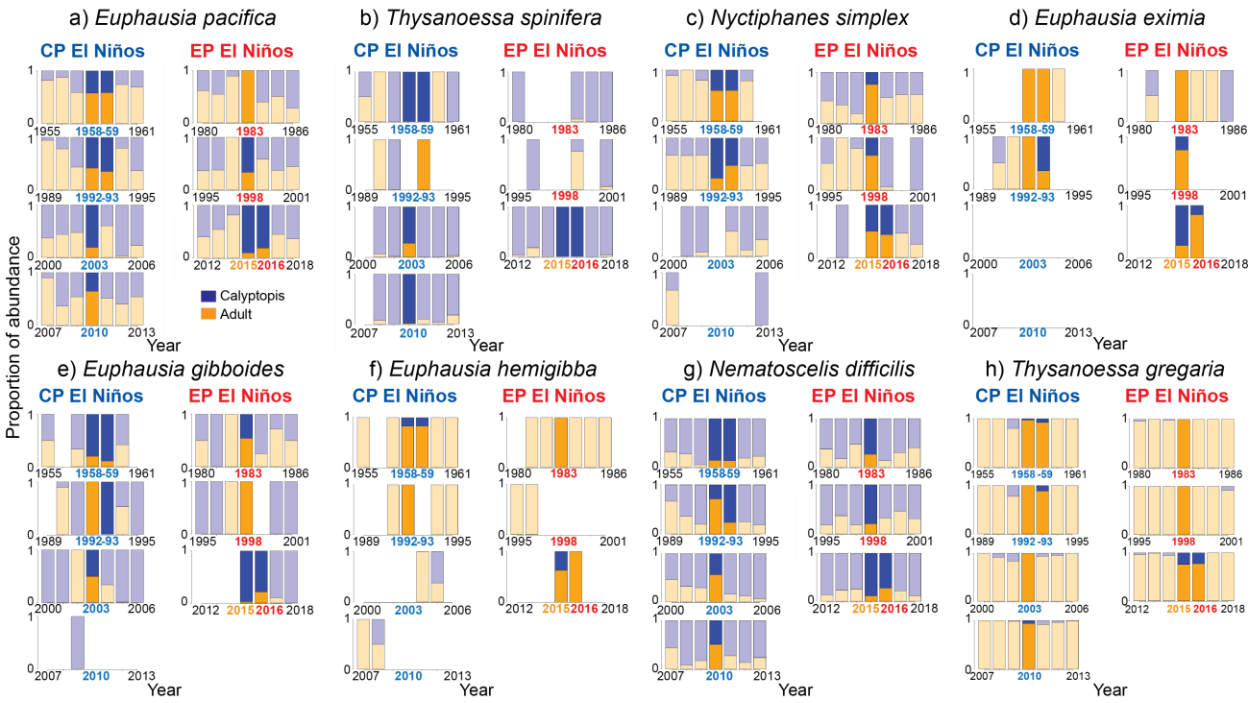

Figure 2.12. Average proportions of adult (orange) and calyptopis (blue) SC region spring abundance during each El Niño year (bold colors) and the three prior and three following years (pale colors). Proportions are calculated of the sum(adult+calyptopis). Lack of bars indicates a lack of both the adult and calyptopis phases, although furcilia or juvenile phases may be present.

the Eastern North Pacific, so short-term dominance by one phase likely reflects temporary increases or decreases in reproduction. In contrast, *T. spinifera* is the species most consistently dominated by the calyptopis phase in the SC region in spring (Fig. 2.12b; Brinton, 1962). However, in three post-Niño years (1960, 1993, 1999), notably after complete absences of both adult and calyptopis phases in 1992 and 1997-1998, *T. spinifera* was only present in adult forms. Calyptopis phases of both *E. pacifica* and *T. spinifera* had similar habitat ranges to their total populations, suggesting reproduction habitat-wide rather than only in a subset of conditions (Fig. S2.7a-h).

2.3.3.2. Subtropical Coastal species

Nyctiphanes simplex had higher calyptopis proportions during the 1958-59 and 1992-93 CP Niños and the 2015-2016 Warm Anomaly-El Niño springs compared to surrounding years (Fig. 2.12c), suggesting enhanced *in situ* reproduction under prolonged favorable conditions. In the 1983 and 1998 Niño springs, proportions of *N. simplex* calyptopes were relatively low (Fig. 2.12c), perhaps due to wintertime increases in abundance that grew to adult populations by spring. *N. simplex* calyptopes inhabit fresher, higher-oxygen, higher-Chl-*a* waters than the total population during non-Niño years, suggesting preferential reproduction in California Current waters rather than off Baja California (Fig. S2.7i-l). During El Niños, *N. simplex* calyptopis and total population habitats are similar, suggesting consistent advection across life history phases.

2.3.3.3. Tropical Pacific-Baja California species

Euphausia eximia has a consistently adult-dominated population stage structure across years in the SC region (Fig. 2.12d; see Brinton, 1962). Only springs 1993 and 2015 had significant calyptopis proportions, perhaps due to favorable reproductive habitat following entire years of sustained elevated temperatures. *Euphausia eximia* calyptopes inhabit similar waters to the total population in non-Niño years but upwelling-characteristic waters during EP and CP Niños, suggesting possible coastal reproduction following advection of adults (Fig. S2.7m-p).

2.3.3.4. Subtropical Offshore species

Euphausia gibboides occurs mostly in calyptopis form in upper waters of the SC region (Brinton, 1962), except before and during some Niño events (1983, 1992, 1998, 2003; Fig. 2.12e). Increased adult proportions during those years could suggest increased advection from offshore Baja California, where shallower waters tend to be dominated by adult rather than calyptopis forms. Subsequent increases in calyptopis phase could indicate increased *in situ* reproduction by adult populations. Unlike *E. gibboides*, however, both *E. recurva* and *S. affine*

are generally dominated by the adult phase in the SC region (Fig. S2.6), consistent with previous measurements of shallower adult and deeper calyptopis phases (Brinton, 1962). Notably, *S. affine* occurs in entirely adult forms across all years analyzed except 1998, 2003, and four non-Niño years (Fig. S2.6b). Calyptopis habitat of *E. gibboides* is slightly warmer and higher-oxygen than for its total population, suggesting preferential reproduction and calyptopis dominance offshore (Fig. S2.7q-t). Calyptopis habitat of *E. recurva* is nearly identical to its total population, although slightly saltier and lower-oxygen, while the *S. affine* calyptopis phase inhabits fresher, higher-oxygen waters than its total population, notably during El Niño, suggesting elevated reproduction in the core California Current (Fig. S2.7u-bb).

Euphausia hemigibba is almost entirely adult phase in the SC region except during the 1958-59 El Niño and 2015 Warm Anomaly (Fig. 2.12f). As for *E. eximia*, dominance by adult forms of *E. hemigibba* may reflect preferential survival of adults and only *in situ* reproduction during periods of prolonged or sufficiently elevated temperatures in the SC region. Non-Niño calyptopis distributions of *E. hemigibba* have similar mean values to the total population, although broader distributions (Figs. 2.10u-x, S2.7cc-ff), but El Niño calyptopis abundances were too sparse to determine habitat ranges.

2.3.3.5. Regionwide Temperate Species

Nematoscelis difficilis shows predominantly calyptopis phase in the SC region, while *T. gregaria* is dominated by adult forms (Fig. 2.12g-h; Brinton, 1962). The exceptions are increased proportions of *N. difficilis* adult forms during some CP Niños, perhaps reflecting decreased reproduction *in situ*, and minor presences of *T. gregaria* calyptopes at the ends of two-year CP Niños and the 2015-2016 Warm Anomaly-El Niño combination. The *N. difficilis* calyptopis habitat distributions are similar to its total population, with slightly lower mean oxygen and

higher Chl-*a* across all Niño categories suggesting slight preferential reproduction in upwelling waters (Figs. 2.10y-bb, S2.7gg-jj). The *T. gregaria* calyptopis habitat is higher temperature, salinity, and Chl-*a* and lower oxygen relative to its total population during both EP and CP Niños, similarly suggesting preferential reproduction in nearshore waters (Figs. 2.10cc-ff, S2.7kk-nn).

2.3.4. Generalized Additive Models and future predictions of distributional shifts

2.3.4.1. Generalized Additive Models of current habitat

We developed generalized additive models (GAMs) to evaluate dominant habitat influences on each species (see figures 2.13 and S2.8 for equations and component plots, and Table S2.9 for model statistics). Inclusion of 'Year' as a categorical variable was essential to account for substantial interannual variability in abundances of several species and to produce appropriate model residuals. Further adding Niño categories (non, EP, CP) or Niño indices (e.g., Niño3.4, San Diego Sea Level Anomaly) did not improve model results, so we considered one model for each species across all Niño categories. Models for all species except *N. difficilis* explain at least 40% of distributional deviance; *N. simplex* has highest deviance explained (70.8%; Table S2.9). Every GAM has a significant latitude/longitude term except for *E. recurva*.

Optimal GAMs are similar, though not identical, for spatially similar species: *E. pacifica* and *T. spinifera* both have dominant temperature terms and an influence of Chl-*a*, although *T. spinifera* is also affected by oxygen (Fig. 2.13). Unlike *E. pacifica,* the *N. simplex* GAM includes interaction terms of oxygen with temperature and Chl-*a*. *Euphausia eximia* and *E. hemigibba* are both modeled only by temperature-oxygen interactive effects and geographic positions,

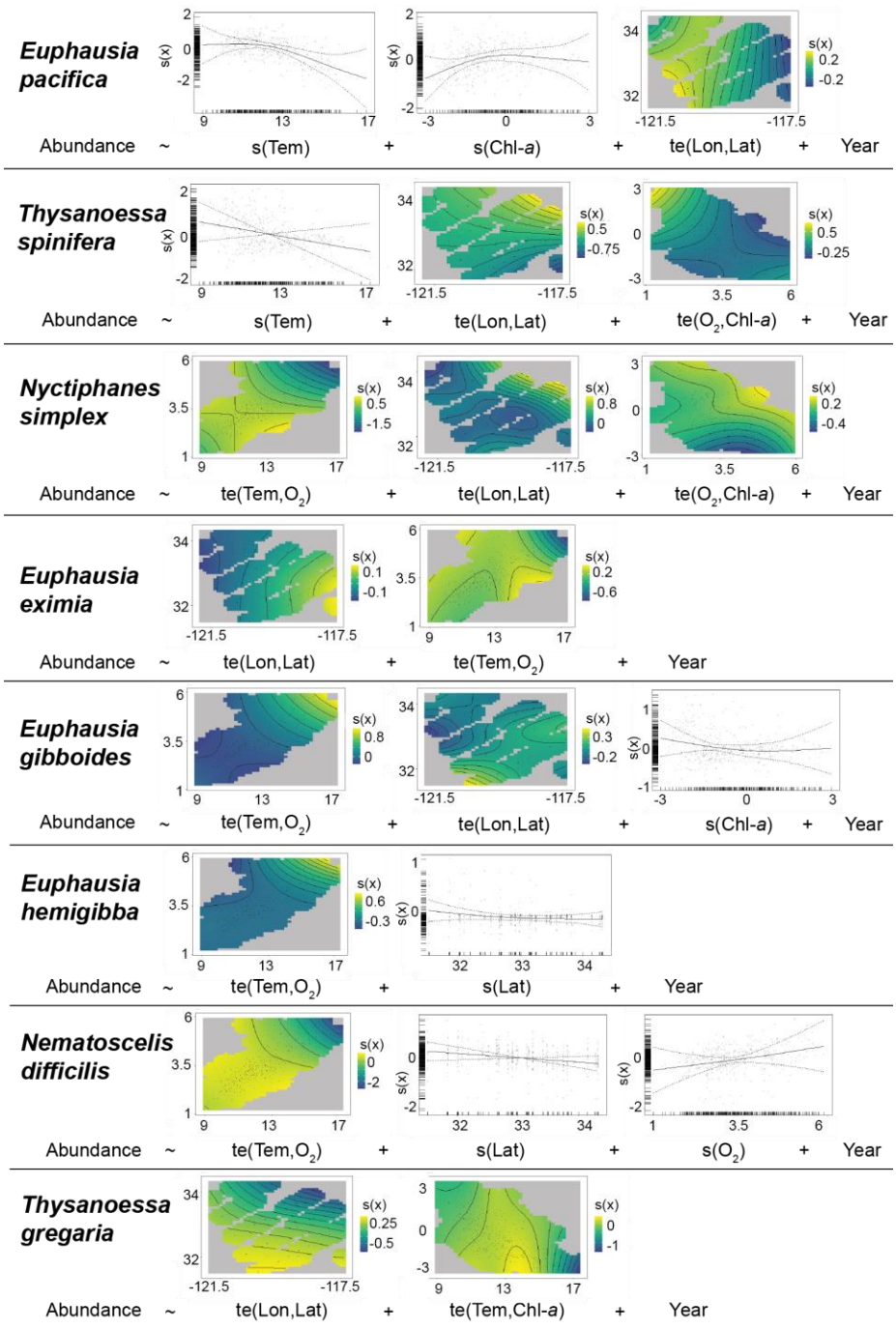

Figure 2.13. Generalized additive model (GAM) optimal equations and outputs, where species spring abundance is modeled as a combination of habitat variables. Abundance is $\log_{10}$-transformed; Chl-*a* is natural log-transformed. Model terms and plots are ordered by decreasing significance (*left to right*). For two-variable terms, the first term listed in parentheses is the x-axis term, and the second is the y-axis term. Numbers of knots associated with each term are listed in Table S2.7. 's' = single-variable smoothers, 'te' = tensor smoothers for interactive terms. GAMs were modeled for the SC region only, 1984-2017.

indicating the dominant effect of warm, high-oxygen waters in defining their habitats. Subtropical offshore species (*E. gibboides* [Fig. 2.13], *E. recurva* and *S. affine* [Fig. S2.8]) are best modeled by combinations of temperature, oxygen, and Chl-*a*, reflecting consistent habitats defined by specific ranges of conditions. Of the two cool-water cosmopolitan species, *N. difficilis* is strongly influenced by oxygen while *T. gregaria* shows stronger temperature and Chl-*a* effects. GAMs showed only minimal increases in AIC and decreases in percent deviance explained when latitude/longitude terms were removed, with all remaining terms still significant (Table S2.9, bottom rows for first four species). Cross-validation tests subsetting out a single year and using all other years to predict its abundances produced significant correlation values (measured against GAM-predicted abundance) for 80% of years.

2.3.4.2. Future predictions of distributional shifts

Using the GAMs developed for each species, as well as documented trends of increasing temperature and Chl-*a* and decreasing dissolved oxygen, we projected future (Year 2100) expected distributions of each species for each Niño category, including future non-Niño conditions (Figs. 2.14, S2.9; see Methods Section 2.2.7). These analyses assume euphausiid associations with habitat variables will remain unchanged through time and across the spatial domain of the southern CCS.

2.3.4.2.1. Cool-Water, Coastally-Associated species

Future predictions of *E. pacifica* distributions suggest moderate regionwide increases during non-Niño years but decreased abundance coastally during EP Niños compared to the present EP distribution (Fig. 2.14a). This change is likely due to reduced suitable habitat resulting from predicted temperature increases. Future EP Niño predictions show patchy areas of

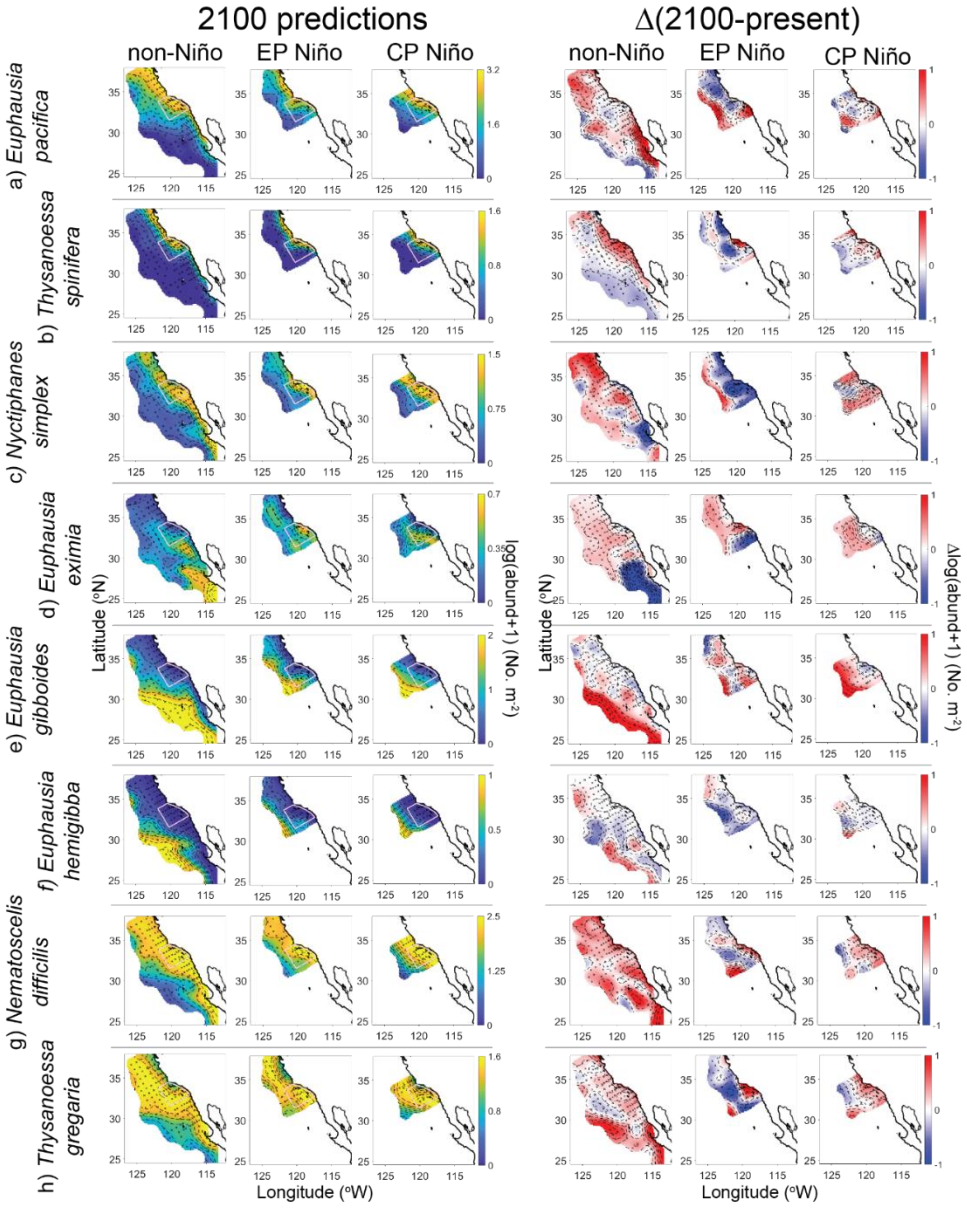

Figure 2.14. (*left panel*) Predictions of euphausiid species spring distributions under average non-Niño, EP Niño, and CP Niño conditions in 2100, using GAMs from figure 2.13 and habitat variables adjusted to Year 2100 predicted values. (*right panel*) Differences between Year 2100 predictions and current average distributions. Spatial coverage during El Niño years is lower than in Figs. 2.2d-2.9d due to lack of input variables at certain stations. All units are log(abundance+1), as (No. m^{-2}).

increase or decrease, while CP predictions show broader areas of minor to moderate increase

(Fig. 2.14a, right panels). *Thysanoessa spinifera* shows similar predicted distributions for all

Niño categories, with populations confined to a narrow nearshore band (Fig. 2.14b, left panels).

Changes from present distributions vary, however: predictions for non-Niño conditions suggest

distributional increases across the nearshore region, likely related to predicted increases in Chl-*a*. In contrast, future EP abundances of *T. spinifera* are lower than the present average, and total area of decrease is substantially greater than area of increase (Fig. 2.14b, right panels). These projected decreases are likely due to comparison to the inflated present distributional average caused by high 2016 EP abundance, as noted in Section 2.3.1.1.

2.3.4.2.2. Subtropical Coastal species

Nyctiphanes simplex increases regionwide and extends northward under future non-Niño and CP Niño conditions but decreases coastally during EP Niños (Fig. 2.14c, left panels), with a greater total area of decrease than of increase from the current EP distribution (Fig. 2.14c, right panels, sum of red regions). This decrease may reflect the importance of enhanced Niño poleward advection, which our GAMs did not include, in increasing *N. simplex* populations.

2.3.4.2.3. Tropical Pacific-Baja California species

Euphausia eximia shows similar future non-Niño distributions to present, with lower abundance off Baja California possibly due to declining oxygen (Fig. 2.14d, left panels). However, total area of increase during future non-Niño conditions is substantially greater than area of decrease (Fig. 2.14d, first panel of right column). Future EP and CP Niño conditions also produce favorable regionwide habitat and greater total areas of increase than of decrease from corresponding present distributions (Fig. 2.14d, right panels). Presence of *E. eximia* calyptopes during the 1991-93 El Niño and 2014-15 Warm Anomaly suggests reproduction can occur in the SC region under sufficiently warm conditions, although populations likely still require initial seeding via advection.

2.3.4.2.4. Subtropical Offshore species

Euphausia gibboides shows substantial offshore population increases under future non-Niño conditions, perhaps due to increasing temperatures and reduced Chl-*a* (Fig. 2.14e, first panel of right column). However, total area of increase under future non-Niño conditions is only moderately greater than total area of decrease (Fig. 2.14e, red and blue regions, respectively). A similar pattern appears for CP Niños. EP Niños show only minor, patchy increases regionwide although twice as much area of increase as decrease. Future distributions for *E. recurva* and *S. affine* are nearly identical to *E. gibboides* despite different GAM equations, although *S. affine* 2100 predictions show regionwide decreases compared to present (Fig. S2.9; note lower abundance scale for *S. affine*). Both species show similar predicted Niño decreases in 2100 compared to current Niño averages, perhaps due to lack of advection terms, and hence population seeding, in our models. Similarly, *E. hemigibba* shows only minimal presence offshore during all predicted 2100 Niño states and overall moderate decreases during both EP and CP Niños, again likely due to a lack of model advection (Fig. 2.14f). The exception for *E. hemigibba* is non-Niño future predictions, which show increases in the southern, offshore region, likely due to increased temperatures.

2.3.4.2.5. Regionwide Temperate Species

Nematoscelis difficilis and *T. gregaria* are predicted to increase regionwide during non-Niño and CP Niño years, producing up to five times more area of increase than decrease. During EP Niños, total areas of decrease are modestly greater than areas of increase, although patches of increased populations appear across the nearshore and offshore SCB (Fig. 2.14g-h).

2.4. Discussion

2.4.1. El Niño impacts on euphausiid spatial distributions

Spatial distributions of the dominant euphausiid species in the southern California Current System (CCS) are strongly influenced by El Niño and vary to a large extent between Eastern Pacific (EP) and Central Pacific (CP) events. Euphausiid responses show additional differences among events of the same type, reflecting known physical variability in CCS expressions of El Niño.

2.4.1.1. Eastern Pacific (EP) El Niño events

The three major Eastern Pacific (EP) El Niño events on record (1982-83, 1997-98, 2015-16) produced corresponding greatest changes in euphausiid species abundances and spatial distributions in the southern CCS, consistent with past observations of greatest community responses during strongest El Niño events (Brinton, 1960; Brinton & Townsend, 2003; Lilly & Ohman, 2018; Pares-Escobar et al., 2018; see our Supporting Information for a full physical description of each El Niño event). However, population shifts varied between the three events, reflecting different CCS physical expressions of each EP Niño. The 1982-83 event was dominated by onshore flow into the southern CCS from southwestern offshore waters, apparently forced by anomalous local atmospheric circulation, and induced regionwide warming and freshening (Lynn, 1983; Simpson, 1983, 1984). Enhanced poleward advection occurred north of Point Conception, CA, in February 1983 (Glynn, 1988; Huyer, 1983; Ramp et al., 1997). The 1997-98 event had the strongest physical expression of any El Niño on record, particularly in the Eastern Equatorial Pacific region (L'Heureux et al., 2017; McPhaden, 1999b). The El Niño signal traveled to the CCS predominantly via oceanic coastally trapped waves (CTWs) that strengthened and broadened poleward nearshore flow off California (Lynn & Bograd, 2002; Schwing et al., 2002; Schwing et al., 2005; Strub & James, 2002).

The 2015-16 EP Niño evolved more moderately than the other two EP events: it warmed waters off South America but produced greatest SST anomalies in the Central Equatorial Pacific, ultimately characterizing as a mixed EP-CP event (L'Heureux et al., 2017; Newman et al., 2018; Timmermann et al., 2019). California Current physical impacts were similarly moderate: positive SST anomalies occurred but were strongest south of Pt. Conception and attributed to alongshore advection from southern waters and possibly coastally-trapped waves (Chao et al., 2017; Frischknecht et al., 2017; Zaba et al., 2020). Downwelling also occurred, but thermocline deepening was not as strong as in 1982-83 and 1997-98, and unusual upwelling winds developed in fall 2015, moderating otherwise potentially strong El Niño effects (Jacox et al., 2016; Zaba et al., 2020).

2.4.1.1.1. EP Niños: Cool-Water Coastal and Regionwide Temperate species responses

Distributional shifts of euphausiid species reflect the varying contributions of enhanced shoreward and poleward flows and warming waters during each EP event. The 1982-83 and 1997-98 events induced significant poleward shifts of coastal euphausiid species, both cool-water (*Euphausia pacifica*, *Thysanoessa spinifera*) and subtropical (*Nyctiphanes simplex*), in narrow nearshore bands. The 1982-83 event confined coastal species to the nearshore region, likely via both anomalous onshore flow and significantly elevated offshore temperatures (+1-4^{o}C) (Ramp et al., 1997; Simpson, 1983, 1984). The 1997-98 event induced moderate offshore expansions of coastal populations, likely due to broadening of the Inshore Countercurrent (Lynn & Bograd, 2002). A prior study notes complete absence of *E. pacifica* and *T. spinifera* off Baja California in 1997-98 (Pares-Escobar et al., 2018), consistent with our observations of poleward retraction out of the southern CCS. Decreased total abundances of *E. pacifica* and *T. spinifera* in 1982-83 and 1997-98, and spatial retractions coastward in 1998 without any physical evidence

for enhanced shoreward flow, suggest these species experienced overall population mortality and reduced reproduction in response to unfavorable habitat conditions, rather than advection-induced coastward compression of normal population levels.

In the CCS, *E. pacifica* has been shown to associate predominantly with waters below 15^{o}C (Brinton, 1981). We found similar habitat ranges across all years except EP Niño winters, when *E. pacifica* occurred in waters up to 18^{o}C. Elevated EP Niño winter temperatures, even short-term, are likely severe enough to reduce cool-water populations through the following spring. It is possible that normal population levels simply retracted northward out of the CalCOFI sampling region, but it is unlikely that the normally high abundances of *E. pacifica* observed here would be sufficiently supported in a substantially smaller region. Acoustic surveys of aggregated krill biomass (apparently dominated by *E. pacifica* and *T. spinifera*) have shown hotspots over shelf-bisecting underwater canyons, which concentrate cold, high-productivity upwelling waters (Santora et al., 2018). During EP Niños, in particular, canyons may provide refugia from warm offshore waters, but they are unlikely to shelter entire populations of *E. pacifica*, which extend into waters well offshore. Significantly elevated *E. pacifica* and *T. spinifera* abundances off Pt. Conception during the 2015-16 EP Niño, and increased proportions of *E. pacifica* calyptopis phase, were likely positive *in situ* responses to moderate spring upwelling, although effects were confined to a relatively nearshore region compared to non-Niño years, suggesting an inability to tolerate the extended 2014-16 warming offshore. Lavaniegos et al. (2019) observed continued low abundances of *E. pacifica* and *T. spinifera* off Baja California through April 2016, likely reflecting slow recovery following prolonged warm conditions.

Regionwide temperate species (*Nematoscelis difficilis, T. gregaria*) also decreased moderately in total abundances during both 1982-83 and 1997-98, although with only minor

shoreward compression and poleward retraction. We note that *N. difficilis* and *T. gregaria* likely have more muted El Niño responses than other euphausiid species because they live in and below the thermocline (Brinton & Reid, 1986) and are likely less affected by El Niño-induced habitat changes to the upper 200 m. Near-normal abundances of *N. difficilis* off central and southern California in spring 2016 suggest either a similar upwelling response to those of *E. pacifica* and *T. spinifera* or an ability to tolerate altered El Niño conditions by living at depth. Lavaniegos et al. (2019) noted significant declines in *N. difficilis* biomass off Baja California in summers 2014 and 2015 and particularly into January 2016. Our SC region may have been far enough north and experienced sufficient upwelling and cool conditions in spring 2016 to either provide a habitat refuge or induce new reproduction of *N. difficilis* off California.

Temperature was the consistent term in generalized additive models of all four cool-water species, suggesting that *in situ* temperature changes or other associated variables are the predominant influence on cool-water species distributions. A prior canonical correspondence analysis (CCA) by Pares-Escobar et al. (2018) of euphausiid species with habitat variables off Baja California revealed an inverse association of *E. pacifica* and *T. spinifera* with the dominant axis (temperature), but no covariance of *N. difficilis* and *T. gregaria* with any physical variable, perhaps due to their warmer habitat ranges or deeper distributions.

2.4.1.1.2. EP Niños: Subtropical Coastal species responses

Nyctiphanes simplex responses to EP Niños reflect its unique biogeographic position between cool-water coastal and true subtropical-tropical habitats, with temperature distribution means similar to *E. pacifica* for all Niño groups but temperature ranges spanning from the *T. spinifera* means to the *E. gibboides* means and slightly cooler than the *N. difficilis* and *T. gregaria* means. These findings support the description by Brinton (1962) of *N. simplex* as a

nearshore species present in coastal upwelling regions at transition zones between warm and cool regions, as well as his findings that *N. simplex* was generally limited in its northward extension in the CCS to 35ºN (temperatures of 11ºC at 100 m to 17ºC at the surface). Similar to cool-water coastal species, *N. simplex* shifted poleward during all EP Niños, but these shifts indicated extensions from southern habitat rather than poleward contraction. Rapid poleward expansions of *N. simplex* along the West Coast in 1982-83 (Brinton & Reid, 1986; Brodeur, 1986; Miller et al., 1985) and 1997-98 (Brinton & Townsend, 2003; Keister et al., 2005; Mackas & Galbraith, 2002; Marinovic et al., 2002; Peterson et al., 2002), as far north as Vancouver Island, British Columbia (Mackas & Galbraith, 2002), suggest initial Niño-related transport via enhanced poleward advection. Brinton and Reid (1986) noted five times higher biomass of *N. simplex* off southern California in 1983-84 than in 1969 (a non-El Niño year), which they attributed to enhanced northerly coastal flow. Marinovic et al. (2002) attribute the sudden presence of *N. simplex* off Monterey Bay, CA, in July 1997 to pre-Niño enhanced poleward flow, as described by Lynn and Bograd (2002).

However, *N. simplex* also appears capable of *in situ* reproduction in the northern CCS during El Niño. Post-larval (calyptopis, furcilia) stages were collected off Oregon between Dec 1997-Nov 1998 (Keister et al., 2005). Initial presence was attributed to northward population advection, while continued presence in summer 1998 was likely due to *in situ* reproduction despite weakening poleward flows. Populations of *N. simplex* persisted off central California through winter 1999, corroborating evidence for *in situ* northern reproduction. Elevated abundances of *N. simplex* in 2015-16 may have resulted from combined *in situ* reproduction (indicated by elevated proportions of calyptopis phase compared to the 1983 and 1998 EP Niños) during the Warm Anomaly and moderate population seeding due to moderately enhanced

nearshore poleward flows into the SC region, described by Rudnick et al. (2017). However, neither mechanism was sufficient to extend populations to the northern CCS as during previous EP Niños.

2.4.1.1.3. EP Niños: Tropical Pacific and Subtropical Offshore species responses

Influxes of Tropical Pacific (*E. eximia*) and subtropical offshore (*E. gibboides, E. recurva, Stylocheiron affine, E. hemigibba*) species to the SC region suggest direct advection with enhanced onshore and poleward flows during EP Niños; magnitudes of population increase appear to be modulated by biogeographic origins and event physical magnitude. *Euphausia eximia* is known to extend northward into the Southern California Bight in fall even during non-Niño years, as shown by Brinton (1967, 1973) for falls 1949-50. These northward fall movements highlight natural spatial variability due to seasonality, which our interannual study resolution cannot capture. However, *E. eximia* is rarely observed off California in spring (Brinton, 1967, 1973; Brinton & Reid, 1986), so its presence in springs 1983-84 was significant evidence for poleward transport of southern waters, including of oceanic origin. Significant decreases in *E. eximia* temperature and salinity habitat ranges, changes in water mass associations, and absence of post-larval forms in springs 1983 and 1998 further support the hypothesis of population advection into the SC region during EP Niños, consistent with prior speculation about *E. eximia* appearances due to enhanced Countercurrent flow (McLain & Thomas, 1983). Low SC abundance of *E. eximia* in spring 1998 compared to 1983 may reflect a combination of reduced shoreward advection of oceanic waters and earlier (winter) peak event expression in 1997-98. We note the potential for sampling bias toward the adult phase due to possible calyptopis undersampling with 505 µm mesh nets, particularly for smaller species such as *E. eximia.* However, given the high proportions of calyptopis phases for other small species

(e.g., *N. simplex*) across most years, and the fact that several years did show high proportions of *E. eximia* calyptopes, our adult/calyptopis proportions represent true interannual fluctuations.

As with *N. simplex*, moderate *E. eximia* presence in the southern SC region in spring 2016 may have resulted from either El Niño-enhanced poleward advection from Baja California or gradual southward population retraction following the 2014-15 Warm Anomaly. Recent analysis of pelagic mollusc populations in the SC region during 2014-16 suggests that elevated abundance in 2016 occurred due to multiyear population persistence following enhanced northward advection in 2014-2015, rather than a new seeding event (Lilly et al., 2019). However, Lavaniegos et al. (2019) measured elevated populations of *E. eximia* and *E. recurva* off Baja California in summer 2015 and through January 2016 compared to summer 2014, which they attributed to enhanced northward transport during El Niño compared to the Warm Anomaly. Our contrasting findings may indicate that enhanced transport did not extend into the SC region or that a return of moderate upwelling in spring 2016 produced unfavorable habitat for subtropical species despite northward transport. The *E. eximia* calyptopis phase had lower proportions in 2016 than 2015, suggesting reduced reproduction in the SC region. Total *E. eximia* abundance declined to zero off California by spring 2017, indicating the population could not sustain itself *in situ* due to lack of continued advection or to mortality in cooler waters.

Offshore subtropical species were likely advected into the SC region with onshore flows during all three EP Niños. Unlike coastal species, they maintain consistent habitat conditions and water mass preferences across all years and winter-spring transitions, suggesting transport with parent water masses. In addition to onshore flow, North Pacific Central Gyre waters can wrap around into the nearshore Southern California Bight and flow poleward via the Inshore Countercurrent (Bograd et al., 2019). The strongest combination of enhanced onshore and

poleward flows was described for the 1982-83 EP Niño (Ramp et al., 1997; Simpson, 1984), explaining high subtropical abundances nearshore. However, increases in *E. gibboides* calyptopes during and following 1983 and through the early 1990s indicate moderate persistent post-Niño reproduction *in situ*, unlike for *E. eximia*.

The 1997-98 El Niño corroborates the importance of physical event magnitude in determining extent of euphausiid presence: offshore subtropical species were only moderately elevated and remained farther offshore in the SC region compared to 1982-83, reflecting weaker onshore flows and a stronger, broader nearshore countercurrent. Shoreward advection may have varied across the CCS, however; Keister et al. (2005) observed elevated *E. recurva* off Oregon in 1997-98, which they attribute to onshore flow. In 2016, offshore subtropical populations appeared to be buffeted even more from shoreward expansion; their distributions mirrored coastal species, with no nearshore presence around Pt. Conception, likely prevented from shoreward movement by offshore flows of cool upwelled waters. As with *E. eximia*, subtropical offshore species distributions in spring 2016 likely reflect retractions back offshore from the SC region following significant onshore expansion in 2015.

2.4.1.2. Central Pacific (CP) El Niño events

Central Pacific El Niño events show substantially more variability than EP Niños in their equatorial and CCS physical impacts. Some CP Niño signals propagate to the CCS solely via atmospheric teleconnections, while others induce moderate oceanic CTWs (Ashok et al., 2007; Ramp et al., 1997; Timmermann et al., 2019). The 1957-59 CP Niño displaced the California Current offshore, depressed nearshore upwelling, and broadened the Inshore Countercurrent in winter 1958 (Lynn, 1983; Wyllie, 1966), similar to 1997-98, although event forcing was

attributed to altered regional wind-driven circulation rather than CTWs (Reid, 1960). Warm conditions persisted through January 1960 (Brinton, 1981). The 1991-93 CP Niño has been characterized as mixed EP-CP (Timmermann et al., 2019) and produced both onshore flow and CTW propagation to the CCS in winter 1992 (Hayward, 1993; Ramp et al., 1997). Normal upwelling occurred in spring 1992, but elevated SSTs subsequently reappeared and persisted through spring 1993 (Chavez, 1996; Hayward, 1993).

The 2002-03 CP Niño was also characterized as mixed EP-CP (Timmermann et al., 2019) but induced strongest Kelvin wave initiation and SST anomalies in the Central Equatorial Pacific (Harrison & Chiodi, 2009; McPhaden, 2004). Its CCS expression was preceded by an anomalously cool, high-salinity subarctic water intrusion in summer 2002 (Bograd & Lynn, 2003; Wheeler et al., 2003), while the El Niño event itself was characterized by moderate warming and salinity-induced stratification (Lavaniegos, 2009; Lavaniegos & Ambriz-Arreola, 2012). The 2009-10 El Niño classified unequivocally as a CP event in the equatorial Pacific (Ashok & Yamagata, 2009; Kim et al., 2011). The Niño signal propagated to the CCS exclusively via atmospheric teleconnections, and depressed the thermocline and warmed upper ocean waters but did not induce anomalous poleward advection (Rudnick et al., 2017; Todd et al., 2011).

2.4.1.2.1. CP Niños: Cool-Water Coastal and Regionwide Temperate species responses

As with physical signatures, euphausiid distributional responses to CP Niños separate into i) two-year events physically similar to EP Niños, and ii) cool CP Niños of the 2000s. Although cool-water coastal (*E. pacifica, T. spinifera*) and regionwide temperate (*N. difficilis, T. gregaria*) species decreased in the SC region during both 1957-59 and 1991-93, elevated populations off central California in 1958-59 suggest moderate poleward compression rather

than regionwide decreases. Spatial changes during 1957-59 and 1991-93 were similar to 1997-98 but more moderate, likely due to cooler background conditions (1957-59) or weaker Niño signal transport (both events). Elevated abundances of *E. pacifica* and subtropical coastal *N. simplex* only in narrow nearshore bands around Pt. Conception in 1992, and absence of neritic *T. spinifera*, again suggest compression from onshore flows preventing outward expansion of cool and subtropical coastal populations. Shoreward compression appeared to weaken by spring 1993, in line with diminished onshore flows compared to 1992, although impacts of warm temperatures persisted.

Both the 2002-03 and 2009-10 CP Niño events changed CCS euphausiid community composition in opposite ways from past El Niño events. Cool-water species maintained average abundances or increased during both events and expanded outward from the coast in spring 2010. Lavaniegos and Ambriz-Arreola (2012) note similar increases in *E. pacifica* and *T. spinifera* off Baja California in July 2002-spring 2003, which they attribute to increased southward flow via Subarctic water intrusions and cooler habitat conditions.

2.4.1.2.2. CP Niños: Subtropical Coastal, Tropical Pacific, and Subtropical Offshore species responses

Subtropical and tropical species increases were more muted and showed less poleward expansion during 1957-59 and 1991-93 compared to 1982-83 and 1997-98. However, subtropical-tropical intrusions appeared to persist and even strengthen by the second spring of each event (1959, 1993), even for the usually rare *E. eximia*, likely due to some *in situ* reproduction under prolonged warm conditions. Elevated post-Niño subtropical abundances persisted through winter 1960 (data not shown) but decreased by spring, suggesting return of upwelling. The 1957-59 event occurred against cool conditions of a negative Pacific Decadal

Oscillation (PDO) phase (McGowan, 1998), which likely explains why subtropical species did not persist longer-term as for the 1982-83 El Niño. Surprisingly, despite strong onshore flows in February 1992, two subtropical offshore species (*E. gibboides, S. affine*) did not show significant shoreward expansions, although *E. recurva* did. *Stylocheiron affine* is not a vertically migrating species, which may explain its difference from *E. recurva.* The distributions of *E. gibboides* and *E. recurva* are nearly identical, so we cannot explain this apparent temporary divergence.

Subtropical-tropical species, both coastal and offshore, were near-zero or absent in nearshore waters during the 2002-03 and 2009-10 CP Niños. Offshore subtropical species did expand poleward offshore of the California Current during both events, more so in 2009-10. Subtropical euphausiid responses to the 2002-03 and 2009-10 CP Niños are consistent with past El Niño responses if we consider the anomalous physical characteristics of these two events. Stronger southward flow of the California Current in 2002-03 and lack of enhanced poleward flow in 2009-10 eliminated poleward and shoreward advection of subtropical-tropical euphausiid species into the SC region. Any populations that arrived or already existed *in situ* were likely unable to grow and reproduce under cooler temperatures. Offshore subtropical species and *N. simplex* did increase in the SC region in springs 2005 and 2007, which classified as equatorial CP Niños but fell short of our 'CCS El Niño' classification. Analyzing these years may provide further insight into mechanisms that cause subtropical species movements during CP-like events.

Physically atypical El Niño events such as the 2009-10 CP Niño, which did not show anomalous poleward advection in the southern CCS but had elevated temperatures (Rudnick et al., 2017) and sea level anomaly (Lilly & Ohman, 2018), highlight the importance of developing 'CCS El Niño indices' that consider multiple physical factors in both the equatorial Pacific and CCS, as we have done here. The two regions may show markedly different responses, or a region

may have different physical signals depending on the specific El Niño event, so we developed an index to distinguish events that show one or more of a suite of anomalous characteristics in both regions. Likewise, analyzing CCS zooplankton responses during these events can provide greater clues to the physical forcing mechanisms that cause population changes by evaluating how the community responds differently when one of those physical mechanisms (e.g., anomalous advection) is absent.

2.4.1.3. 2014-15 Warm Anomaly

The anomalously warm conditions in the Eastern North Pacific from late 2013-15 were not attributed to direct El Niño forcing (Bond et al., 2015), but they produced unprecedented surface-enhanced warming (+1-5^{o}C), onshore flows, and stratified, low-productivity conditions in the CCS on par with major El Niño events (Gentemann et al., 2017; Lilly et al., 2019; Zaba & Rudnick, 2016). Anomalous warming appeared definitively in nearshore waters off California by late spring 2014 and persisted through summer 2015, temporarily interrupted by moderate upwelling in spring 2015 (Gentemann et al., 2017; Jacox et al., 2016; Leising et al., 2015; Lilly et al., 2019; Robinson, 2016; Zaba & Rudnick, 2016). All cool-water euphausiid species and *N. simplex* responded to the Warm Anomaly in a similar manner to past El Niño events characterized by regionwide warming and onshore flow (e.g., 1957-59, 1982-83, 1991-93). Cool-water species contracted to nearshore Pt. Conception but maintained moderate abundances there, suggesting nearshore refugia from the offshore warming, further reinforced by upwelling in spring 2015. Subtropical species flooded the SC region by spring 2015, increasing from near-zero abundances in 2014; three offshore species (*E. gibboides, E. recurva, S. affine*) reached coastal waters. *Euphausia eximia* and subtropical offshore species reached their highest levels in

the entire timeseries. Increased proportions of *E. eximia* and *E. gibboides* calyptopis phases compared to EP Niños suggest that persistent warm conditions and shallow stratification promoted significant *in situ* reproduction, also described for Baja California (Pares-Escobar et al., 2018).

2.4.2. Proposed El Niño forcing mechanisms on euphausiids

Our analyses suggest that cool-water euphausiid species respond predominantly to altered *in situ* habitat conditions during El Niño events, while subtropical and tropical species appear in the SC region initially due to anomalous advection. Under non-Niño conditions, cool-water species dominate CCS waters off California (Fig. 2.15, left panel; dark and light blue shapes), with only minor poleward intrusions of subtropical coastal species (light orange band) into the SC region. During EP Niños, regionwide decreases and nearshore compression of cool-water coastal species into only upwelling areas suggest that negative *in situ* habitat conditions induced population mortality or reduced reproduction in offshore and southern waters (Fig. 2.15, middle panel; dark blue shape; 'x' indicates inferred *in situ* population mortality or reduced growth). Cool-water coastal species decreases are not as severe during CP Niños, reflecting less extreme habitat changes, although some amount of reduced population growth likely occurs in the southern part of the distribution (Fig. 2.15, right panel; dark blue shape and symbols). Regionwide temperate species appear overall less impacted by El Niño events, as previously noted (Lilly & Ohman, 2018), but still appear to experience some *in situ* die-off or reduced population growth in the southern and offshore parts of their ranges during both EP and CP Niños (Fig. 2.15; light blue shape and symbols; small 'x's indicate minor population mortality).

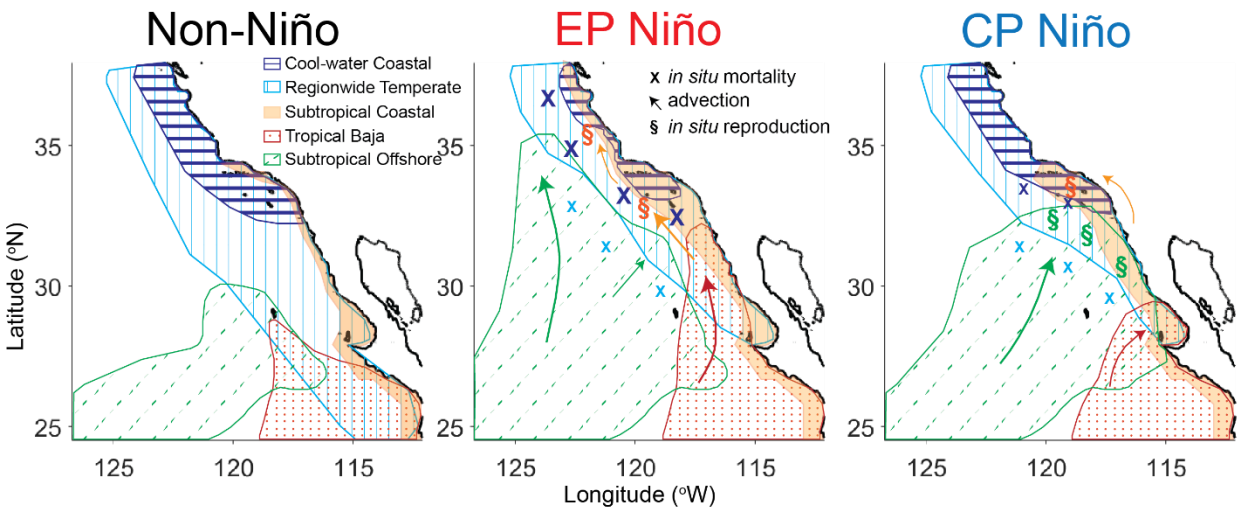

Figure 2.15. Schematic distributions of the five main types of euphausiid species spring responses to Eastern Pacific (EP) and Central Pacific (CP) El Niño events. *(center and right panels*) 'X' symbols indicate inferred *in situ* mortality or reduced reproduction, causing coastward compression or poleward retraction; arrows indicate population transport via enhanced advection; '§' indicates inferred *in situ* reproduction and population growth. Symbol colors correspond to the group they affect. Larger symbols indicate a hypothesized larger influence of that process.

In contrast, subtropical coastal species (*N. simplex*) and Tropical Pacific-Baja California species (*E. eximia*) likely move northward into novel CCS habitats during El Niño events predominantly due to advection. The most significant poleward extensions of subtropical coastal species during EP Niños are apparently due to strongest levels of poleward advection during those events (Fig. 2.15, middle and right panels; light orange and red arrows). However, subsequent *in situ* reproduction by *N. simplex* likely occurs during and following major El Niños, even when it extends anomalously northward, prolonging its anomalous northern presence (Fig. 2.15, middle panel; light orange '§' symbols). In contrast, offshore subtropical species (*E. gibboides, E. recurva, S. affine, E. hemigibba*) are likely advected shoreward to varying degrees with their parent water masses, depending on the specific strength of onshore flow during each El Niño event (Fig. 2.15; green shape and arrows). They appear to reach the nearshore SCB only during years of anomalously strong onshore flow, which occurred more often in our timeseries

during CP Niños (e.g., 1958) and the Warm Anomaly than during EP Niños, although spring 1983 showed substantial shoreward species incursions in line with observed onshore flow.

As with subtropical coastal species, subtropical offshore species appear to secondarily undergo *in situ* reproduction during and following El Niño events that have sustained warm conditions or a warm background PDO phase (i.e., 1982-83, 1991-93, 2014-16; Fig. 2.15, green '§' in right panel). However, more southerly tropical species (*E. eximia, E. hemigibba*) show little post-Niño persistence except following multiyear anomalous warming (e.g., 1992-93, 2014-15), likely due to their requirement for significantly warmer reproductive habitat. Thus, although all subtropical and tropical species are influenced by anomalous El Niño-related advection, the extent of advective transport and resulting population persistence depends on a species' biogeographic origins and tolerance for El Niño-induced habitat changes, as well as the physical characteristics of each event. We note that our conclusions are limited by a lack of higher temporal resolution (i.e., seasonality) of sampling, so we cannot truly track *in situ* reproduction or advection. However, our proposed forcing mechanisms are based on patterns in the available data and are intended to be framework hypotheses to be tested in future studies of modeled advection or further measurements of *in situ* population growth.

2.4.3. Future species distributions and implications for higher trophic levels

Long-term abundance trends combined with predictions of future distributions suggest that cool-water euphausiids will maintain or moderately expand population levels and distributional patterns under non-Niño conditions, while subtropical species will expand into the SC region. The combination of minimal predicted warming in the nearshore southern CCS (compared to regions farther offshore) and increasing Chl-*a* due to enhanced upwelling (Hazen

et al., 2013; Rykaczewski & Dunne, 2010) likely explains our findings of cool-water species increases long-term despite temporary El Niño-related population decreases. Pares-Escobar et al. (2018) note that, given predictions that global warming will induce stronger coastal upwelling (see Bakun et al., 2015; Wang et al., 2015), upwelling-adapted species such as *T. spinifera* will likely continue to increase in the future. Cool-water species will likely tolerate moderate temperature increases and benefit from elevated primary production, while subtropical species may better reproduce under sustained warmer temperatures, as already shown for 1993 and 2015. Although *N. difficilis* and *T. gregaria* live deeper in the water column and are less likely to be affected by changes in coastal upwelling, their long-term increases are likely also due to increasing primary production. Future El Niño events, superimposed on long-term climate trends in the CCS, may continue to result in marked short-term declines in cool-water euphausiid abundances during EP Niños but moderate regionwide increases in all species during CP Niños.

Our predictions of future increases in both cool-water and subtropical species by Year 2100 highlight the importance of understanding the specific mechanisms that cause sub-regional changes in species distributions in the southern CCS. Our observations of long-term increases in cool-water euphausiids over the past 70 years, but no long-term trends for subtropical species in the southern CCS, are contrary to recent findings of increasing subtropicalization of mesopelagic forage fishes in the southern CCS (McClatchie et al., 2018). Strong El Niño-related variability in subtropical species suggests they currently depend predominantly on advection into the SC region and cannot yet sustainably reproduce *in situ* long-term. The lack of advective terms in our GAM predictions limits our ability to fully forecast future changes in subtropical species distributions. Assessing advective influences on euphausiids via particle-tracking models will be a topic of future study.

Seasonal-to-interannual variations in euphausiid distributions can significantly affect highly mobile planktivore foraging patterns and management strategies. Whales, seabirds, and mobulid rays off California and Baja California show distinct preferences for certain species of euphausiids, particularly *E. pacifica* (by humpback whales, *Megaptera novaeangliae*: Fleming et al., 2016, Santora et al., 2020; Cassin's auklets, *Ptychoramphus aleuticus*: Lee et al., 2007, Sydeman et al., 2006), *T. spinifera* (blue whales, *Balaenoptera musculus*: Croll et al., 1998, Fiedler et al., 1998, Nickels et al., 2018, 2019; Cassin's auklets, *Ptychoramphus aleuticus*: Lee et al., 2007, Sydeman et al., 2006), and *N. simplex* (fin whales, *Balaenoptera physalus*, and mobulids, *Mobula mobular*: Croll et al., 2012; Stewart et al., 2017). Some highly mobile species face significant threats from ship strikes and fishing gear entanglements (Abrahms et al., 2019; Hazen et al., 2017; Office of Protected Resources, 2018a, 2018b; Santora et al., 2020). Oceanography-based models (e.g., WhaleWatch, Abrahms et al., 2019; Hazen et al., 2017) are emerging to track blue whale movements in the CCS using physical habitat conditions, but do not yet include zooplankton distributional information (but see Szesciorka et al., 2020). Lack of appropriate zooplankton data limits model accuracy by only establishing 'habitat suitability', not potentially variable whale densities due to targeted foraging on krill hotspots. Zooplanktivorous consumers may also preferentially forage on certain growth stages of euphausiids, which may vary spatially within a species (Nickels et al., 2018). Such models need also to account for rapid switching to alternative prey (i.e., humpback whales to anchovy when *E. pacifica* is low; Santora et al., 2020; Santora et al., 2011) that may not simply correspond to physical oceanographic conditions. Incorporating euphausiid spatial distributions and life-histories into foraging models may clarify highly mobile species preferences and produce more accurate spatiotemporal predictions to reduce needs for fishery closures and vessel diversions.

Appendix 2A. Multi-sample averaging per station and year

CalCOFI cruises have occasionally sampled the same station multiple times within a single season, either on multiple cruises or as multiple samples on one cruise, so we used a two-part system to produce only one abundance value per station per year: for spring samples, 1) if multiple samples existed at the same station but only in different months (i.e., one April sample and one March sample at Station 90.50), we used a selection hierarchy of: i) April sample (if present), ii) if not, then March sample, iii) if neither, then May sample, iv) if no other months, then February sample. All four months are considered 'spring' in CalCOFI because spring cruises can start as early as February 15 and extend into May; 2) if multiple samples still existed at a station within the same month after we completed the selection hierarchy (i.e., two April samples at Stn 90.50), we averaged those samples to get one mean abundance value for the station. We chose the above month hierarchy to obtain each year's sample as close as possible to April for consistency and because we expect April to be the peak of biological responses to January peak CCS El Niño physical signals, assuming an average three-month lag of biological responses behind physical change. We used the same method for winter zooplankton samples, with a month hierarchy of i) January, ii) December, iii) February (Days 1-15). Enumerated winter samples are only available for 1951-2002 and 2009.

Appendix 2B. Objective mapping decorrelation length-scales

To determine object mapping input parameters, we calculated an autocovariance matrix for each species from all available abundance values (averaged to one value per station per year; see Appendix A2). For each species, we first removed a plane mean from all values in the timeseries to obtain anomalies from the mean. We chose a rotation angle of -60^{o} based on visual determination of the angle that produced the straightest x/y orientation of the CalCOFI sampling grid, to align the cross-shore and alongshore components to x and y. Using the rotated values, we calculated all station-station covariance values within a year and binned those values by their station-station distances, using bin increments of 95 and 80 km for the x- and y-directions, respectively. For each distance bin, we averaged all covariance values within a year and then summed all yearly mean covariance values within that bin to obtain its autocovariance. The full autocovariance matrix consists of each distance bin's sum of all yearly averages in that bin. As a secondary check on our selection of optimal input angle, we visually assessed each autocovariance matrix under different input rotation angles to ensure closest alignment to an x/y grids. To determine optimal x and y decorrelation length-scales for mapping, we fit Gaussian curves to the zero-bin (center) distributions separately for the x- and y-directions, and varied the numbers of input bins (i.e., distances from zero) to determine optimal curve fits. Decorrelation scales of 160 km (x-direction) and 190 km (y-direction) produced the best overall fits, so we used those distances as our optimal decorrelation length-scales for objective maps. All species showed similar optimal bin numbers, so we used the same decorrelation length-scales and rotation angles for each species.

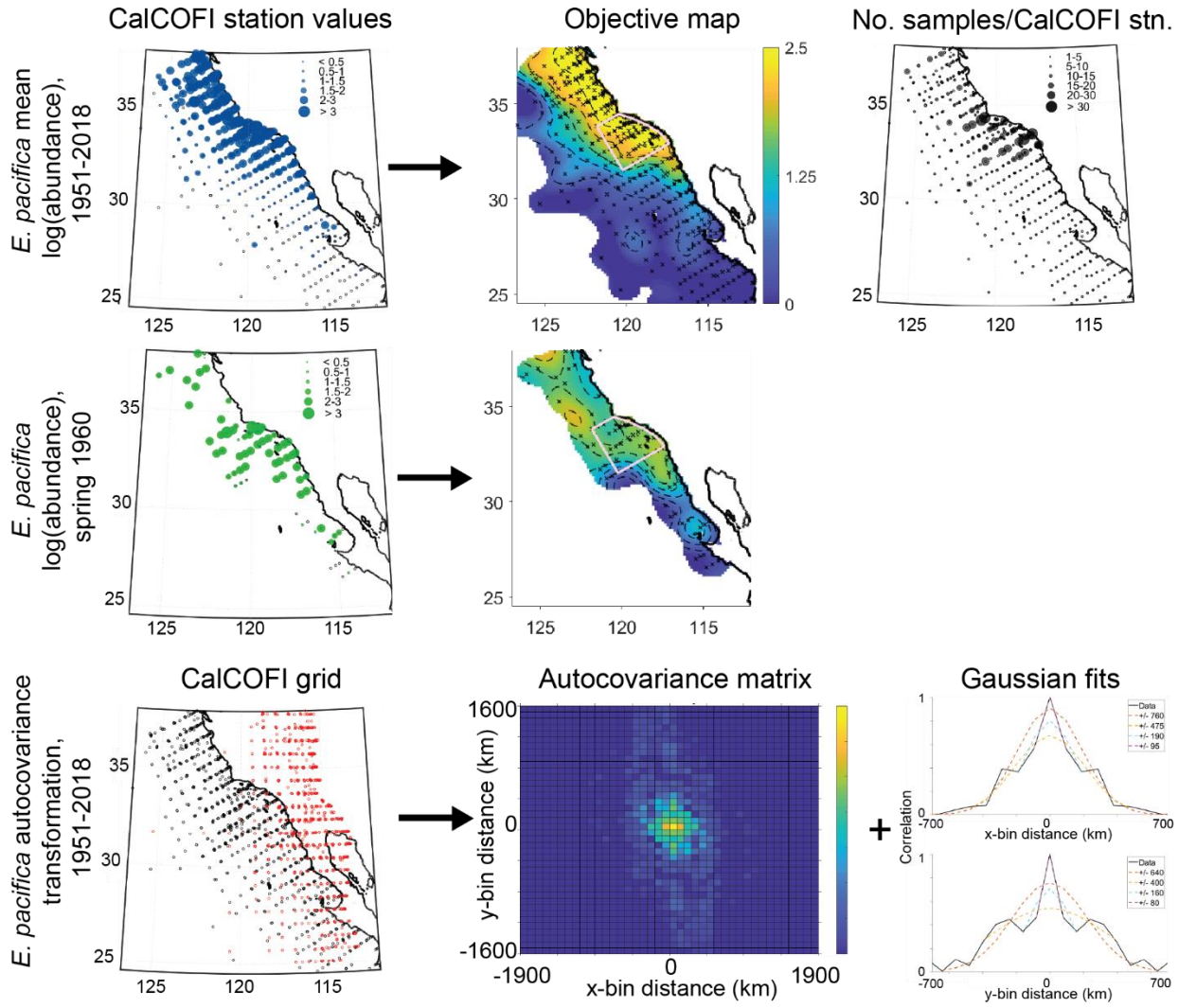

Figure 2.B1. Objective mapping fit steps and explanation: *(top row)* comparison of *E. pacifica* CalCOFI station-by-station datapoints (left panel) and objectively mapped distribution (center panel) for the 1951-2018 mean; right panel shows the number of times each CalCOFI station was sampled; *(middle row)* same comparison but for a single year (1960); *(bottom row)* -60º rotation of CalCOFI grid for objective mapping (left panel), autocovariance matrix of all station-station covariances for *E. pacifica* (center panel), and Gaussian fits of decorrelation lengths (colored lines, in km) to actual data (black lines) for x (top) and y (bottom) directions (right panel).

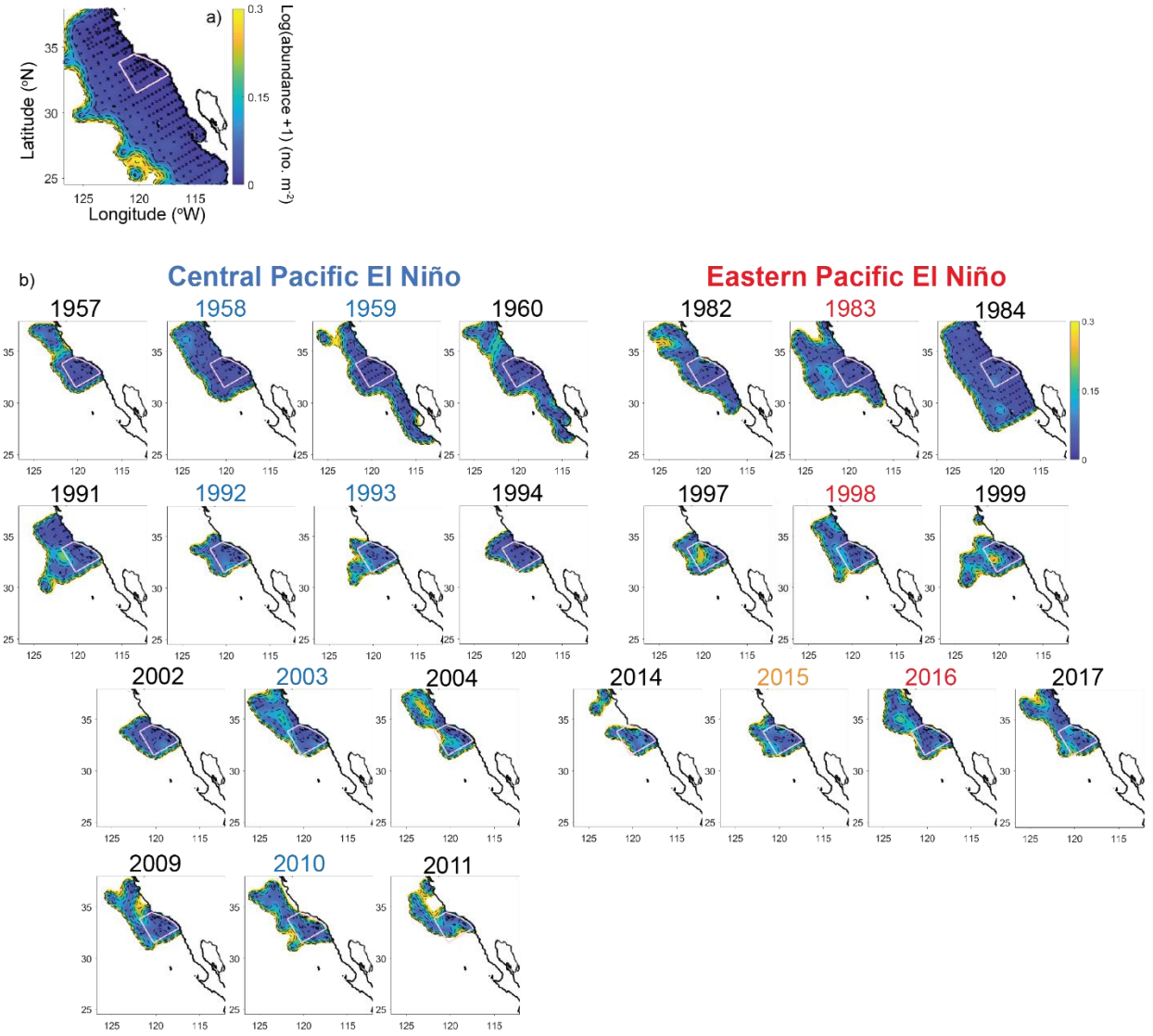

Figure 2.B2. Error maps associated with yearly objective maps for all species. Error threshold of 0.3 for all years.

Appendix 2C. Spatial statistical calculations

To determine annual changes in the spatial distribution of each species, we calculated yearly mean regionwide abundance and centers of gravity (COG) in the x (cross-shore) and y (alongshore) directions. We present results from both the 'Southern California only' and 'full CalCOFI' regions (see Section 2.2.1 for region descriptions). We calculated yearly means and standard errors using $\log_{10}$-transformed abundance (see Figs. 2.2-2.9c, S2.2-S2.3c). We calculated changes in x- and y-centers of gravity using untransformed abundance data, to emphasize centroid shifts without damping effects from log-transformation. We used the rotated CalCOFI grid (-60^{o}) for COG calculations so that x- and y-directional changes would correspond to cross-shore and alongshore. We used a 'zero point' of lat0 = 32.84^{o}N, lon0 = -118.73^{o}W (the approximate center point of the SC region) from which to calculate all other station distances. For center of gravity calculations, we converted each station's coordinates from latitude/longitude to kilometers, and used the following equation:

cogx = (1/sum(year_abund))*sum(year_abund.*xn)

where 'cogx' is the vector of center of gravity offsets in the x-direction from the zero point, 'year_abund' is the vector of zooplankton untransformed abundance values at each station for that year, and 'xn' is the vector of x-distance values from the zero point. The same equation applies to changes in y-direction center of gravity, replacing 'xn' with 'yn'. We estimated the effects of sampling error on yearly change in center of gravity using a random normal distribution multiplied by the abundance data and iterated 1000 times to produce 1000 'pseudo-shifts' in center of gravity, from which we calculated a standard deviation.

For distance values in center of gravity calculations, we converted each station's coordinates from latitude/longitude to km as described in Appendix 2B. To estimate the effects

of sampling errors on yearly change in center of gravity, we calculated the standard deviations from each COG value (separate for x and y) using the following steps: 1) we produced a random normal distribution of the same length as the number of occupied stations for a year; 2) we multiplied this random normal distribution by the abundance value at each station and by 0.1 to incorporate an expected 10% sampling error into the distribution; 3) we added these 'error' distribution values to the station abundances; 4) we calculated the changes in x and y centers of gravity:

$$abund_{err} = year\_abundance+(random\_dist* year\_abundance *0.1)$$

$$cogx_{err} = (1/nansum(abund\_err))*nansum(abund\_err *xn)$$

We repeated these steps 1000 times to produce a distribution changes in center of gravity, from which we calculated the standard deviation as a metric of likely sampling error.

To calculate the 'area of influence' of each CalCOFI station for total areas of population increase or decrease in 'EP Niño-non Niño' maps (e.g., figure 2.2e), we assumed individual station 'area boxes' which represent the total area around each station that we expected to have the same abundance as the station does. We assumed that each station represents an area around it out to halfway to the next station or line. The average inter-station and inter-line distances in the SC region are 30 km and 70 km, respectively, and we expect each station to have a halfway distance (15 km and 35 km) on each side, so we used 30 km and 70 km for box length and width, giving us a total 'area of influence' of 2100 km^2.

We did not include 1968 in our statistical calculations because CalCOFI only sampled off southern Baja California in that year, which skewed those centers of gravity significantly southward.

Acknowledgements and Author Contributions

We thank all contributors to CalCOFI data collection and analysis, particularly the at-sea technicians and ship crews for rigorous and high-quality sampling sustained over so many decades. We dedicate this study to the late E. Brinton in recognition of his career's work and extensive insight into euphausiid biogeography and biology, without which this analysis would not have been possible. We thank A. Townsend, and currently L. Sala, for continued detailed enumerations. S. Bograd and I. Schroeder developed and generously provided the water mass indices used here. We thank D. L. Rudnick, B. D. Cornuelle, and K. D. Zaba for extensive help with objective mapping and spatial statistics, and J. B. Shurin, S. Gastauer, and J. P. Zwolinski for assistance with GAMs. This work was supported by an NSF Graduate Research Fellowship to L. E. Lilly, by NSF OCE-1614359 and OCE-1637632 to the California Current Ecosystem-LTER site, and by Gordon and Betty Moore Foundation support to M. D. Ohman.

L.E.L. and M.D.O. developed the study. L.E.L. conducted all analyses and wrote the manuscript. L.E.L. and M.D.O. analyzed results and edited the manuscript. The authors declare no competing interests.

Chapter 2, in full, is a reprint of the material as it appears in Progress in Oceanography, 2021. Lilly, Laura E.; Ohman, Mark D. The dissertation author was the primary investigator and author of this paper.

Table S2.1. Mean values (± standard error) of habitat variables (temp @ 50 m, sal @ 50 m, oxygen @ 100 m, ln(Chl-a) @ 10 m) for each euphausiid species' spring total abundance distribution in figures 2.10 and S2.4 (lower rows), during non-Niño years (grey bars and black vertical line), EP Niño years (pink bars and line), and CP Niño years (blue bars and line).

	Temperature @ 50 m			Salinity @ 50 m			Oxygen @ 100 m			ln(Chl-a) @ 10 m		
Species	**Non**	**EP**	**CP**	**Non**	**EP**	**CP**	**Non**	**EP**	**CP**	**Non**	**EP**	**CP**
Euphausia pacifica	11.47 (0.001)	10.61 (0.003)	12.09 (0.003)	33.54 (<0.001)	33.59 (<0.001)	33.43 (<0.001)	3.26 (0.001)	2.87 (0.001)	3.39 (0.003)	0.06 (0.001)	0.90 (0.003)	0.52 (0.005)
Thysanoessa spinifera	10.72 (0.005)	10.77 (0.011)	10.82 (0.014)	33.66 (0.001)	33.66 (0.001)	33.72 (0.003)	2.83 (0.004)	2.68 (0.003)	3.08 (0.011)	0.74 (0.005)	0.78 (0.012)	1.51 (0.014)
Nyctiphanes simplex	12.16 (0.005)	11.87 (0.008)	12.56 (0.015)	33.63 (0.001)	33.57 (0.001)	33.54 (0.001)	3.18 (0.003)	3.07 (0.005)	3.64 (0.008)	0.13 (0.004)	0.32 (0.007)	0.52 (0.016)
Euphausia eximia	16.05 (0.015)	14.36 (0.026)	13.33 (0.051)	33.79 (0.003)	33.41 (0.003)	33.40 (0.006)	4.30 (0.009)	4.01 (0.024)	3.77 (0.017)	-1.88 (0.014)	-1.64 (0.025)	-1.07 (0.031)
Euphausia gibboides	14.87 (0.011)	15.03 (0.034)	15.17 (0.022)	33.43 (0.002)	33.27 (0.009)	33.49 (0.003)	4.80 (0.008)	4.86 (0.023)	4.69 (0.014)	-1.99 (0.008)	-1.93 (0.023)	-1.37 (0.095)
Euphausia recurva	14.51 (0.010)	14.80 (0.018)	14.66 (0.020)	33.39 (0.002)	33.26 (0.004)	33.44 (0.003)	4.79 (0.008)	5.09 (0.015)	4.43 (0.014)	-1.79 (0.008)	-1.71 (0.015)	-1.76 (0.041)
Stylocheiron affine	14.61 (0.018)	14.34 (0.043)	14.37 (0.057)	33.42 (0.003)	33.32 (0.006)	33.43 (0.007)	4.69 (0.012)	4.65 (0.039)	4.36 (0.034)	-1.79 (0.013)	-1.53 (0.029)	-1.18 (0.104)
Euphausia hemigibba	15.13 (0.032)	15.01 (0.046)	15.36 (0.066)	33.45 (0.006)	33.27 (0.010)	33.40 (0.017)	5.28 (0.019)	5.33 (0.025)	5.10 (0.046)	-2.20 (0.022)	-1.80 (0.042)	-2.49 (0.079)
Nematoscelis difficilis	12.56 (0.003)	12.99 (0.012)	13.11 (0.010)	33.46 (<0.001)	33.41 (0.003)	33.40 (0.001)	3.72 (0.002)	3.50 (0.009)	3.76 (0.005)	-0.62 (0.003)	-0.30 (0.011)	-0.48 (0.012)
Thysanoessa gregaria	12.90 (0.007)	13.65 (0.021)	13.50 (0.021)	33.40 (0.001)	33.32 (0.004)	33.31 (0.003)	4.03 (0.005)	4.31 (0.018)	4.11 (0.014)	-1.01 (0.006)	-0.85 (0.021)	-0.87 (0.025)

Table S2.2. Kruskal-Wallis and post-hoc multicomparison test values (p-values in parentheses) for spring total abundance distributions of the three El Niño categories (non, EP=Eastern Pacific, CP=Central Pacific) at four habitat variables (temp @ 50 m, sal @ 50 m, oxygen @ 100 m, ln(Chl-a) @ 10 m) shown in figures 2.10 and S2.4 (lower rows). See Table S2.1 for mean values.

	Oxygen @ 100 m				ln(Chl-a) @ 10 m			
Species	**K-W X^2**	**Non-EP**	**Non-CP**	**EP-CP**	**K-W X^2**	**Non-EP**	**Non-CP**	**EP-CP**
Euphausia pacifica	8.06 (0.02)	140.84 (0.02)	38.24 (0.51)	-102.61 (0.21)	6.58 (0.04)	-65.71 (0.13)	-59.77 (0.16)	5.94 (0.99)
Thysanoessa spinifera	24.58 (5e-6)	-243.49 (2e-16)	-37.54 (0.49)	205.95 (1e-3)	4.36 (0.11)	7.15 (0.97)	-64.34 (0.10)	-71.49 (0.22)
Nyctiphanes simplex	15.75 (4e-4)	-109.31 (3e-3)	-53.74 (0.04)	55.57 (0.32)	12.32 (2e-3)	53.60 (0.02)	-39.56 (0.10)	-93.15 (1e-3)
Euphausia eximia	21.28 (2e-5)	-152.04 (3e-3)	-108.65 (1e-3)	43.39 (0.70)	12.33 (2e-3)	70.73 (0.05)	-68.15 (0.05)	-138.87 (1e-3)
Euphausia gibboides	7.87 (0.02)	-81.79 (0.15)	-64.52 (0.07)	17.26 (0.94)	0.24 (0.89)	-14.16 (0.88)	0.14 (0.99)	14.30 (0.93)
Euphausia recurva	28.48 (7e-7)	-183.86 (5e-4)	-131.21 (1e-4)	52.65 (0.62)	9.13 (0.01)	66.22 (0.09)	-59.65 (0.12)	-125.87 (7e-3)
Stylocheiron affine	21.20 (2e-5)	-215.90 (2e-16)	-24.11 (0.72)	191.79 (1e-3)	19.01 (7e-5)	90.04 (8e-3)	-85.35 (0.01)	-175.39 (2e-16)
Euphausia hemigibba	5.58 (0.06)	-62.05 (0.16)	-36.58 (0.23)	25.47 (0.79)	2.08 (0.35)	25.18 (0.45)	-14.15 (0.77)	-39.33 (0.34)
Nematoscelis difficilis	7.06 (0.03)	-139.23 (0.02)	-7.17 (0.98)	132.06 (0.07)	2.79 (0.25)	-12.98 (0.92)	-54.02 (0.23)	-41.04 (0.64)
Thysanoessa gregaria	9.61 (8e-3)	-156.04 (7e-3)	19.98 (0.83)	176.02 (0.01)	3.18 (0.20)	42.89 (0.41)	-37.20 (0.49)	-80.09 (0.18)

	Temperature @ 50 m				Salinity @ 50 m			
Species	**K-W X^2**	**Non-EP**	**Non-CP**	**EP-CP**	**K-W X^2**	**Non-EP**	**Non-CP**	**EP-CP**
Euphausia pacifica	3.64 (0.16)	110.88 (0.19)	36.38 (0.65)	-74.50 (0.57)	6.49 (0.04)	128.98 (0.10)	66.22 (0.23)	-62.76 (0.66)
Thysanoessa spinifera	31.03 (2e-7)	-328.91 (2e-16)	-62.18 (0.25)	266.73 (4e-4)	30.30 (2e-7)	-317.95 (2e-16)	-66.03 (0.20)	251.91 (1e-3)
Nyctiphanes simplex	13.85 (1e-3)	-124.28 (7e-3)	-62.97 (0.04)	61.31 (0.40)	15.63 (4e-4)	-125.56 (5e-3)	-68.62 (0.02)	56.94 (0.44)
Euphausia eximia	31.96 (1e-7)	-187.29 (3e-3)	-172.67 (<2e-16)	14.62 (0.97)	33.22 (6e-8)	-181.57 (3e-3)	-177.42 (2e-16)	4.15 (0.99)
Euphausia gibboides	10.55 (5e-3)	-120.20 (0.06)	-84.03 (0.04)	36.37 (0.82)	7.58 (0.02)	-110.08 (0.09)	-65.01 (0.14)	45.07 (0.74)
Euphausia recurva	39.48 (3e-9)	-222.75 (4e-4)	-197.70 (<2e-16)	25.05 (0.93)	39.79 (2e-9)	-213.06 (1e-3)	-200.51 (2e-16)	12.56 (0.98)
Stylocheiron affine	22.30 (1e-5)	-264.12 (2e-16)	-41.63 (0.49)	222.49 (2e-3)	21.09 (3e-5)	-253.52 (2e-16)	-38.78 (0.54)	214.74 (3e-3)
Euphausia hemigibba	6.32 (0.04)	-73.90 (0.16)	-47.24 (0.16)	26.65 (0.83)	7.08 (0.03)	-74.30 (0.14)	-50.95 (0.11)	23.35 (0.87)
Nematoscelis difficilis	12.45 (2e-3)	-220.54 (2e-3)	-37.35 (0.63)	183.18 (0.03)	8.52 (0.01)	-182.36 (0.01)	1.03 (0.99)	183.38 (0.03)
Thysanoessa gregaria	13.04 (2e-3)	-227.21 (1e-3)	6.45 (0.99)	233.66 (4e-3)	12.40 (2e-3)	-212.07 (2e-3)	26.98 (0.78)	239.05 (3e-3)

Table S2.3. Mean values (± standard error) of habitat variables (temp @ 50 m, sal @ 50 m, oxygen @ 100 m, ln(Chl-a) @ 10 m) for each euphausiid species' winter total abundance distribution in figure S2.4 (top rows) during non-Niño years (corresponding to grey bars and black vertical line), EP Niño years (pink bars and line), and CP Niño years (blue bars and line).

	Temperature @ 50 m			Salinity @ 50 m			Oxygen @ 100 m			ln(Chl-a) @ 10 m		
Species	**Non**	**EP**	**CP**	**Non**	**EP**	**CP**	**Non**	**EP**	**CP**	**Non**	**EP**	**CP**
Euphausia pacifica	12.17 (0.002)	15.84 (0.168)	13.51 (0.004)	33.45 (<0.001)	33.34 (0.033)	33.29 (<0.001)	3.48 (0.002)	4.41 (0.070)	4.03 (0.002)	-0.08 (0.003)	-0.52 (0.042)	-0.83 (0.002)
Thysanoessa spinifera	11.99 (0.013)	16.62 (<0.001)	12.85 (0.086)	33.50 (0.002)	NaN	33.43 (0.014)	3.15 (0.008)	3.84 (<0.001)	3.65 (0.052)	0.32 (0.017)	-0.19 (<0.001)	-0.04 (<0.001)
Nyctiphanes simplex	13.91 (0.008)	16.15 (0.002)	13.97 (0.011)	33.51 (0.001)	33.64 (<0.001)	33.35 (0.002)	3.71 (0.003)	3.94 (0.008)	4.08 (0.006)	-0.11 (0.005)	-0.53 (0.006)	-0.56 (0.008)
Euphausia eximia	16.00 (0.034)	16.59 (0.027)	15.30 (0.125)	33.63 (0.005)	33.62 (0.005)	33.57 (0.014)	4.22 (0.012)	4.05 (0.011)	3.96 (0.023)	-1.24 (0.021)	-0.72 (0.024)	-0.59 (0.026)
Euphausia gibboides	14.80 (0.029)	15.99 (0.084)	14.85 (0.081)	33.39 (0.005)	33.38 (0.028)	33.43 (0.011)	4.69 (0.015)	4.91 (0.059)	4.25 (0.033)	-1.40 (0.020)	-1.18 (0.055)	-0.95 (0.043)
Euphausia recurva	14.92 (0.014)	15.68 (0.024)	15.00 (0.026)	33.38 (0.002)	33.37 (0.008)	33.41 (0.004)	4.90 (0.007)	5.07 (0.016)	4.50 (0.015)	-1.59 (0.008)	-1.26 (0.020)	-1.16 (0.019)
Stylocheiron affine	15.30 (0.021)	16.54 (0.035)	15.42 (0.043)	33.46 (0.003)	33.51 (0.010)	33.45 (0.006)	4.78 (0.010)	4.46 (0.026)	4.61 (0.022)	-1.51 (0.013)	-0.86 (0.028)	-1.24 (0.040)
Euphausia hemigibba	15.65 (0.052)	15.88 (0.045)	16.23 (0.089)	33.45 (0.008)	33.51 (0.001)	33.49 (0.021)	5.22 (0.023)	5.26 (0.043)	5.01 (0.064)	-1.77 (0.030)	-1.60 (0.078)	-1.92 (0.047)
Nematoscelis difficilis	12.93 (0.005)	16.27 (0.016)	13.99 (0.011)	33.42 (0.001)	33.43 (0.006)	33.35 (0.002)	3.80 (0.003)	4.16 (0.007)	4.25 (0.006)	-0.59 (0.004)	-0.54 (0.008)	-0.88 (0.007)
Thysanoessa gregaria	13.38 (0.010)	15.60 (0.034)	13.86 (0.020)	33.38 (0.001)	33.28 (0.009)	33.31 (0.003)	4.15 (0.006)	4.61 (0.016)	4.37 (0.013)	-0.98 (0.007)	-0.91 (0.016)	-0.85 (0.011)

Table S2.4. Kruskal-Wallis and post-hoc multicomparison test values (p-values in parentheses) for winter total abundance distributions of the three El Niño categories (non, EP=Eastern Pacific, CP=Central Pacific) at four habitat variables (temp @ 50 m, sal @ 50 m, oxygen @ 100 m, ln(Chl-a) @ 10 m) shown in figure S2.4 (top rows). See Table S2.3 for mean values.

	Oxygen @ 100 m				ln(Chl-a) @ 10 m			
Species	**K-W X^2**	**Non-EP**	**Non-CP**	**EP-CP**	**K-W X^2**	**Non-EP**	**Non-CP**	**EP-CP**
Euphausia pacifica	35.51 (2e-8)	266.94 (2e-16)	71.22 (0.01)	-195.72 (1e-3)	14.27 (1e-3)	-95.96 (0.01)	52.95 (0.06)	148.91 (1e-3)
Thysanoessa spinifera	5.51 (0.06)	28.97 (0.51)	28.32 (0.08)	-0.64 (0.99)	0.09 (0.96)	5.39 (0.95)	-0.55 (0.99)	-5.93 (0.96)
Nyctiphanes simplex	3.92 (0.14)	-43.28 (0.63)	-43.57 (0.17)	-0.28 (0.99)	11.39 (3e-3)	53.57 (0.22)	66.63 (7e-3)	13.06 (0.94)
Euphausia eximia	25.86 (2e-6)	-186.42 (2e-16)	5.56 (0.95)	191.97 (2e-16)	15.09 (1e-3)	94.65 (4e-4)	-7.04 (0.91)	-101.69 (1e-3)
Euphausia gibboides	10.81 (5e-3)	-128.15 (0.02)	-45.97 (0.12)	82.19 (0.24)	4.45 (0.11)	65.37 (0.10)	12.21 (0.84)	-53.16 (0.32)
Euphausia recurva	32.56 (8e-8)	-164.41 (2e-3)	-117.14 (<1e-3)	47.27 (0.64)	10.46 (5e-3)	77.31 (0.05)	53.41 (0.05)	-23.90 (0.81)
Stylocheiron affine	25.17 (3e-6)	-221.78 (<1e-3)	-48.13 (0.11)	173.65 (2e-3)	8.40 (0.02)	92.52 (0.01)	-1.17 (0.99)	-93.69 (0.03)
Euphausia hemigibba	4.83 (0.09)	-59.17 (0.20)	-25.85 (0.30)	33.32 (0.65)	2.98 (0.23)	35.90 (0.27)	-10.74 (0.78)	-46.64 (0.20)
Nematoscelis difficilis	6.01 (0.05)	-118.23 (0.05)	10.64 (0.91)	128.87 (0.05)	19.27 (6e-5)	85.53 (0.03)	87.08 (5e-4)	1.55 (0.99)
Thysanoessa gregaria	11.41 (3e-3)	-158.04 (4e-3)	22.26 (0.65)	180.30 (2e-3)	12.57 (2e-3)	82.33 (0.04)	63.20 (0.02)	-19.13 (0.88)

	Temperature @ 50 m				Salinity @ 50 m			
Species	**K-W X^2**	**Non-EP**	**Non-CP**	**EP-CP**	**K-W X^2**	**Non-EP**	**Non-CP**	**EP-CP**
Euphausia pacifica	46.37 (9e-9)	360.37 (2e-16)	106.46 (1e-3)	-253.91 (3e-4)	24.47 (5e-6)	293.51 (1e-3)	96.24 (1e-3)	-197.28 (0.06)
Thysanoessa spinifera	7.54 (0.02)	44.34 (0.37)	40.10 (0.04)	-4.24 (0.99)	6.35 (0.04)	54.50 (0.45)	33.18 (0.06)	-21.33 (0.89)
Nyctiphanes simplex	11.31 (4e-3)	-58.99 (0.57)	-92.93 (3e-3)	-33.94 (0.85)	10.18 (6e-3)	27.53 (0.94)	-81.47 (5e-3)	-109.00 (0.38)
Euphausia eximia	26.03 (2e-6)	-229.11 (2e-16)	-4.83 (0.97)	224.29 (2e-16)	2.42 (0.30)	-89.75 (0.32)	-12.35 (0.81)	77.39 (0.45)
Euphausia gibboides	13.12 (1e-3)	-160.24 (0.01)	-65.09 (0.05)	95.15 (0.26)	7.21 (0.03)	-92.20 (0.45)	-61.12 (0.04)	31.09 (0.92)
Euphausia recurva	42.93 (5e-9)	-193.08 (3e-3)	-168.25 (2e-16)	24.83 (0.92)	27.53 (1e-6)	-112.74 (0.34)	-133.51 (2e-16)	-20.77 (0.97)
Stylocheiron affine	24.35 (5e-6)	-259.64 (2e-16)	-58.45 (0.09)	201.19 (3e-3)	3.18 (0.29)	-24.52 (0.95)	-39.55 (0.26)	-15.03 (0.98)
Euphausia hemigibba	6.82 (0.03)	-64.39 (0.26)	-43.45 (0.08)	20.94 (0.89)	3.18 (0.20)	-8.85 (0.99)	-32.74 (0.18)	-23.90 (0.91)
Nematoscelis difficilis	4.24 (0.12)	-121.23 (0.11)	10.64 (0.93)	131.87 (0.11)	1.82 (0.40)	-28.17 (0.94)	34.85 (0.40)	63.02 (0.74)
Thysanoessa gregaria	11.55 (3e-3)	-175.03 (0.01)	47.46 (0.25)	222.48 (2e-3)	4.12 (0.13)	-12.67 (0.99)	54.21 (0.11)	66.88 (0.72)

Table S2.5. Mean values (± standard error) of associations of each euphausiid species' spring total abundance with proportions of three water masses (PSUW @ 150 m, PEW @ 200 m, ENPCW @ 100 m) shown in figures 2.11 and S2.5 during non-Niño years (corresponding to grey bars and black vertical line), EP Niño years (pink bars and line), and CP Niño years (blue bars and line).

	PSUW @ 150 m			PEW @ 200 m			ENPCW @ 100 m		
Species	**Non**	**EP**	**CP**	**Non**	**EP**	**CP**	**Non**	**EP**	**CP**
Euphausia pacifica	0.50 (<0.001)	0.51 (<0.001)	0.38 (<0.001)	0.38 (<0.001)	0.33 (<0.001)	0.51 (0.001)	0.12 (0.001)	0.12 (0.001)	0.07 (0.001)
Thysanoessa spinifera	0.46 (0.001)	0.35 (0.001)	0.37 (0.001)	0.40 (0.001)	0.48 (0.001)	0.49 (0.003)	0.10 (0.001)	0.19 (0.001)	0.07 (0.001)
Nyctiphanes simplex	0.49 (0.001)	0.45 (0.001)	0.41 (0.003)	0.37 (0.001)	0.41 (0.001)	0.46 (0.003)	0.17 (0.001)	0.18 (0.001)	0.08 (0.002)
Euphausia eximia	0.50 (0.004)	0.42 (0.003)	0.45 (0.004)	0.32 (0.004)	0.40 (0.006)	0.44 (0.003)	0.28 (0.006)	0.32 (0.006)	0.12 (0.002)
Euphausia gibboides	0.57 (0.001)	0.55 (0.004)	0.62 (0.007)	0.32 (0.001)	0.36 (0.004)	0.36 (0.006)	0.37 (0.003)	0.45 (0.006)	0.31 (0.014)
Euphausia recurva	0.58 (0.001)	0.54 (0.002)	0.63 (0.005)	0.30 (0.001)	0.33 (0.003)	0.34 (0.003)	0.36 (0.002)	0.59 (0.005)	0.26 (0.008)
Stylocheiron affine	0.56 (0.002)	0.49 (0.005)	0.60 (0.009)	0.30 (0.002)	0.40 (0.004)	0.33 (0.006)	0.34 (0.003)	0.44 (0.008)	0.19 (0.014)
Euphausia hemigibba	0.53 (0.005)	0.56 (0.006)	0.67 (0.008)	0.27 (0.004)	0.33 (0.006)	0.31 (0.006)	0.50 (0.008)	0.63 (0.010)	0.46 (0.021)
Nematoscelis difficilis	0.51 (<0.001)	0.40 (0.001)	0.50 (0.002)	0.37 (0.001)	0.44 (0.002)	0.42 (0.001)	0.19 (0.001)	0.31 (0.002)	0.11 (0.001)
Thysanoessa gregaria	0.52 (0.001)	0.49 (0.001)	0.51 (0.001)	0.36 (0.001)	0.38 (0.001)	0.42 (0.003)	0.23 (0.003)	0.41 (0.001)	0.13 (0.003)

Table S2.6. Kruskal-Wallis and post-hoc multicomparison test values (p-values in parentheses) for spring total abundance distributions of the three El Niño categories (non, EP=Eastern Pacific, CP=Central Pacific) at three water mass proportions (PSUW @ 150 m, PEW @ 200 m, ENPCW @ 100 m) shown in figures 2.11 and S2.5. See Table S2.5 for mean values.

	PSUW @ 150 m				PEW @ 200 m				ENPCW @ 100 m			
Species	**K-W X^2**	**Non-EP**	**Non-CP**	**EP-CP**	**K-W X^2**	**Non-EP**	**Non-CP**	**EP-CP**	**K-W X^2**	**Non-EP**	**Non-CP**	**EP-CP**
Euphausia pacifica	22.63 (1e-5)	135.15 (2e-16)	44.45 (0.15)	-90.70 (0.03)	14.50 (7e-4)	112.39 (4e-4)	15.45 (0.79)	-96.94 (0.02)	11.36 (3e-3)	56.93 (0.13)	68.50 (0.01)	11.58 (0.94)
Thysanoessa spinifera	4.98 (0.08)	-26.01 (0.56)	-41.31 (0.10)	-15.30 (0.87)	6.82 (0.03)	-30.53 (0.44)	-47.62 (0.04)	-17.09 (0.84)	3.48 (0.18)	-32.73 (0.36)	-26.75 (0.34)	5.98 (0.98)
Nyctiphanes simplex	26.25 (2e-6)	-126.96 (2e-16)	42.91 (0.13)	169.87 (2e-16)	25.90 (2e-6)	-127.82 (2e-16)	37.01 (0.21)	164.84 (2e-16)	35.33 (2e-8)	-145.77 (2e-16)	46.91 (0.08)	192.68 (2e-16)
Euphausia eximia	67.99 (2e-15)	-126.04 (2e-16)	-20.37 (0.22)	105.68 (2e-16)	65.06 (2e-16)	-119.57 (2e-16)	-21.31 (0.17)	98.26 (2e-16)	58.45 (2e-12)	-118.07 (2e-16)	-18.01 (0.31)	100.06 (2e-16)
Euphausia gibboides	8.21 (0.02)	-71.26 (0.02)	14.42 (0.77)	85.68 (0.02)	8.47 (0.01)	-72.44 (0.01)	12.47 (0.82)	84.90 (0.02)	14.81 (6e-4)	-90.80 (1e-3)	25.10 (0.44)	11.60 (7e-4)
Euphausia recurva	5.64 (0.06)	-65.45 (0.05)	4.31 (0.98)	69.76 (0.10)	6.44 (0.04)	-69.70 (0.03)	1.65 (0.99)	71.35 (0.09)	12.02 (3e-3)	-91.00 (3e-3)	14.79 (0.77)	105.79 (4e-3)
Stylocheiron affine	17.49 (2e-4)	-88.22 (4e-3)	52.07 (0.04)	140.29 (1e-4)	21.46 (2e-5)	-103.72 (4e-3)	49.20 (0.06)	152.92 (2e-16)	25.82 (2e-6)	-110.81 (1e-4)	53.94 (0.03)	164.74 (2e-16)
Euphausia hemigibba	3.10 (0.21)	-30.21 (0.260	10.22 (0.78)	40.43 (0.20)	2.48 (0.29)	-26.01 (0.36)	9.97 (0.79)	35.98 (0.27)	3.87 (0.14)	-34.05 (0.17)	9.58 (0.80)	43.64 (0.14)
Nematoscelis difficilis	8.73 (0.01)	11.83 (0.92)	70.11 (9e-3)	58.27 (0.25)	3.00 (0.22)	-12.25 (0.91)	38.58 (0.23)	50.83 (0.34)	25.70 (3e-6)	-112.04 (4e-4)	70.97 (7e-3)	183.01 (2e-16)
Thysanoessa gregaria	3.24 (0.20)	-40.20 (0.37)	25.41 (0.53)	65.61 (0.17)	7.44 (0.02)	-80.63 (0.02)	-5.07 (0.97)	75.56 (0.09)	17.76 (1e-4)	-106.40 (8e-4)	42.54 (0.16)	148.94 (1e-4)

Table S2.7. Mean values (± standard error) of habitat variables (temp @ 50 m, sal @ 50 m, oxygen @ 100 m, ln(Chl-a) @ 10 m) for each euphausiid species' spring calyptopis abundance distribution in figure S2.7 during non-Niño years (corresponding to grey bars and black vertical line), EP Niño years (pink bars and line), and CP Niño years (blue bars and line).

	Temperature @ 50 m			Salinity @ 50 m			Oxygen @ 100 m			ln(Chl-a) @ 10 m		
Species	**Non**	**EP**	**CP**	**Non**	**EP**	**CP**	**Non**	**EP**	**CP**	**Non**	**EP**	**CP**
Euphausia pacifica	11.35 (0.003)	10.45 (0.002)	12.00 (0.010)	33.55 (0.001)	33.60 (<0.001)	33.44 (0.002)	3.18 (0.003)	2.83 (<0.001)	3.49 (0.009)	0.52 (0.003)	1.04 (0.003)	0.96 (0.013)
Thysanoessa spinifera	10.82 (0.013)	10.85 (0.013)	11.58 (0.055)	33.64 (0.002)	33.57 (0.001)	33.61 (0.005)	2.76 (0.010)	2.88 (0.004)	2.74 (0.030)	0.72 (0.014)	0.79 (0.017)	1.64 (0.052)
Nyctiphanes simplex	12.20 (0.008)	12.03 (0.011)	12.81 (0.051)	33.56 (0.001)	33.55 (0.001)	33.54 (0.004)	3.25 (0.007)	2.94 (0.007)	3.57 (0.026)	0.32 (0.008)	0.64 (0.01)	-0.01 (0.080)
Euphausia eximia	16.2 (0.038)	13.30 (0.135)	13.07 (0.124)	33.76 (0.006)	33.51 (0.022)	33.38 (0.015)	4.41 (0.020)	2.87 (0.067)	3.80 (0.038)	-2.14 (0.015)	-0.70 (0.182)	-1.20 (0.064)
Euphausia gibboides	15.01 (0.019)	15.48 (0.047)	15.11 (0.035)	33.41 (0.004)	33.37 (0.009)	33.50 (0.004)	4.92 (0.013)	4.85 (0.031)	4.72 (0.020)	-2.12 (0.011)	-2.02 (0.034)	-1.58 (0.177)
Euphausia recurva	14.57 (0.025)	14.88 (0.101)	14.79 (0.057)	33.37 (0.005)	33.31 (0.016)	33.55 (0.005)	4.88 (0.021)	4.60 (0.085)	4.33 (0.034)	-1.79 (0.027)	-1.89 (0.056)	-1.50 (0.192)
Stylocheiron affine	15.05 (0.077)	14.76 (0.102)	13.66 (0.132)	33.29 (0.017)	33.24 (0.034)	33.12 (0.001)	5.23 (0.056)	5.00 (0.061)	4.56 (0.113)	-2.19 (0.052)	-1.76 (0.122)	-1.47 (0.122)
Euphausia hemigibba	15.04 (0.233)	NaN	NaN	33.48 (0.034)	NaN	NaN	4.82 (0.153)	NaN	NaN	-1.77 (0.124)	NaN	NaN
Nematoscelis difficilis	12.51 (0.006)	12.86 (0.019)	13.22 (0.019)	33.46 (0.001)	33.47 (0.003)	33.37 (0.003)	3.62 (0.005)	3.21 (0.012)	3.85 (0.011)	-0.39 (0.006)	0.07 (0.016)	-0.74 (0.023)
Thysanoessa gregaria	12.86 (0.058)	12.87 (0.112)	13.08 (0.090)	33.45 (0.010)	33.49 (0.005)	33.21 (0.021)	4.11 (0.055)	3.52 (0.102)	4.29 (0.073)	-0.60 (0.074)	0.15 (0.105)	-1.06 (0.065)

Table S2.8. Kruskal-Wallis and post-hoc multicomparison test values (p-values in parentheses) for spring calyptopis abundance distributions of the three El Niño categories (non, EP=Eastern Pacific, CP=Central Pacific) at four habitat variables (temp @ 50 m, sal @ 50 m, oxygen @ 100 m, ln(Chl-a) @ 10 m) shown in figure S2.6. See Table S2.7 for mean values.

	Oxygen @ 100 m				ln(Chl-a) @ 10 m			
Species	**K-W X^2**	**Non-EP**	**Non-CP**	**EP-CP**	**K-W X^2**	**Non-EP**	**Non-CP**	**EP-CP**
Euphausia pacifica	3.70 (0.16)	-60.89 (0.40)	-47.07 (0.28)	13.81 (0.97)	1.11 (0.57)	-33.01 (0.55)	-8.09 (0.96)	24.92 (0.83)
Thysanoessa spinifera	30.63 (2e-7)	-154.33 (2e-16)	-17.58 (0.61)	136.76 (1e-4)	0.32 (0.85)	-10.14 (0.88)	-6.51 (0.94)	3.63 (0.99)
Nyctiphanes simplex	15.40 (5e-4)	-141.84 (3e-4)	-20.54 (0.67)	121.31 (0.011)	5.36 (0.07)	-58.90 (0.05)	-2.22 (0.99)	56.68 (0.22)
Euphausia eximia	0.08 (0.96)	-4.83 (0.96)	0.63 (0.99)	5.46 (0.96)	0.51 (0.77)	-7.71 (0.76)	-1.50 (0.99)	6.21 (0.90)
Euphausia gibboides	9.66 (8e-3)	-14.79 (0.90)	-68.80 (6e-3)	-54.01 (0.35)	5.23 (0.07)	-13.16 (0.80)	-45.41 (0.06)	-32.26 (0.48)
Euphausia recurva	9.84 (7e-3)	-59.85 (0.12)	-52.04 (0.03)	7.81 (0.97)	4.71 (0.09)	28.26 (0.33)	-29.57 (0.28)	-57.83 (0.08)
Stylocheiron affine	8.57 (0.01)	-38.91 (0.02)	7.41 (0.71)	46.32 (0.01)	4.43 (0.11)	21.68 (0.09)	0.30 (0.99)	-21.37 (0.27)
Euphausia hemigibba	NaN	NaN	NaN	NaN	NaN	NaN	NaN	NaN
Nematoscelis difficilis	2.75 (0.25)	-80.83 (0.25)	-18.48 (0.84)	62.35 (0.53)	1.95 (0.38)	-41.97 (0.41)	-21.01 (0.79)	20.96 (0.88)
Thysanoessa gregaria	13.56 (0.001)	-76.01 (7e-4)	-6.78 (0.87)	69.23 (0.01)	0.58 (0.75)	10.14 (0.73)	1.87 (0.99)	-8.27 (0.89)

	Temperature @ 50 m				Salinity @ 50 m			
Species	**K-W X^2**	**Non-EP**	**Non-CP**	**EP-CP**	**K-W X^2**	**Non-EP**	**Non-CP**	**EP-CP**
Euphausia pacifica	4.52 (0.10)	-101.87 (0.17)	-46.20 (0.42)	55.67 (0.67)	2.50 (0.29)	-83.94 (0.30)	-22.82 (0.81)	61.12 (0.62)
Thysanoessa spinifera	35.91 (2e-7)	-204.32 (2e-16)	-9.34 (0.91)	194.98 (2e-16)	32.73 (8e-8)	-195.54 (2e-16)	0.22 (0.99)	195.76 (2e-16)
Nyctiphanes simplex	21.17 (3e-5)	-208.71 (2e-16)	-22.52 (0.72)	186.18 (1e-3)	20.00 (4e-5)	201.91 (2e-16)	-19.99 (0.78)	181.93 (2e-3)
Euphausia eximia	0.07 (0.96)	0.95 (0.99)	3.92 (0.96)	2.98 (0.99)	0.10 (0.95)	2.12 (0.99)	4.49 (0.95)	2.36 (0.99)
Euphausia gibboides	16.87 (2e-4)	-12.50 (0.95)	-107.33 (1e-4)	-94.82 (0.11)	16.47 (3e-4)	-8.73 (0.97)	-106.21 (1e-4)	-97.48 (0.09)
Euphausia recurva	14.50 (7e-4)	-68.97 (0.14)	-79.96 (2e-3)	-10.99 (0.96)	14.36 (8e-4)	-65.98 (0.16)	-80.20 (2e-3)	-14.22 (0.94)
Stylocheiron affine	8.00 (0.02)	-44.35 (0.03)	10.99 (0.58)	55.34 (0.01)	8.01 (0.02)	-43.80 (0.03)	10.43 (0.61)	54.23 (0.01)
Euphausia hemigibba	NaN	NaN	NaN	NaN	NaN	NaN	NaN	NaN
Nematoscelis difficilis	5.93 (0.05)	-147.80 (0.04)	-21.27 (0.85)	126.53 (0.17)	4.53 (0.10)	-126.65 (0.09)	10.62 (0.96)	137.27 (0.12)
Thysanoessa gregaria	18.25 (1e-4)	-104.22 (1e-4)	-5.57 (0.93)	98.64 (1e-3)	15.94 (3e-4)	-99.01 (2e-4)	-2.66 (0.99)	96.34 (2e-3)

Table S2.9. Parameters for optimal generalized additive model (GAM) equation for each species (see figures 2.13 and S2.8 for equations). 'd.f.' is the total degrees of freedom of the model; 'AIC' is Akaike Information Criterion; '-REML' indicates the score using the method of maximum likelihood (ML) for smoothing selection, treating smooth components as random effects; '%dev. exp.' is the percent deviance explained by the model (akin to adjusted R^2); and 'Terms' indicate knots ('kts'), degrees of freedom, and significance of each term ('p'). Terms were only included in a model if they reached a significance of $p < 0.05$. For first four species, top row is term values for GAM with lat/lon terms; bottom row is for GAM without lat/lon terms.

Species	d.f.	AIC	-REML	%dev. exp.	Term 1		Term 2		Term 3	
					kts	d.f. (p)	kts	d.f. (p)	kts	d.f. (p)
Euphausia pacifica	44.9	798.0	397.2	63.6%	(5)	3.09 (4e-11)**	(5)	3.00 (6e-5)**	(5,5)	4.79 (1e-4)**
no (Lat,Lon)	41.6	823.0	403.9	60.8%		4.76 (2e-08)***		2.88 (1e-06)***	---	---
Nyctiphanes simplex	49.9	742.2	360.6	70.8%	(5,5)	3.00 (8e-8)**	(5,5)	9.01 (6e-4)**	(5,5)	3.90 (7e-3)**
no (Lat,Lon)	40.5	764.4	371.9	67.1%		3 (<2e-16)***	---	---		3.472 (0.046)*
Euphausia eximia	44.0	212.3	120.7	44.2%	(7,6)	6.50 (5e-3)**	(6,5)	6.05 (0.046)*	---	---
no (Lat,Lon)	40.0	229.6	131.8	38.2%	---	---		5.97 (0.014)*		---

Euphausia gibboides	46.4	501.9	256.2	56.9%	(6,5)	3.30 (6e-7)**	(6,6)	7.37 (0.022)*	(3)	1.77 (0.044)*
no (Lat,Lon)	39.0	510.9	261.7	54.0%		3.28 (1e-11)***	---	---		1.79 (1e-3)**
Thysanoessa spinifera	42.3	941.9	454.2	51.6%	7	1.00 (2e-3)**	(7,7)	4.17 (0.014)*	(7,7)	3.17 (0.05)^
Euphausia recurva	42.7	583.4	294.0	60.8%	(5,5)	3.00 (4e-3)**	(5,5)	3.13 (4e-3)**	(5,6)	2.54 (0.04)*
Stylocheiron affine	42.5	583.4	293.0	40.5%	(5,5)	5.54 (9e-5)***	(5,5)	3.00 (3e-4)***	---	---
Euphausia hemigibba	42.0	-190.4	-57.0	49.3%	(5,5)	5.91 (2e-16)***	5	2.12 (0.02)*	---	---
Nematoscelis difficilis	40.7	696.2	348.2	34.2%	(6,5)	4.40 (2e-10)**	6	1.00 (4e-4)**	6	1.30 (0.014)*
Thysanoessa gregaria	45.9	780.1	382.9	48.2%	(5,5)	5.21 (3e-5)***	(5,5)	6.66 (2e-4)***	---	---

Figure S2.1. Metrics of population distribution change for the 10 species analyzed, corresponding to individual year distribution maps in Figs. S2.10-S2.19. Plots are (*top*) changes in x-direction center of gravity (COGx) and (*bottom*) y-direction center of gravity (COGy). All centers of gravity are calculated from a constant centroid (x = -118.73^{o}W, y= 32.84^{o}N), so a species may have consistently negative values if its population is always offset from that centroid. Positive values denote shoreward (x) and northward (y) shifts. Pink lines show values for the full CalCOFI region (variable sampling); blue lines are for the SC region only. Vertical grey bars denote El Niño events. See Appendix 2C for explanation of calculations.

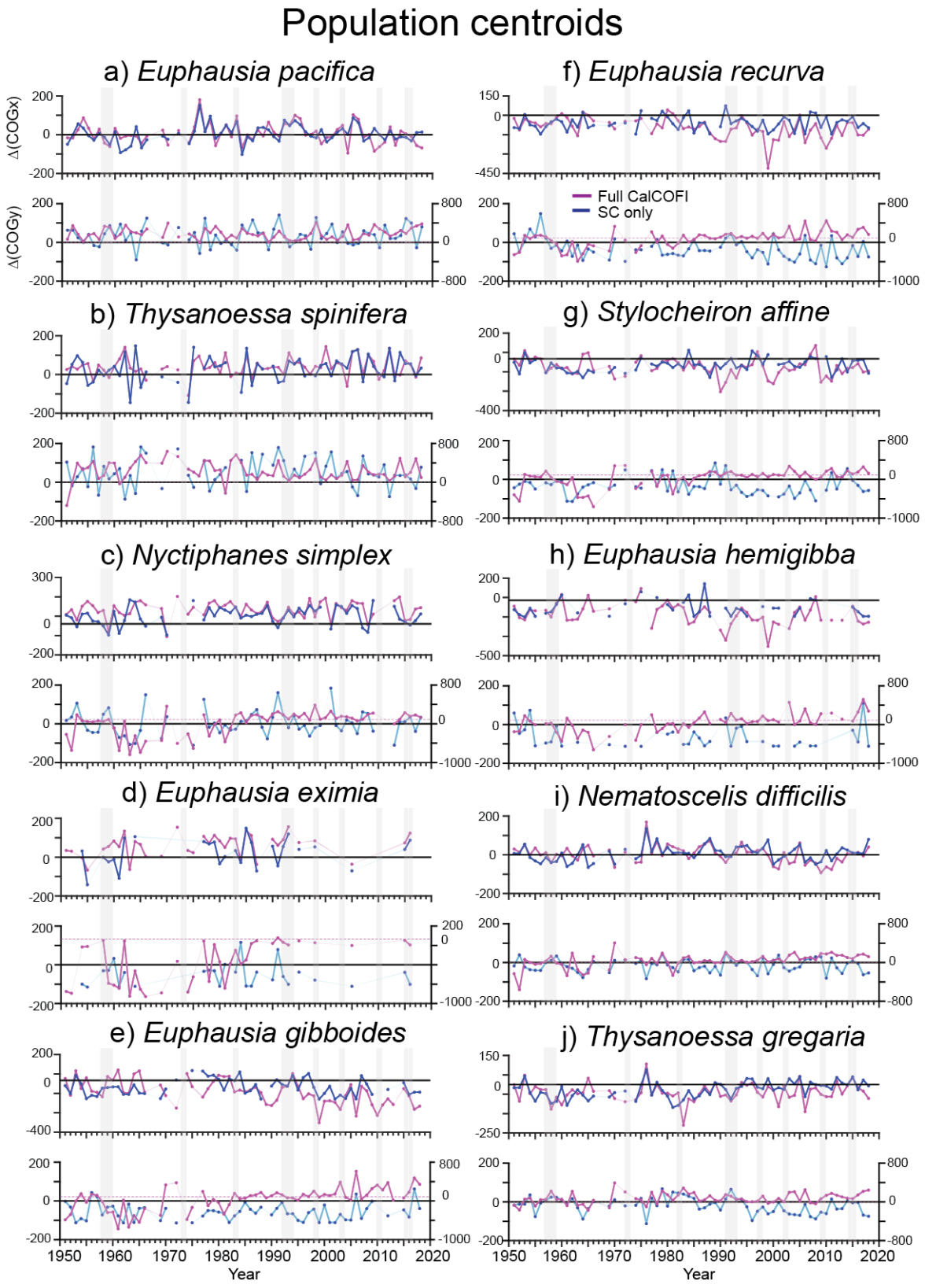
Population centroids
a) Euphausia pacifica
f) Euphausia recurva
b) Thysanoessa spinifera
g) Stylocheiron affine
c) Nyctiphanes simplex
h) Euphausia hemigibba
d) Euphausia eximia
i) Nematoscelis difficilis
e) Euphausia gibboides
j) Thysanoessa gregaria
Δ(COGx)
Δ(COGy)
Full CalCOFI
SC only
Year
1950 1960 1970 1980 1990 2000 2010 2020

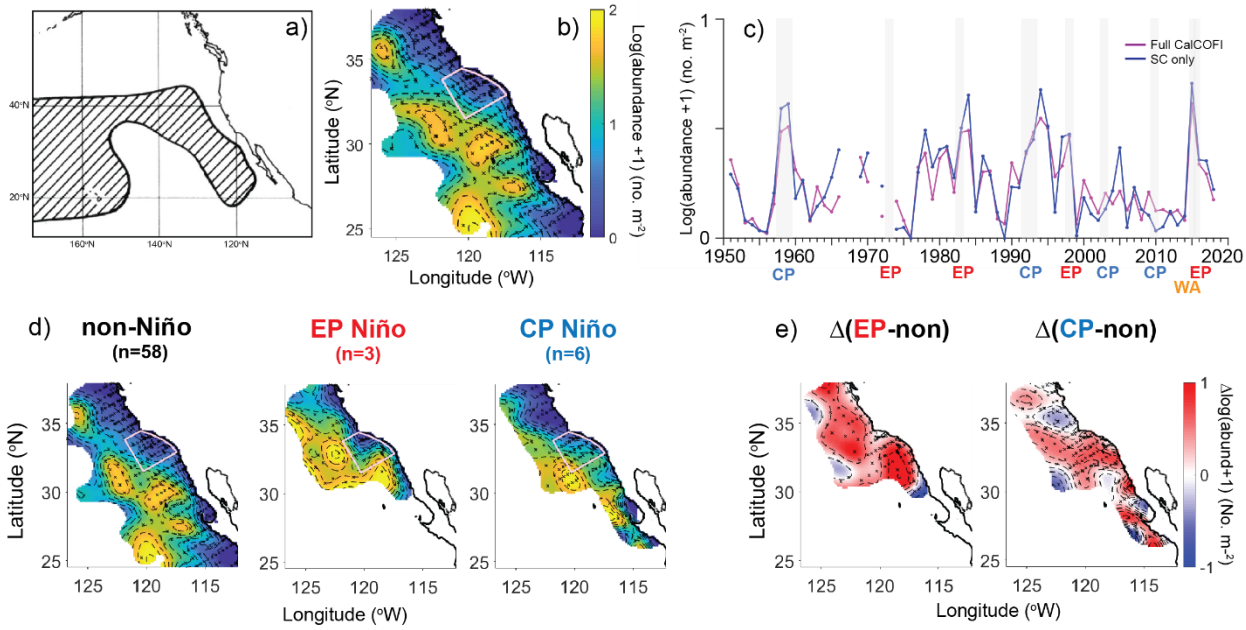

Figure S2.2. As in figure 2.2, but for *Euphausia recurva*. Lack of linear trendline in 'c' indicates no significant long-term trend ($p > 0.05$).

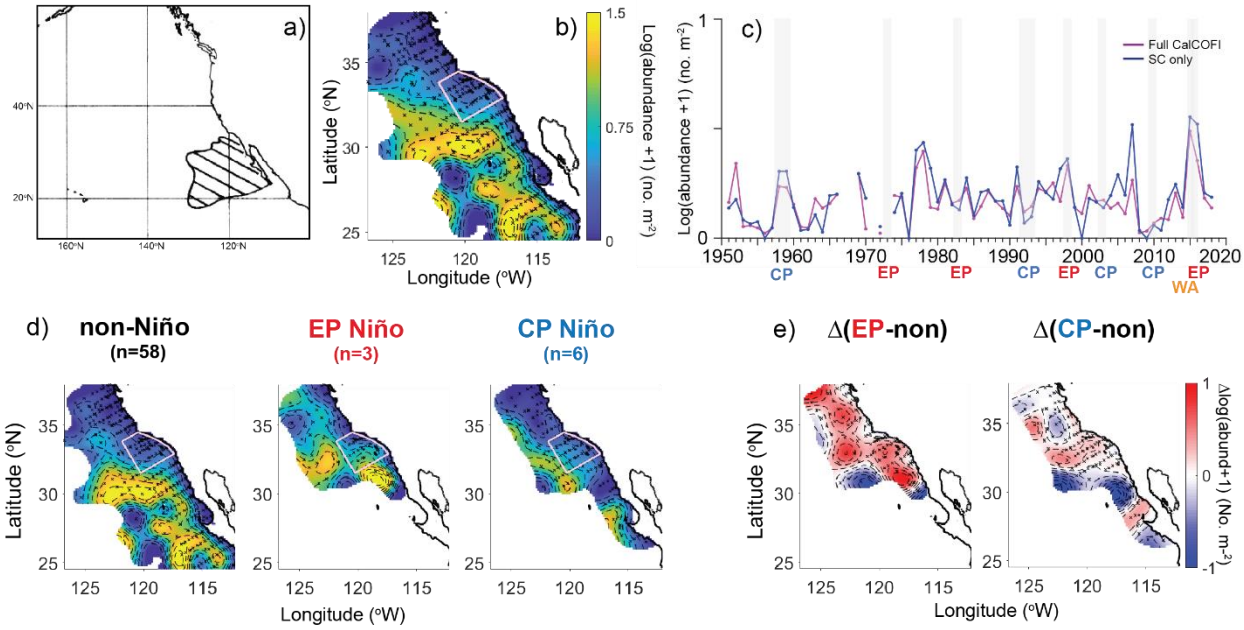

Figure S2.3. As in figure 2.2, but for *Stylocheiron affine*. Lack of linear trendline in 'c' indicates no significant long-term trend ($p > 0.05$).

Figure S2.4. As in figure 2.10 but for both winter (*top row, each species*) and spring (bottom rows) habitat distributions. Spring plots are identical to figure 2.10 but are shown for direct comparison to winter distributions.

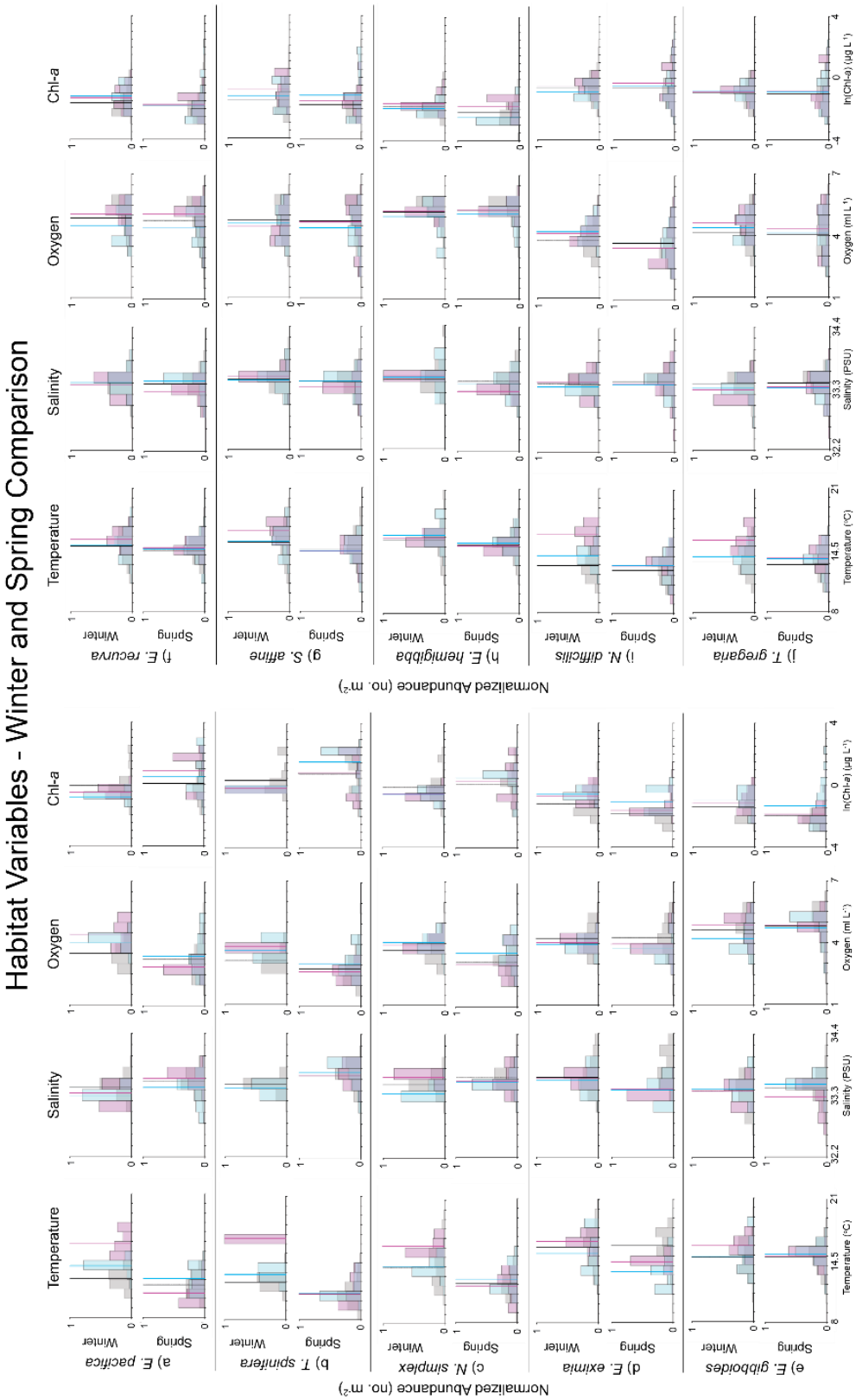
Habitat Variables - Winter and Spring Comparison
Temperature
Salinity
Oxygen
Chl-a
Spring
Winter
Temperature (°C)
Salinity (PSU)
Oxygen (ml L⁻¹)
ln(Chl-a) (µg L⁻¹)
Normalized Abundance (no. m⁻²)
a) E. pacifica
b) T. spinifera
c) N. simplex
d) E. eximia
e) E. gibbolides
f) E. recurva
g) S. affine
h) E. hemigibba
i) N. difficilis
j) T. gregaria

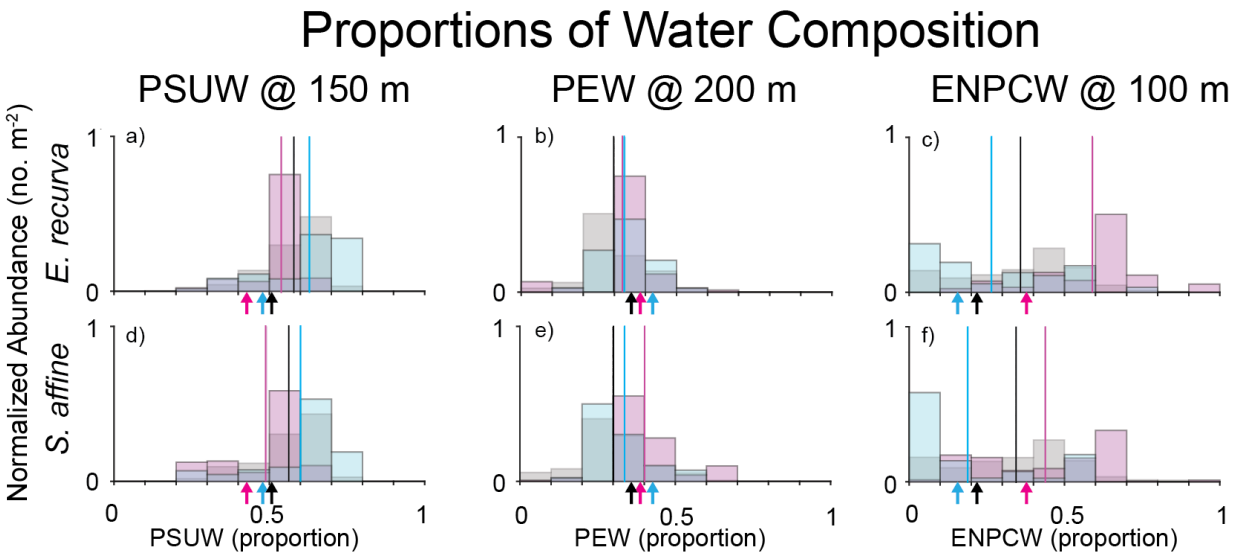

Figure S2.5. As in figure 2.11 but for the remaining two species.

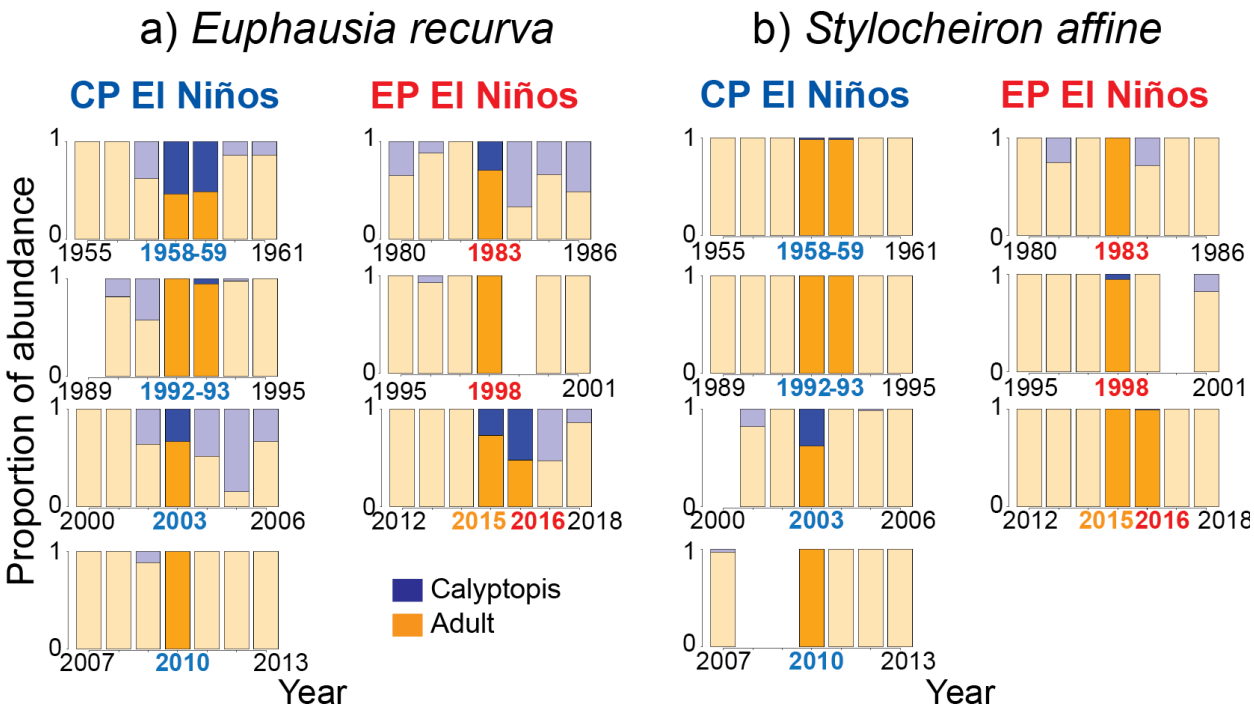

Figure S2.6. As in figure 2.12 but for the remaining two species.

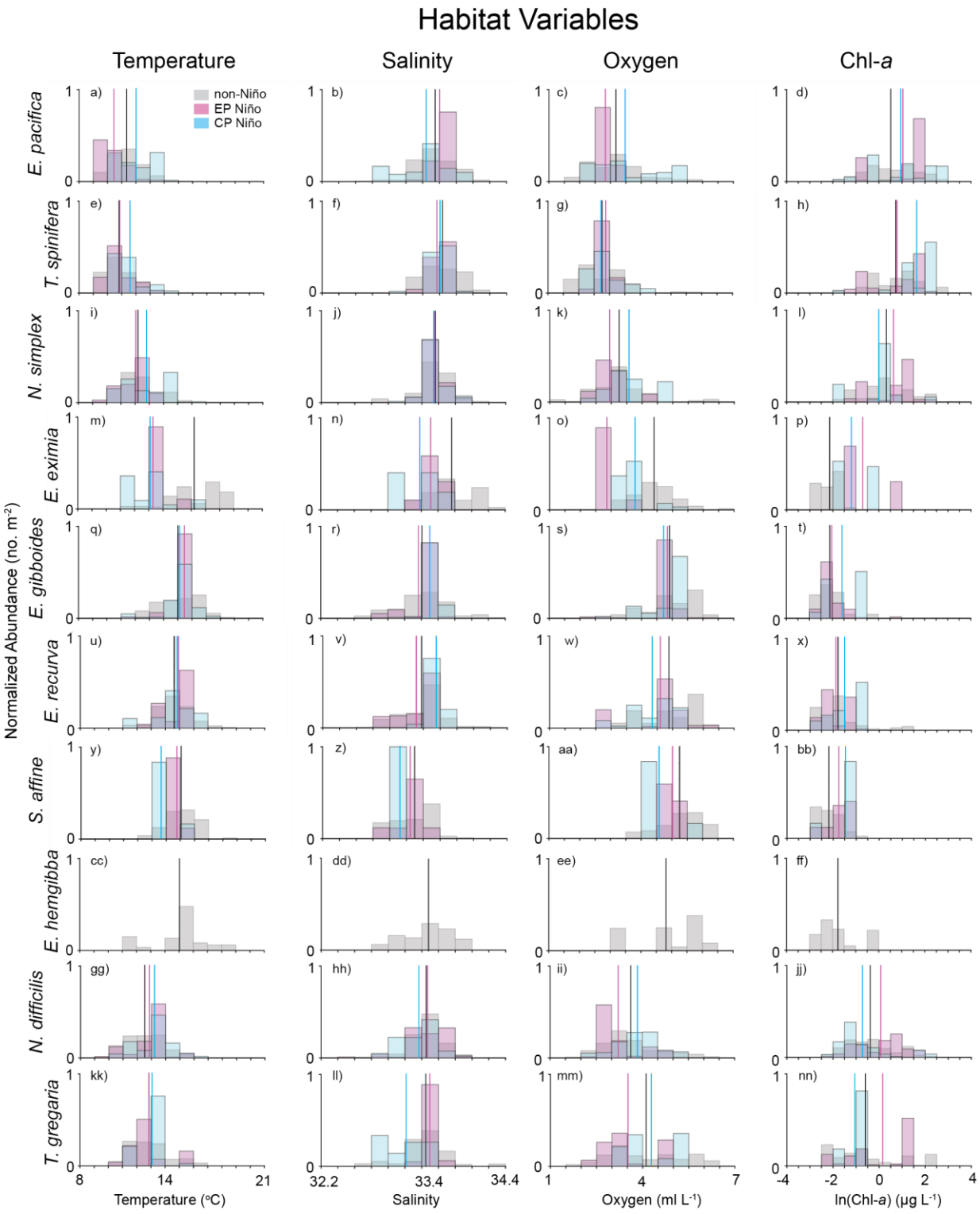

Figure S2.7. As in figure 2.10 but spring habitat distributions for calyptopis phase only.

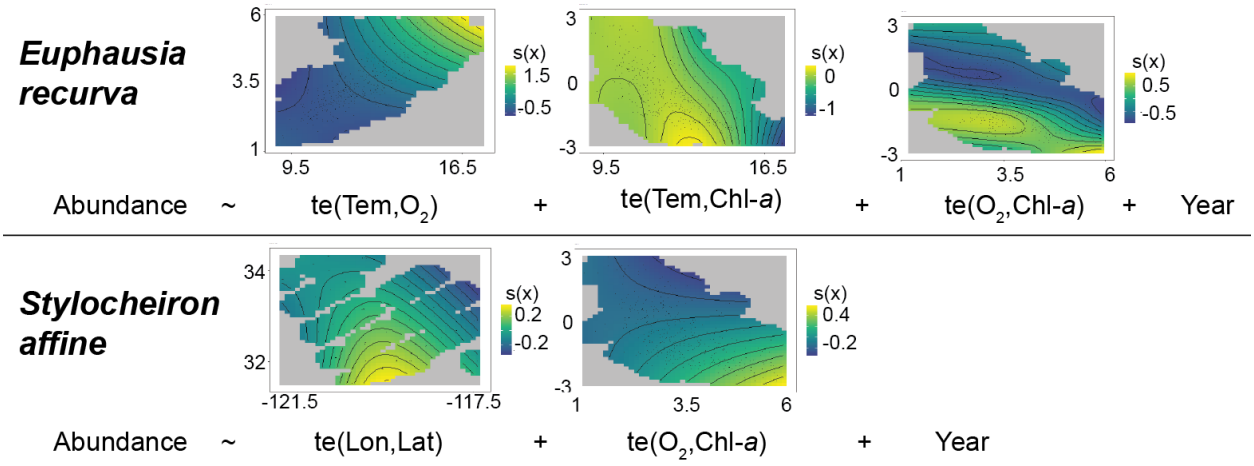

Figure S2.8. As in figure 2.13 but for the remaining two species.

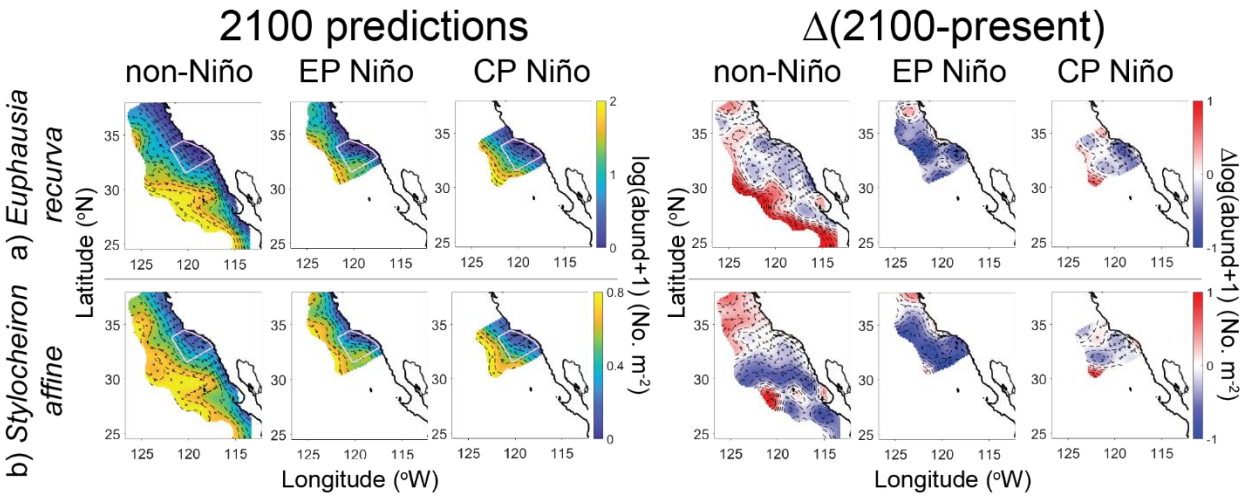

Figure S2.9. As in figure 2.14 but for the remaining two species.

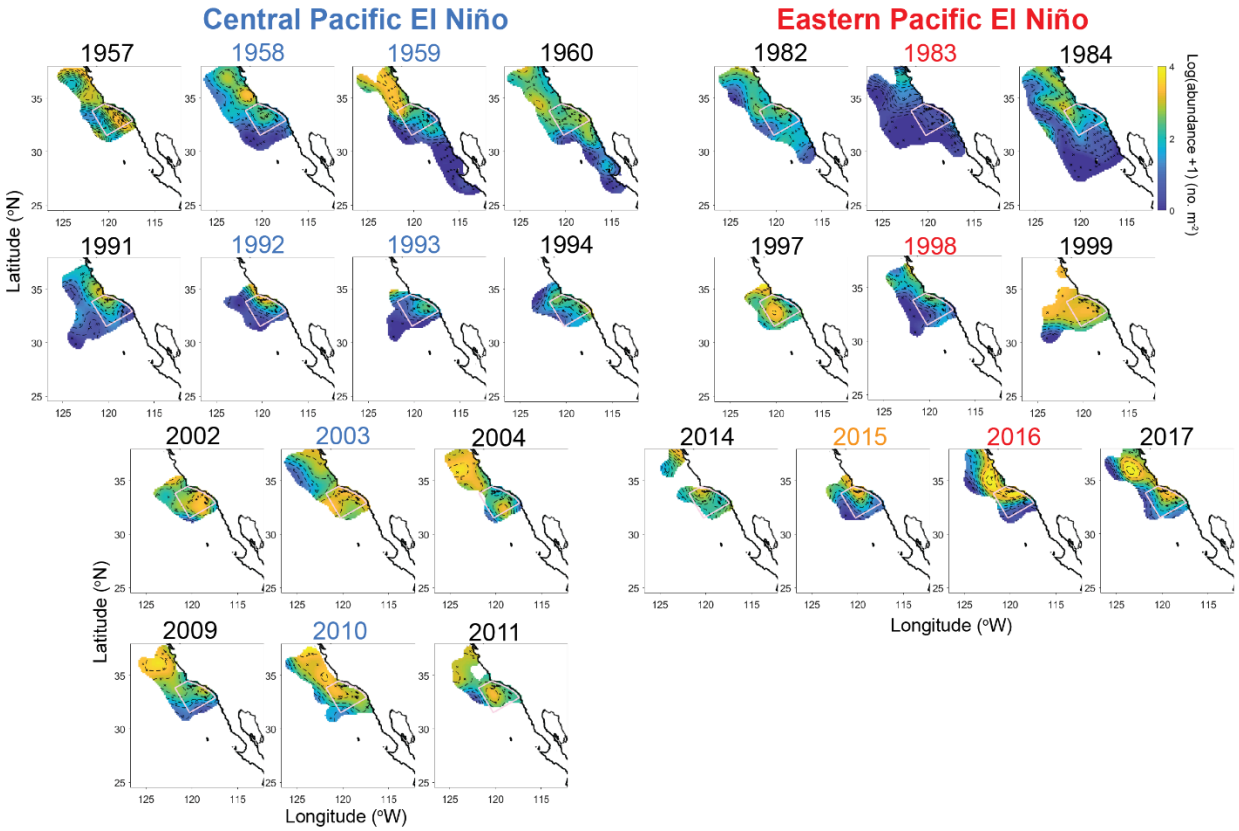

Figure S2.10. Individual year spring distributions for *E. pacifica.* Color scale shown for 1984 is the same for all years. El Niño springs are shown as central plots with colored year-labels. Spring 2015 was the Warm Anomaly (orange label), although it was also a precursor to the 2015-16 Eastern Pacific El Niño.

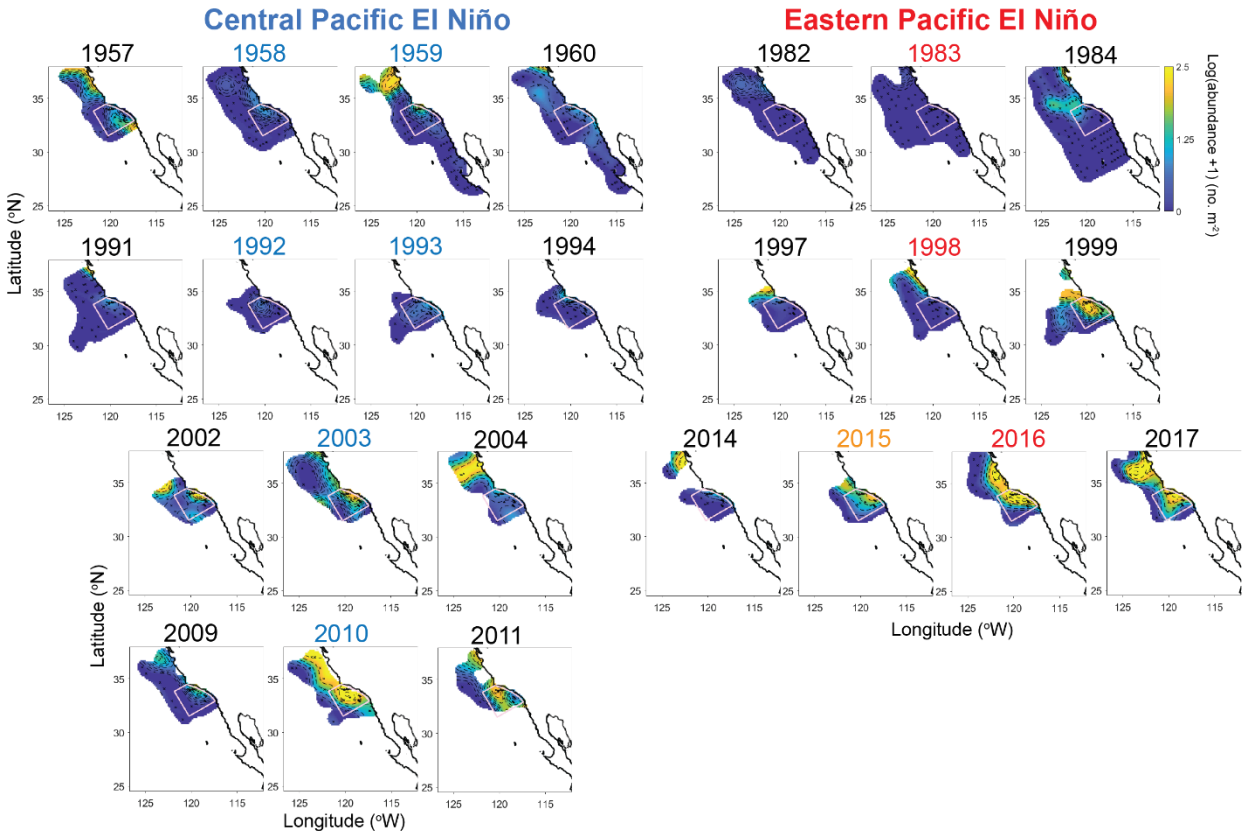

Figure S2.11. As in figure S2.10, but for *T. spinifera*.

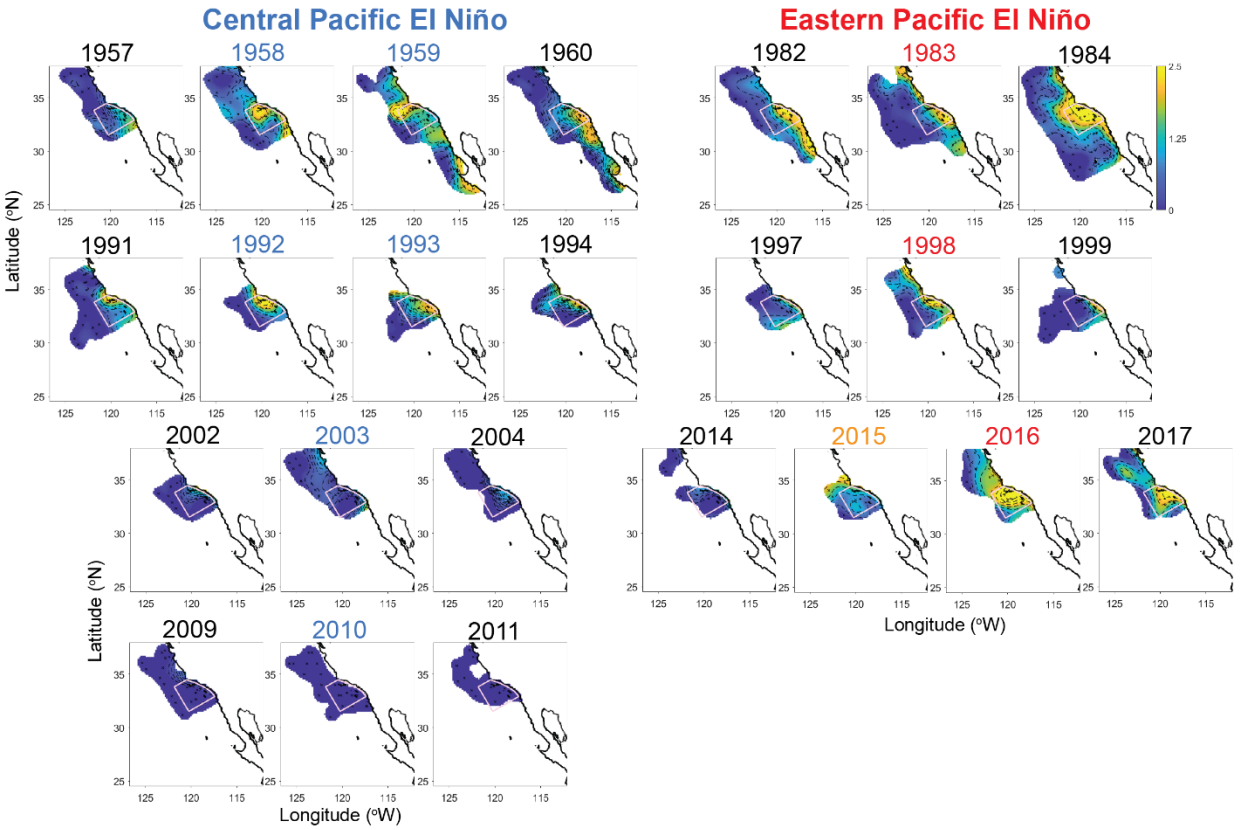

Figure S2.12. As in figure S2.10, but for *N. simplex*

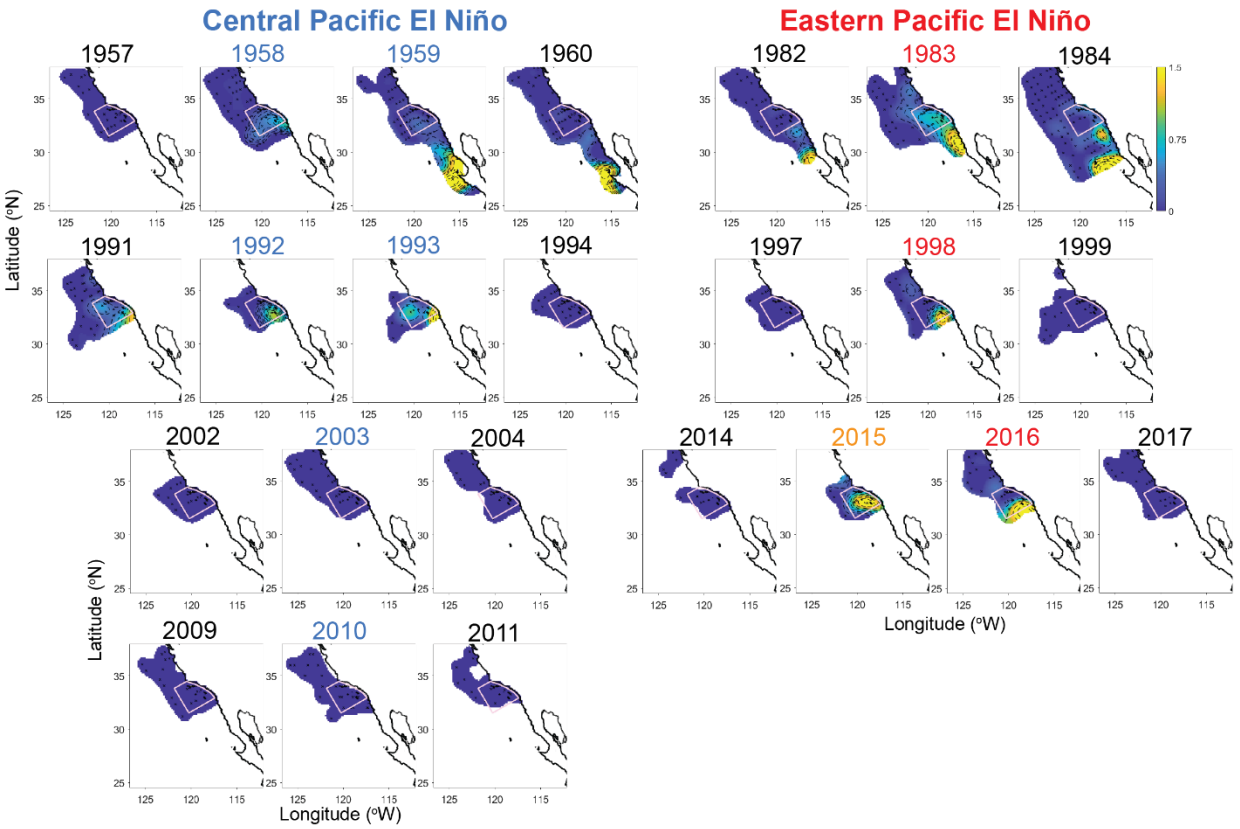

Figure S2.13. As in figure S2.10, but for *E. eximia*.

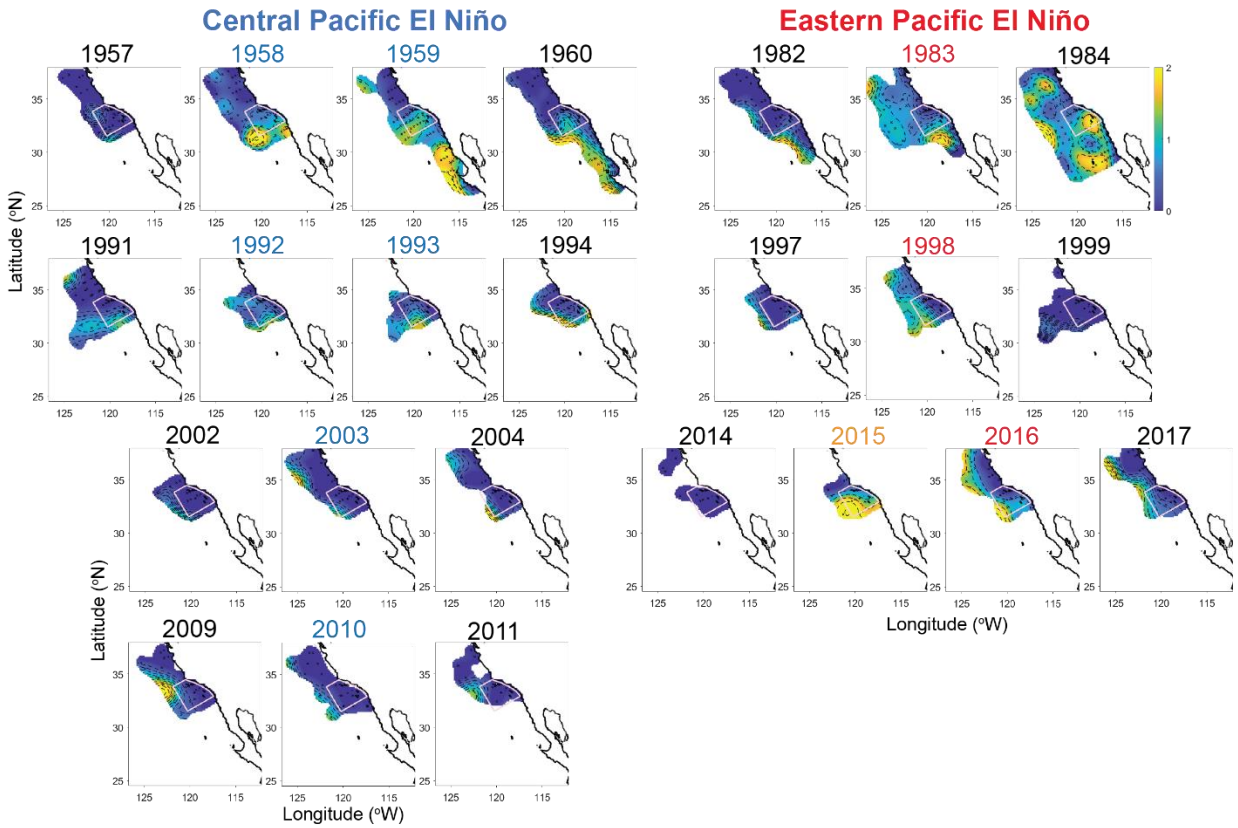

Figure S2.14. As in figure S2.10, but for *E. gibboides.*

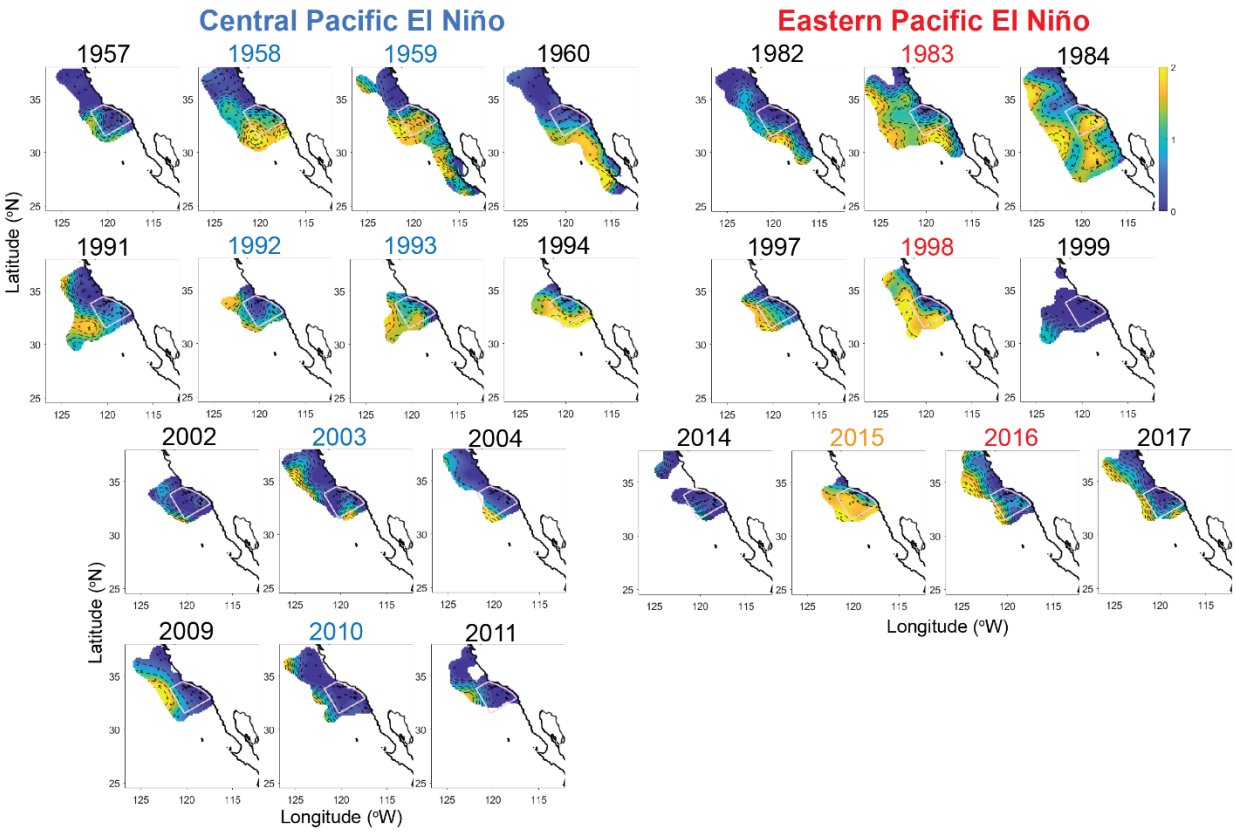

Figure S2.15. As in figure S2.10, but for *E. recurva*.

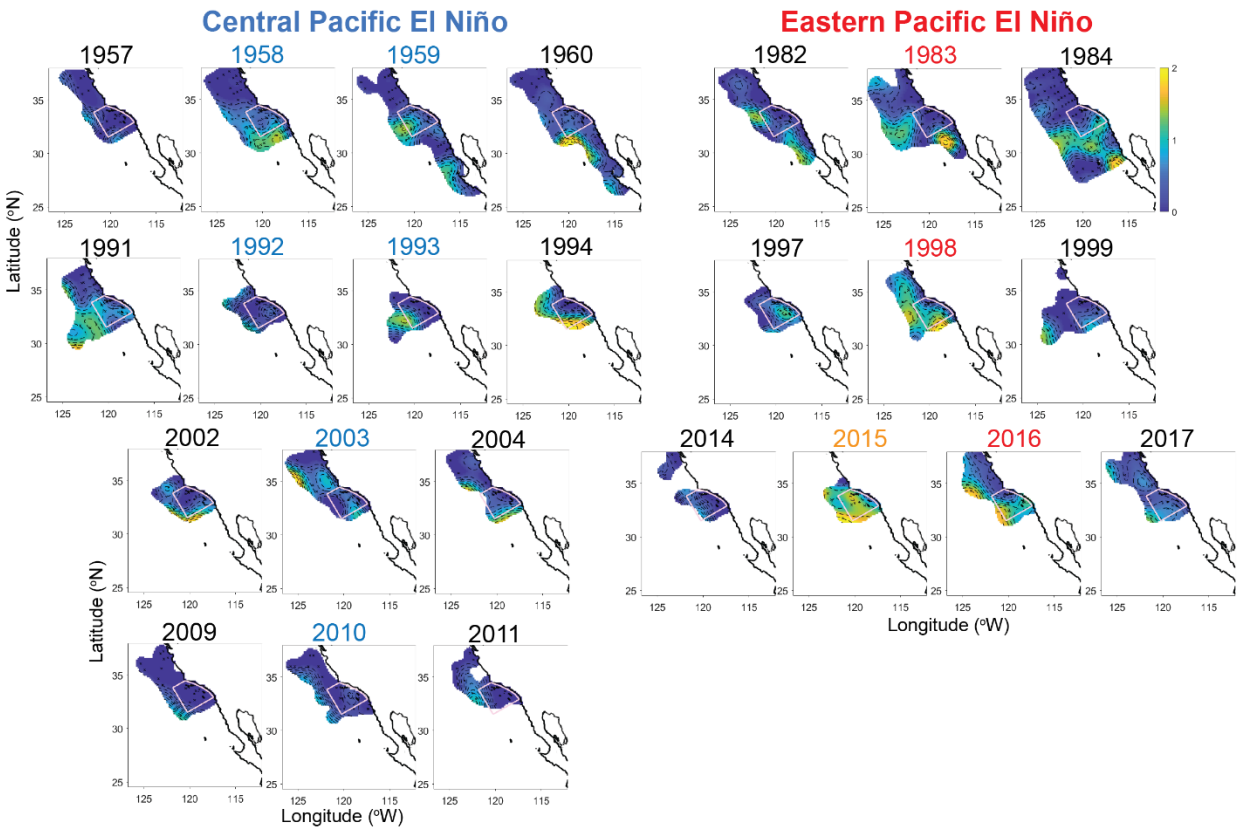

Figure S2.16. As in figure S2.10, but for *S. affine.*

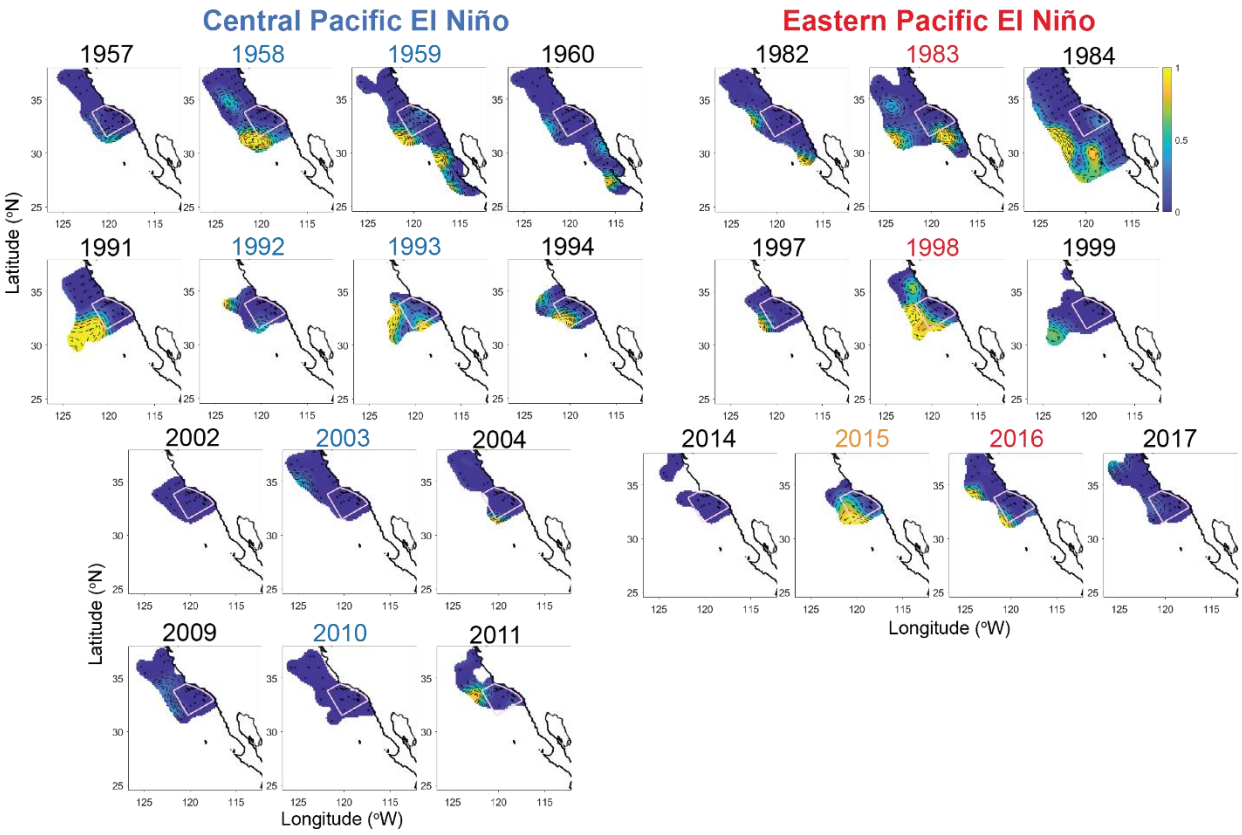

Figure S2.17. As in figure S2.10, but for *E. hemigibba.*

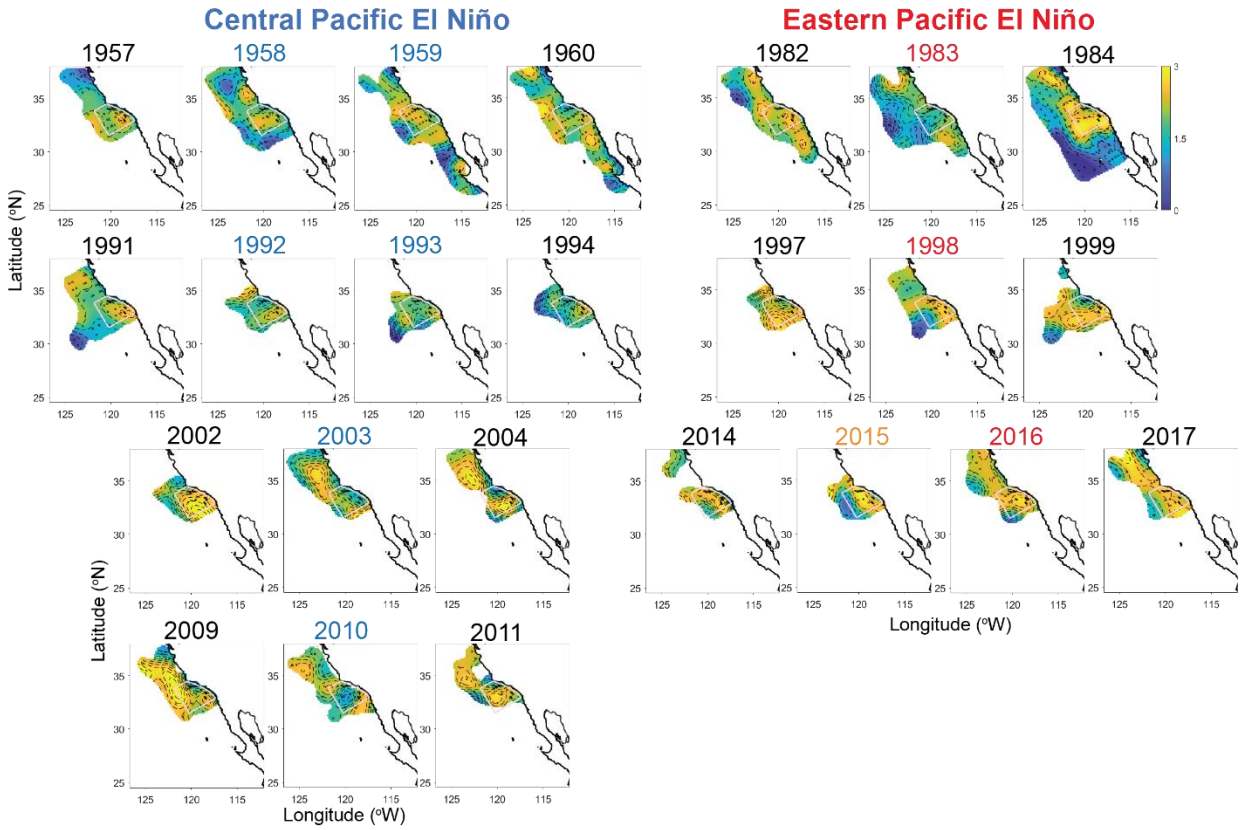

Figure S2.18. As in figure S2.10, but for *N. difficilis.*

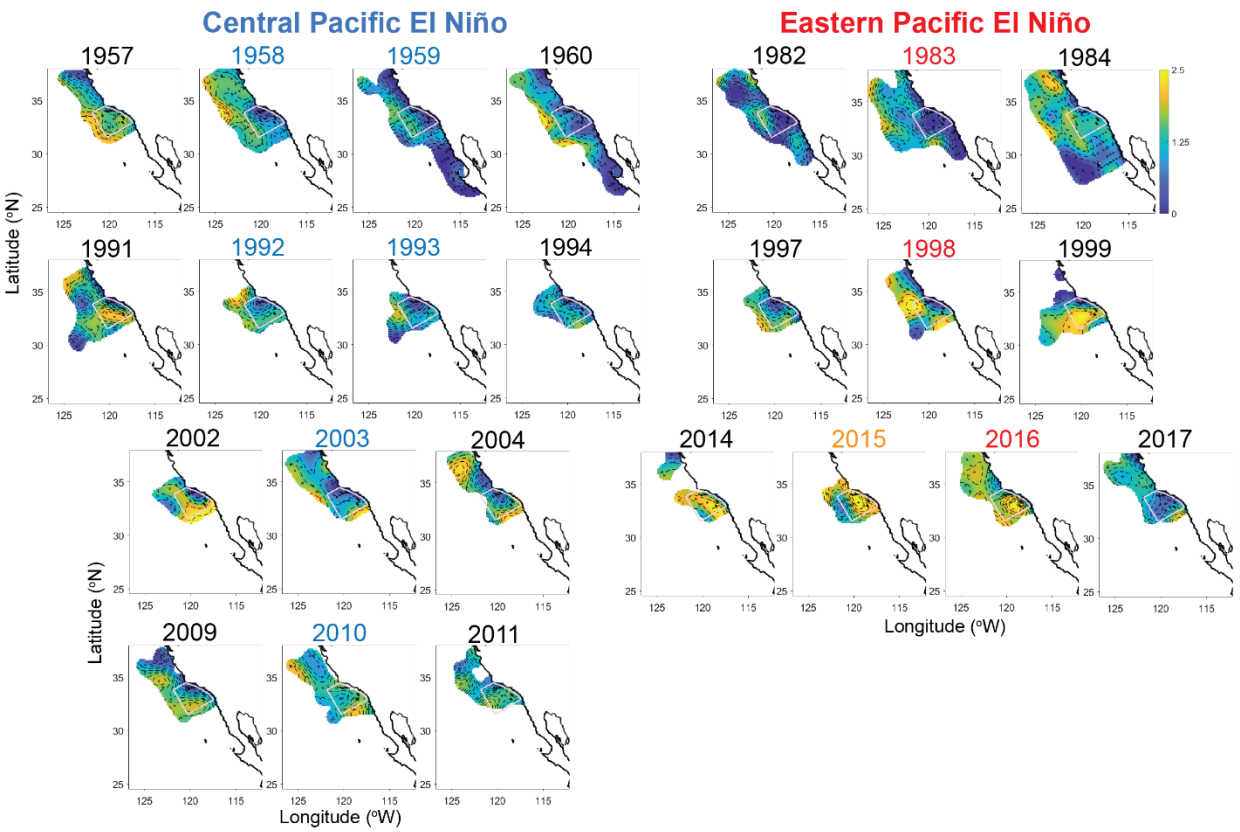

Figure S2.19. As in figure S2.10, but for *T. gregaria*.

SUPPORTING INFORMATION: Physical characterizations of individual El Niño events, 1951-2018

We present here additional information on the physical development and impacts in the equatorial Pacific and California Current System of each El Niño event considered in our analyses. See references for detailed event descriptions.

S.1. Eastern Pacific El Niño events

S.1.1. 1982-83

The 1982-82 Eastern Pacific (EP) Niño was one of the two strongest events on record in the equatorial Pacific. It was the first El Niño for which the initial development of warm conditions was observed in the western equatorial Pacific (WEP) rather than the eastern equatorial Pacific (EEP) off South America, although whether that development sequence was unprecedented or was simply the first record is not clear (Barber & Chavez, 1986; Philander, 1983). The 1982-83 EP Niño produced the strongest temperature anomalies besides the 1997-98 El Niño in the Niño1+2 region off South America, but anomalies occurred much later in event development (fall through following summer, rather than initial spring-summer) (L'Heureux et al., 2017). The 1982-83 EP Niño was dominated by onshore flow into the southern CCS from southwestern offshore waters, apparently forced by anomalous local atmospheric circulation, although it also showed characteristics of enhanced poleward advection north of Point Conception, CA, in February 1983. Poleward flow was also attributed predominantly to altered local atmospheric circulation rather than coastally trapped wave (CTW) propagation (Huyer, 1983; Simpson, 1983, 1984). Nearshore flows reversed to their normal spring equatorward

direction in March, driven by the return of normal upwelling (Ramp et al., 1997). Significant surface and subsurface warming, freshening, and oxygen increases occurred regionwide (Lynn, 1983; Ramp et al., 1997).

S.1.2. 1997-98

The 1997-98 EP Niño is considered the canonical El Niño event in both the equatorial Pacific and CCS. Its physical signature remains the strongest on record, particularly in the EEP region (L'Heureux et al., 2017; McPhaden, 1999b). In the normal cold tongue region off South America, sea surface temperature anomalies were +4^{o}C in summer-fall 1997, and eastward-propagating Kelvin waves depressed the thermocline by 90 m (McPhaden, 1999b). Positive event feedback occurred due to eastward expansion of the Western Pacific Warm Pool, which increased the area over which westerly wind bursts blew, further strengthening the event (McPhaden, 1999a, 1999b) The El Niño signal traveled to the CCS predominantly via oceanic coastally trapped waves (CTWs) that strengthened and broadened the poleward nearshore flow off California (Lynn & Bograd, 2002; Schwing et al., 2002; Schwing et al., 2005; Strub & James, 2002). Nearshore dynamic height increased significantly and nutricline depth decreased by > 80 m, and upper layer waters warmed +3-4^{o}C regionwide, due to both changes in flow patterns and thermal expansion in winter 1997-98 (Bograd & Lynn, 2001; Lynn & Bograd, 2002). The 1997-98 El Niño was also followed by the most dramatic reversal to a significant La Niña event (1998-99) on record (McPhaden, 1999a, 1999b).

S.1.3. 2015-16

The 2015-16 El Niño developed in the Equatorial Pacific initially in line with the 1997-98 event, although temperature anomalies did not develop as strongly in the EEP. In contrast, SST anomalies in the Central Equatorial Pacific (CEP) were the strongest of any El Niño on record (L'Heureux et al., 2017; Newman et al., 2018). Although our method of El Niño classification labels the 2015-16 El Niño as an EP event, it weighed equally on the E and C indices, suggesting a mixture of EP and CP characteristics (Takahashi et al., 2011; Timmermann et al., 2019). Similarly, the 2015-16 El Niño impact in the CCS was more moderate than the previous two EP Niños: positive SST anomalies did occur, strongest south of Pt. Conception, but they were weaker and also had a smaller cross-shore temperature gradient because offshore temperatures were still elevated from the 2014-15 Warm Anomaly (Jacox et al., 2016). Thermocline depression was similarly established in mid-2014 during the Warm Anomaly and remained constant and moderate (~1 standard deviation shallower than predicted) through spring 2016, suggesting weak oceanic teleconnections from the tropical Pacific (Jacox et al., 2016).

S.2. Central Pacific El Niño events

S.2.1. 1957-59

The 1957-59 El Niño was the first event recognized and studied as a significant global phenomenon with impacts beyond the equatorial Pacific (Schwing et al., 2005). The event was anomalous in that it produced significant regionwide upper ocean warming across the southern CCS but occurred against the cool background conditions of a negative Pacific Decadal Oscillation (PDO) phase (McGowan, 1998). Similar to the 1997-98 El Niño, the core California Current was displaced offshore and reduced in strength in winter 1958, and nearshore upwelling

was depressed, while the Inshore Countercurrent surface flow intensified and broadened (Brinton, 1981; Lynn, 1983; Wyllie, 1966). However, Reid (1960) posited that the 1957-59 El Niño was forced in the CCS by changes in wind-driven regional circulation rather than oceanic CTWs. Warm El Niño conditions persisted in the California Current through January 1960, over a year beyond the end of the equatorial Pacific event (Brinton, 1981).

S.2.2. 1991-93

The 1991-93 El Niño was just below our Niño1+2 cutoff for EP Niño events, and has been characterized in the equatorial Pacific as a mixed EP-CP event (Timmermann et al., 2019). Kelvin waves propagated east at the equator, though more weakly than in true EP events, and induced poleward CTW propagation (Chavez, 1996; Ramp et al., 1997). Two CTWs arrived in the CCS between Feb-Apr 1992 (Ramp et al., 1997); their arrival later in the event sequence likely induced the prolonged warm anomalies that lasted through spring 1993. The CCS experienced warm, fresh anomalies and isopycnal depression in February 1992 due to onshore flows driven by the southward-displaced Aleutian Low. Hayward (1993) described elevated SSTs and strong poleward countercurrent flows off California during fall 1991-Apr 1992, with low total zooplankton displacement volume. This period was followed by a rapid reversal to strong upwelling, decreased nearshore sea surface height (SSH), and a strong southward California Current. However, elevated SSTs persisted throughout 1992, and El Niño-related high SSH anomalies returned from late 1992-early 1993, prolonging the impact of the event in the CCS. Sea surface height anomalies from 1991-92 were comparable to those during 1982-83, but of shorter duration (eight months), at least during the initial event onset. Hayward (1993) also noted that no large salinity anomalies occurred during 1991-92, which would suggest a lack of

advection of southern waters from the Eastern Tropical Pacific; this appears to contradict the assertion by Ramp et al. (1997) that two CTWs arrived to the CCS in spring 1992, although the timings of the two studies may not overlap.

S.2.3. 2002-03

As with 1991-93, the 2002-03 El Niño characterized as a mixed EP-CP event of moderate strength in the equatorial Pacific (Timmermann et al., 2019), although its signature was very different than 1991-93 (Harrison & Chiodi, 2009). Westerly wind bursts induced subsurface Kelvin waves that generated the event, but they were weaker and farther west than during past major El Niños. Resulting strongest SST anomalies occurred in the CEP region, and the event most resembled the equatorial 1994-95 El Niño, which did not classify as a 'CCS Niño' by our metrics (McPhaden, 2004). Physical event development in the CCS in 2002-03 was preceded by an anomalously cool, high-salinity Subarctic water intrusion and strengthening of the southward core California Current in summer 2002 (Bograd & Lynn, 2003; Wheeler et al., 2003). Cool subarctic waters reached Baja California by October 2002 and induced high phytoplankton production but low zooplankton biomass (Lavaniegos, 2009; Lavaniegos & Ambriz-Arreola, 2012). The PDO also switched to a positive phase in 2002 (Lavaniegos, 2009). The 2002-03 El Niño itself was characterized by moderate warming, although low-salinity surface waters and resulting stratification persisted throughout and following the event (Lavaniegos, 2009; Lavaniegos & Ambriz-Arreola, 2012).

S.2.4. 2009-10

The 2009-10 El Niño characterizes unequivocally as a CP event in the equatorial Pacific, with record-breaking SST anomalies in the CEP (Kim et al., 2011; Lee & McPhaden, 2010). Unlike other CP events, it had a rapid decay phase to cool conditions resembling a strong EP Niño but no off-equator heat discharge as in major EP events (Kim et al., 2011). Instead, El Niño signals propagated to the CCS exclusively via atmospheric teleconnections, depressing the thermocline and warming upper ocean waters but not inducing anomalous poleward advection (Todd et al., 2011).

S.3. 2014-15 Warm Anomaly

The 2014-15 Warm Anomaly was not attributed to direct equatorial El Niño forcing. Equatorial El Niño conditions developed in spring 2014 but stalled and weakened over the summer due to anomalous eastward wind bursts (Hu & Fedorov, 2016; Li et al., 2015). However, the 2014-15 event produced unprecedented surface-enhanced warming (> +1^{o}C) and stratified, low-productivity conditions in the CCS, on par with major El Niño events. Anomalously warm conditions appeared offshore of California as early as January 2014 (Gentemann et al., 2017; Zaba & Rudnick, 2016), and definitively in the nearshore region by late spring (Leising et al., 2015; Robinson, 2016), although normal nearshore upwelling occurred in spring 2014 (Lilly et al., 2019). Regionwide anomalously warm conditions and near-zero nitrate and chlorophyll-*a* levels persisted from summer 2014-late winter 2015. Moderate upwelling reappeared off California in spring 2015, before renewed persistence of the Warm Anomaly and the subsequent El Niño arrival (Jacox et al., 2016; Lilly et al., 2019).

REFERENCES

Abrahms, B., Welch, H., Brodie, S., Jacox, M. G., Becker, E. A., Bograd, S. J., et al. (2019). Dynamic ensemble models to predict distributions and anthropogenic risk exposure for highly mobile species. *Diversity and Distributions, 25*(8), 1182-1193. doi:10.1111/ddi.12940

Aksnes, D. L. & Ohman, M. D. (2009). Multi-decadal shoaling of the euphotic zone in the southern sector of the California Current System. *Limnology and Oceanography, 54*(4), 1272-1281. doi:DOI 10.4319/lo.2009.54.4.1272

Alexander, M. A., Blade, I., Newman, M., Lanzante, J. R., Lau, N. C. & Scott, J. D. (2002). The atmospheric bridge: The influence of ENSO teleconnections on air-sea interaction over the global oceans. *Journal of Climate, 15*(16), 2205-2231.

Amante, C. & Eakins, B. W. (2009). *ETOPO1 1 Arc-Minute Global Relief Model: Procedures, Data Sources and Analysis*. Retrieved from: https://www.ngdc.noaa.gov/mgg/global/

Ashok, K., Behera, S. K., Rao, S. A., Weng, H. & Yamagata, T. (2007). El Niño Modoki and its possible teleconnection. *Journal of Geophysical Research: Oceans, 112*(C11).

Ashok, K. & Yamagata, T. (2009). The El Niño with a difference. *Nature, 461*(7263), 481-484.

Bakun, A., Black, B. A., Bograd, S. J., Garcia-Reyes, M., Miller, A. J., Rykaczewski, R. R. & Sydeman, W. J. (2015). Anticipated Effects of Climate Change on Coastal Upwelling Ecosystems. *Current Climate Change Reports, 1*(2), 85-93. doi:10.1007/s40641-015-0008-4

Barber, R. T. & Chavez, F. P. (1986). Ocean Variability in Relation to Living Resources during the 1982-83 El-Nino. *Nature, 319*(6051), 279-285. doi:DOI 10.1038/319279a0

Bograd, S. J., Castro, C. G., Di Lorenzo, E., Palacios, D. M., Bailey, H., Gilly, W. & Chavez, F. P. (2008). Oxygen declines and the shoaling of the hypoxic boundary in the California Current. *Geophysical Research Letters, 35*(12). doi:10.1029/2008gl034185

Bograd, S. J., Checkley, D. A. & Wooster, W. S. (2003). CalCOFI: a half century of physical, chemical, and biological research in the California Current System. *Deep-Sea Research Part Ii-Topical Studies in Oceanography, 50*(14-16), 2349-2353. doi:10.1016/S0967-0645(03)00122-X

Bograd, S. J. & Lynn, R. J. (2001). Physical-biological coupling in the California Current during the 1997-99 El Niño-La Niña cycle. *Geophysical Research Letters, 28*(2), 275-278.

Bograd, S. J. & Lynn, R. J. (2003). Anomalous subarctic influence in the southern California Current during 2002. *Geophysical Research Letters, 30*(15). doi:10.1029/2003gl017446

Bograd, S. J., Schroeder, I. D. & Jacox, M. G. (2019). A water mass history of the Southern California current system. *Geophysical Research Letters, 46*(12), 6690-6698. doi:10.1029/2019gl082685

Bond, N. A., Cronin, M. F., Freeland, H. & Mantua, N. (2015). Causes and impacts of the 2014 warm anomaly in the NE Pacific. *Geophysical Research Letters, 42*(9), 3414-3420. doi:10.1002/2015gl063306

Bretherton, F. P., Davis, R. E. & Fandry, C. B. (1976). A technique for objective analysis and design of oceanographic experiments applied to MODE-73. *Deep Sea Research and Oceanographic Abstracts, 23*(7), 559-582.

Brinton, E. (1960). Changes in the distribution of euphausiid crustaceans in the region of the California Current. *CalCOFI Rep., 7*, 137-146.

Brinton, E. (1962). The distribution of Pacific euphausiids. *Bulletin of the Scripps Institution of Oceanography, University of California, San Diego*(8), 51-270.

Brinton, E. (1967). Distributional atlas of Euphausiacea (Crustacea) in the California current region, Part I. In *California Cooperative Oceanic Fisheries Investigations Atlas* (Vol. 5, pp. 275 p.).

Brinton, E. (1973). Distributional atlas of euphausiacea (crustacean) in the California Current region, Part II. *CalCOFI Atlas, 18*.

Brinton, E. (1976). Population Biology of Euphausia-Pacifica Off Southern-California. *Fishery Bulletin, 74*(4), 733-762.

Brinton, E. (1979). Parameters relating to the distributions of planktonic organisms, especially euphausiids in the eastern tropical Pacific. *Progress in Oceanography, 8*(3), 125-189.

Brinton, E. (1981). Euphausiid distributions in the California Current during the warm winter-spring of 1977–78, in the context of a 1949–1966 time series. *California Cooperative Oceanic Fisheries Investigations Reports, 22*, 135-154.

Brinton, E., Ohman, M. D., Townsend, A. W., Knight, M. D. & Bridgeman, A. L. (Producer). (2000). Euphausiid of the World Ocean.

Brinton, E. & Reid, J. L. (1986). On the effects of interannual variations in circulation and temperature upon euphausiids of the California Current. *UNESCO Tech. Pap. Mar. Sci, 49*(25-34).

Brinton, E. & Townsend, A. (2003). Decadal variability in abundances of the dominant euphausiid species in southern sectors of the California Current. *Deep-Sea Research Part Ii-Topical Studies in Oceanography, 50*(14-16), 2449-2472. doi:10.1016/S0967-0645(03)00126-7

Brinton, E. & Townsend, A. W. (1981). A comparison of euphausiid abundances from bongo and 1-m CalCOFI nets. *California Cooperative Oceanic Fisheries Investigations Reports, 22*, 111-125.

Brodeur, R. D. (1986). Northward Displacement of the Euphausiid Nyctiphanes-Simplex Hansen to Oregon and Washington Waters Following the El-Nino Event of 1982-83. *Journal of Crustacean Biology, 6*(4), 686-692. doi:Doi 10.2307/1548382

Cane, M. A. (1986). El-Nino. *Annual Review of Earth and Planetary Sciences, 14*, 43-70. doi:DOI 10.1146/annurev.ea.14.050186.000355

Capotondi, A. (2013). ENSO diversity in the NCAR CCSM4 climate model. *Journal of Geophysical Research-Oceans, 118*(10), 4755-4770. doi:10.1002/jgrc.20335

Capotondi, A., Wittenberg, A. T., Newman, M., Di Lorenzo, E., Yu, J. Y., Braconnot, P., et al. (2015). Understanding ENSO diversity. *Bulletin of the American Meteorological Society, 96*(6), 921-938.

Chao, Y., Farrara, J. D., Bjorkstedt, E., Chai, F., Chavez, F., Rudnick, D. L., et al. (2017). The origins of the anomalous warming in the California coastal ocean and San Francisco Bay during 2014-2016. *Journal of Geophysical Research-Oceans, 122*(9), 7537-7557. doi:10.1002/2017jc013120

Chavez, F. P. (1996). Forcing and biological impact of onset of the 1992 El Niño in central California. *Geophysical Research Letters, 23*(3), 265-268.

Croll, D. A., Marinovic, B., Benson, S., Chavez, F., Black, N., Temullo, R. & Tershy, B. R. (2005). From wind to whales: trophic links in a coastal upwelling ecosystem. *Marine Ecology Progress Series, 289*, 117-130. doi:10.3354/meps289117

Croll, D. A., Newton, K. M., Weng, K., Galvan-Magana, F., O'Sullivan, J. & Dewar, H. (2012). Movement and habitat use by the spine-tail devil ray in the Eastern Pacific Ocean. *Marine Ecology Progress Series, 465*, 193-200. doi:10.3354/meps09900

Croll, D. A., Tershy, B. R., Hewitt, R. P., Demer, D. A., Fiedler, P. C., Smith, S. E., et al. (1998). An integrated approach to the foraging ecology of marine birds and mammals. *Deep-Sea Research Part Ii-Topical Studies in Oceanography, 45*(7), 1353-+. doi:Doi 10.1016/S0967-0645(98)00031-9

Davis, R. E. (1985). Objective mapping by least squares fitting. *Journal of Geophysical Research: Oceans, 90*(C3), 4773-4777.

Di Lorenzo, E. & Mantua, N. (2016). Multi-year persistence of the 2014/15 North Pacific marine heatwave. *Nature Climate Change, 6*(11), 1042-1047.

Di Lorenzo, E. & Ohman, M. D. (2013). A double-integration hypothesis to explain ocean ecosystem response to climate forcing. *Proceedings of the National Academy of Sciences, 110*(7), 2496-2499.

Dorman, J. G., Powell, T. M., Sydeman, W. J. & Bograd, S. J. (2011). Advection and starvation cause krill (Euphausia pacifica) decreases in 2005 Northern California coastal populations: Implications from a model study. *Geophysical Research Letters, 38*(L04605).

Fasiolo, M., Nedellec, R., Goude, Y. & Wood, S. N. (2019). Scalable Visualization Methods for Modern Generalized Additive Models. *Journal of Computational and Graphical Statistics*. doi:10.1080/10618600.2019.1629942

Fiedler, P. C., Reilly, S. B., Hewitt, R. P., Demer, D., Philbrick, V. A., Smith, S., et al. (1998). Blue whale habitat and prey in the California Channel Islands. *Deep-Sea Research Part Ii-Topical Studies in Oceanography, 45*(8-9), 1781-1801. doi:Doi 10.1016/S0967-0645(98)80017-9

Frischknecht, M., Munnich, M. & Gruber, N. (2017). Local atmospheric forcing driving an unexpected California Current System response during the 2015-2016 El Nino. *Geophysical Research Letters, 44*(1), 304-311. doi:10.1002/2016gl071316

Gentemann, C. L., Fewings, M. R. & Garcia-Reyes, M. (2017). Satellite sea surface temperatures along the West Coast of the United States during the 2014-2016 northeast Pacific marine heat wave. *Geophysical Research Letters, 44*(1), 312-319. doi:10.1002/2016gl071039

Glynn, P. W. (1988). El-Nino Southern Oscillation 1982-1983 - Nearshore Population, Community, and Ecosystem Responses. *Annual Review of Ecology and Systematics, 19*, U309-+.

Gomez, J. G. (1995). Distribution Patterns, Abundance and Population-Dynamics of the Euphausiids Nyctiphanes-Simplex and Euphausia-Eximia Off the West-Coast of Baja-California, Mexico. *Marine Ecology Progress Series, 119*(1-3), 63-76. doi:DOI 10.3354/meps119063

Harrison, D. E. & Chiodi, A. M. (2009). Pre-and post-1997/98 westerly wind events and equatorial Pacific cold tongue warming. *Journal of Climate, 22*(3), 568-581.

Hastie, T. & Tibshirani, R. (1987). Generalized Additive-Models - Some Applications. *Journal of the American Statistical Association, 82*(398), 371-386. doi:Doi 10.2307/2289439

Hayward, T. L. (1993). Preliminary observations of the 1991–1992 El Niño in the California Current. *California Cooperative Oceanic Fisheries Investigations Reports, 34*(21-29).

Hazen, E. L., Jorgensen, S., Rykaczewski, R. R., Bograd, S. J., Foley, D. G., Jonsen, I. D., et al. (2013). Predicted habitat shifts of Pacific top predators in a changing climate. *Nature Climate Change, 3*(3), 234-238. doi:10.1038/Nclimate1686

Hazen, E. L., Palacios, D. M., Forney, K. A., Howell, E. A., Becker, E., Hoover, A. L., et al. (2017). WhaleWatch: a dynamic management tool for predicting blue whale density in the California Current. *Journal of Applied Ecology, 54*(5), 1415-1428. doi:10.1111/1365-2664.12820

Hu, S. N. & Fedorov, A. V. (2016). Exceptionally strong easterly wind burst stalling El Nino of 2014. *Proceedings of the National Academy of Sciences of the United States of America, 113*(8), 2005-2010. doi:10.1073/pnas.1514182113

Huyer, A. (1983). Coastal upwelling in the California Current System. *Progress in Oceanography, 12*, 259-284.

Jacox, M. G., Fiechter, J., Moore, A. M. & Edwards, C. A. (2015). ENSO and the California Current coastal upwelling response. *Journal of Geophysical Research-Oceans, 120*(3), 1691-1702. doi:10.1002/2014jc010650

Jacox, M. G., Hazen, E. L., Zaba, K. D., Rudnick, D. L., Edwards, C. A., Moore, A. M. & Bograd, S. J. (2016). Impacts of the 2015-2016 El Nino on the California Current System: Early assessment and comparison to past events. *Geophysical Research Letters, 43*(13), 7072-7080. doi:10.1002/2016gl069716

Kao, H. Y. & Yu, J. Y. (2009). Contrasting Eastern-Pacific and Central-Pacific Types of ENSO. *Journal of Climate, 22*(3), 615-632. doi:10.1175/2008jcli2309.1

Karnauskas, K. B. (2013). Can we distinguish canonical El Nino from Modoki? *Geophysical Research Letters, 40*(19), 5246-5251. doi:10.1002/grl.51007

Keister, J. E., Johnson, T. B., Morgan, C. A. & Peterson, W. T. (2005). Biological indicators of the timing and direction of warm-water advection during the 1997/1998 El Nino off the central Oregon coast, USA. *Marine Ecology Progress Series, 295*, 43-48. doi:DOI 10.3354/meps295043

Kim, W., Yeh, S. W., Kim, J. H., Kug, J. S. & Kwon, M. (2011). The unique 2009–2010 El Niño event: A fast phase transition of warm pool El Niño to La Niña. *Geophysical Research Letters, 38*(15).

Kug, J. S., Jin, F. F. & An, S. I. (2009). Two Types of El Nino Events: Cold Tongue El Nino and Warm Pool El Nino. *Journal of Climate, 22*(6), 1499-1515. doi:10.1175/2008jcli2624.1

L'Heureux, M. L., Takahashi, K., Watkins, A. B., Barnston, A. G., Becker, E. J., Di Liberto, T. E., et al. (2017). Observing and Predicting the 2015/16 El Nino. *Bulletin of the American Meteorological Society, 98*(7), 1363-1382. doi:10.1175/Bams-D-16-0009.1

Larkin, N. K. & Harrison, D. E. (2005). On the definition of El Niño and associated seasonal average US weather anomalies. *Geophysical Research Letters, 32*(12).

Lavaniegos, B. E. (1992). Growth and larval development of Nyctiphanes simplex in laboratory conditions. *CalCOFI Rep., 33*, 162-171.

Lavaniegos, B. E. (2009). Influence of a multiyear event of low salinity on the zooplankton from Mexican eco-regions of the California Current. *Progress in Oceanography, 83*(1-4), 369-375.

Lavaniegos, B. E. & Ambriz-Arreola, I. (2012). Interannual variability in krill off Baja California in the period 1997-2005. *Progress in Oceanography, 97*, 164-173. doi:10.1016/j.pocean.2011.11.008

Lavaniegos, B. E., Jiménez-Herrera, M. & Ambriz-Arreola, I. (2019). Unusually low euphausiid biomass during the warm years of 2014–2016 in the transition zone of the California Current. *Deep Sea Research Part II: Topical Studies in Oceanography*, 104638.

Lavaniegos, B. E., Jimenez-Perez, L. C. & Gaxiola-Castro, G. (2002). Plankton response to El Nino 1997-1998 and La Nina 1999 in the southern region of the California Current. *Progress in Oceanography, 54*(1-4), 33-58. doi:10.1016/S0079-6611(02)00042-3

Lavaniegos, B. E. & Ohman, M. D. (2007). Coherence of long-term variations of zooplankton in two sectors of the California Current System. *Progress in Oceanography, 75*(1), 42-69. doi:10.1016/j.pocean.2007.07.002

Lee, D. E., Nur, N. & Sydeman, W. J. (2007). Climate and demography of the planktivorous Cassin's auklet Ptychoramphus aleuticus off northern California: implications for population change. *Journal of Animal Ecology, 76*(2), 337-347. doi:10.1111/j.1365-2656.2007.01198.x

Lee, T. & McPhaden, M. J. (2010). Increasing intensity of El Nino in the central-equatorial Pacific. *Geophysical Research Letters, 37*. doi:Artn L1460310.1029/2010gl044007

Leising, A. W., Schroeder, I. D., Bograd, S. J., Abell, J., Durazo, R., & & Warybok, P. (2015). State of the California Current 2014-15: Impacts of the Warm-Water" Blob". *California Cooperative Oceanic Fisheries Investigations Reports, 56*, 31-68.

Li, J. Y., Liu, B. Q., Li, J. D. & Mao, J. Y. (2015). A Comparative Study on the Dominant Factors Responsible for the Weaker-than-expected El Nino Event in 2014. *Advances in Atmospheric Sciences, 32*(10), 1381-1390. doi:10.1007/s00376-015-4269-6

Lilly, L. E. & Ohman, M. D. (2018). CCE IV: El Niño-related zooplankton variability in the southern California Current System. *Deep-Sea Research Part I: Oceanographic Research Papers*.

Lilly, L. E., Send, U., Lankhorst, M., Martz, T. R., Feely, R. A., Sutton, A. J. & Ohman, M. D. (2019). Biogeochemical anomalies at two southern California Current System moorings during the 2014-16 Warm Anomaly-El Niño sequence. *Journal of Geophysical Research: Oceans*.

Lynn, R. J. (1983). The 1982-83 warm episode in the California Current. *Geophysical Research Letters, 10*(11), 1093-1095.

Lynn, R. J. & Bograd, S. J. (2002). Dynamic evolution of the 1997-1999 El Nino-La Nina cycle in the southern California Current System. *Progress in Oceanography, 54*(1-4), 59-75. doi:Pii S0079-6611(02)00043-5

Mackas, D. L. & Galbraith, M. (2002). Zooplankton community composition along the inner portion of Line P during the 1997-1998 El Nino event. *Progress in Oceanography, 54*(1-4), 423-437. doi:10.1016/S0079-6611(02)00062-9

Mackas, D. L., Peterson, W. T., Ohman, M. D. & Lavaniegos, B. E. (2006). Zooplankton anomalies in the California Current system before and during the warm ocean conditions of 2005. *Geophysical Research Letters, 33*(22).

Marinovic, B. B., Croll, D. A., Gong, N., Benson, S. R. & Chavez, F. P. (2002). Effects of the 1997-1999 El Nino and La Nina events on zooplankton abundance and euphausiid community composition within the Monterey Bay coastal upwelling system. *Progress in Oceanography, 54*(1-4), 265-277. doi:10.1016/S0079-6611(02)00053-8

Matthews, S. A., Goetze, E. & Ohman, M. D. (2020). *Cross-shore Changes in Vertical Habitats of Mesozoplankton: A Paired Metabarcoding and Morphological Approach*. Paper presented at the Ocean Sciences Meeting 2020, San Diego, CA, USA.

McClatchie, S., Gao, J., Drenkard, E. J., Thompson, A. R., Watson, W., Ciannelli, L., et al. (2018). Interannual and secular variability of larvae of mesopelagic and forage fishes in the Southern California current system. *Journal of Geophysical Research: Oceans, 123*(9), 6277-6295.

McGowan, J. A. (1998). Climate-ocean variability and ecosystem response in the northeast Pacific (vol 281, pg 210, 1998). *Science, 282*(5388), 417-417.

McLain, D. R. & Thomas, D. H. (1983). Year-to-year fluctuations of the California Countercurrent and effects on marine organisms. *CalCOFI Rep., 24*(165-181).

McPhaden, M. J. (1999a). El Nino - The child prodigy of 1997-98. *Nature, 398*(6728), 559-+. doi:Doi 10.1038/19193

McPhaden, M. J. (1999b). Genesis and evolution of the 1997-98 El Nino. *Science, 283*(5404), 950-954. doi:DOI 10.1126/science.283.5404.950

McPhaden, M. J. (2004). Evolution of the 2002/03 El Nino. *Bulletin of the American Meteorological Society, 85*(5), 677-695. doi:10.1175/Bams-85-5-677

Miller, C. B., Batchelder, H. P., Brodeur, R. D. & Pearcy, W. G. (1985). Response of the zooplankton and ichthyoplankton off Oregon to the El Niño event of 1983. In W. S. Wooster & A. L. Fluharty (Eds.), *El Niño North* (pp. 185-187): Washington Sea Grant Program.

Newman, M., Wittenberg, A. T., Cheng, L. Y., Compo, G. P. & Smith, C. A. (2018). The Extreme 2015/16 El Nino, in the Context of Historical Climate Variability and Change. *Bulletin of the American Meteorological Society*, *99*(1), S16-S20. doi:10.1175/Bams-D-17-0116.1

Nickels, C. F., Sala, L. M. & Ohman, M. D. (2018). The morphology of euphausiid mandibles used to assess selective predation by blue whales in the southern sector of the California Current System. *Journal of Crustacean Biology, 38*(5), 563-573.

Nickels, C. F., Sala, L. M. & Ohman, M. D. (2019). The euphausiid prey field for blue whales around a steep bathymetric feature in the southern California current system. *Limnology and Oceanography, 64*(1), 390-405. doi:10.1002/lno.11047

Notarbartolo-di-Sciara, G. (1988). Natural history of the rays of the genus Mobula in the Gulf of California. *Fishery Bulletin, 86*(1), 45-66.

Office of Protected Resources, N. (2018a). *BLUE WHALE (Balaenoptera musculus musculus): Eastern North Pacific Stock*. Retrieved from https://www.fisheries.noaa.gov/national/marine-mammal-protection/marine-mammal-stock-assessment-reports-species-stock#cetaceans---large-whales

Office of Protected Resources, N. (2018b). HUMPBACK WHALE (Megaptera novaeangliae): California/Oregon/Washington Stock.

Ohman, M. D. & Lavaniegos, B. E. (2002). Comparative zooplankton sampling efficiency of a ring net and bongo net with comments on pooling of subsamples. *California Cooperative Oceanic Fisheries Investigations Reports*, 162-173.

Ohman, M. D., Mantua, N., Keister, J., Garcia-Reyes, M. & McClatchie, S. (2017). ENSO impacts on ecosystem indicators in the California Current System. *US Clivar Variations, 15*(1), 8-15.

Ohman, M. D. & Romagnan, J. B. (2016). Nonlinear effects of body size and optical attenuation on Diel Vertical Migration by zooplankton. *Limnology and Oceanography, 61*(2), 765-770. doi:10.1002/lno.10251

Ohman, M. D. & Smith, P. E. (1995). A comparison of zooplankton sampling methods in the CalCOFI time series. *California Cooperative Oceanic Fisheries Investigations Reports*, 153-158.

Pares-Escobar, F., Lavaniegos, B. E. & Ambriz-Arreola, I. (2018). Interannual summer variability in oceanic euphausiid communities off the Baja California western coast during 1998-2008. *Progress in Oceanography, 160*, 53-67. doi:10.1016/j.pocean.2017.11.009

Peterson, W. T., Keister, J. E. & Feinberg, L. R. (2002). The effects of the 1997-99 El Nino/La Nina events on hydrography and zooplankton off the central Oregon coast. *Progress in Oceanography, 54*(1-4), 381-398. doi:Doi 10.1016/S0079-6611(02)00059-9

Philander, S. G. H. (1983). Meteorology - Anomalous El-Nino of 1982-83. *Nature, 305*(5929), 16-16. doi:DOI 10.1038/305016a0

Ramp, S. R., McClean, J. L., Collins, C. A., Semtner, A. J. & Hays, K. A. S. (1997). Observations and modeling of the 1991-1992 El Nino signal off central California. *Journal of Geophysical Research-Oceans, 102*(C3), 5553-5582. doi:Doi 10.1029/96jc03050

Reid, J. L. (1960). *Oceanography of the eastern North Pacific in the last 10 years*. Retrieved from

Ren, H. L. & Jin, F. F. (2011). Niño indices for two types of ENSO. *Geophysical Research Letters, 38*(4).

Robinson, C. J. (2016). Evolution of the 2014–2015 sea surface temperature warming in the central west coast of Baja California, Mexico, recorded by remote sensing. *Geophysical Research Letters, 43*(13), 7066-7071.

Ross, R. M. (1982). Energetics of Euphausia-Pacifica .1. Effects of Body Carbon and Nitrogen and Temperature on Measured and Predicted Production. *Marine Biology, 68*(1), 1-13. doi:10.1007/Bf00393135

Rudnick, D. L., Zaba, K. D., Todd, R. E. & Davis, R. E. (2017). A climatology of the California Current System from a network of underwater gliders. *Progress in Oceanography, 154*, 64-106. doi:10.1016/j.pocean.2017.03.002

Rykaczewski, R. R. & Dunne, J. P. (2010). Enhanced nutrient supply to the California Current Ecosystem with global warming and increased stratification in an earth system model. *Geophysical Research Letters, 37*. doi:10.1029/2010gl045019

Santora, J. A., Mantua, N. J., Schroeder, I. D., Field, J. C., Hazen, E. L., Bograd, S. J., et al. (2020). Habitat compression and ecosystem shifts as potential links between marine

heatwave and record whale entanglements. *Nature Communications, 11*(1). doi:10.1038/s41467-019-14215-w

Santora, J. A., Sydeman, W. J., Schroeder, I. D., Wells, B. K. & Field, J. C. (2011). Mesoscale structure and oceanographic determinants of krill hotspots in the California Current: Implications for trophic transfer and conservation. *Progress in Oceanography, 91*(4), 397-409. doi:10.1016/j.pocean.2011.04.002

Santora, J. A., Zeno, R., Dorman, J. G. & Sydeman, W. J. (2018). Submarine canyons represent an essential habitat network for krill hotspots in a large marine ecosystem. *Scientific Reports, 8*(1), 1-9.

Schwing, F. B., Murphree, T. & Green, P. M. (2002). The evolution of oceanic and atmospheric anomalies in the northeast Pacific during the El Niño and La Niña events of 1995–2001. *Progress in Oceanography, 54*(1), 459-491.

Schwing, F. B., Palacios, D. M. & Bograd, S. J. (2005). El Nino impacts of the California current ecosystem. *US CLIVAR Newsletter, 3*(2), 5-8.

Simpson, J. J. (1983). Large-Scale Thermal Anomalies in the California Current during the 1982-1983 El-Nino. *Geophysical Research Letters, 10*(10), 937-940. doi:DOI 10.1029/GL010i010p00937

Simpson, J. J. (1984). El-Nino-Induced Onshore Transport in the California Current during 1982-1983. *Geophysical Research Letters, 11*(3), 241-242.

Smiles, M. C. & Pearcy, W. G. (1971). Size Structure and Growth Rate of Euphausia-Pacifica Off Oregon Coast. *United States Fish and Wildlife Service Fishery Bulletin, 69*(1), 79-&.

Stewart, J. D., Rohner, C. A., Araujo, G., Avila, J., Fernando, D., Forsberg, K., et al. (2017). Trophic overlap in mobulid rays: insights from stable isotope analysis. *Marine Ecology Progress Series, 580*, 131-151. doi:10.3354/meps12304

Strub, P. T. & James, C. (2002). The 1997-1998 oceanic El Niño signal along the southeast and northeast Pacific boundaries - an altimetric view. *Progress in Oceanography, 54*(1-4), 439-458.

Sydeman, W. J., Bradley, R. W., Warzybok, P., Abraham, C. L., Jahncke, J., Hyrenbach, K. D., et al. (2006). Planktivorous auklet Ptychoramphus aleuticus responses to ocean climate, 2005: Unusual atmospheric blocking? *Geophysical Research Letters, 33*(22). doi:10.1029/2006gl026736

Szesciorka, A. R., Ballance, L. T., Širović, A., Rice, A., Ohman, M. D., Hildebrand, J. A. & Franks, P. J. (2020). Timing is everything: Drivers of interannual variability in blue whale migration. *Scientific Reports, 10*(1), 1-9.

Takahashi, K., Montecinos, A., Goubanova, K. & Dewitte, B. (2011). ENSO regimes: Reinterpreting the canonical and Modoki El Nino. *Geophysical Research Letters, 38*. doi:10.1029/2011gl047364

Tanasichuk, R. W. (1998). Interannual variations in the population biology and productivity of Euphausia pacifica in Barkley Sound, Canada, with special reference to the 1992 and 1993 warm ocean years. *Marine Ecology Progress Series, 173*, 163-180. doi:Doi 10.3354/Meps173163

Timmermann, A., An, S.-I., Kug, J. S., Jin, F. F., Cai, W., Capotondi, A., et al. (2019). El Niño-Southern Oscillation complexity. *Nature, 559*, 535-545.

Todd, R. E., Rudnick, D. L., Davis, R. E. & Ohman, M. D. (2011). Underwater gliders reveal rapid arrival of El Nino effects off California's coast. *Geophysical Research Letters, 38*. doi:10.1029/2010gl046376

Wang, D. W., Gouhier, T. C., Menge, B. A. & Ganguly, A. R. (2015). Intensification and spatial homogenization of coastal upwelling under climate change. *Nature, 518*(7539), 390-394. doi:10.1038/nature14235

Wheeler, P. A., Huyer, A. & Fleischbein, J. (2003). Cold halocline, increased nutrients and higher chlorophyll off Oregon in 2002. *Geophysical Research Letters, 30*(14). doi:10.1029/2003gl017395

Wickett, W. P. (1967). Ekman transport and zooplankton concentration in the North Pacific Ocean. *Journal of the Fisheries Board of Canad, 24*(3), 581-594.

Wood, S. N., Li, Z. Y., Shaddick, G. & Augustin, N. H. (2017). Generalized Additive Models for Gigadata: Modeling the UK Black Smoke Network Daily Data. *Journal of the American Statistical Association, 112*(519), 1199-1210. doi:10.1080/01621459.2016.1195744

Wyllie, J. G. (1966). Geostrophic flow of the California Current at the surface and at 200 m. In *CalCOFI Atlas* (Vol. 4). University of California, San Diego.

Wyrtki, K. (1975). El Nino - Dynamic-Response of Equatorial Pacific Ocean to Atmospheric Forcing. *Journal of Physical Oceanography, 5*(4), 572-584. doi:Doi 10.1175/1520-0485(1975)005<0572:Entdro>2.0.Co;2

Yeh, S. W., Kug, J. S., Dewitte, B., Kwon, M. H., Kirtman, B. P. & Jin, F. F. (2009). El Nino in a changing climate (vol 461, pg 511, 2009). *Nature, 462*(7273). doi:10.1038/nature08546

Zaba, K. D. & Rudnick, D. L. (2016). The 2014-2015 warming anomaly in the Southern California Current System observed by underwater gliders. *Geophysical Research Letters, 43*(3), 1241-1248. doi:10.1002/2015gl067550

Zaba, K. D., Rudnick, D. L., Cornuelle, B., Gopalakrishnan, G. & Mazloff, M. (2020). Volume and heat budgets in the coastal California Current System: Means, annual cycles and interannual anomalies of 2014-2016. *Journal of Physical Oceanography*.

Chapter 3

Using a Lagrangian particle tracking model to evaluate impacts of El Niño-related anomalous advection on euphausiids in the southern California Current System

Abstract

The relative influences of advection and *in situ* population growth in explaining zooplankton changes off California during El Niño events are not well understood. Here we examine whether variability in advection alone can explain biomass fluctuations and distributional shifts of five euphausiid species in the southern California Current System (CCS) from 2008-2017, a period encompassing a Central Pacific El Niño (2009-10), Warm Anomaly (2014-15), and Eastern Pacific El Niño (2015-16). We employ the California State Estimate (CASE), a regionally-optimized implementation of the MIT general circulation model, to quantify El Niño- and Warm Anomaly-associated variability in likely source water flows for each species. Anomalies of spring biomass of each species covaried positively with anomalous flows from their respective source waters in the preceding November-January, indicating winter advection most affects subsequent spring population changes. Subtropical coastal (*Nyctiphanes simplex*) and tropical Pacific (*Euphausia eximia*) species show consistent time-lagged correlation patterns across larval (calyptopis) and adult phases, suggesting initial advection of multiple life history phases into the Southern California Bight. In contrast, cool-water species (*Euphausia pacifica, Nematoscelis difficilis*) and an offshore subtropical species (*Euphausia gibboides*) show differential temporal phasing of calyptopes and adults; strongest associations of calyptopes with flow anomalies in February-March suggest *in situ* reproduction increases with enhanced flow of

source waters. Winter source waters for cool-water species during the 2015-16 EP Niño originated inshore off central California, rather than the core California Current, suggesting *in situ* recirculation instead of favorable habitat sourcing from the north. Subtropical and tropical species were influenced predominantly by southern offshore waters, which likely transported favorable habitat for temporary *in situ* reproduction. While favorable advection contributes to species changes, it alone does not completely account for observed biomass variability. Explicit measurements of growth and mortality rates are needed to unambiguously resolve the dominant forcing mechanisms that affect euphausiid species during El Niño events and improve future predictions of community change, with implications for carbon export and higher trophic levels.

3.1. Introduction

Unusual zooplankton occurrences (e.g., tropical species sightings, short-term dominance by rare taxa) have been observed periodically in the southern California Current System (CCS) for as long as observations have been made. Such appearances are often considered indicators of anomalous physical ocean conditions, which are in turn forced primarily by basin-wide atmosphere-ocean interannual anomalies (e.g., El Niño) or interdecadal variability (e.g., Pacific Decadal Oscillation (PDO), Mantua et al. (1997); North Pacific Gyre Oscillation (NPGO), Di Lorenzo et al. (2008)). The general consensus on unusual zooplankton appearances in the CCS is that anomalous advection transports novel species directly into the region (Bernal, 1981; Bernal & McGowan, 1981; Brinton, 1960; Chelton et al., 1982; Peterson, 1998; Peterson et al., 2017), while altered habitat conditions influence the survival and reproduction of both non-native and resident species (Brinton, 1981; Lavaniegos & Ambriz-Arreola, 2012).

Anomalous advection into the southern CCS is usually defined as increased transport of Tropical Pacific waters poleward along Baja California and into the Southern California Bight (SCB) (Lynn & Bograd, 2002; Ramp et al., 1997; Schwing et al., 2002; Strub & James, 2002) or onshore transport of offshore subtropical waters associated with the North Pacific Central Gyre (Simpson, 1984; Zaba & Rudnick, 2016), to magnitudes and spatial extents beyond normal seasonal fluctuations. Anomalous advection into the CCS occurs notably in conjunction with El Niño events, which can propagate to extratropical latitudes via combinations of oceanic coastally trapped waves (CTWs) and atmospheric teleconnections, producing a range of anomalous physical conditions. Mechanisms of anomalous advection into the CCS include: 1) enhanced nearshore poleward transport due to CTW propagation from the equatorial Pacific (Lynn & Bograd, 2002; Ramp et al., 1997; Schwing et al., 2002; Strub & James, 2002); 2) changes in wind-driven circulation due to atmospheric teleconnections and resulting shifts in the Aleutian Low pressure system (Alexander et al., 2002; Simpson, 1984); or 3) onshore advection of warm, salty, southern offshore waters due to altered atmospheric circulation (Jacox et al., 2016; Simpson, 1984). See Lilly and Ohman (submitted, Supplemental Information) for a summary of the dominant CCS physical forcing mechanisms during El Niño events from 1951-2018.

Recent studies have suggested grouping the equatorial Pacific expressions of El Niño events into either Eastern Pacific (EP) or Central Pacific (CP) events (Ashok & Yamagata, 2009; Capotondi et al., 2015; Kao & Yu, 2009; Kug et al., 2009; Ren & Jin, 2011; Yeh et al., 2014). However, both Niño categories can produce various combinations of the three above-mentioned types of advection into the CCS. Within the timeseries analyzed for this study (2008-2017), three anomalous interannual events affected the CCS, each with distinct forcing mechanisms and physical characteristics. The 2009-10 CP Niño had the strongest positive temperature anomaly

on record in the central equatorial Pacific (Kim et al., 2011) but only induced shallow (50 m) temperature anomalies in the Southern California Bight (Rudnick et al., 2017). The event altered circulation patterns in the CCS but did not produce anomalous poleward transport from the Tropical Pacific (Rudnick et al., 2017; Todd et al., 2011). The 2015-16 EP Niño induced significant temperature anomalies in the eastern equatorial Pacific but was eventually characterized as a mixed EP/CP Niño (L'Heureux et al., 2017; Newman et al., 2018; Timmermann et al., 2019). The event induced CTW propagation to the CCS and anomalous poleward transport to Pt. Conception (Chao et al., 2017; Rudnick et al., 2017; Zaba et al., 2020), but anomalous upwelling winds and minimal thermocline deepening in fall 2015 muted the strength of the event (Jacox et al., 2016). A third anomalous event, the 2014-15 Warm Anomaly, was initially expressed at high latitudes (Bond et al., 2015) but eventually produced unprecedented and sustained shallow positive temperatures across the Eastern North Pacific (Gentemann et al., 2017; Lilly et al., 2019; Zaba & Rudnick, 2016) and onshore flow in the southern CCS (Zaba & Rudnick, 2016), both comparable to the magnitude of El Niño anomalies. Zooplankton species vary in their biogeographic affinities and optimal habitat conditions within the CCS, so the specific combination of anomalous flow direction and strength and *in situ* habitat changes of an individual El Niño event can produce unique zooplankton community rearrangements (Brinton, 1960, 1962, 1981; Lavaniegos & Ambriz-Arreola, 2012; Lilly & Ohman, submitted; Pares-Escobar et al., 2018; Peterson et al., 2017).

Past studies of zooplankton in the CCS have found evidence for both direct advection of populations and variability in population growth rates due to *in situ* habitat changes. Brinton (1981) attributed intrusions of subtropical euphausiid species into the southern CCS during the 1957-59 El Niño to poleward and shoreward transport anomalies, but also noted range

contraction of a cool-water species to only waters <15^{o}C and also post-Niño retraction of subtropical species offshore due to cooling in the SCB. More recent analyses of euphausiid species variability in the southern CCS (Lilly & Ohman, submitted) and off Baja California (Pares-Escobar et al., 2018) across multiple El Niño events found associations of species variability with changing habitat conditions. However, Lilly and Ohman (submitted) also suggested anomalous poleward or onshore advection as the likely mechanisms explaining the initial appearances of subtropical species during El Niño events. Other studies have correlated certain euphausiid species (notably *Nyctiphanes simplex*) with variability in PDO-related advection (Brinton & Townsend, 2003; time-lagged in the case of Di Lorenzo & Ohman, 2013).

Keister et al. (2011) and Dorman et al. (2011b) conducted two of the only known particle-tracking studies of zooplankton in the CCS, and showed an important role of anomalous advection in transporting zooplankton-like particles to new regions. However, Dorman et al. (2011b) noted the role of delayed upwelling, in addition to anomalous poleward advection, in reducing abundance of the dominant coastal CCS euphausiid, *Euphausia pacifica*, off Northern California during anomalous conditions in winter-spring 2005. Thus, although anomalous advection appears to serve a significant role in altering zooplankton populations in the CCS, the question of whether species are actually transported into or out of the southern CCS with anomalous flows or respond *in situ* to enhanced transport of favorable habitat or other means of *in situ* physical changes is still largely unanswered.

The CCS euphausiid community undergoes notable changes in species dominance during El Niño events (Brinton, 1960, 1981; Brinton & Townsend, 2003; Lavaniegos & Ambriz-Arreola, 2012; Lavaniegos et al., 2019; Lavaniegos et al., 2002; Lilly & Ohman, 2018, submitted; Pares-Escobar et al., 2018). A recent analysis of ten CCS euphausiid species

identified five “El Niño response” groups based on shared biogeographic affinities and El Niño-related spatial changes, with the goal of determining the dominant forcing mechanisms that affect each group. The five groups are as follow (see Lilly and Ohman (submitted) for details):

1. **Cool-Water Coastally-Associated** (*Euphausia pacifica, Thysanoessa spinifera*) – dominant species in CCS; significant nearshore, poleward retractions during EP Niños; moderate regionwide decrease during CP Niños. Proposed forcing mechanism: mortality due to unfavorable *in situ* habitat conditions (e.g., warm temperatures, low productivity).
2. **Regionwide Temperate** *(Nematoscelis difficilis, Thysanoessa gregaria)* **–** similar to above group, although with CCS regionwide distributions; less affected by El Niño, likely due to deeper habitat (~400 m daytime).
3. **Subtropical Coastal** (*Nyctiphanes simplex*) – population center off coastal Baja California; regularly extends poleward coastally into SCB, and farther during some EP Niños; localized expansion in SCB during CP Niños. Proposed forcing mechanisms: initial poleward advection with subsequent *in situ* reproduction during and post-Niño.
4. **Tropical Pacific/Baja California** (*Euphausia eximia*) – centered offshore of Baja California; only present off southern California during major El Niños. Proposed forcing mechanism: direct poleward advection with anomalous poleward flow; requires above-average water temperatures in SCB to survive.
5. **Subtropical Offshore** (*Euphausia gibboides, Euphausia recurva, Stylocheiron affine, Euphausia hemigibba*) – inhabit offshore North Pacific Central Gyre waters; expand shoreward to SCB during some El Niños, with short-term post-event reproduction. Proposed forcing mechanism: shoreward advection (occasionally poleward offshore) due to anomalous flow; *in situ* reproduction under sustained favorable habitat conditions.

Despite past analyses of El Niño-related euphausiid population rearrangements, questions remain about the relative influences of advection and *in situ* population growth or mortality in causing short-term distributional shifts. The overarching goal of this study is to analyze whether advection alone can explain euphausiid species distributional and biomass variability in the southern CCS during El Niño events. Specifically:

1. Does any euphausiid species vary in biomass proportionally with changes in its source flow?
2. Do non-resident (i.e., subtropical, tropical) species always appear in the southern CCS during periods of anomalous advection?
3. Do adult and calyptopis (larval) stages of a species have similar responses to variability in flow?
4. Do winter source waters for any species vary between non-Niño years and the three anomalously warm conditions?

Euphausiids form essential components of diets of fishes (Genin et al., 1988; Tanasichuk, 1999; Yamamura et al., 1998), marine mammals (Croll et al., 2005; Nickels et al., 2018, 2019), and seabirds (Lee et al., 2007; Thayer & Sydeman, 2007), with many higher trophic species preferentially foraging on single euphausiid species (Croll et al., 1998; Nickels et al., 2018, 2019; Thayer & Sydeman, 2007). Detecting and predicting fluctuations in the species-specific euphausiid community can therefore inform predictions of altered foraging patterns of higher trophic levels.

3.2. Methods

3.2.1. Euphausiid data

3.2.1.1. Sample collection and species enumerations

We analyzed five euphausiid species (*Euphausia pacifica, Nematoscelis difficilis, Nyctiphanes simplex, Euphausia eximia, Euphausia gibboides*) that inhabit different subregions of the CCS and have unique El Niño population responses. All euphausiid data come from the California Cooperative Oceanic Fisheries Investigations (CalCOFI) sampling program, which conducts four quarterly cruises per year off Central and Southern California. The program samples on a regular station grid (see https://calcofi.org/ for complete station map), but the actual subset of stations successfully sampled in a year can vary depending on weather conditions and ship time. Zooplankton are sampled on all cruises but are only enumerated taxonomically from the spring (usually April/May) cruise (see Lavaniegos et al. (2002) and Lilly and Ohman (2018) for complete sampling and preservation procedures). For each CalCOFI station, an aliquot is sorted and all euphausiids are identified to species level and life-history phase. Body lengths are converted to carbon biomass using known taxon-specific length-carbon relationships (Lavaniegos & Ohman, 2007; Ross, 1982). We considered only nighttime samples to eliminate complications from day/night vertical migration and daytime net avoidance. For the current study, we conducted all calculations using log(carbon biomass (mg C m^{-2})+1), to reduce skew from single values of extremely high biomass.

3.2.1.2. Biomass anomalies

To determine changes in species biomass within the period of interest, we calculated station-by-station annual anomalies by removing the station-specific 2008-2017 mean from the biomass of each year at that station. The 2008-2017 mean corresponds to the temporal availability of modeled flow fields available (see Section 3.2.2.1). We used objective mapping

(described in Lilly & Ohman, submitted) to convert the grid of CalCOFI station biomasses into smoothed distribution maps. For each year's mapped distribution, we then calculated the threshold contours above which occurred 50% and 80% of the maximum biomass for that year (e.g., for a year of maximum species biomass = 1.0 log(mg C m^{-2}), the 80% threshold included all regions of >0.8 log(mg C m^{-2}) and the 50% threshold included all regions of >0.5-0.8 log(mg C m^{-2})).

To calculate correlations of species biomass anomalies with flow anomalies, we first calculated the regionwide mean species biomass anomaly for each year from all stations within that year. Some years in the timeseries had no detection (zero biomass) of *N. simplex* or *E. eximia*; these years are indicated in figure 3.2 by '*' symbols on the x-axes. Years of zero biomass differ slightly in their (negative) anomalies because each year consists of a different subset of CalCOFI stations sampled, each of which has a different mean to remove from zero, resulting in slightly different negative average anomalies. For correlations of *E. eximia* and *E. gibboides* calyptopis phases with flow, we used abundance (no. m^{-2}), rather than biomass, because calyptopes of these species were sparse and small enough that their abundances did not register as biomass. Correlations of total population with flow were nearly identical for biomass and abundance, so we retained the biomass correlations of total populations in figure 3.4, for consistency with figures 3.2 and 3.3.

3.2.2. CASE model and study region

3.2.2.1. Model description

We used current fields from the California State Estimate (CASE) as the source of flow fields to force particle backtrack runs. CASE is a regionally optimized subset of the

Massachusetts Institute of Technology general circulation model (MITgcm; Marshall et al., 1997) and Estimating the Circulation and Climate of the Ocean (ECCO; Stammer et al., 2002) four-dimensional variational (4DVAR) assimilation system. The CASE model domain used here encompasses the region 116^{o}W-128^{o}W x 30^{o}N-38^{o}N and is integrated onto a (1/16)^{o} x (1/16)^{o} x (8 km) spherical polar grid with 72 *z*-depth levels of varying thickness. The physical data assimilated include profiles from Argo floats (Roemmich et al., 2009), the California Underwater Glider Network (CUGN, Rudnick et al., 2017), and expendable bathythermographs (NOAA, 2021). The resulting flow fields are cross-validated against the CalCOFI hydrography dataset. See Zaba et al. (2018) for more information about model data assimilation and forcing. We used a version of the model that consists of 41 non-overlapping three-month estimates between 1 January 2007-31 March 2017. Flow values are calculated to daily resolution.

3.2.2.2. Flow anomalies

We considered flow only on the 55 m depth level, which integrates the surrounding 10 m of flow (50-60 m). We chose this depth because it corresponds to the midpoint depth of nighttime vertical distributions (100-0 m) of the five species analyzed here (Brinton, 1962; Matthews et al., 2020). We calculated and removed interannual means and seasonal cycles from the u- and v-velocity timeseries (separately) to produce flow anomalies, and then averaged those values point-by-point across all days in a month to produce monthly-averaged flow anomalies.

We applied a smoothing filter to the flow fields to smooth finer-scale variability in the model output. The filter was a 2D Gaussian with a standard deviation of 60 km (isotropic in x and y), with influence truncated beyond 5x the standard deviation (300 km total). All flow values within that range (150 km on either side of the center flowpoint) were averaged using their

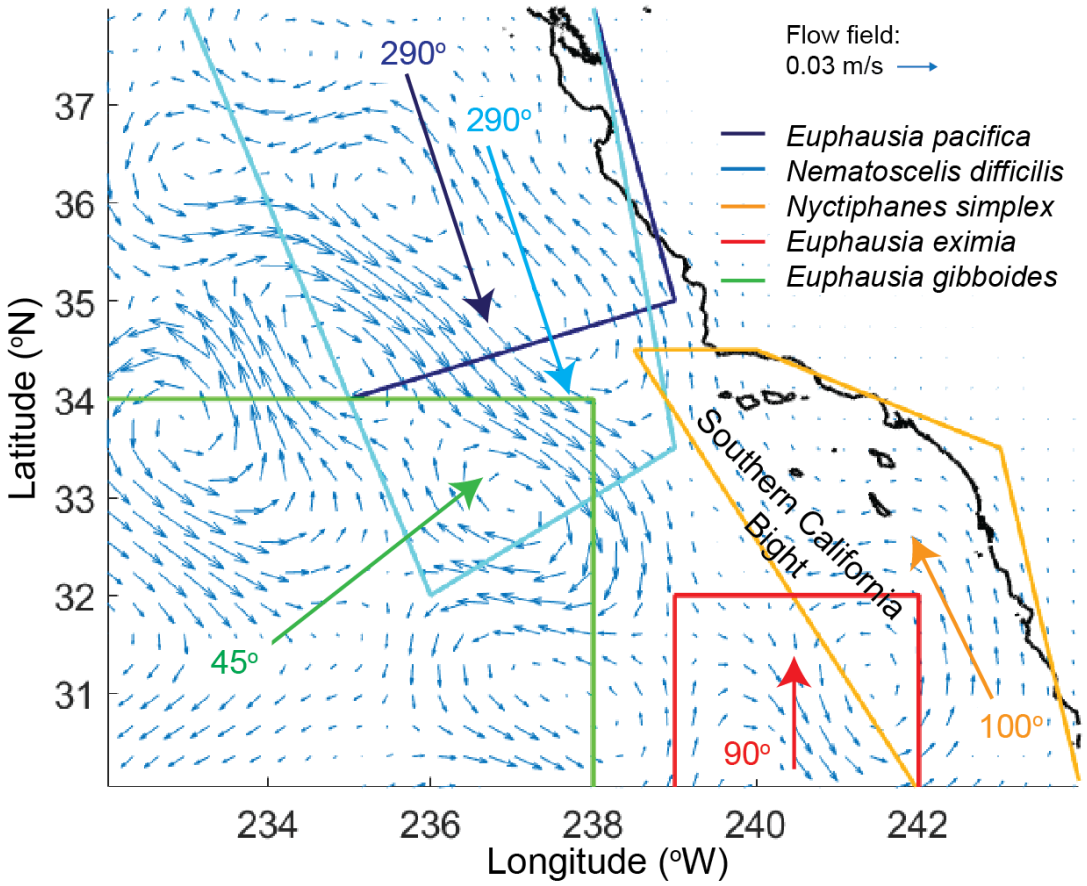

Figure 3.1. Monthly averaged flow anomalies for December 2009 (small blue arrows in background) overlain with locations of source flow boxes and expected dominant direction of transport for the five 'El Niño response' euphausiid groups (colored boxes and large arrows). The direction corresponding to each arrow is noted in degrees (oriented to 0 = East). Source boxes and directions of dominant flow were defined based on known habitat distributions and El Niño-related spatial variability of each species (see Methods 3.2.2.3). Magnitude of flow field anomalies is shown in top right corner.

Gaussian weights (i.e., flow values farthest away had the smallest weights) to produce a weighted-average value at that point. All flow anomalies for correlations were calculated from the filtered flow field, but particle tracks (Section 3.2.3) were calculating using the unfiltered flow field.

3.2.2.3. Source boxes

For each of the five euphausiid species, we defined a flow 'source box' as the subregion of the CASE model within which we expected flow anomalies to have the greatest influence in terms of transporting a species into the CalCOFI sampling region (Fig. 3.1). We defined each species' source box by drawing upon its previously described biogeographic affinity within the CCS (Brinton, 1962) and objectively mapped CalCOFI distribution (Lilly & Ohman, submitted) to define its expected non-Niño population center. We used the same criteria to define the dominant direction of flow for each species, which we considered the direct track that source waters (and potentially euphausiid populations) would follow from a species' population center to the sampled CalCOFI region. These directions were also based on the directions of most consistent population expansion during El Niño events; in the case of cool-water species, flows were the opposite direction from the species' El Niño-related population contractions.

3.2.3. Particle-tracking model

To determine the winter origins of source waters and possible seed populations impacting spring euphausiid distributions, we used a particle-tracking model forced by the CASE u and v flow fields at 55 m to backtrack particles from 31 March to the prior 1 December for each year of interest (see figure 3.5 for example particle backtracks). The model interpolates gridded velocity to particle positions, with an integration timestep of 0.01 day (100 timesteps for each 24-hr flow point). Particles were seeded on 31 March within the contours of the 50% and 80% thresholds defined from each year's objective map of population (see Section 3.2.1.2). Particles for individual anomalous year backtracks (springs 2010, 2015, 2016; see figure 3.5) were seeded at resolutions of one particle per 0.24^{o} longitude and 0.16^{o} latitude spacing (50 particles spanning the full latitude and 50 particles spanning the full longitude ranges of CASE). Although a new

model estimate begins on 1 Jan of each year, creating potential discontinuities between the 1 Jan and 31 Dec flow-days, the integrative nature of the particle-tracking model reduced any impacts of discontinuities on the appearances of trajectories. Because the CASE current fields are forward run, we conducted forward/backward comparative particle runs before backtracking the full region, to verify that backtracking did not produce significant chaotic displacement. Particles were forward-run from 1 Dec to 31 Mar, and their end-locations were then backtracked to 1 Dec. Spatial displacements of the 1 Dec particle backtracks from their original 1 Dec start points were minimal ($<10^{-6}$ m in both x and y, not shown), signifying that chaotic motion did not appear to skew backtracks compared to forward tracks. To determine whether small spatial displacements in the seeding locations of particles produced substantially different end-locations due to small-scale features in the flow field, we calculated the 'end-spreads' between groups of 25 particles seeded within 0.1^o, 0.05^o, or 0.01^o grid cells. In almost all cases, the end-spread between particles within a grid cell was $<0.2^o$ in x and y for the 0.1^o cells, so we concluded that particle seeding at a resolution of several tenths of a degree was sufficient to depict the resolution of water parcel circulation we were interested in.

In addition to backtracks for the individual anomalous years, we also created 'non-Niño composite backtracks,' which consisted of overlays of all the individual spring backtracks from each non-Niño year (all years between 2008-2017 except 2010, 2015, and 2016; see figure 3.5a). The composite backtracks for *E. pacifica* and *N. difficilis* only seeded particles at 0.6^o longitude and 0.4^o latitude spacing (20 particles spanning the full longitude and latitude ranges, respectively, of the model) to reduce the total number of backtracked particles for easier viewing. Composites for the other three species used the same particle seeding resolution as did individual years. Composite backtracks were overlain by 'average non-Niño' spring distributions, which

were calculated by first averaging the station-by-station biomasses of a species across all non-Niño years, then calculating an objective map from the station averages and identifying the 80% and 50% thresholds from the average map.

Proportions of winter backtracked particles in each of the four quadrants for each year in the timeseries (Fig. 3.A1) were calculated as the number of particles in a region divided by the total number of particles that remained in the CASE region at the end of the backtrack (some particles seeded in spring ended up beyond the region boundaries and were thus not counted).

3.3. Results

3.3.1. Covariability of flow and euphausiid biomass

3.3.1.1. Flow anomalies, 2007-2017

Figure 3.2 illustrates timeseries of the monthly-averaged flow anomalies within each source box for its defined dominant direction of flow (colored lines in figure 3.2 correspond to boxes and arrows in figure 3.1). Arrows on left axes of figure 3.2 indicate rough cardinal directions corresponding to positive and negative flow for that box. See figures S3.1-S3.5 for spatial depictions of Nov-Mar monthly flows for the 2009-10, 2014-15, and 2015-16 anomalies, as well as 2012-13 (a representative non-Niño year). We first describe variability in flow anomalies for each source box; in the next section, we analyze correspondence of altered flow with variability in euphausiid species biomasses.

Anomalously positive (southward) flows in the source boxes of the two cool-water species, *Euphausia pacifica* and *Nematoscelis difficilis*, were strongest and most persistent from late 2007-late 2008 and again from spring-fall 2016, two non-Niño periods (Fig. 3.2a-b).

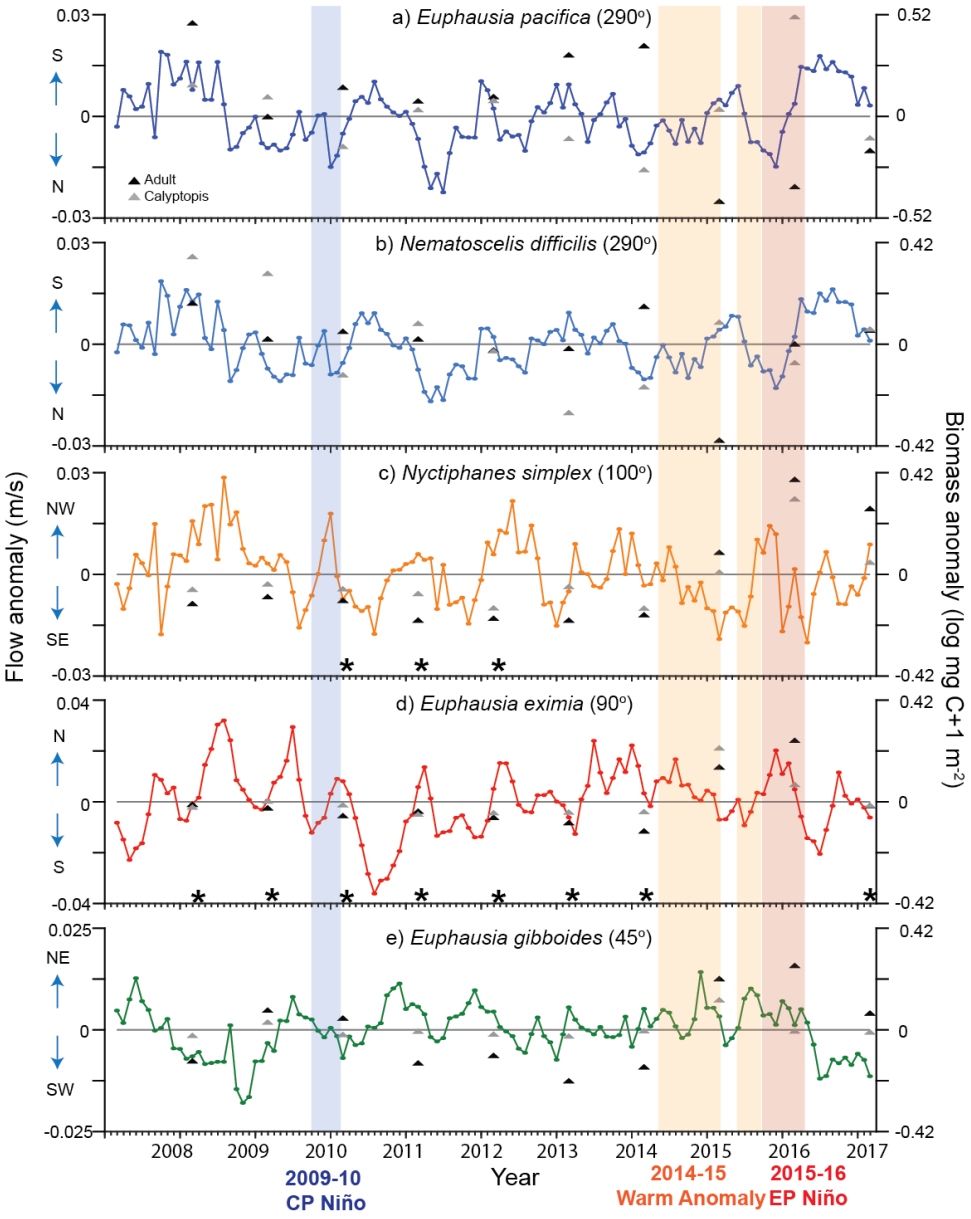

Figure 3.2. Timeseries of monthly averaged component along the expected direction of water flow (solid lines) averaged within the source box defined for each euphausiid species in figure 3.1. Dominant directions of flow are shown in degrees after species names. Interannual spring biomass anomalies for total biomass (black triangles) and calyptopis phase only (grey triangles) are overlain and correspond to the right axes (biomass as log(mgC+1 m^{-2}); calyptopis anomalies are multiplied by 5 to align with total anomalies. Calyptopis anomalies for *E. eximia* and *E. gibboides* are abundance, log (no.+1 m^{-2})). Shaded vertical regions indicate the 2009-10 CP Niño (blue), 2014-15 Warm Anomaly (two orange segments), and 2015-16 EP Niño (red). Arrows next to left axes indicate flow directions corresponding to positive and negative anomalies. Asterisks ('*') on x-axes for *Nyctiphanes simplex* and *Euphausia eximia* indicate years of zero biomass; anomalies for those years differ slightly from each other based on each year's individual combination of CalCOFI stations averaged (see Methods 3.2.1.2).

Strongest negative (northward) flow anomalies also occurred in a non-Niño period (mid-2011), but the second-strongest negative anomalies occurred in January 2010 and December 2015, during the 2009-10 CP Niño (purple shaded bar) and 2015-16 EP Niño (red shaded bar), respectively. Moderately negative flow also occurred immediately preceding and intermittently throughout the first part of the Warm Anomaly (late 2013-2014) but reversed to positive southward flow during the Spring 2015 upwelling period (denoted by gap between vertical orange bars in figure 3.2). Thus, much of the anomalous time-periods for these two species were characterized by at least moderately negative (unfavorable) source flows.

Source flow for the subtropical species *Nyctiphanes simplex* shows several periods of sustained enhanced poleward flow unrelated to the anomalous years analyzed here: early 2008-early 2009, 2012, and mid 2013-mid 2014 (Fig. 3.2c). However, the third- and fourth-strongest single months of poleward flow anomalies were January 2010 (during the 2009-10 CP Niño) and November 2015 (2015-16 EP Niño), respectively, suggesting favorable transport of either source waters or seed populations during these periods. The Tropical Pacific species *Euphausia eximia* showed elevated poleward flows during many of the same periods as *N. simplex*, although anomalies were not sustained for as long (Fig. 3.2d). Magnitudes of variability for *E. eximia* source flow were also the greatest of the five boxes. Similar to *N. simplex*, *E. eximia* source flow was positive during the anomalous periods of the 2009-10 CP Niño (positive flow in January-February 2010) and the 2015-16 EP Niño (October 2015-February 2016), although the 2010 anomalies were only moderate compared to other anomalously positive periods. Unlike *N. simplex*, however, the *E. eximia* flow showed a period of low-magnitude but prolonged favorable poleward flow throughout the first part of the Warm Anomaly (spring-summer 2014).

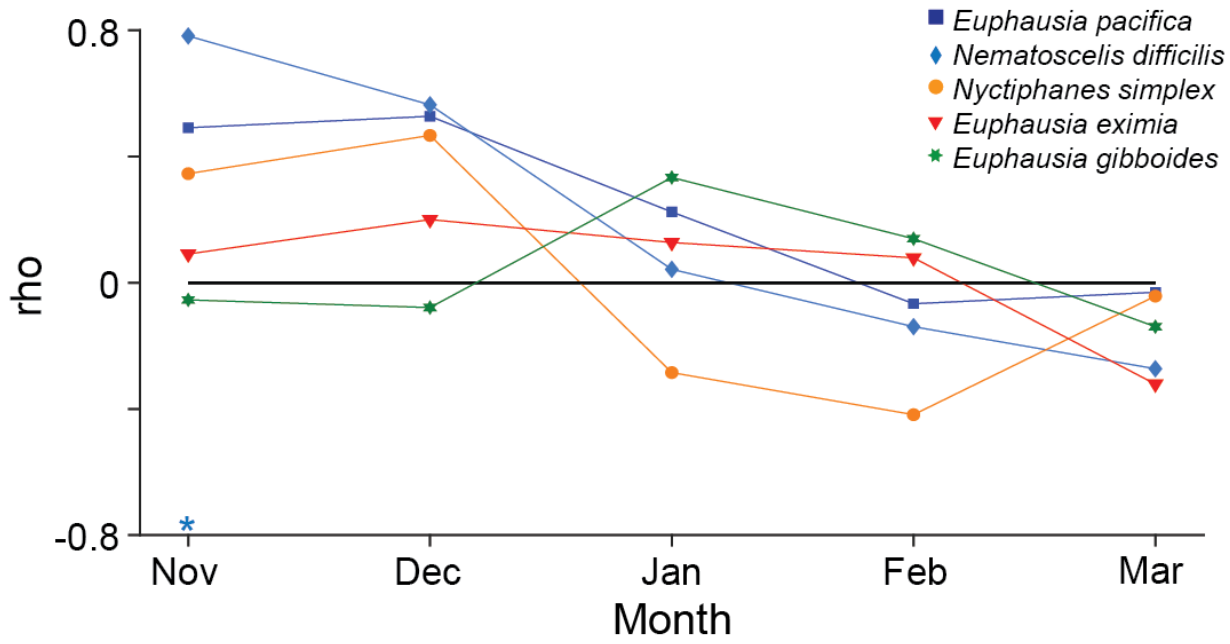

Figure 3.3. Timeseries of lagged correlations between flow anomalies (Nov-Mar) and euphausiid spring biomass (black triangles in figure 3.2). Asterisk above x-axis indicates significant correlation ($p < 0.05$) of *N. difficilis* with November flow.

Source flows for *Euphausia gibboides* had the lowest-magnitude variability of the five species (Fig. 3.2e). The 2009-10 CP Niño period showed zero flow anomalies (i.e., no deviations from the mean). However, the 2014-15 Warm Anomaly showed multiple periods of positive (northeastward) flow, and the 2015-16 EP Niño showed moderate but still positive flow. The single month of strongest positive flow was December 2014, at the height of the Warm Anomaly. The *E. gibboides* flow timeseries also shows a clear negative effect of the spring 2015 upwelling period, which appeared to reverse flow to slightly anomalously offshore, as would be expected during upwelling. However, positive flow anomalies reemerged in summer 2015 at almost the same strength as in late 2014.

3.3.1.2. Time-lagged correlations of flow and biomass anomalies

To determine whether biomass anomalies tracked flow anomalies either directly or with a time-lag, we analyzed visual correspondence of euphausiid biomass anomalies with flow anomalies (Fig. 3.2) and calculated time-lagged correlations of spring biomass with the five preceding months of source flow anomalies (Nov-Mar) across the 2007-2017 timeseries (Fig. 3.3). Given evidence for euphausiid lifespans in the CCS region of 7-8 months (*N. simplex,* Gomez, 1995; Lavaniegos, 1992) to 1 year (*E. pacifica*, Ross, 1982; Ross et al., 1982), we hypothesized that spring populations would be most strongly impacted by direct advection from approximately the five preceding months. Extending time-lagged correlations back to include flow from 10 months prior yielded weaker correlations than 3- to 5-month lags for all species (data not shown).

All five species showed highest positive correlations of spring biomass with flow from the preceding late fall-winter (Fig. 3.3; November – *N. difficilis*, $p < 0.05$; December – *E. pacifica, N. simplex, E. eximia;* January – *E. gibboides*), suggesting that late fall-early winter flow patterns have the greatest impact on spring biomass. In contrast, almost all correlations of spring biomass with February-March flow were negative or neutral, suggesting populations had reached sufficiently established levels to withstand reversals of spring flows back out of the CalCOFI region (i.e., elimination of population seeding or favorable source habitat). The apparent later influence of flow on the offshore subtropical species (*E. gibboides*) may reflect the greater distance it initially has to travel to reach the SCB.

Analysis of euphausiid biomass anomalies from individual years help explain the correlation patterns. Total biomass anomalies of both *E. pacifica* and *N. difficilis* are notably elevated in springs 2008 (both species) and 2013 (*E. pacifica*), periods of sustained southward flow (Fig. 3.2a-b; black triangles denote total biomass). Elevated biomass of both species in

spring 2014 does not obviously follow a period of strong or sustained southward flow, so it may reflect continued population persistence and reproduction throughout 2013 in the presence of favorable habitat conditions. Negative biomass anomalies of both species in spring 2015 and *E. pacifica* in spring 2016 follow periods of negative (enhanced northward) flow, suggesting the populations off central and southern California experienced either reduced seeding or reduced advection of favorable habitat. Biomass of both species recovered somewhat by spring 2017, following a prolonged period of strongly elevated and sustained southward flow.

The three subtropical-tropical species present greater challenges to calculating correlations because they were only present at very low levels or not detected at all in the CalCOFI region during several springs (Fig. 3.2c-e; '*' on x-axes denote years of no detection. Anomalies for zero-biomass years vary slightly due to different combinations of CalCOFI stations averaged). *Nyctiphanes simplex* was not detected in the sampled CalCOFI region in springs 2010-2012 and had very low biomass in all other years except 2015-2017. Elevated biomass in all three of those springs followed periods of either moderate but sustained poleward flow (spring 2015, following poleward flow in 2014) or short-term but strong poleward flow (springs 2016 and 2017, following elevated poleward flows the prior fall and summer, respectively). *Euphausia eximia* was below the threshold of detection in the CalCOFI region except in springs 2015 and 2016, both of which followed periods of at least moderately enhanced poleward flow. However, strong, persistent poleward flows in 2008, 2009, and 2013 did not induce any detected presence of *E. eximia* in the CalCOFI region.

Euphausia gibboides was detected in at least some part of the CalCOFI region during every year analyzed, but only springs 2015 and 2016 showed notably positive biomass anomalies (Fig. 3.2e). These were also the only two years of notable *E. gibboides* presence in the nearshore

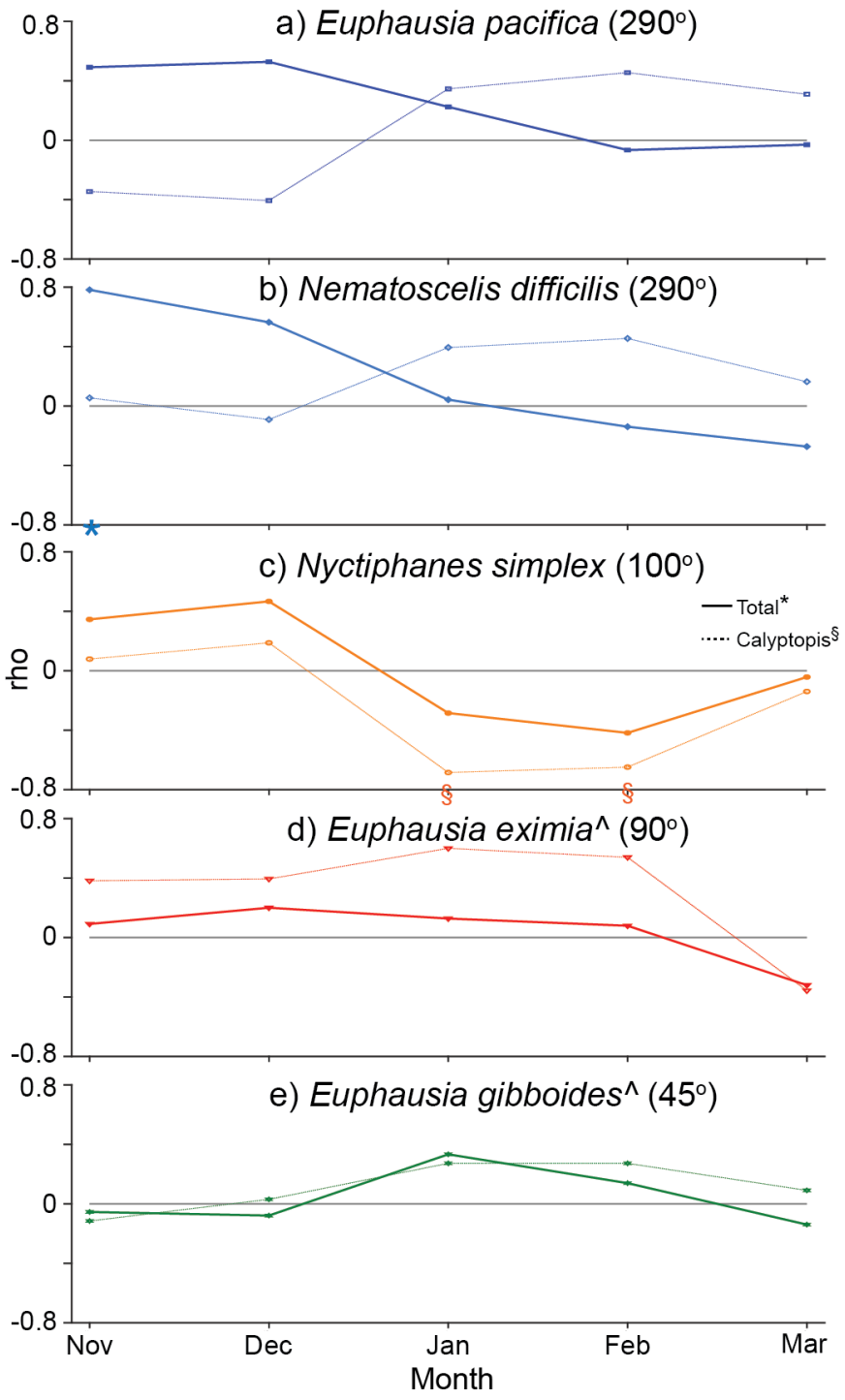

Figure 3.4. Timeseries of lagged correlations between flow anomalies (Nov-Mar) and euphausiid spring biomass (single spring timepoints; black triangles in figure 3.2). Solid lines are correlation values for total biomass, identical to figure 3; dotted lines are for calyptopis stage only for each species. Correlations for *E. eximia* and *E. gibboides* calyptopis phases used log abundance (no.+1 m^{-2}) due to instances of zero calyptopis biomass despite non-zero abundance. Symbols indicate significant correlation for total (*) or calyptopis (§) population.

Southern California Bight (Fig. S3.10). Both springs followed periods of at least moderately enhanced favorable (combined onshore-poleward) flow. As for the other subtropical-tropical species, not all years of anomalously favorable flow induced elevated *E. gibboides* population presence (e.g., 2010-11, 2012 in figure 3.2e).

3.3.1.3. Consistency of calyptopis phase response with total population

In addition to time-lagged correlations for total species biomass (which is dominated by adult and juvenile phases), we also calculated correlations of only the calyptopis phase with flow anomalies, to assess whether larval stages, indicative of active population growth, were also advected (Fig. 3.4; see grey triangles in figure 3.2 for calyptopis biomass anomalies). Both *E. pacifica* and *N. difficilis* show out-of-phase timing of propagation of the calyptopis phase from total population biomass (Fig. 3.4a-b). In contrast to declining, and negligible, correlations of total biomass with flow in February-March, calyptopis phases of both species show temporal increases in correlations with flow, from negative values in December to positive in January-March. We do not believe these results suggest the calyptopis phase is preferentially advected later than adults and juveniles. Rather, elevated *in situ* reproduction of larvae in late winter-early spring within the CalCOFI region likely occurs in years of stronger southward flow, which would transport favorable habitat conditions (cooler waters, higher nutrients, and elevated food availability) that promote *in situ* reproduction and larval growth. Spring 2014 had very low *E. pacifica* calyptopis presence despite high total biomass, suggesting little *in situ* reproduction (Fig. 3.2a). Flow anomalies were correspondingly negative from November 2013-March 2014, which we interpret to indicate that either the population could not reproduce or larval stages did not survive, likely due to reduced southward flow of cool, high-nutrient waters. In contrast, spring 2016 had anomalously elevated calyptopis biomass despite low total population. Flow

anomalies were negative from November-January but reversed to positive in February-March, contributing to the overall positive correlation with *E. pacifica* calyptopis phase in late winter-spring. In contrast to *E. pacifica*, the calyptopis phase of *N. difficilis* was anomalously low in 2016, but its source flow was also negative (anomalously northward) in January-February 2016, while years of positive *N. difficilis* calyptopis anomalies corresponded to positive southward flow. Thus *N. difficilis* also showed a positive correlation of calyptopis biomass with January-March flow.

In contrast, *N. simplex* and *E. eximia* show consistency between the calyptopis phase and total biomass in their correlations with flow (Fig. 3.4c-d). We interpret such close tracking of post-larval organisms with the total population as an indicator that these species reproduce in their external source waters, and then all stages are advected into the CalCOFI region rather than undergoing *in situ* reproduction following transport. We note that *in situ* reproduction of both species likely does occur in the CalCOFI region during periods of favorable habitat conditions, particularly prolonged elevated temperatures, but such physical changes are not obviously or exclusively related to enhanced poleward flow, as indicated by lack of differential patterns for total and calyptopis biomass.

Euphausia gibboides shows a mixed time-lagged correlation pattern of calyptopis phase with flow, aligning its peak with the highest correlation of total population biomass in January but maintaining an elevated correlation through February before decreasing in March (Fig. 3.4e). The consistently strong correlation of *E. gibboides* calyptopes with flow anomalies from January-February appears to be influenced predominantly by spring 2015. The calyptopis phase in spring 2015 showed the only notably positive anomalies of the timeseries, corresponding to strongly positive shoreward flow in December 2014 and through March 2015 (Fig. 3.2e).

However, the highest positive correlation of total biomass with January flow resulted from the correspondence of increased onshore flow anomalies in January 2016 and highest positive total biomass in spring 2016, influencing the overall correlation across years. Thus, for the total population, anomalous flow in January 2015 and 2016 produced a positive biomass-flow correlation, while exceptionally high calyptopis anomalies in spring 2015 alone produced positive correlations of calyptopes with flow across multiple months. We thus suggest that the total *E. gibboides* population is most affected by variability in January flow into the SCB, but that *in situ* reproduction also likely occurs under favorable habitat conditions, as evidenced by high calyptopis biomass in spring 2015 following a prolonged period of elevated temperatures.

3.3.2. Winter origins of spring source waters and populations

We next used a particle tracking model to backtrack the spring distribution of each species during the three anomalous events (2009-10 CP Niño, 2014-15 Warm Anomaly, 2015-16 EP Niño) in comparison to composites of all non-Niño years (2008-2017) to determine variability in winter origins of source waters and possible seed populations (Figs. 3.5-3.9). Our findings in Section 3.3.1 suggest that direct population advection alone does not fully explain biomass variability, so we do not expect the backtracks to reveal exact population winter origins. However, the particle tracking model does show interannual variability in the likely winter origins of spring water parcels, which can further inform our interpretations from Section 3.3.1.3 of altered reproduction in response to changes in source water origins.

For each year, we evaluated only the high-population core of a species' distribution, which we defined using two thresholds: a '>80% biomass' threshold as the region of biomass values that were >80% of the maximum biomass value for that year, and a secondary threshold

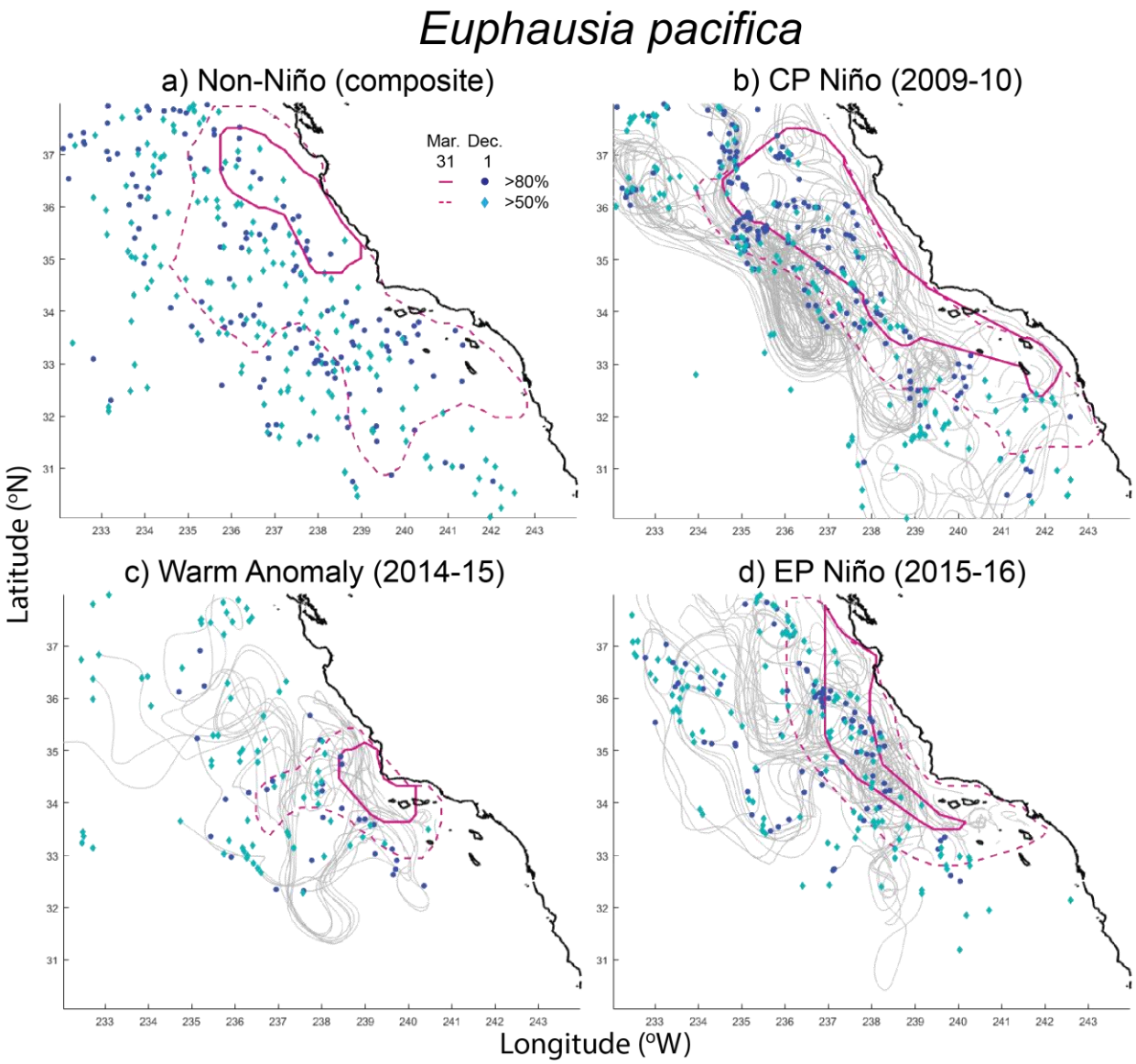

Figure 3.5. Four-month backtracks (Mar. 31 → Dec. 1) from spring distributions for a) the composite of all non-Niño years (2008-2017, minus the anomalous years in b-d), b) 2009-10 CP Niño, c) 2014-15 Warm Anomaly, and d) 2015-16 EP Niño. Pink lines are Mar. 31 distribution (solid – 80% of max, dashed – 50%); symbols are Dec. 1 backtrack (blue dots – 80%, turquoise diamonds – 50%). Grey lines indicate individual particle paths (only shown for every fifth particle). Composite spring distribution (a) is averaged from spring distributions of all non-Niño years, but backtracked winter origins were run separately for each year.

for >50% biomass (Figs. 3.5-3.9; 80% threshold defined by solid pink line (spring population) and dark blue dots (winter origins); 50% threshold defined by dashed pink line and turquoise dots). For the non-Niño composite, we backtracked the 80% and 50% regions for each separate year and then overlaid all backtracks. For the average spring distribution, we calculated station-by-station average biomass values, then objectively mapped the average distribution and plotted its 50% and 80% contours (see figure 5a for example).

We then divided the CASE model region into four quadrants depicting major hydrographic regions of the CCS (Fig. 3.A1): Q1 – Northern Inshore, including coastal waters off central California and the inshore portion of the core California Current (cCC); Q2 – Northern Offshore, including the offshore part of the cCC and northern waters of the North Pacific Central Gyre; Q3 – Southern Offshore, dominated by offshore waters of the North Pacific Central Gyre and subtropical intrusions, and also encompassing the southern portion of the cCC; Q4 – Southern California Bight, comprised of the waters south of Pt. Conception and inshore of the cCC. For each quadrant, we calculated the proportion of particles that backtracked into that region as a quantitative indicator of interannual variability in source waters (Fig. 3.10; proportions are only shown for the two expected dominant source quadrants for each species. See figure 3.A2 for proportions for all four quadrants). We note that all euphausiid species distributions depicted here are affected by variable CalCOFI sampling coverage between years, so interannual comparisons and interpretations require some consideration of sampling coverage (see black ‘x’ marks in Figs. S3.6-S3.10 for full CalCOFI sampling range by year).

The *E. pacifica* spring distribution extended farther south and offshore during non-Niño years than during the three anomalous years; 2010 had similar north-to-south extension but slight shoreward compression (Fig. 3.5, pink solid and dashed lines). Spring distributions in 2015 and

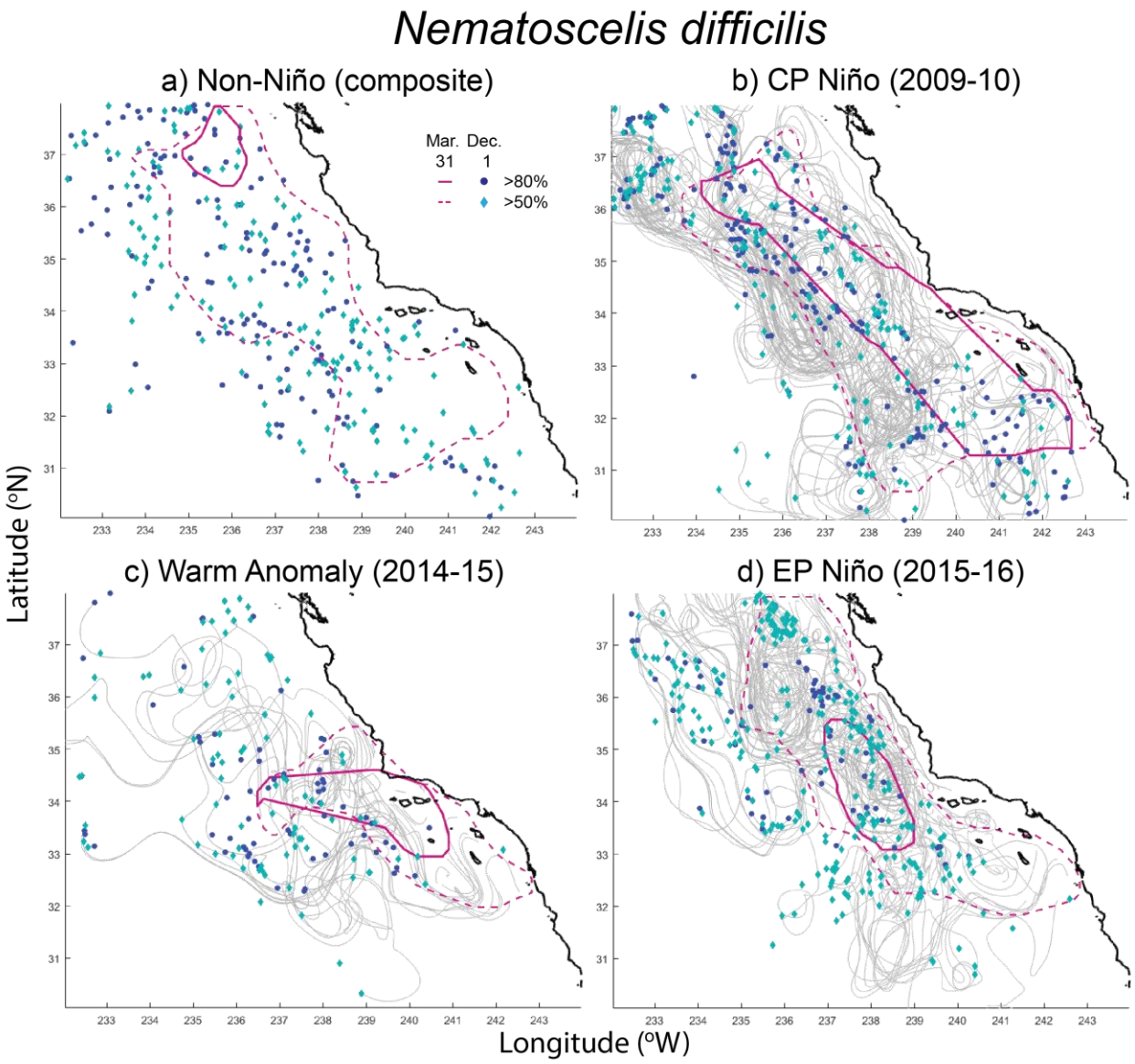

Figure 3.6. As in figure 3.5, but for *Nematoscelis difficilis.* Particle backtrack lines are only shown for every fifth particle.

2016 were compressed notably poleward, although the 2016 distribution still extended into the northern portion of the SCB. We primarily analyzed *E. pacifica* source waters from the northern inshore (Q1) and northern offshore (Q2) regions because we expect those areas to be its dominant winter water source (Fig. 3.A1). Visual analysis of backtrack maps suggests winter

source waters for both 2010 and the non-Niño composite originated throughout the region, with concentrated presence in the northern area (Fig. 3.5, blue and turquoise dots; note that only every 5th particle backtrack line (grey) is shown, although all particles are shown). Quantification of proportions of winter source waters shows that over half of source waters for spring 2010 originated in the northern offshore region, the highest of any year in the timeseries (Fig. 3.10a, purple diamond). Although the winter preceding spring 2015 was the height of the 2014-15 Warm Anomaly, which produced some onshore flow (Zaba & Rudnick, 2016), spring 2015 had a lower proportion of waters originating in the northern offshore region (~40%) compared to 2010, around the median of non-Niño years (Fig. 3.10a, yellow triangle). Spring 2016 had a similar proportion of northern offshore-origin winter waters to spring 2015 but the highest proportion of northern inshore contributions of any year, suggesting that the primary source for spring was closer inshore (Fig. 3.10a, red triangle).

The *N. difficilis* spring distribution showed farthest southward extent of core biomass (>80%) in spring 2010, farther south than the non-Niño average (Fig. 3.6a-b). However, all four years showed southward extensions of moderate biomass (50-80% of maximum biomass, dashed pink lines) into the SCB, although springs 2015 and 2016 were confined closer to shore. Visual analysis of winter source origins (blue and turquoise dots in figure 3.6) suggests source waters originated throughout the CCS region in all years, although 2010 showed lower offshore contributions. For *N. difficilis*, we expected the two dominant source quadrants to be the northern offshore (Q2) and southern offshore (Q3) regions. Quantifications of winter source waters indicate that 2010 had highest proportion of source waters from the northern offshore region, similar to *E. pacifica*, and the second-lowest proportion of southern offshore source waters (Fig. 3.10b). Spring 2015 had median source water proportions for both northern and southern

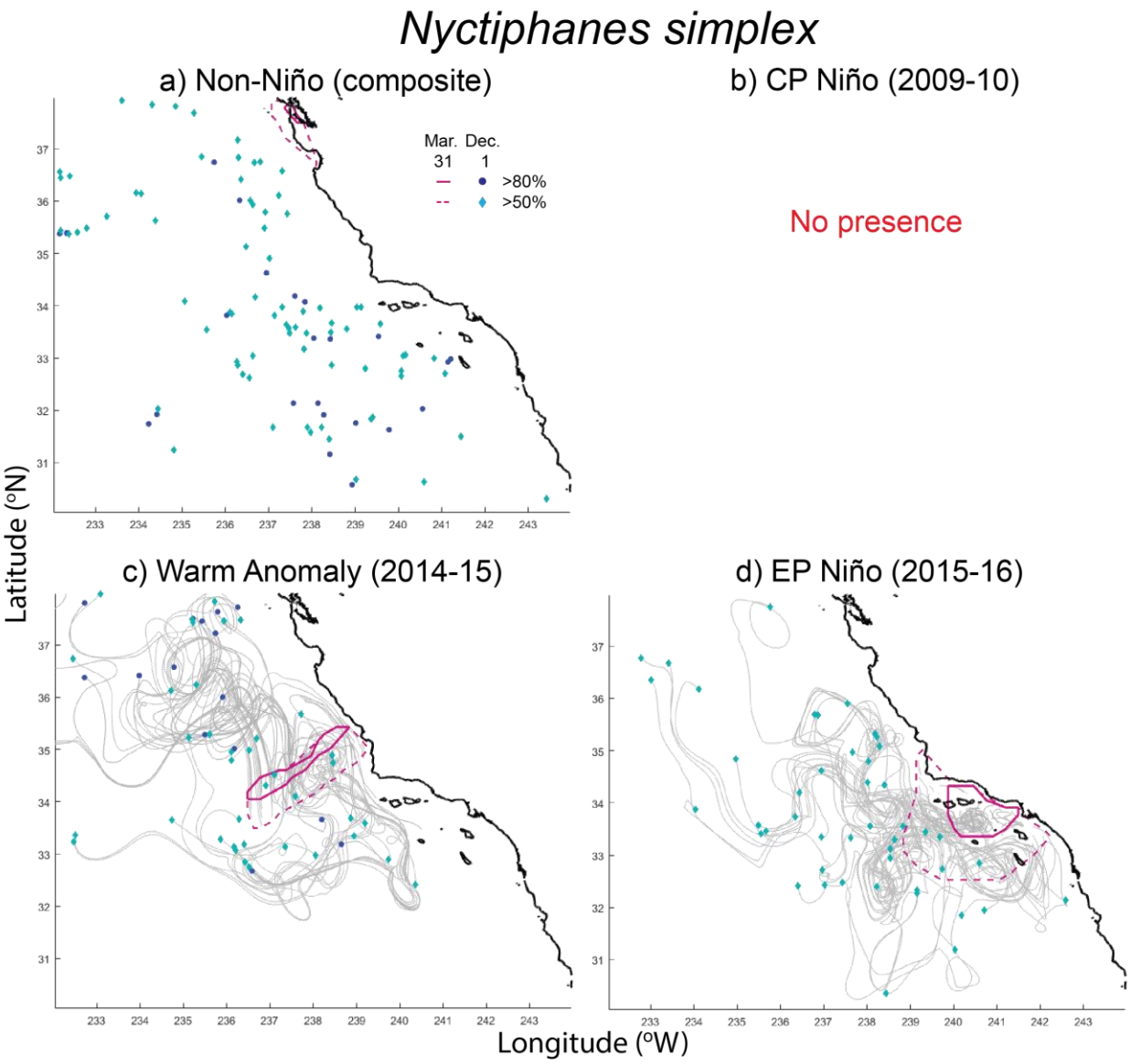

Figure 3.7. As in figure 3.5, but for *Nyctiphanes simplex.* Particle backtrack lines are shown for all symbols.

offshore regions, while spring 2016 had relatively low proportions of source waters from both offshore regions, particularly offshore southern waters.

Subtropical coastal *N. simplex* showed clear northward population extensions in springs 2015 and 2016 (Fig. 3.7) compared to its known non-Niño population (Brinton, 1962; Lilly &

Ohman, submitted). We believe that the small area of maximum average *N. simplex* population off San Francisco Bay (~37.5ºN) depicted in figure 3.7a for the non-Niño composite is an artifact of overall very low presence of *N. simplex* in the CalCOFI region during the 2008-2017 non-Niño period. Two years (2008, 2014) showed *N. simplex* presence off San Francisco (Fig. S3.8); this presence was not averaged out by other years due to lack of sampling, so it became the 'maximum', and no other areas of average biomass reached 50% of this value, thus contributing to the appearance of a lack of population presence except for this northern enclave. However, because the particle backtracks were conducted for individual years, they reveal the true winter origins of source waters across non-Niño years. Visual analysis suggests that spring 2015 appeared to be sourced at least partially from northern offshore waters, overlapping the northern and offshore portions of the non-Niño composite, while spring 2016 was sourced more from waters within and around the SCB (Fig. 3.7; blue and turquoise symbols). We note that the spring 2016 CalCOFI cruise sampled north to 37ºN, covering the same region sampled in 2015, so we do not attribute the apparent north/south offset of particle origins between 2015 and 2016 to an artifact of differential sampling; the spring 2016 distribution truly had shifted south to the SCB, as depicted.

We anticipated that *N. simplex* would be influenced most by waters of southern offshore and nearshore origin, so we first analyzed Q3 and Q4 for backtrack particle proportions. Spring 2015 had among the lowest contributions from southern offshore waters (Fig. 3.10c; *N. simplex* has fewer symbols because it was absent in 2010-2012 and only retained one particle in the CASE region in 2014. See Animation S3 for temporally-resolved particle backtracks). However, winter source contributions from southern nearshore (SCB) waters were also low, particularly for the 2015 and 2016 anomalies. Consideration of the other quadrants shows that highest winter

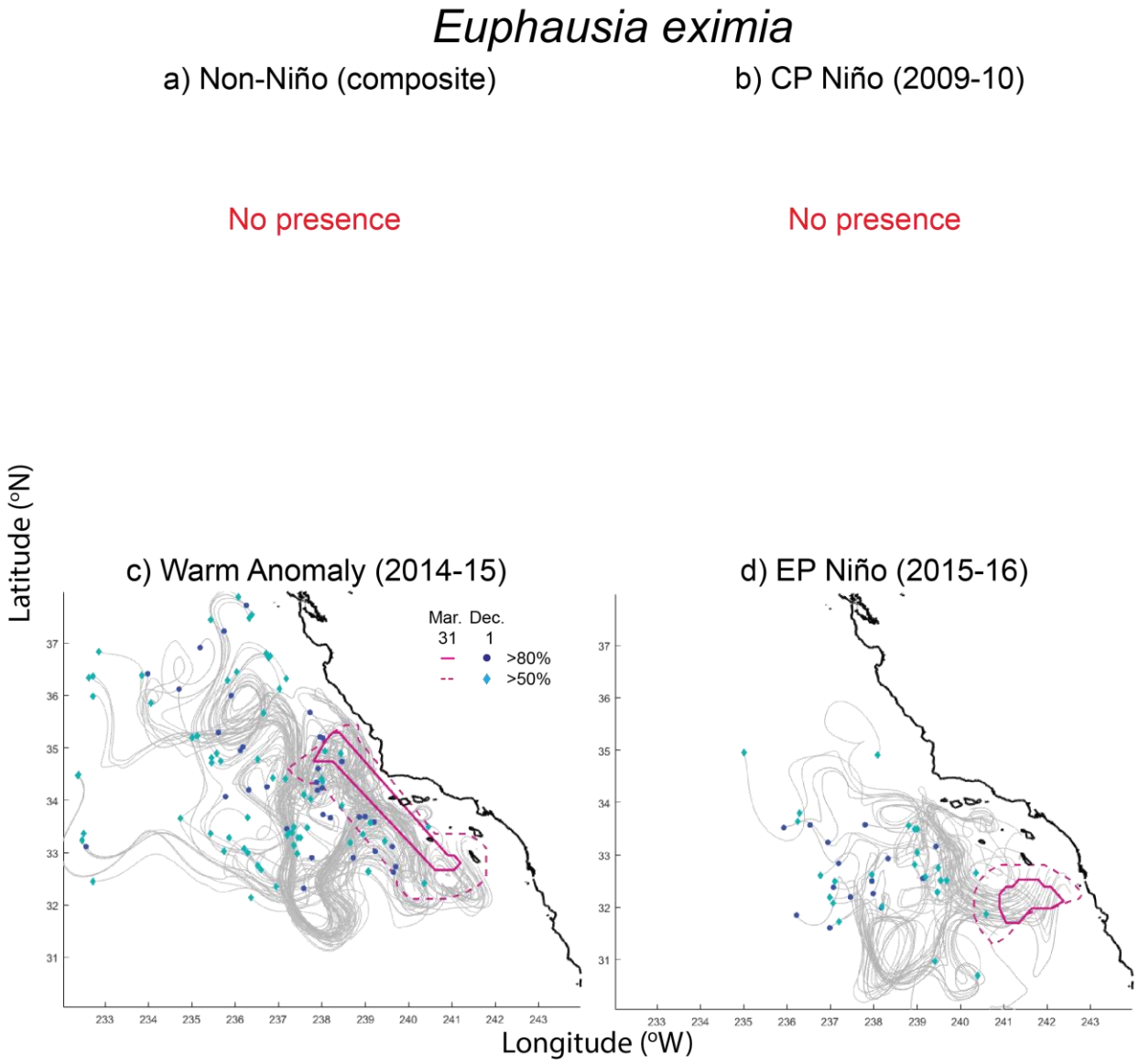

Figure 3.8. As in figure 3.5, but for *Euphausia eximia.* Particle backtrack lines are shown for all symbols.

source water contributions for *N. simplex* came from northern offshore waters (Q2, Fig. 3.A2c), as mentioned from visual analysis. Spring 2016 was moderately influenced by the southern offshore region (Q3), which contributed the highest proportion of the four quadrants.

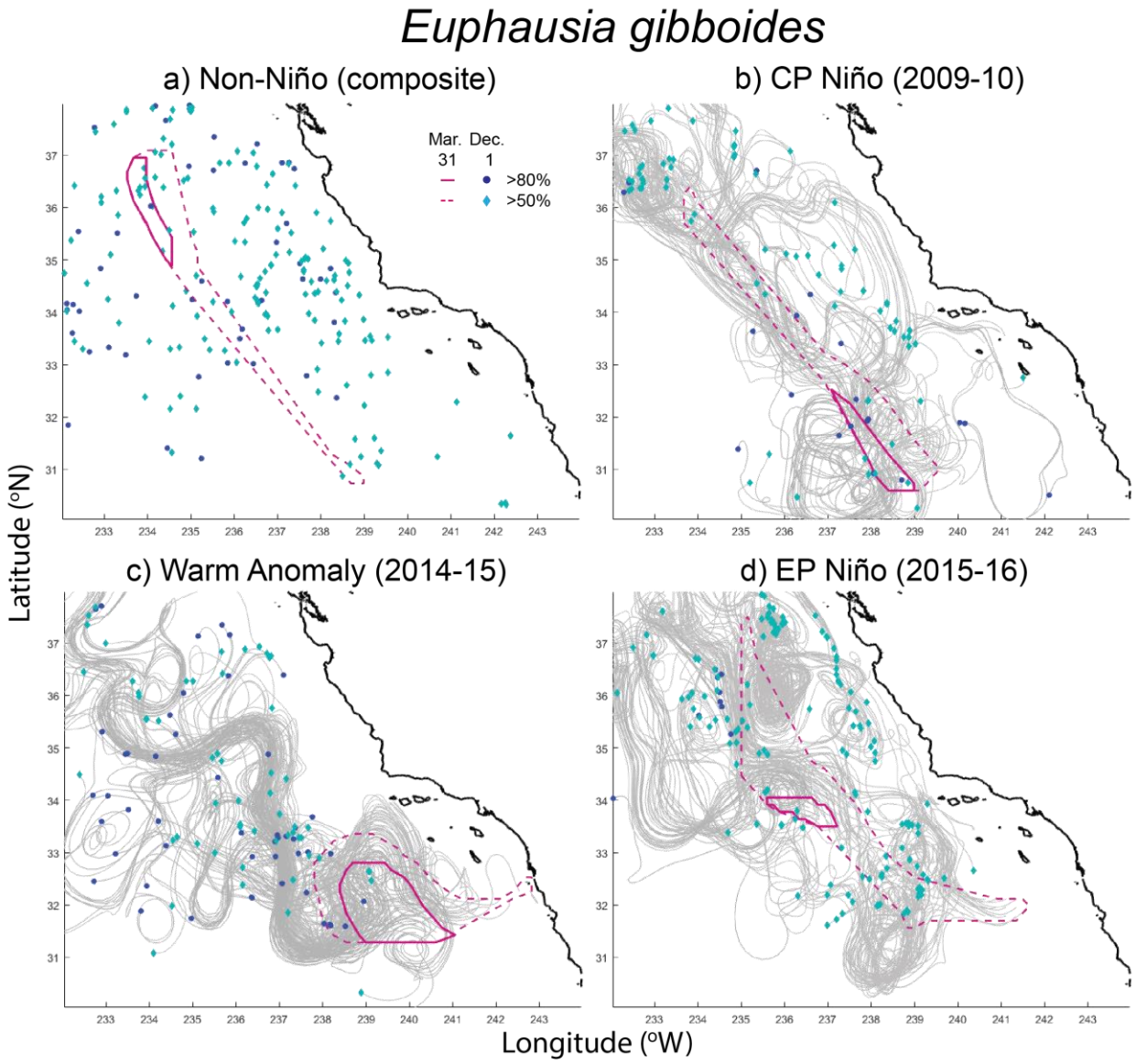

Figure 3.9. As in figure 3.5, but for *Euphausia gibboides.* Particle backtrack lines are shown for all symbols.

As noted above, *E. eximia* was only detected in the CalCOFI region in springs 2015 and 2016, so we do not have information on how its source waters may have varied compared to non-anomalous years. However, its population showed a farther northward extent in spring 2015 than

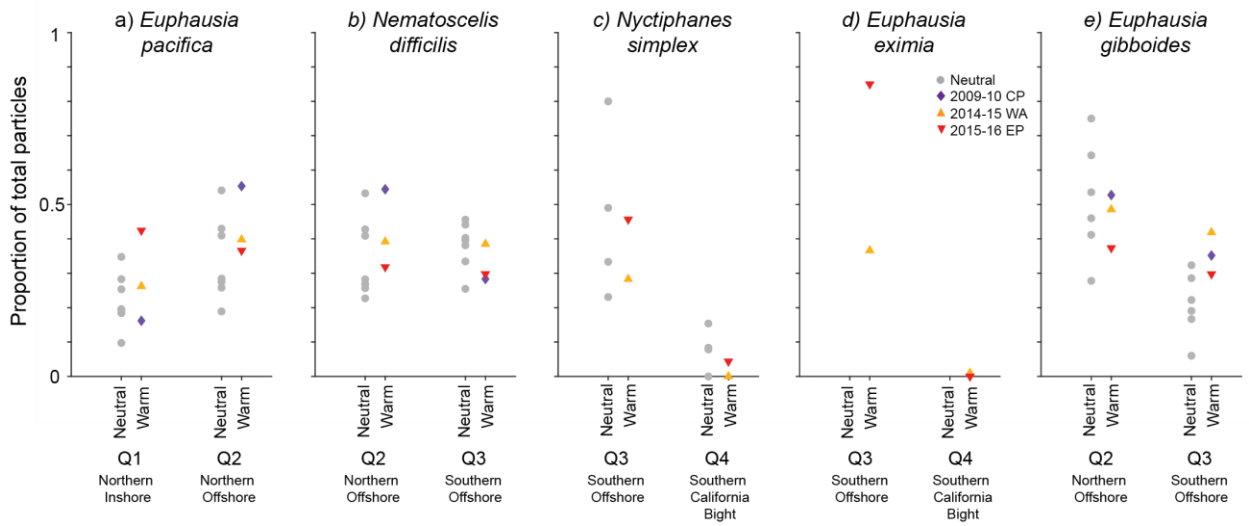

Figure 3.10. Proportions of winter backtracked particles (blue and turquoise symbols in figures 3.5-3.9) that originated in the dominant source quadrants for each species within the CASE model region (see figure 3.A1 for quadrant delineations and figure 3.A2 for the proportions of particles in all four quadrants for each species). Proportions are calculated from the total combined numbers of particles for both the >50% and >80% thresholds. The three anomalous years are offset from all non-Niño years (light grey dots). *Nyctiphanes simplex* and *Euphausia eximia* have fewer symbols because they were not present in certain years.

2016, including high levels north to Pt. Conception (Fig. 3.8). Winter source waters for spring 2015 were fairly evenly distributed between the northern and southern offshore regions, while sources for spring 2016 came predominantly from southern offshore waters (Figs. 3.10d, 3.A2d).

The *E. gibboides* spring distributions in non-Niño years and 2010 were limited to only the very offshore portion of CalCOFI sampling (Fig. 3.9). Springs 2015 and 2016 each showed different manifestations of anomalous distributions: the spring 2015 distribution shifted substantially shoreward in the southern CCS, while the spring 2016 distribution extended farther north but only in offshore waters. We expected winter source waters for *E. gibboides* to originate predominantly in the northern and southern offshore regions (Q2 and Q3). Every non-Niño year except one had >40% of source water origins from the northern offshore region, while springs

2010 and 2015 showed ~50% (Fig. 3.10e; note that *E. gibboides* was absent in one non-Niño year, 2014, so there are only 6 grey dots). Those two springs also had highest proportions of southern offshore waters of any year, although still lower contributions than from northern offshore waters. In contrast, spring 2016 had relatively low proportions of source waters from both offshore regions (although higher in Q3 than most non-Niño years) but a relatively high contribution from northern inshore waters (Q1, Fig. 3.A2e).

3.4. Discussion

All five euphausiid species show some degree of correspondence between biomass and interannual flow anomalies across their respective source boxes, but direct advection of populations via the source waters as we have defined them cannot alone completely explain biomass variability in the CalCOFI region. Not surprisingly, altered *in situ* population variability (growth and reproduction, mortality) must also exist to explain the observed patterns. Furthermore, correlation of population biomass with flow anomalies may indicate either or both of two mechanisms of population change: 1) advection of populations into the region ('seeding'), or 2) responses of existing *in situ* populations to altered habitat conditions induced by anomalous flow. Consideration of flow correlations of the calyptopis phase allowed us to deduce whether species were likely directly advected into the region or grew *in situ*. Below, we propose three types of advection-habitat response combinations based on the correlation patterns and source water variability of the five euphausiid species considered here.

3.4.1. Population and reproductive responses to source flow

3.4.1.1. Cool-water and Regionwide Temperate ("resident") species: in situ *calyptopis production in response to favorable flow*

Populations of cool-water coastal (*Euphausia pacifica*) and regionwide temperate (*Nematoscelis difficilis*) species in the southern CCS appear to be influenced by reproductive responses in spring, with possible additional population seeding via winter transport. Correlations of total spring populations of both species with winter flow supports two hypotheses: i) organisms grow *in situ* in response to advection of favorable source waters, increasing total biomass by spring; ii) favorable advection physically transports organisms, further 'seeding' existing *in situ* populations. These hypotheses are not mutually exclusive, and we expect that they serve complementary roles across years. However, reproduction, as evidenced by the calyptopis phase, appears to respond differently than total population survival. Negative correlations of spring calyptopes with winter flow suggest they are not physically transported into the CalCOFI region in winter. However, negative correlations of total population in February-March, when calyptopis correlations with flow are positive, suggest that late winter-spring advection is not likely, either. Thus, enhanced *in situ* reproduction in late winter-spring in response to enhanced winter source water flows is the likely primary mode of calyptopis production of *E. pacifica* and *N. difficilis*, and an important source of population increase during years of favorable reproductive conditions. Brinton (1962) noted the importance of nearshore spawning for *E. pacifica* populations off California, including year-round spawning in the 34^{o}-40^{o}N range, and that populations of *N. difficilis* in the inshore southern CCS are primarily in larval form. Those observations reinforce our hypothesis that calyptopis production of both species occurs primarily *in situ* within the CalCOFI region.

Several years of opposite biomass anomalies between the total and calyptopis populations for both *E. pacifica* and *N. difficilis* further suggest different forcing mechanisms for total population survival and calyptopis production, with resulting differential impacts to the subsequent year's population. As previously suggested by Lilly and Ohman (submitted), years of low total biomass (springs 2015, 2016) were likely caused by *in situ* population mortality due to prolonged (~1 year) elevated *in situ* temperatures and below-average food availability. Such conditions would be exacerbated by reduced southward flow of cool, high-nutrient waters of the core California Current (CC), as observed for springs 2015 and 2016, when winter source waters for both *E. pacifica* and *N. difficilis* originated predominantly from farther south offshore (2015) or the northern nearshore region (2016) rather than the core CC. However, springs 2015 and 2016 both showed elevated *E. pacifica* and *N. difficilis* spring calyptopis biomass, suggesting rapid reproductive rebound with the return of favorable habitat conditions, even for low total population levels. We posit that these rebounds are likely due to moderate nearshore upwelling, which occurred to varying degrees in springs 2015 and 2016 (Jacox et al., 2016; Lilly et al., 2019). Such rapid reproductive re-emergence reiterates that, although some dominant zooplankton species decrease substantially during El Niño events, the impacts of such events have so far not induced long-term population declines, and increased reproduction can occur as soon as favorable conditions return (Lilly & Ohman, 2018, submitted; Lindegren et al., 2018).

In contrast, although spring 2010 and several non-Niño years had high contributions of source waters from the northern offshore region, as well as elevated total population biomass of both *E. pacifica* and *N. difficilis*, calyptopis biomasses were anomalously low. It is possible that existing adult populations benefited from later-spring enhanced source water delivery to reproduce after our sampling period. However, shoreward compression of *E. pacifica* and *N.*

difficilis distributions in spring 2010 suggests negative influences of reduced upwelling and enhanced downwelling due to anomalous alongshore wind stress (Todd et al., 2011) and reduced offshore flow of upwelled waters (Chabert et al., 2021) during the 2009-10 CP Niño. Both of these factors corroborate our hypothesis that physical compression or reduced upwelling, combined with subsequent shoreward expansion of warm offshore waters, negatively impacted reproductive conditions despite favorable source flows and possible population seeding from the north.

3.4.1.2. Subtropical Coastal and Tropical Pacific species: whole-population transport

In contrast to cool-water and regionwide temperate species, subtropical coastal (*Nyctiphanes simplex*) and Tropical Pacific (*Euphausia eximia*) species show remarkable consistency of flow correlations across all developmental stages, suggesting that whole-population transport, rather than proliferation of *in situ* populations, is the dominant response mechanism during periods of enhanced flow into the CalCOFI region. Both *N. simplex* and *E. eximia* have population centers off Baja California, so they likely require some initial forcing via enhanced population advection. Brinton (1981) attributed prior incursions of these species into the southern CCS during the 1957-59 El Niño to direct transport with anomalous flow. However, *N. simplex* has shown cyclical multiyear presence of at least low abundances in the southern CCS since the 1950s (Brinton & Townsend, 2003; Lilly & Ohman, submitted). We thus expect some level of *in situ* reproduction of *N. simplex*, which has also shown a somewhat eurythermal range (Lilly & Ohman, submitted). Reproduction of *N. simplex* in northern waters, notably off Oregon, was previously observed during the strong 1997-98 EP Niño even after truncation of anomalous poleward flow (Keister et al., 2005), so the species may simply require prolonged anomalously warm conditions to undergo reproduction in the southern CCS. Origination of source waters in

winter-spring 2016 predominantly from the southern offshore region of the CCS, which also encompasses the North Pacific Central Gyre and was further warmed during the 2015-16 EP Niño, likely provided the prolonged warm habitat conditions to promote enhanced reproduction.

The late 2000s-early 2010s were notable for very low presence or complete absence of both *N. simplex* and *E. eximia* throughout most years. Advection alone does not fully explain fluctuations in biomass of either species. Multiple years of regionally enhanced favorable source flow did not result in elevated biomass or even moderate presence of either species, notably in springs 2008-2010, including the 2009-10 CP Niño. We suggest three possible reasons for these discrepancies: 1) anomalous advection observed in the CASE model region did not extend far enough south to reach the population of either species off Baja California; 2) anomalous advection did not persist for long enough to transport organisms from population centers off Baja California to the SCB; or 3) anomalous advection did transport subtropical and tropical organisms northward, but *in situ* SCB habitat conditions were not sufficiently warm for population survival to spring. Including flow patterns from the region off Baja California would provide a clearer picture of the magnitude and spatial extent of flow required to transport these species to the southern CCS. Additionally, the complete absence of *E. eximia* in all years except 2015 and 2016 presents challenges in identifying trends. A longer timeseries of transport anomalies that spans more years of *E. eximia* presence would provide a fuller picture of the impact of advection.

3.4.1.3. Subtropical Offshore species: initial shoreward transport, then in situ *reproduction while favorable habitat conditions persist*

The increase in *E. gibboides* total biomass in the SCB in spring 2015, and across the broader CCS region in spring 2016, is striking (Figs. 3.9, S3.10). That these two springs of

elevated biomass immediately follow periods of notable shoreward advection suggests the species is heavily influenced by variability in transport. High offshore biomass in springs 2009 and 2010 but no nearshore presence is slightly surprising, as the 2009-10 CP Niño was characterized by reduced offshore extent of nearshore waters (Chabert et al., 2021) and downwelling-favorable alongshore winds (Todd et al., 2011), as noted above in relation to shoreward compression of *E. pacifica* and *N. difficilis*. We would expect such a reduction to enhance shoreward expansion of *E. gibboides*, although continued strong presence of the southward-flowing core California Current may have acted as a barrier to onshore population expansion.

In addition to an apparently strong influence of advection on population variability, however, *E. gibboides* likely also responds to favorable *in situ* conditions, notably temperature. Exceptionally high calyptopis anomalies in 2015 could have been due to either, or a combination of, strong onshore flow in January 2015 or the prolonged period of anomalously warm temperatures across the CCS region from mid-2014 to winter 2015. The *E. gibboides* population likely underwent some amount of *in situ* reproduction in 2015 regardless of initial mechanism of increase, because its distribution had spread across the CCS region by spring 2016. Furthermore, it showed gradual retraction offshore by spring 2017, which supports the hypothesis of decreasingly favorable habitat following eventual cooling from 2016 to 2017. In both 2016 and 2017, *E. gibboides* was absent in the coastal region, perhaps due to the re-emergence of cool upwelling conditions, although its source waters appeared to originate in somewhat nearshore waters at least in 2016. Such responses to temperature changes, both favorable and unfavorable, following perceived initial advection into the region agree with the supposition by Brinton (1981) that *E. gibboides* undergoes initial shoreward advection with favorable flow but retracts

back offshore with the return of cool conditions. We note that the later seasonal correlation of *E. gibboides* with flow (January instead of November-December for the other species) could be due to the greater distance of its population center from the SCB.

3.4.2. Variability in source flows

Winter source water origins for spring 2010 were distinct from other warm years for cool-water and offshore subtropical species, originating predominantly in the northern offshore region and emphasizing a strong contribution of enhanced flow from the core California Current. Such an enhanced, northern-origin flow would likely benefit populations of resident cooler-water species via favorable habitat temperatures and enhanced nutrient inputs to fuel primary production. However, that alone did not appear to induce elevated production of calyptopis phases in those species. Neither *N. simplex* nor *E. eximia* was detected in the CalCOFI region in spring 2010, perhaps due in part to inhibition of northward population progression by enhanced southward flow. However, the CP Niño event did induce moderate warm anomalies *in situ* (Rudnick et al., 2017; Todd et al., 2011).

We expected spring 2015 populations to show source water origins in offshore waters due to previously described evidence for enhanced shoreward flow across the central and southern CCS (Zaba & Rudnick, 2016). Both northern and southern offshore waters influenced *N. simplex* and *E. gibboides* in spring 2015, although northern origins were slightly greater. Offshore winter source waters for *E. gibboides* meandered southward before reaching the SCB. In notable contrast, spring 2016 showed the most consistent nearshore origins in northern waters off central California for cool-water and subtropical offshore species, consistent with reduced offshore flow (Chabert et al., 2021) and perhaps reflecting enhanced within-region circulation

during the 2015-16 EP Niño. However, *N. simplex* (subtropical coastal) and *E. eximia* (Tropical Pacific) were influenced by winter source waters originating in the southern offshore region, which may have promoted continued *in situ* reproduction in anomalously warm habitat from offshore.

We note several caveats that likely affect our outcomes. First, our source water boxes are statically defined across the timeseries and do not encompass either the entire extent of any species or its variable core distribution between years. Second, we assume direct, straight-line transport of species from their source boxes to the CalCOFI region; in reality, transport likely involves meanders and may come from different directions depending on the year. We also note that spatial averaging of both source flows and regionwide biomass may mask spatial subtleties, i.e., sub-regions of anomalously high or low biomass due to corridors of flow. Last, correlations for the three subtropical-tropical species were predominantly influenced by the few years of true population presence in the CalCOFI region. More accurate correlations of biomass anomalies with flow would benefit from longer timeseries that include more years of non-zero population. However, the overall patterns of biomass variability with flow in all five species across the timeseries suggest that even large-scale flow anomalies can help inform and predict regionwide changes in species-specific patterns of euphausiid biomass.

3.4.3. Conclusions

Our findings lend further credence to previous interpretations that advection serves an important role in initially transporting subtropical and tropical euphausiid species into the southern CCS at anomalous levels, while cool-water species respond more to changing *in situ* habitat (Brinton, 1960, 1981; Lilly & Ohman, submitted; Marinovic et al., 2002). The temporal

differences in responses of larval and adult phases of both *E. pacifica* and *N. difficilis* to flow suggest at least partial influence of variable source waters on reproduction. Advection thus impacts these species indirectly by altering their habitat conditions, affecting both reproduction and population survival or mortality. We note, however, that these species are also likely influenced by *in situ* habitat changes caused by direct atmospheric forcing (e.g., warming due to increased heat flux, Zaba & Rudnick, 2016). The extent to which these species benefit from additional population seeding via source flows remains unknown.

The strong evidence for initial advection of *N. simplex* into the SCB is surprising, since the species is regularly observed in the SCB at low to moderate levels even during non-Niño years (Brinton & Townsend, 2003; Lilly & Ohman, submitted). As noted above, our findings may be limited by our time-period, which spanned only the relatively cool late 2000s-2010s and the singular anomalous period of 2014-16. Given its known association with PDO cycles (Brinton & Townsend, 2003; Di Lorenzo & Ohman, 2013), *N. simplex* may show a greater ability to reproduce *in situ* without initial transport during years of warmer and otherwise favorable background conditions (i.e., positive PDO phase).

Given the population centers of *E. eximia* and *E. gibboides* far south or offshore of the southern CCS, and their near-complete absence in the nearshore SCB in most years, we expected these species to require some initial transport to appear in the SCB. However, anomalous advection needs to extend sufficiently far south or offshore to reach population centers, as not all years of enhanced advection in our source boxes defined within the CASE region resulted in presence of *E. eximia* (anywhere) or *E. gibboides* (in the nearshore southern CCS); we note the same also for *N. simplex*. The levels and durations of habitat conditions required for *in situ*

reproduction of any of the three subtropical-tropical species in the southern CCS also require further examination.

Euphausiids are not the only zooplankton that appeared to benefit from combinations of advection and *in situ* habitat changes during the 2014-16 Warm Anomaly-El Niño sequence. Lilly et al. (2019) observed a significant increase in the pteropod population in the Southern California Bight in spring 2014, coincident with increased poleward flow and dominated by an anomalous subtropical species. However, a similar increase in spring 2016 occurred in the absence of anomalous poleward flow but corresponded to sustained elevated aragonite saturation levels, suggesting a positive population response to favorable *in situ* conditions in spring 2016. Responses of zooplankton species, and resulting changes in community composition, thus likely vary substantially by event depending on the specific changes in individual source flows and other means of *in situ* habitat change.

Acknowledgements and Author Contributions

We are indebted to G. Gopalakrishnan for development and further refinement of the California State Estimate, and to R. Musgrave and J. Garwood for generously sharing previous versions of our particle tracking model. We thank the CalCOFI program for at-sea sample collection and the late E. Brinton, as well as A. Townsend, and L. Sala of the Scripps Institution of Oceanography Pelagic Invertebrate Collection (PIC) for detailed enumerations of euphausiid species. This work was supported by an NSF Graduate Research Fellowship to L. E. Lilly, NSF OCE-1614359 and OCE-1637632 to the California Current Ecosystem-LTER site, Gordon and Betty Moore Foundation support to M. D. Ohman, and NOAA Office of Naval Research support to B. D. Cornuelle and the CASE model.

L.E.L. and M.D.O. developed the study. L.E.L. conducted analyses with substantial model and methodological assistance from B.D.C. All authors analyzed results and edited the manuscript. The authors declare no competing interests.

Chapter 3, in full, is currently being prepared for submission for publication of the material. Lilly, Laura E.; Cornuelle, Bruce D.; Ohman, Mark D. The dissertation author was the primary investigator and author of this paper.

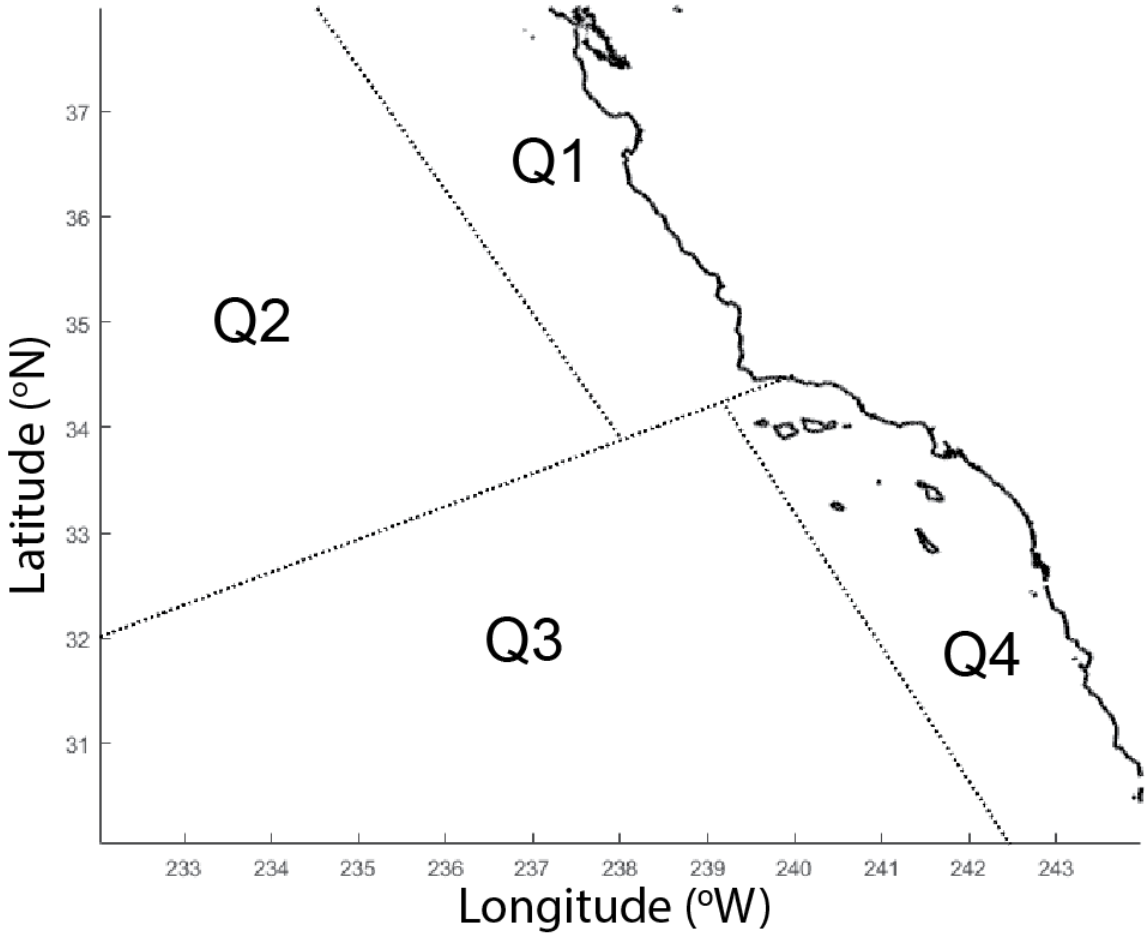

Figure 3.A1. Delineations of the four quadrants used to count proportions of particles in winter backtracks. Regions are as follows (see Section 3.3.2): Q1 – Northern Inshore region; Q2 – Northern Offshore region; Q3 – Southern Offshore region; Q4 – Southern California Bight region.

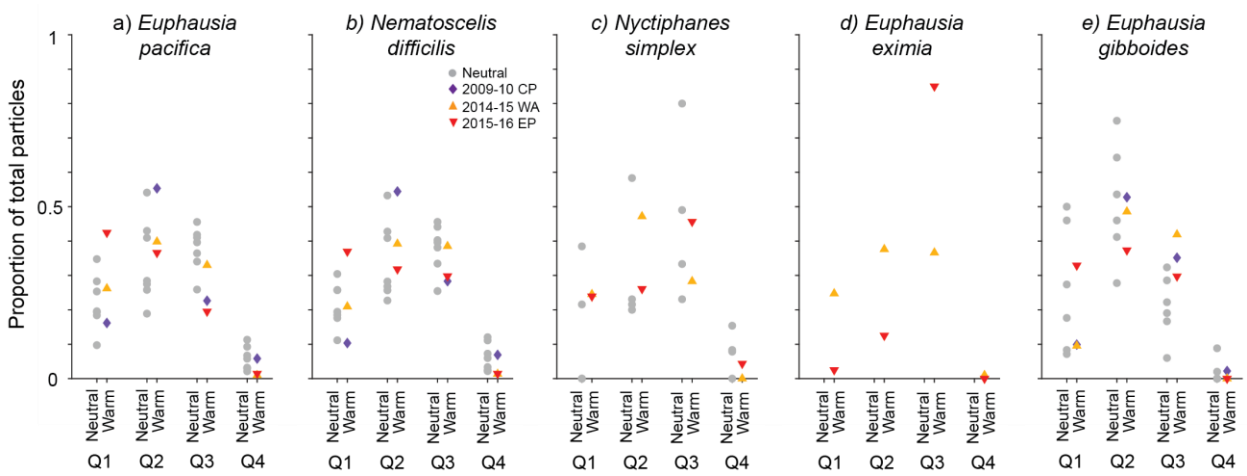

Figure 3.A2. As in figure 3.10, but proportions of particles in all four quadrants for each species.

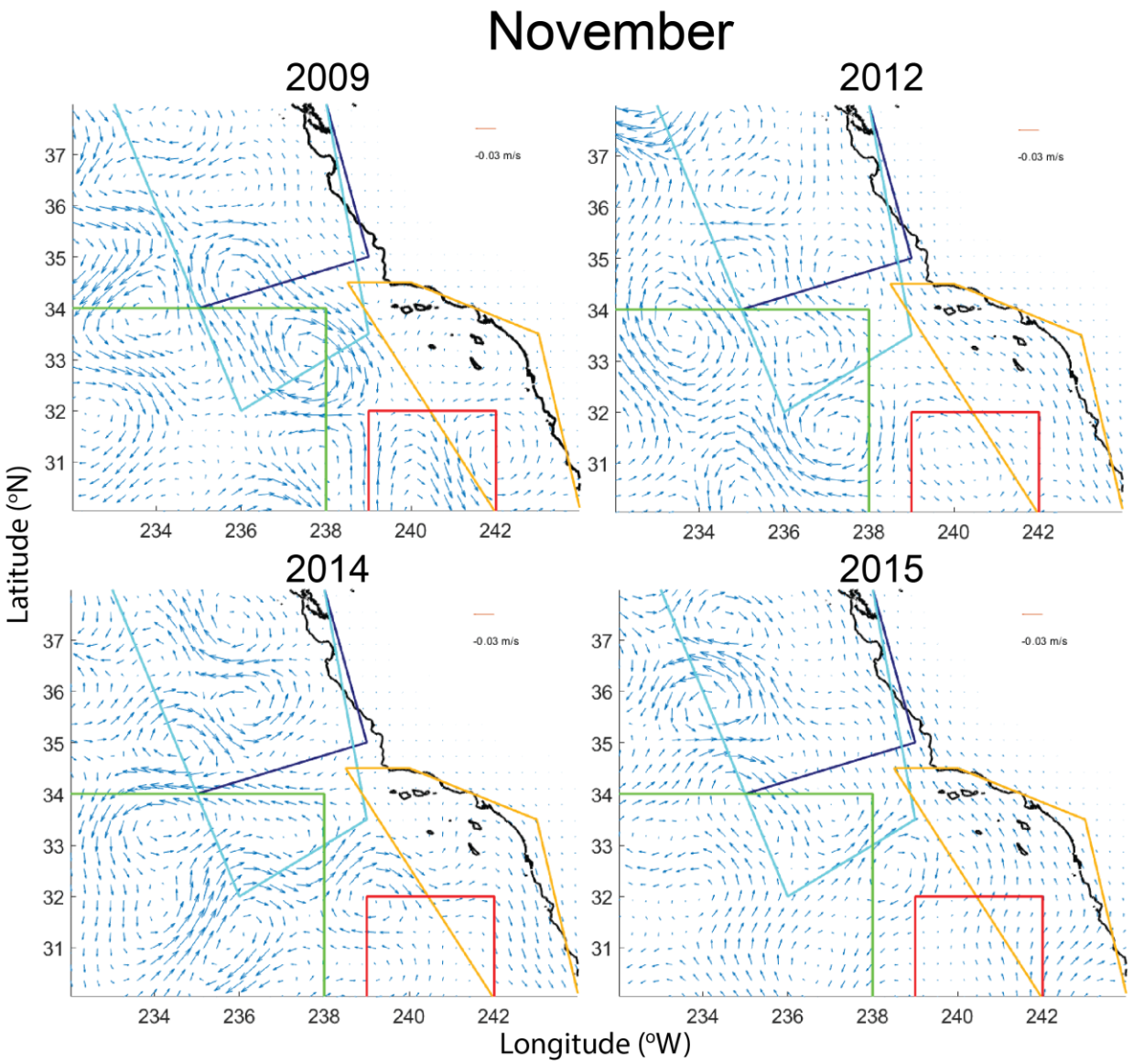

Figure S3.1. Flow anomalies on the 55 m level for the CASE region averaged for the month of November (Days 1-30) preceding the three anomalous springs (2010, 2015, and 2016) and a non-Niño spring (2013). Boxes indicate the source flow regions for the five euphausiid species analyzed (see figure 3.1 and Methods 3.2.2.3).

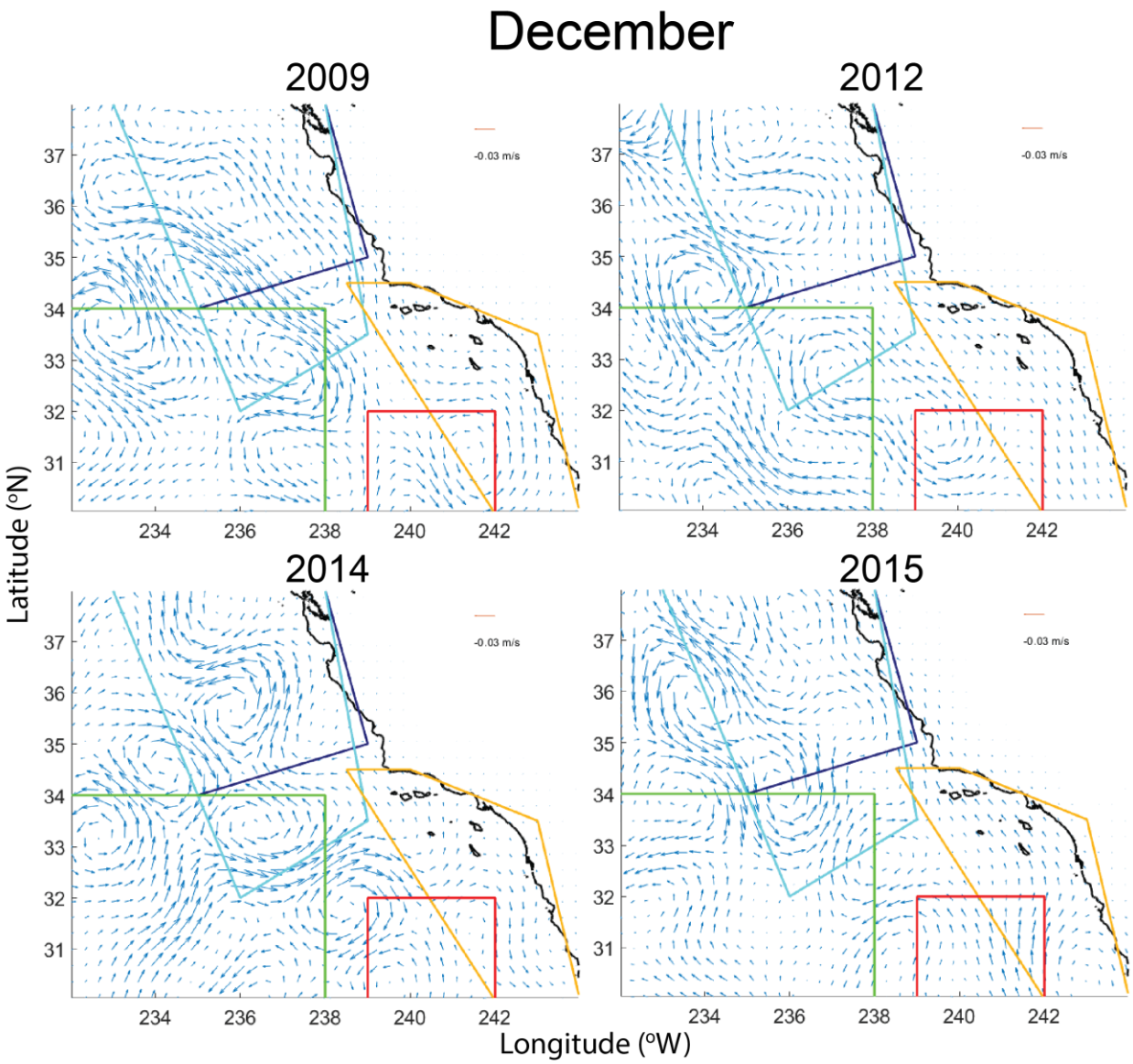

Figure S3.2. As in figure S3.1, but for December averages.

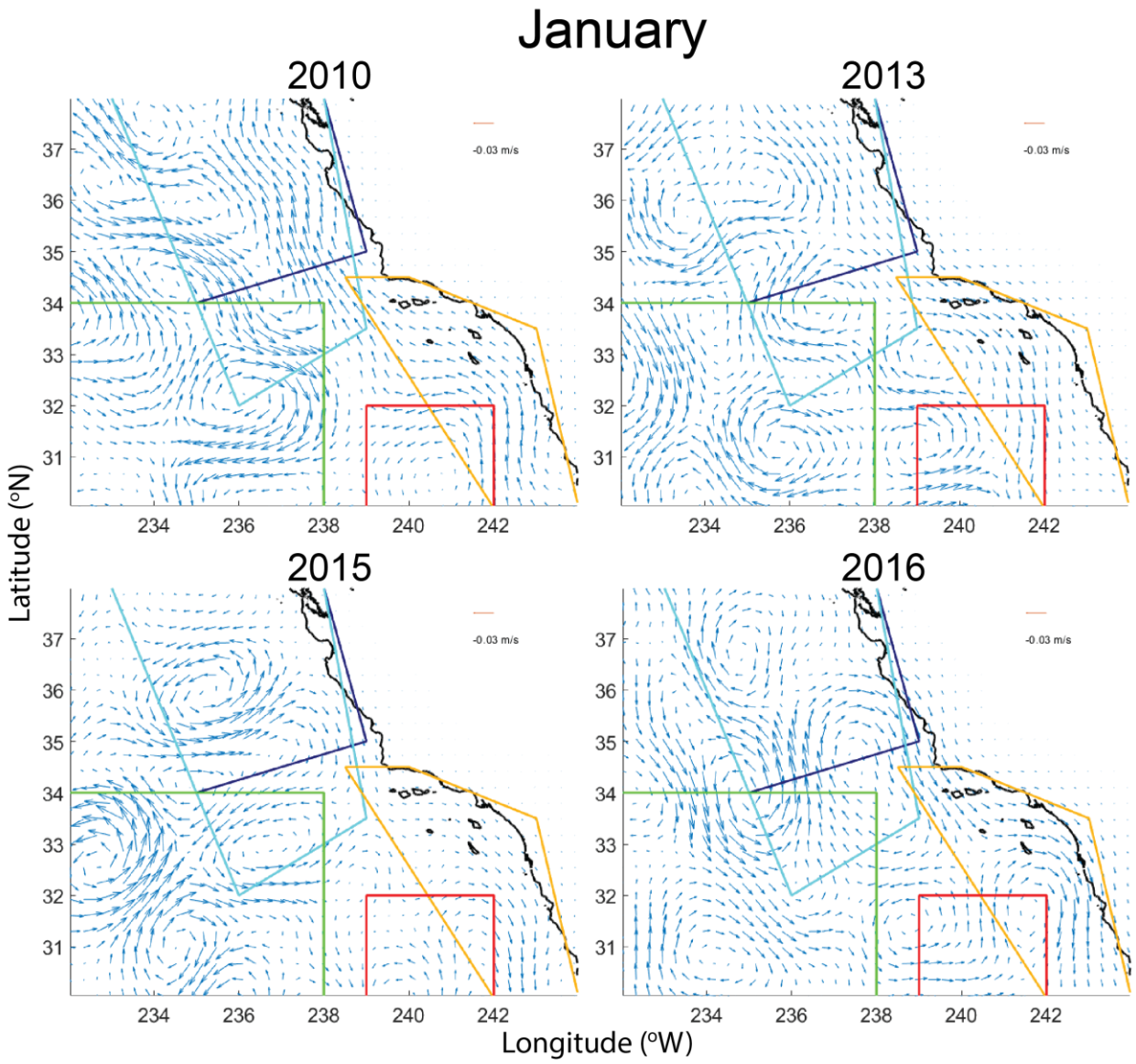

Figure S3.3. As in figure S3.1, but for January averages.

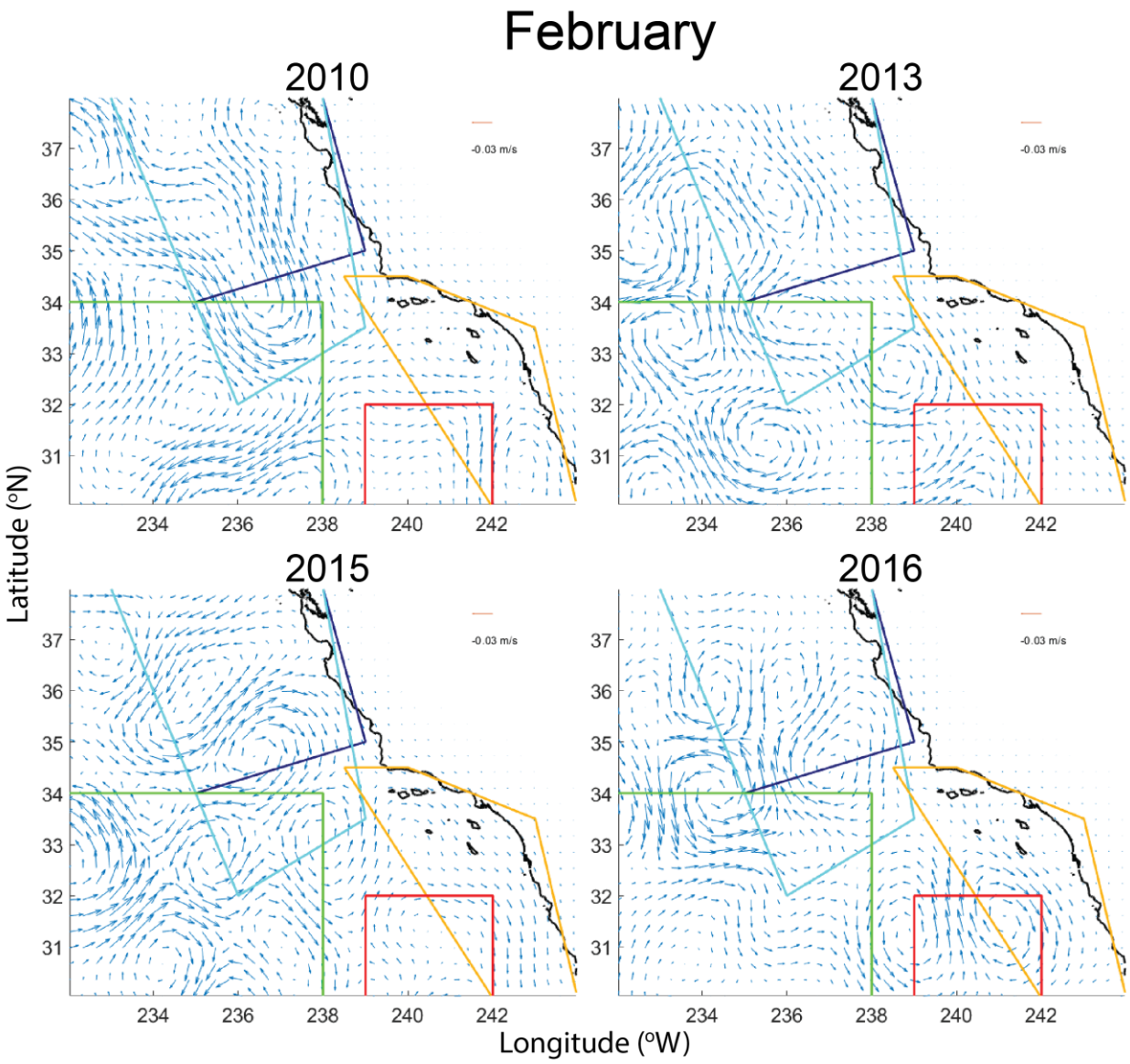

Figure S3.4. As in figure S3.1, but for February averages.

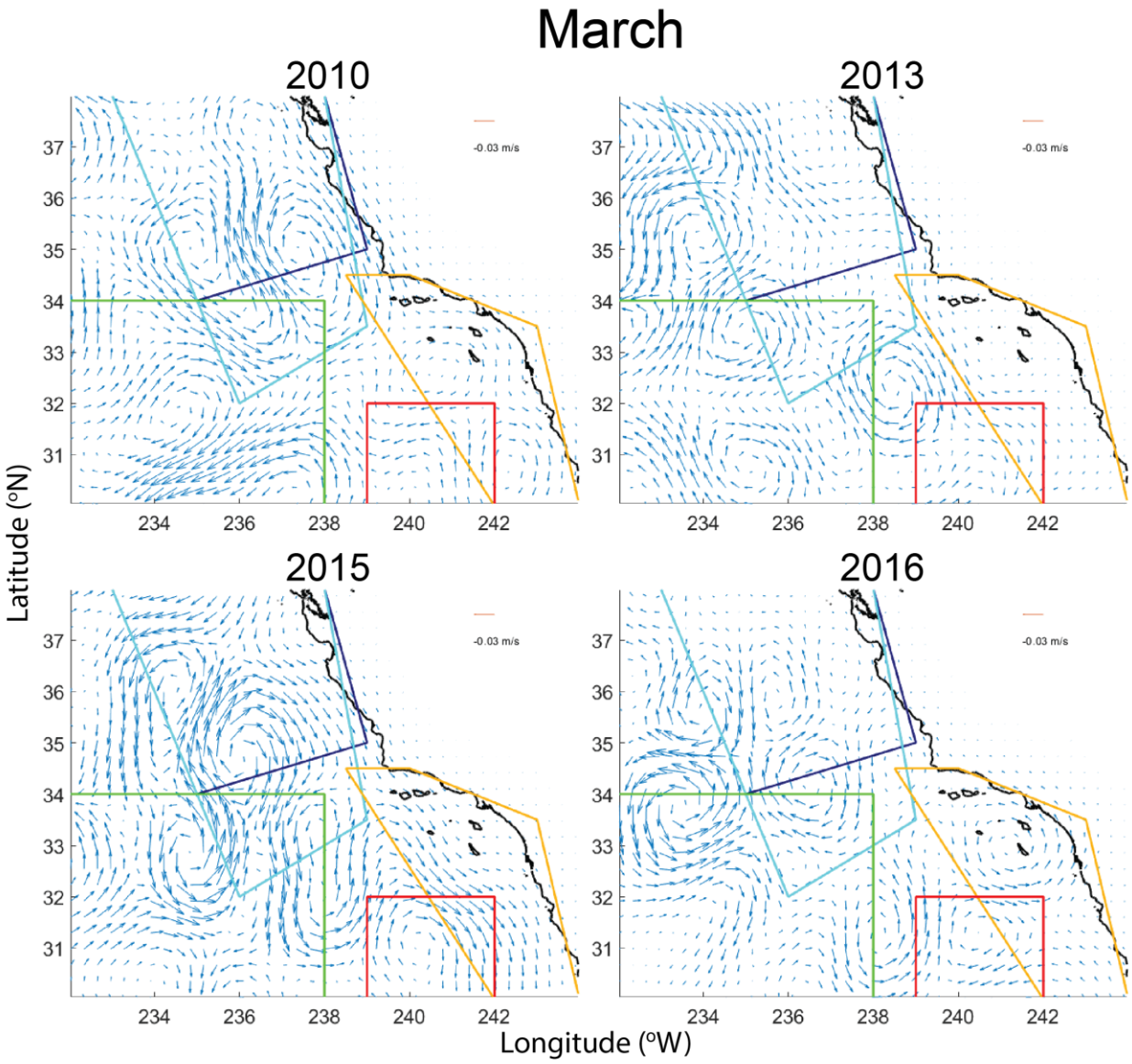

Figure S3.5. As in figure S3.1, but for March averages.

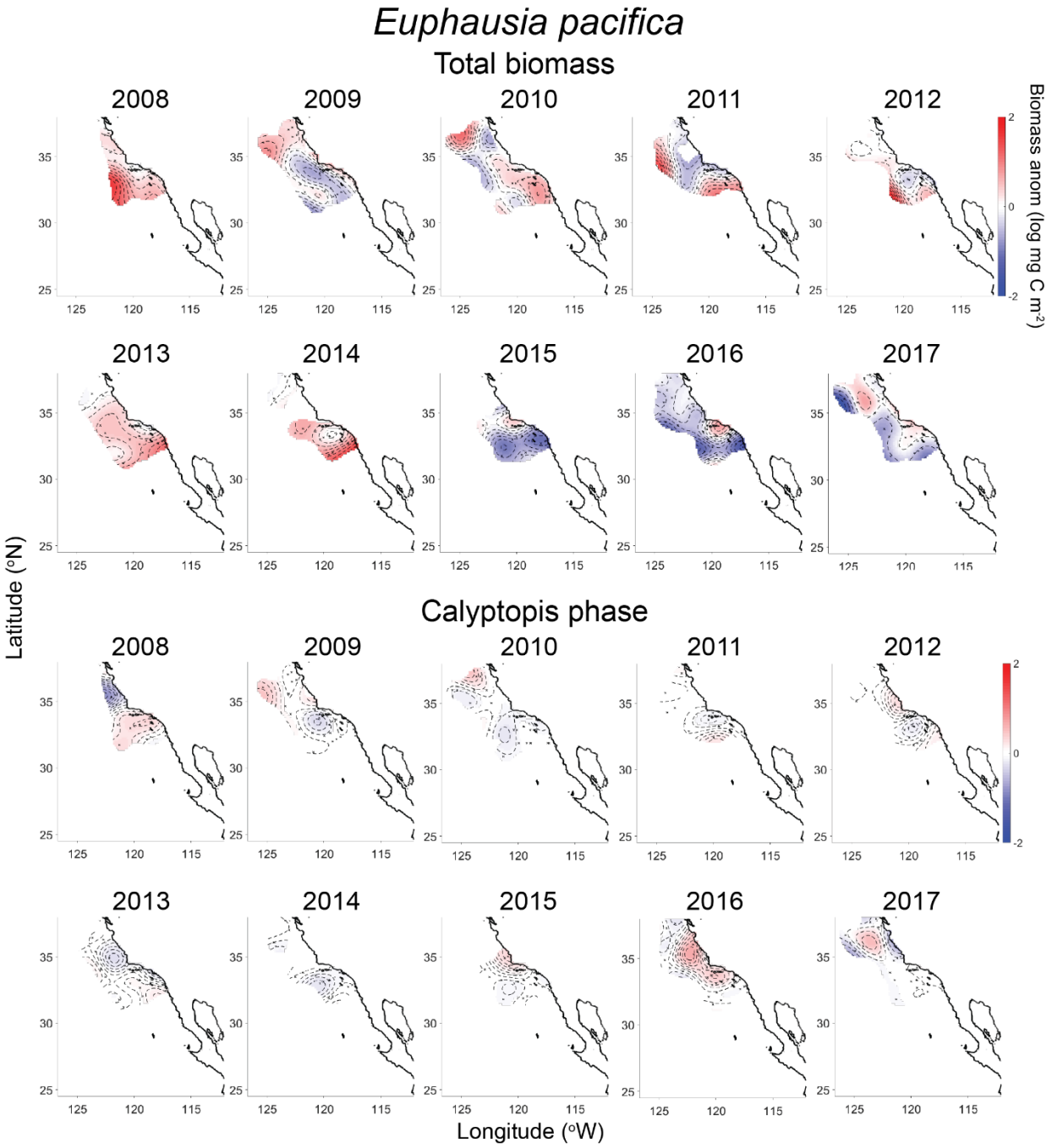

Figure S3.6. Biomass anomalies for total population (top) and calyptopis phase only (bottom) of *Euphausia pacifica*. Anomalies were calculated by removing station-by-station means (2008-2017) from each year's distribution.

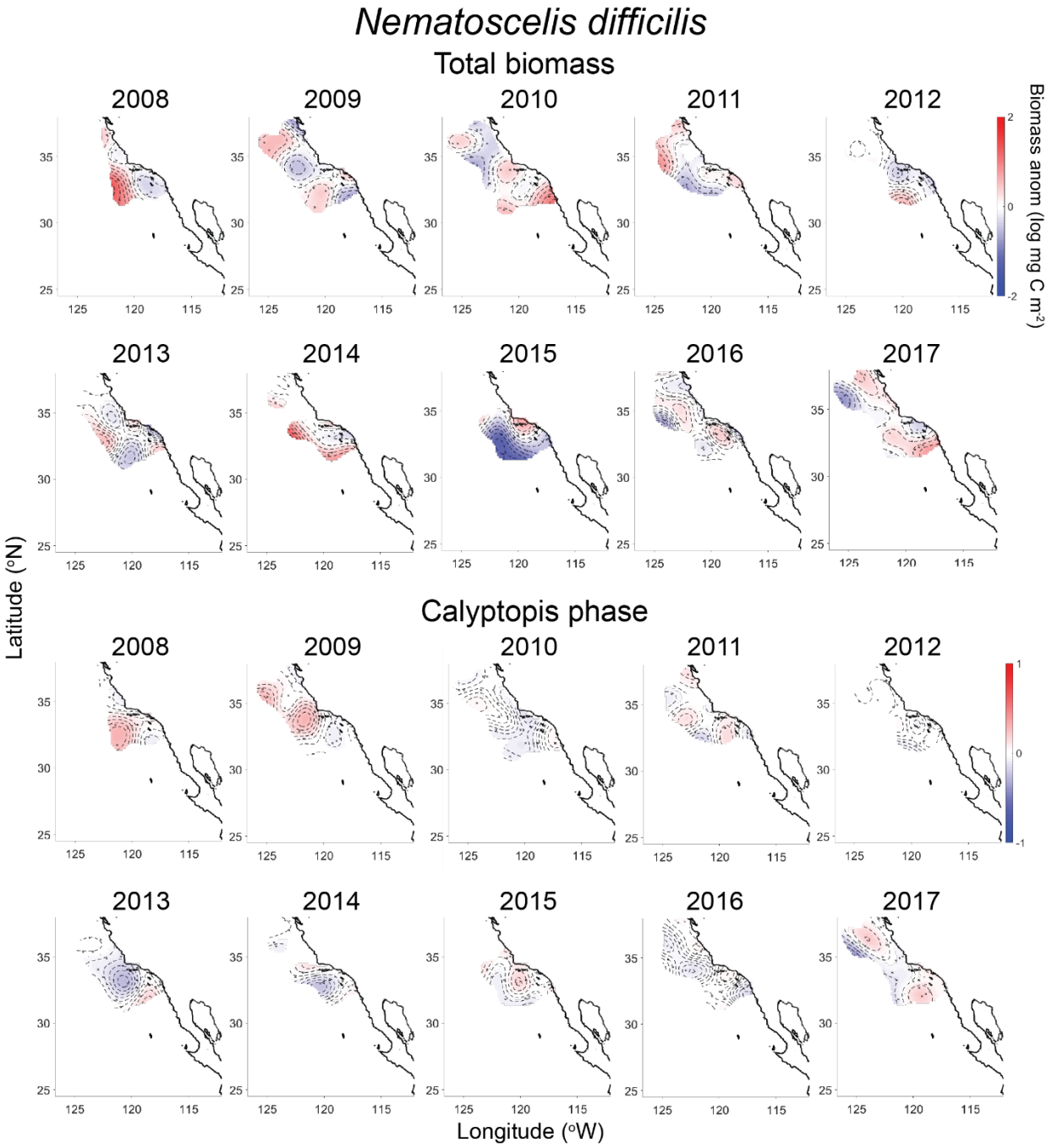

Figure S3.7. As in figure S3.6, but for *Nematoscelis difficilis*.

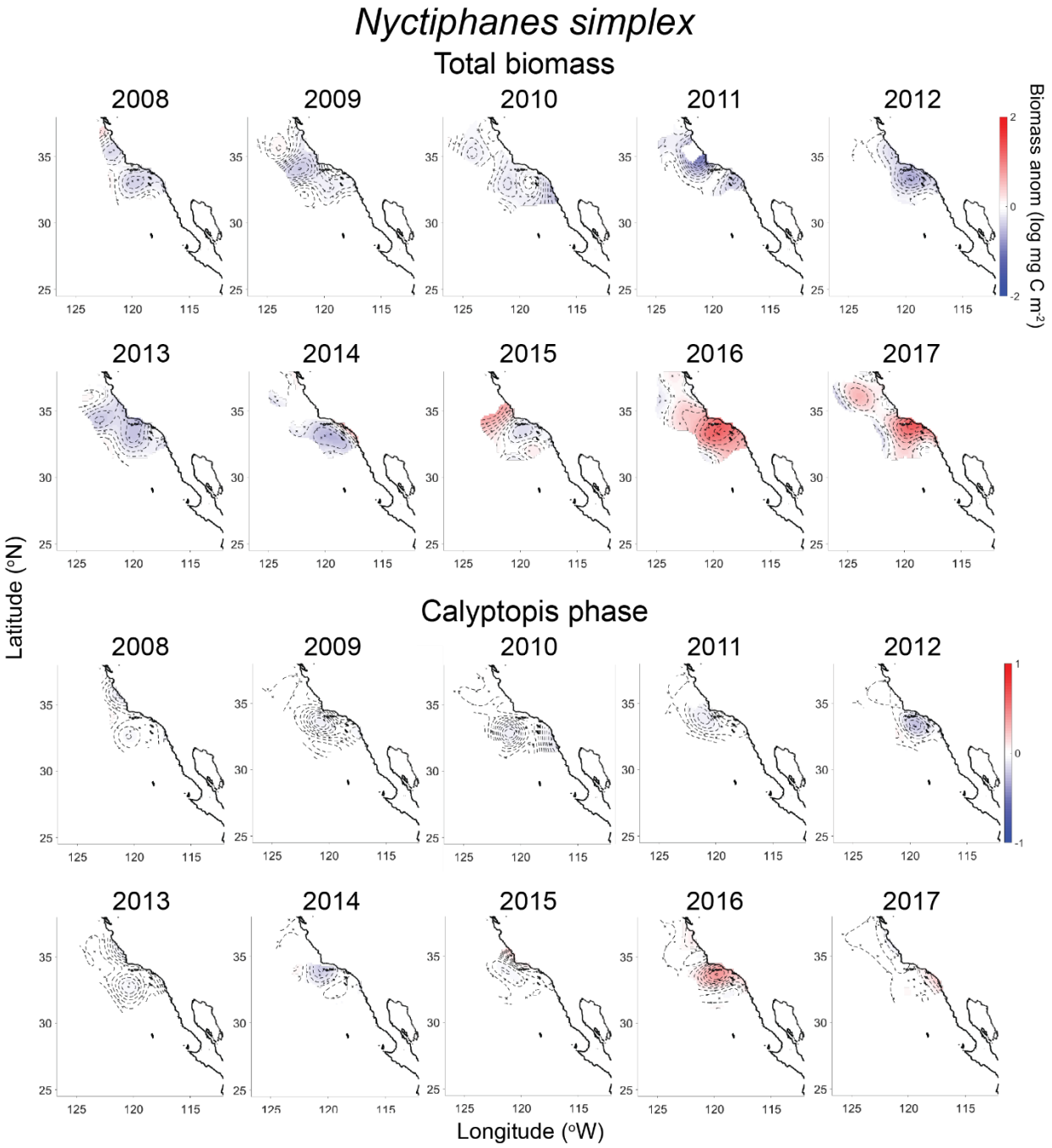

Figure S3.8. As in figure S3.6, but for *Nyctiphanes simplex*.

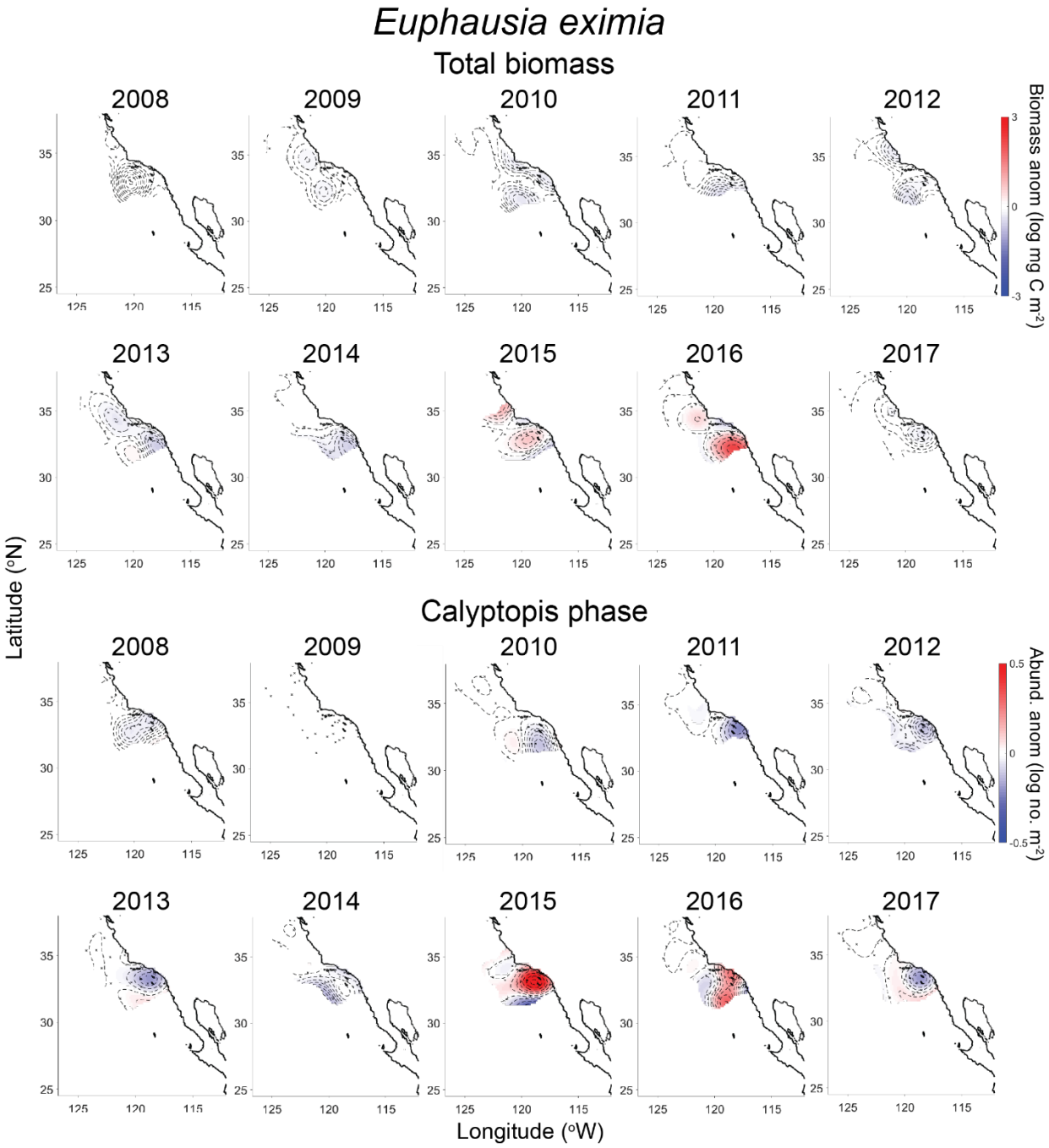

Figure S3.9. As in figure S3.6, but for *Euphausia eximia*. Calyptopis anomalies are shown for abundance (no. individuals m^{-2}) because many stations recorded zero biomass even for some calyptopis presence.

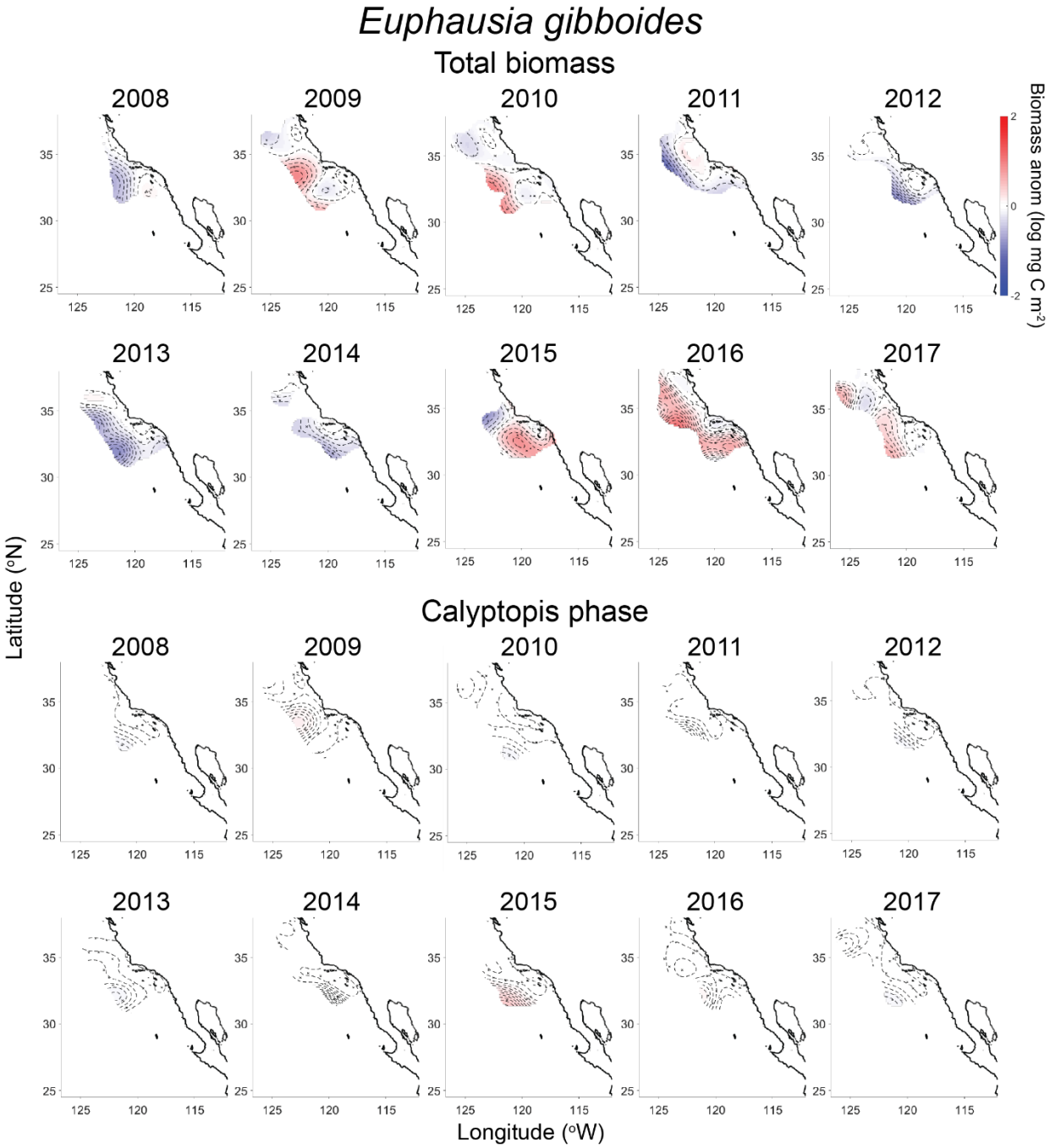

Figure S3.10. As in figure S3.9, but for *Euphausia gibboides*.

REFERENCES

Alexander, M. A., Blade, I., Newman, M., Lanzante, J. R., Lau, N. C. & Scott, J. D. (2002). The atmospheric bridge: The influence of ENSO teleconnections on air-sea interaction over the global oceans. *Journal of Climate, 15*(16), 2205-2231.

Ashok, K. & Yamagata, T. (2009). The El Niño with a difference. *Nature, 461*(7263), 481-484.

Bernal, P. A. (1981). A Review of the Low-Frequency Response of the Pelagic Ecosystem in the California Current. *CalCOFI Rep., 22*.

Bernal, P. A. & McGowan, J. A. (1981). Advection and upwelling in the California Current. *Coastal Upwelling, 1*, 381-399.

Bond, N. A., Cronin, M. F., Freeland, H. & Mantua, N. (2015). Causes and impacts of the 2014 warm anomaly in the NE Pacific. *Geophysical Research Letters, 42*(9), 3414-3420. doi:10.1002/2015gl063306

Brinton, E. (1960). Changes in the distribution of euphausiid crustaceans in the region of the California Current. *CalCOFI Rep., 7*, 137-146.

Brinton, E. (1962). The distribution of Pacific euphausiids. *Bulletin of the Scripps Institution of Oceanography, University of California, San Diego*(8), 51-270.

Brinton, E. (1981). Euphausiid distributions in the California Current during the warm winter-spring of 1977–78, in the context of a 1949–1966 time series. *California Cooperative Oceanic Fisheries Investigations Reports, 22*, 135-154.

Brinton, E. & Townsend, A. (2003). Decadal variability in abundances of the dominant euphausiid species in southern sectors of the California Current. *Deep-Sea Research Part Ii-Topical Studies in Oceanography, 50*(14-16), 2449-2472. doi:10.1016/S0967-0645(03)00126-7

Capotondi, A., Wittenberg, A. T., Newman, M., Di Lorenzo, E., Yu, J. Y., Braconnot, P., et al. (2015). Understanding ENSO diversity. *Bulletin of the American Meteorological Society, 96*(6), 921-938.

Chabert, P., d'Ovidio, F., Echevin, V., Stukel, M. R. & Ohman, M. D. (2021). Cross-shore flow and implications for Carbon Export in the California Current Ecosystem: a Lagrangian analysis. *Journal of Geophysical Research: Oceans, e2020JC016611*.

Chao, Y., Farrara, J. D., Bjorkstedt, E., Chai, F., Chavez, F., Rudnick, D. L., et al. (2017). The origins of the anomalous warming in the California coastal ocean and San Francisco Bay during 2014-2016. *Journal of Geophysical Research-Oceans, 122*(9), 7537-7557. doi:10.1002/2017jc013120

Chelton, D. B., Bernal, P. A. & Mcgowan, J. A. (1982). Large-Scale Interannual Physical and Biological Interaction in the California Current. *Journal of Marine Research, 40*(4), 1095-1125.

Croll, D. A., Marinovic, B., Benson, S., Chavez, F. P., Black, N., Ternullo, R. & Tershy, B. R. (2005). From wind to whales: trophic links in a coastal upwelling system. *Marine Ecology Progress Series, 289*, 117-130. doi:DOI 10.3354/meps289117

Croll, D. A., Tershy, B. R., Hewitt, R. P., Demer, D. A., Fiedler, P. C., Smith, S. E., et al. (1998). An integrated approach to the foraging ecology of marine birds and mammals. *Deep-Sea Research Part Ii-Topical Studies in Oceanography, 45*(7), 1353-+. doi:Doi 10.1016/S0967-0645(98)00031-9

Di Lorenzo, E. & Ohman, M. D. (2013). A double-integration hypothesis to explain ocean ecosystem response to climate forcing. *Proceedings of the National Academy of Sciences, 110*(7), 2496-2499.

Di Lorenzo, E., Schneider, N., Cobb, K. M., Franks, P. J. S., Chhak, K., Miller, A. J., et al. (2008). North Pacific Gyre Oscillation links ocean climate and ecosystem change. *Geophysical Research Letters, 35*(8).

Dorman, J. G., Powell, T. M., Sydeman, W. J. & Bograd, S. J. (2011). Advection and starvation cause krill (Euphausia pacifica) decreases in 2005 Northern California coastal populations: Implications from a model study. *Geophysical Research Letters, 38*. doi:Artn L0460510.1029/2010gl046245

Genin, A., Haury, L. & Greenblatt, P. (1988). Interactions of Migrating Zooplankton with Shallow Topography - Predation by Rockfishes and Intensification of Patchiness. *Deep-Sea Research Part a-Oceanographic Research Papers, 35*(2), 151-+. doi:Doi 10.1016/0198-0149(88)90034-9

Gentemann, C. L., Fewings, M. R. & Garcia-Reyes, M. (2017). Satellite sea surface temperatures along the West Coast of the United States during the 2014-2016 northeast Pacific marine heat wave. *Geophysical Research Letters, 44*(1), 312-319. doi:10.1002/2016gl071039

Gomez, J. G. (1995). Distribution Patterns, Abundance and Population-Dynamics of the Euphausiids Nyctiphanes-Simplex and Euphausia-Eximia Off the West-Coast of Baja-California, Mexico. *Marine Ecology Progress Series, 119*(1-3), 63-76. doi:DOI 10.3354/meps119063

Jacox, M. G., Hazen, E. L., Zaba, K. D., Rudnick, D. L., Edwards, C. A., Moore, A. M. & Bograd, S. J. (2016). Impacts of the 2015-2016 El Nino on the California Current System: Early assessment and comparison to past events. *Geophysical Research Letters, 43*(13), 7072-7080. doi:10.1002/2016gl069716

Kao, H. Y. & Yu, J. Y. (2009). Contrasting Eastern-Pacific and Central-Pacific Types of ENSO. *Journal of Climate, 22*(3), 615-632. doi:10.1175/2008jcli2309.1

Keister, J. E., Di Lorenzo, E., Morgan, C. A., Combes, V. & Peterson, W. T. (2011). Zooplankton species composition is linked to ocean transport in the Northern California Current. *Global Change Biology, 17*(7), 2498-2511.

Keister, J. E., Johnson, T. B., Morgan, C. A. & Peterson, W. T. (2005). Biological indicators of the timing and direction of warm-water advection during the 1997/1998 El Nino off the central Oregon coast, USA. *Marine Ecology Progress Series, 295*, 43-48. doi:DOI 10.3354/meps295043

Kim, W., Yeh, S. W., Kim, J. H., Kug, J. S. & Kwon, M. (2011). The unique 2009–2010 El Niño event: A fast phase transition of warm pool El Niño to La Niña. *Geophysical Research Letters, 38*(15).

Kug, J. S., Jin, F. F. & An, S. I. (2009). Two Types of El Nino Events: Cold Tongue El Nino and Warm Pool El Nino. *Journal of Climate, 22*(6), 1499-1515. doi:10.1175/2008jcli2624.1

L'Heureux, M. L., Takahashi, K., Watkins, A. B., Barnston, A. G., Becker, E. J., Di Liberto, T. E., et al. (2017). Observing and Predicting the 2015/16 El Nino. *Bulletin of the American Meteorological Society, 98*(7), 1363-1382. doi:10.1175/Bams-D-16-0009.1

Lavaniegos, B. E. (1992). Growth and larval development of Nyctiphanes simplex in laboratory conditions. *CalCOFI Rep., 33*, 162-171.

Lavaniegos, B. E. & Ambriz-Arreola, I. (2012). Interannual variability in krill off Baja California in the period 1997-2005. *Progress in Oceanography, 97*, 164-173. doi:10.1016/j.pocean.2011.11.008

Lavaniegos, B. E., Jiménez-Herrera, M. & Ambriz-Arreola, I. (2019). Unusually low euphausiid biomass during the warm years of 2014–2016 in the transition zone of the California Current. *Deep Sea Research Part II: Topical Studies in Oceanography*, 104638.

Lavaniegos, B. E., Jimenez-Perez, L. C. & Gaxiola-Castro, G. (2002). Plankton response to El Nino 1997-1998 and La Nina 1999 in the southern region of the California Current. *Progress in Oceanography, 54*(1-4), 33-58. doi:10.1016/S0079-6611(02)00042-3

Lavaniegos, B. E. & Ohman, M. D. (2007). Coherence of long-term variations of zooplankton in two sectors of the California Current System. *Progress in Oceanography, 75*(1), 42-69.

Lee, D. E., Nur, N. & Sydeman, W. J. (2007). Climate and demography of the planktivorous Cassin's auklet Ptychoramphus aleuticus off northern California: implications for population change. *Journal of Animal Ecology, 76*(2), 337-347. doi:10.1111/j.1365-2656.2007.01198.x

Lilly, L. E. & Ohman, M. D. (2018). CCE IV: El Niño-related zooplankton variability in the southern California Current System. *Deep-Sea Research Part I: Oceanographic Research Papers*.

Lilly, L. E. & Ohman, M. D. (submitted). Euphausiid spatial displacements elucidate El Niño forcing mechanisms in the southern California Current System.

Lilly, L. E., Send, U., Lankhorst, M., Martz, T. R., Feely, R. A., Sutton, A. J. & Ohman, M. D. (2019). Biogeochemical anomalies at two southern California Current System moorings during the 2014-16 Warm Anomaly-El Niño sequence. *Journal of Geophysical Research: Oceans*.

Lindegren, M., Checkley, D. M., Koslow, J. A., Goericke, R. & Ohman, M. D. (2018). Climate-mediated changes in marine ecosystem regulation during El Nino. *Global Change Biology, 24*(2), 796-809. doi:10.1111/gcb.13993

Lynn, R. J. & Bograd, S. J. (2002). Dynamic evolution of the 1997-1999 El Nino-La Nina cycle in the southern California Current System. *Progress in Oceanography, 54*(1-4), 59-75. doi:Pii S0079-6611(02)00043-5

Mantua, N. J., Hare, S. R., Zhang, Y., Wallace, J. M. & Francis, R. C. (1997). A Pacific interdecadal climate oscillation with impacts on salmon production. *Bulletin of the American Meteorological Society, 78*(6), 1069-1079. doi:Doi 10.1175/1520-0477(1997)078<1069:Apicow>2.0.Co;2

Marinovic, B. B., Croll, D. A., Gong, N., Benson, S. R. & Chavez, F. P. (2002). Effects of the 1997-1999 El Nino and La Nina events on zooplankton abundance and euphausiid community composition within the Monterey Bay coastal upwelling system. *Progress in Oceanography, 54*(1-4), 265-277. doi:10.1016/S0079-6611(02)00053-8

Marshall, J., Adcroft, A., Hill, C., Perelman, L. & Heisey, C. (1997). A finite-volume, incompressible Navier Stokes model for studies of the ocean on parallel computers. *Journal of Geophysical Research: Oceans, 102*(C3), 5753-5766.

Matthews, S. A., Goetze, E. & Ohman, M. D. (2020). *Cross-shore Changes in Vertical Habitats of Mesozoplankton: A Paired Metabarcoding and Morphological Approach*. Paper presented at the Ocean Sciences Meeting 2020, San Diego, CA, USA.

Newman, M., Wittenberg, A. T., Cheng, L. Y., Compo, G. P. & Smith, C. A. (2018). The Extreme 2015/16 El Nino, in the Context of Historical Climate Variability and Change. *Bulletin of the American Meteorological Society, 99*(1), S16-S20. doi:10.1175/Bams-D-17-0116.1

Nickels, C. F., Sala, L. M. & Ohman, M. D. (2018). The morphology of euphausiid mandibles used to assess selective predation by blue whales in the southern sector of the California Current System. *Journal of Crustacean Biology, 38*(5), 563-573.

Nickels, C. F., Sala, L. M. & Ohman, M. D. (2019). The euphausiid prey field for blue whales around a steep bathymetric feature in the southern California current system. *Limnology and Oceanography, 64*(1), 390-405. doi:10.1002/lno.11047

NOAA, O. E. a. R. (2021). What is an Expendable Bathythermograph, or "XBT"?

Pares-Escobar, F., Lavaniegos, B. E. & Ambriz-Arreola, I. (2018). Interannual summer variability in oceanic euphausiid communities off the Baja California western coast during 1998-2008. *Progress in Oceanography, 160*, 53-67. doi:10.1016/j.pocean.2017.11.009

Peterson, W. (1998). Life cycle strategies of copepods in coastal upwelling zones. *Journal of Marine Systems, 15*(1-4), 313-326.

Peterson, W. T., Fisher, J. L., Strub, P. T., Du, X., Risien, C., Peterson, J. & Shaw, C. T. (2017). The pelagic ecosystem in the Northern California Current off Oregon during the 2014–2016 warm anomalies within the context of the past 20 years. *Journal of Geophysical Research-Oceans, 122*(9), 7267-7290. doi:10.1002/2017JC012952

Ramp, S. R., McClean, J. L., Collins, C. A., Semtner, A. J. & Hays, K. A. S. (1997). Observations and modeling of the 1991-1992 El Nino signal off central California. *Journal of Geophysical Research-Oceans, 102*(C3), 5553-5582. doi:Doi 10.1029/96jc03050

Ren, H. L. & Jin, F. F. (2011). Niño indices for two types of ENSO. *Geophysical Research Letters, 38*(4).

Roemmich, D., Johnson, G. C., Riser, S., Davis, R., Gilson, J., Owens, W. B., et al. (2009). The Argo Program: Observing the global ocean with profiling floats. *Oceanography, 22*(2), 34-43.

Ross, R. M. (1982). Energetics of Euphausia-Pacifica .1. Effects of Body Carbon and Nitrogen and Temperature on Measured and Predicted Production. *Marine Biology, 68*(1), 1-13. doi:10.1007/Bf00393135

Ross, R. M., Daly, K. L. & English, T. S. (1982). Reproductive-Cycle and Fecundity of Euphausia-Pacifica in Puget Sound, Washington. *Limnology and Oceanography, 27*(2), 304-314. doi:DOI 10.4319/lo.1982.27.2.0304

Rudnick, D. L., Zaba, K. D., Todd, R. E. & Davis, R. E. (2017). A climatology of the California Current System from a network of underwater gliders. *Progress in Oceanography, 154*, 64-106. doi:10.1016/j.pocean.2017.03.002

Schwing, F. B., Murphree, T. & Green, P. M. (2002). The evolution of oceanic and atmospheric anomalies in the northeast Pacific during the El Niño and La Niña events of 1995–2001. *Progress in Oceanography, 54*(1), 459-491.

Simpson, J. J. (1984). El-Nino-Induced Onshore Transport in the California Current during 1982-1983. *Geophysical Research Letters, 11*(3), 241-242.

Stammer, D., Wunsch, C., Giering, R., Eckert, C., Heimbach, P., Marotzke, J., et al. (2002). Global ocean circulation during 1992–1997, estimated from ocean observations and a general circulation model. . *Journal of Geophysical Research: Oceans, 107*(C9), 1.

Strub, P. T. & James, C. (2002). The 1997-1998 oceanic El Niño signal along the southeast and northeast Pacific boundaries - an altimetric view. *Progress in Oceanography, 54*(1-4), 439-458.

Tanasichuk, R. W. (1999). Interannual variation in the availability and utilization of euphausiids as prey for Pacific hake (Merluccius productus) along the south-west coast of Vancouver Island. *Fisheries Oceanography, 8*(2), 150-156.

Thayer, J. A. & Sydeman, W. J. (2007). Spatio-temporal variability in prey harvest and reproductive ecology of a piscivorous seabird, Cerorhinca monocerata, in an upwelling system. *Marine Ecology Progress Series, 329*, 253-265. doi:DOI 10.3354/meps329253

Timmermann, A., An, S.-I., Kug, J. S., Jin, F. F., Cai, W., Capotondi, A., et al. (2019). El Niño-Southern Oscillation complexity. *Nature, 559*, 535-545.

Todd, R. E., Rudnick, D. L., Davis, R. E. & Ohman, M. D. (2011). Underwater gliders reveal rapid arrival of El Nino effects off California's coast. *Geophysical Research Letters, 38*. doi:10.1029/2010gl046376

Yamamura, O., Inada, T. & Shimazaki, K. (1998). Predation on Euphausia pacifica by demersal fishes: predation impact and influence of physical variability. *Marine Biology, 132*(2), 195-208. doi:DOI 10.1007/s002270050386

Yeh, S. W., Kug, J. S. & An, S. I. (2014). Recent progress on two types of El Niño: Observations, dynamics, and future changes. *Asia-Pacific Journal of Atmospheric Sciences, 50*(1), 69-81.

Zaba, K. D. & Rudnick, D. L. (2016). The 2014-2015 warming anomaly in the Southern California Current System observed by underwater gliders. *Geophysical Research Letters, 43*(3), 1241-1248. doi:10.1002/2015gl067550

Zaba, K. D., Rudnick, D. L., Cornuelle, B., Gopalakrishnan, G. & Mazloff, M. (2020). Volume and heat budgets in the coastal California Current System: Means, annual cycles and interannual anomalies of 2014-2016. *Journal of Physical Oceanography*.

Zaba, K. D., Rudnick, D. L., Cornuelle, B. D., Gopalakrishnan, G. & Mazloff, M. R. (2018). Annual and Interannual Variability in the California Current System: Comparison of an Ocean State Estimate with a Network of Underwater Gliders. *Journal of Physical Oceanography, 48*(12), 2965-2988. doi:10.1175/Jpo-D-18-0037.1

Chapter 4

Biogeochemical anomalies at two southern California Current System moorings during the 2014-16 Warm Anomaly-El Niño sequence

Abstract

We analyzed impacts of the 2014-15 Pacific Warm Anomaly and 2015-16 El Niño on physical and biogeochemical variables at two southern California Current System moorings (CCE2, nearshore upwelling off Point Conception; CCE1, offshore California Current). Nitrate and Chl-*a* fluorescence were < 1 µM and < 1 Standardized Fluorescence Unit, respectively, at CCE2 for the entire durations of the Warm Anomaly and El Niño, the two longest periods of such low values in our timeseries. Negative nitrate and Chl-*a* anomalies at CCE2 were interrupted briefly by upwelling conditions in spring 2015. Near-surface temperature anomalies appeared simultaneously at both moorings in spring 2014, indicating region-wide onset of Warm Anomaly temperatures, although sustained negative nitrate and Chl-*a* anomalies only occurred offshore at CCE1 during El Niño (summer 2015-spring 2016). Warm Anomaly temperature changes were expressed more strongly in near-surface (< 40 m) than subsurface (75 m) waters at both moorings, while El Niño produced comparable temperature anomalies at near-surface and subsurface depths. Nearshore $\Omega_{aragonite}$ at 76 m showed notably fewer undersaturation events during both warm periods, suggesting an environment more conducive to calcifying organisms. Planktonic calcifying molluscs (pteropods and heteropods) increased markedly in springs 2014 and 2016 and remained modestly elevated in spring 2015. Moorings provide high-frequency measurements essential for resolving the onset timing of anomalous conditions and frequency

and duration of short-term (days-to-weeks) perturbations (reduced nitrate, aragonite undersaturation events) that can affect marine organisms.

4.1. Introduction

The California Current System (CCS) is an eastern boundary upwelling system that supports high biological production and commercially valuable fisheries. The southern portion of the CCS extends from Point Conception, CA, south to the U.S.-Mexico border, and consists of the southward-flowing core California Current (200-400 km offshore), the nearshore poleward California Undercurrent (inshore of 150 km, centered at 150 m depth), and the Inshore Countercurrent (Di Lorenzo, 2003; Lynn & Simpson, 1987; Rudnick et al., 2017). The nearshore region experiences a spring upwelling season driven by alongshore winds, while wind-stress curl upwelling produces vertical pumping farther offshore; these dynamics deliver nutrients to near-surface waters, sustaining high primary production (Carr & Kearns, 2003; Chelton, 1982; Chelton et al., 1982; Cushing, 1971; Pickett & Paduan, 2003; Rykaczewski & Checkley, 2008). El Niño is the dominant mode of interannual variability in the CCS, and can produce anomalous circulation including advection of water masses into the southern CCS from Baja California or southern offshore waters (Chavez, 1996; Chavez et al., 2002; Jacox et al., 2016; Lynn & Bograd, 2002; Simpson, 1984). El Niño impacts on CCS ecosystems vary substantially, but past major El Niños reduced phytoplankton biomass (Chavez, 1996; Fiedler, 1984; Kahru & Mitchell, 2000), produced anomalous subtropical zooplankton influxes (Bednaršek et al., 2018; Lavaniegos et al., 2002; Lavaniegos & Ohman, 2007; Lilly & Ohman, 2018; Rebstock, 2001), and altered survival and spatial distributions of seabirds and marine mammals (Keiper et al., 2005; Lee et al., 2007; Thayer & Sydeman, 2007).

The CCS can be affected by other modes of variability, including the Pacific Decadal Oscillation, the North Pacific Gyre Oscillation, and regionally-forced non-Niño warm events (Di Lorenzo et al., 2008; Fiedler & Mantua, 2017; Mantua et al., 1997). The 2014-15 Pacific Warm Anomaly that developed in the Eastern North Pacific Ocean showed unprecedented magnitude, spatial extent, and duration (Bond et al., 2015; Di Lorenzo & Mantua, 2016; Zaba & Rudnick, 2016). Anomalous sea surface temperatures (SST) appeared off California in spring 2014 and reached +5^{o} C in the upper 50 m of the water column (Gentemann et al., 2017; Zaba & Rudnick, 2016). The Warm Anomaly was associated with an 'aborted El Niño' and was thus not attributed to direct equatorial El Niño forcing (Hu & Fedorov, 2016; Li et al., 2015), although atmospheric teleconnections from the equatorial Pacific likely influenced temperature anomalies in winter 2014-15 (Chao et al., 2017; Di Lorenzo & Mantua, 2016). The Warm Anomaly persisted through spring 2015, at which point normal upwelling conditions produced cooler temperatures and high nutrients nearshore. Warm temperatures reappeared in summer 2015, and El Niño conditions reached the California Current System (CCS) by fall 2015 (Chao et al., 2017; Jacox et al., 2016). The sequence of the 2014-15 Warm Anomaly followed immediately by the 2015-16 El Niño produced more than two years of anomalous physical oceanographic conditions in the CCS, notably extremely warm temperatures and increased water column stratification (Jacox et al., 2016; Zaba & Rudnick, 2016). Despite known differences in physical forcing mechanisms, the Warm Anomaly had coastwide impacts on CCS ecosystems similar to those observed during El Niño events, including anomalously deep chlorophyll maxima (Zaba & Rudnick, 2016), subtropical zooplankton species appearances and community composition rearrangements (Fisher et al., 2015; Lilly & Ohman, 2018; Peterson et al., 2017), coastwide harmful algal

blooms and associated marine mammal toxicity (McCabe et al., 2016; Ryan et al., 2017), and large-scale seabird mortality events (Peterson et al., 2015).

Ocean acidification is a growing issue due to increased anthropogenic release of CO_2 and subsequent oceanic uptake. The CCS experiences natural intrusions of low-pH, high-CO_2 conditions from upwelling of deep, remineralized waters, although these intrusions are predicted to expand and intensify in the future (Feely et al., 2016; Feely et al., 2018; Feely et al., 2008; Gruber et al., 2012; Hauri et al., 2013a; Hauri et al., 2013b; Leinweber & Gruber, 2013). Ocean acidification threatens calcifying marine organisms because it lowers the saturation states (Ω) of aragonite and calcite, carbonate minerals essential for shell production, requiring organisms to expend more energy on shell formation and growth (Bednaršek et al., 2014; Bednaršek et al., 2017; Bednaršek et al., 2016; Hauri et al., 2013a). Bednaršek et al. (2018) found that the pteropod species *Limacina helicina* in the northern CCS (southern British Columbia to Monterey Bay, CA) experienced synergistic negative impacts from an enhanced upwelling season (low oxygen, pH, and Ω_{arag}) in spring 2016 combined with increased temperatures during the 2013-15 marine heat wave (here referred to as the Warm Anomaly) and 2015-16 El Niño. Analysis of anomalous perturbations to CCS ecosystems and predictions of future impacts must therefore consider not just the event at hand but also its potential combination with background conditions and other perturbations.

Moorings provide continuous high-frequency measurements of a specific region and thus can resolve the onset timing of perturbations such as the Warm Anomaly and El Niño. They also provide information on short-term (days to weeks) habitat changes that organisms experience, such as pulsed nutrient delivery (Chavez, 1996; Chavez et al., 1997; Pennington & Chavez, 2000; Sakamoto et al., 2017) and aragonite undersaturation events. The present paper analyzes

impacts of the 2014-15 Pacific Warm Anomaly and 2015-16 El Niño on sub-seasonal and interannual changes in multiple physical and biogeochemical variables measured at two southern CCS moorings that have been deployed regularly since January 2010. We specifically examined the following questions: 1) Did the 2014-15 Warm Anomaly and 2015-16 El Niño differentially affect physical and biogeochemical conditions in the southern CCS region? 2) Were the timing and magnitude of each event synchronous across CCE2 and CCE1? 3) Did the prior existence of the Warm Anomaly appear to influence subsequent biological responses to the 2015-16 El Niño or long-term effects beyond the events? 4) How did biogeochemical responses to these two perturbations compare to the 2009-10 El Niño?

We hypothesized that near-surface temperatures would be anomalously high and nitrate and chlorophyll-*a* fluorescence anomalously low at both moorings for the entire Warm Anomaly-El Niño sequence (spring 2014-spring 2016). In contrast, we expected that deeper temperature anomalies would only appear during El Niño, and more strongly at CCE2 than at CCE1, due to coastally-enhanced northward propagation of the El Niño signal. We further hypothesized that aragonite saturation state would be elevated at both moorings from spring 2014-spring 2016, with corresponding increases in pelagic mollusc populations due to either advection of subtropical species or favorable in situ conditions.

4.2. Materials and Methods

4.2.1. Mooring locations

Physical and biogeochemical data are from two biogeochemical moorings located in the southern California Current System: CCE1 is located 220 km southwest of Point Conception, CA, in 4100 m of water in the core southward-flowing California Current; CCE2 is located 35

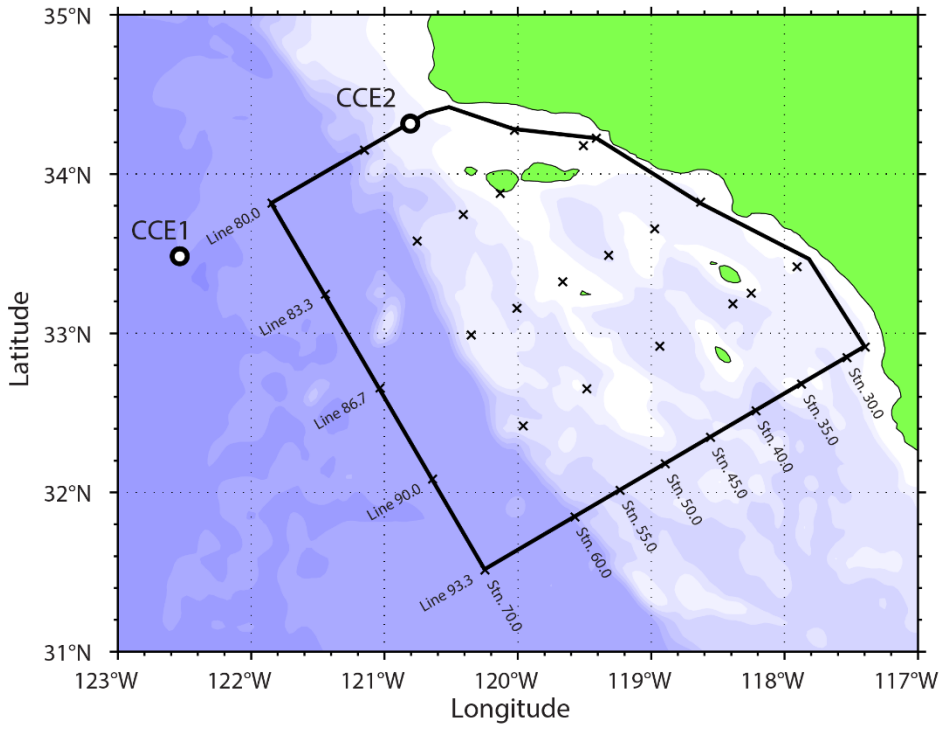

Figure 4.1. Locations of the CCE1 and CCE2 moorings (black circles) and subset of the CalCOFI sampling region from which zooplankton were analyzed (black box) in the southern California Current System. The CalCOFI stations from which zooplankton samples are pooled are shown by black crosses within and along the black box. Note that these stations are only a subset of the larger CalCOFI grid.

km southwest of Point Conception in 800 m of water in the nearshore upwelling region (Fig. 4.1). CCE1 is co-located with CalCOFI station 80.80, CCE2 with CalCOFI 80.55 (California Cooperative Oceanic Fisheries Investigations, Bograd et al. (2003)). CCE1 was initiated in October 2008 and CCE2 in January 2010, although both timeseries have experienced short-term interruptions. We present data here only from January 2010-present. The moorings are maintained by the Ocean Time Series Group and the California Current Ecosystem Long-Term Ecological Research site (CCE-LTER), both based at Scripps Institution of Oceanography, La Jolla, CA.

4.2.2. Mooring design and sensors

Each mooring consists of a surface buoy with a buoy-mounted instrument package, including a Moored Autonomous pCO_2 sensor ($MAPCO_2$) which measures seawater and air mole fractions of CO_2 (xCO_2) to be converted to partial pressure (pCO_2). A conductive wire connects subsurface instruments to the surface to permit real-time data transmission. Each mooring has a subsurface biogeochemical sensor cage: CCE1 at 40 m depth and CCE2 at 16 m depth. The cages include the following sensors: SBE37-IM Microcat (temperature, salinity), SeapHOx (pH sensor, Martz Lab, Scripps Institution of Oceanography) with attached Aanderaa optode (oxygen), WET Labs FLNTUS fluorometer (chlorophyll-*a* fluorescence), and Satlantic SUNA (nitrate). In addition to data from the sensor cages, we analyzed temperature and oxygen data at CCE2 at 76 m depth to calculate deep aragonite saturation (see Section 4.2.4), and temperature and salinity data at CCE1 at 19 m and 75 m to compare onset timing of the Warm Anomaly and El Niño between CCE1 and CCE2. Most of the sensors record data every 30 minutes; for the present study we averaged data to daily values as described below. A detailed description of mooring design is available at: http://mooring.ucsd.edu/projects.

4.2.3. Sensor calibrations and quality control

Microcat and optode sensors are calibrated by attaching sensors to a CTD rosette and conducting pre-deployment and post-recovery calibration casts to compare sensors to concurrent CTD measurements and bottle samples. Nitrate data undergo a two-step quality control process: 1) manual baseline correction to zero data and account for sensor drift, and 2) comparison to in situ bottle-sample nitrate measurements for further correction. Chl-*a* fluorescence data undergo a three-step conversion process: 1) manual baseline correction, 2) conversion to Standardized Fluorescence Units (SFU, *cf*. Powell and Ohman (2015)) by multiplying the raw timeseries by a

slope value calculated by comparing fluorometer voltage readings to laboratory-prepared chlorophyll-*a* standards, and 3) comparison to CalCOFI Chl-*a* measurements for external validation and adjustment (see Appendix 4A and Fig. 4.A1 for additional information). The pH timeseries are quality controlled following Bresnahan et al. (2014) by bringing the subsurface SeapHOx pH sensors into agreement with a calculated surface reference pH at a time when the mixed layer is sufficiently deep to encompass the subsurface sensor. The surface reference pH is calculated from surface-measured pCO_2 data and total alkalinity estimated from temperature and salinity by the proxy relationships described in Alin et al. (2012). pCO_2 is measured as follows from Sutton et al. (2014): mole fraction of CO_2 (xCO_2) in seawater is measured by pumping a sample of air through seawater for 10 minutes, then reading the equilibrated air sample using a LI-COR LI-820 CO_2 gas analyzer. A separate air sample is drawn into the $MAPCO_2$ and air xCO_2 is measured by the gas analyzer. Seawater and air measurements are made every 3 hours and calibrated in situ with a standard CO_2 reference gas. Raw (wet) xCO_2 measurements are converted to (dry) xCO_2 using atmospheric pressure and LI-820 vapor pressure, and dry measurements are used to calculate seawater and air pCO_2. $\Delta pCO_2 = pCO_{2SW} - pCO_{2air}$.

We averaged each timeseries to daily resolution to produce consistency across timeseries. Chl-*a* fluorescence daily values were only averaged from nighttime datapoints (2100-0300 local time) to avoid daylight quenching. Anomalies were computed by removing the 2010-2018 mean for each year-day from the corresponding year-day for each year (e.g., Jan 1 of each year minus the 2010-2018 Jan 1 mean). We compared timeseries to quarterly CalCOFI cruise measurements at the appropriate station and depth as an external data check for all timeseries except pH and pCO_2 (CalCOFI data not available) (Figs. 4.2, 4.4), although these types of pH and pCO_2 checks have been performed as part of previous studies (Sutton et al., 2016; Sutton et al., 2014). The

carbonate chemistry calculations described in this section and the following section were carried out using CO2SYS for Matlab v1.1 (Van Heuven et al., 2011).

4.2.4. Aragonite saturation state calculations

Aragonite saturation state (Ω_{arag}) was calculated using two approaches. The first estimates Ω_{arag} from measured pH and estimated total alkalinity (TA) calculated from the proxy mentioned in Section 4.2.3 above. We applied this approach using the pH sensor data at CCE1 40 m and CCE2 16 m. We used a second proxy relationship to calculate Ω_{arag} at CCE2 76 m using temperature and oxygen, as described in Alin et al. (2012). The relationship between Ω_{arag} and temperature-O_2 holds beneath the mixed layer but is often also valid at shallower depths in upwelling areas such as CCE2. Due to the high correlation between the pH-derived Ω_{arag} and temperature-O_2 proxy at CCE2 16 m (rho = 0.90, $p < 0.01$), we supplemented the pH-derived Ω_{arag} calculations at CCE1 40 m and CCE2 16 m with calculations from the second relationship during periods for which we lacked pH data (see Appendix 4B for more information). For comparison, we also calculated Ω_{arag} from quarterly CalCOFI bottle data corresponding to CCE1 40 m, CCE2 16 m, and CCE2 76 m. We used dissolved inorganic carbon (DIC) and TA measurements at CCE1 40 m and CCE2 16 m from the five cruises for which they are available (pH data are not available from CalCOFI cruises). For other cruises and all calculations at CCE2 76 m, we calculated CalCOFI Ω_{arag} from temperature and oxygen.

To estimate the percentage of aragonite undersaturation days in a year, we summed the number of days of aragonite undersaturation within a yearlong period (Jan 1-Dec 31) or the Warm Anomaly or El Niño and divided by the number of sampled days of aragonite saturation in

that period (see Appendix 4C for start and end date of each anomalous period). The resulting values for '% aragonite undersaturation days/year' are shown in figure 4.3c.

4.2.5. Temperature and nitrate cumulative anomalies

We demarcated the start and end dates of the Warm Anomaly and El Niño as the beginnings and ends of periods of continuous positive temperature anomalies during spring 2014-spring 2016 at the near-surface sensors (16 m for CCE2, 19 m for CCE1; see Appendix 4C for explanation and dates). The resulting periods are shaded in figures 4.2 and 4.4. We calculated average daily anomalies for temperature and nitrate during the Warm Anomaly and El Niño to compare the individual impacts of each perturbation and their differential effects in near-surface and subsurface waters. We used the temperature-derived start and end dates for nitrate anomaly calculations to maintain consistency and because nitrate did not have continuous negative anomalies throughout each perturbation. For each anomalous period, we summed all temperature or nitrate anomalies at a given depth to obtain the total integrated anomaly for that depth, which we then divided by the total number of perturbation days to get the average daily anomaly.

4.2.6. North/South water mass index and particle backtracking

An index of the relative contributions of northern- versus southern-origin flow (hereafter: N/S index) was previously developed to identify origins of water masses arriving at the CCE1 mooring, based on temperature-salinity (T-S) properties. The N/S index was developed from temperature and salinity data from locations in the CCS between Northern California and the southern tip of Baja California using data from the World Ocean Atlas climatologies (Locarnini et al., 2013; Zweng et al., 2013). Locations were assigned N/S index values on a scale from -1

(Northern California) to +1 (southern Baja California) based on where their T-S diagrams fit in relation to the southernmost and northernmost water masses. The CCE1 N/S index at 40 m was then computed by determining where its combined T-S values aligned with the standardized values from -1 to +1. Our N/S index is akin to the spiciness property (Flament, 2002) or to analyzing salinity on a fixed isopycnal, but the -1 to +1 scaling adjusts the values to the local hydrography. Waters at CCE1 with positive N/S index values suggest southern or offshore origins.

The CCE1 site is located in the climatological mean position of the California Current, but as the current meanders back and forth inflow to CCE1 can occur from different directions (see also Fig. 11 in Frischknecht et al., 2018). To investigate whether southern-appearance waters at CCE1 indicated by the N/S index were associated with southern- or coastal-origin flows, we analyzed surface particle trajectories. These were computed from altimetry-derived geostrophic currents, which are distributed as part of the Copernicus Marine Environment Monitoring System (CMEMS, formerly AVISO). From these currents, we computed particle trajectories by solving the equation $\vec{u} = \frac{d\vec{X}}{dt}$, where $\vec{u}$ denotes the Eulerian velocities from the altimeter and $\vec{X}$ denotes the Lagrangian positions along a trajectory. We integrated the resulting velocities backward for 30 days prior to the CCE1 endpoint. Each particle track starts 5 days after the previous track starts, so successive tracks overlap for 25 days; there are 533 tracks total for the entire period from 2010-2018. We compared our altimetry-derived particle trajectories to ADCP-derived trajectories from CCE1 at 30 m depth and found strong correspondence for the 30-day forward projections (See Appendix 4D and figure 4.D1 for more information). Prior results from Hartman et al. (2010; see their Fig. 5) also suggest that qualitative comparisons using these trajectories are reasonable. We did not calculate particle trajectories for CCE2

(located 35 km from land) because altimetry data within 50 km of the coast are generally unreliable and would likely not produce accurate backtracks.

4.2.7. Pelagic mollusc sampling

Zooplankton were collected on CalCOFI cruises as previously described (Lavaniegos & Ohman, 2007; Lilly & Ohman, 2018). Samples were collected by a 505 µm mesh, dual-opening, 0.71-m diameter bongo net towed obliquely from 0-210 m. After collection, samples were preserved in formaldehyde buffered with sodium tetraborate, then archived for identification in the Pelagic Invertebrate Collection at Scripps Institution of Oceanography. All nighttime stations within the Southern California region (CalCOFI Lines 80-93.3 from the coast to Station 70, excluding stations < 200 m depth) were pooled into one aliquot per cruise. Pelagic molluscs (i.e., thecosome and gymnosome pteropods, heteropods) from spring cruises only were identified to genus (where possible) or higher taxon using light microscopy. Within the total pelagic mollusc group, we also present data for the family Limacinidae and for *Hyalocylis* spp., which only appeared in 2014 and was comprised almost exclusively of *H. striata* (L. Sala, personal communication). The family Limacinidae is not enumerated to species level but is likely comprised of the following six species based on past descriptions of pteropod biogeographies in the eastern North Pacific: *Heliconoides inflatus, Limacina helicina helicina, Limacina helicina pacifica, Limacina bulimoides, Limacina lesueruii, Limacina trochiformis* (Janssen et al., 2019; McGowan, 1967).

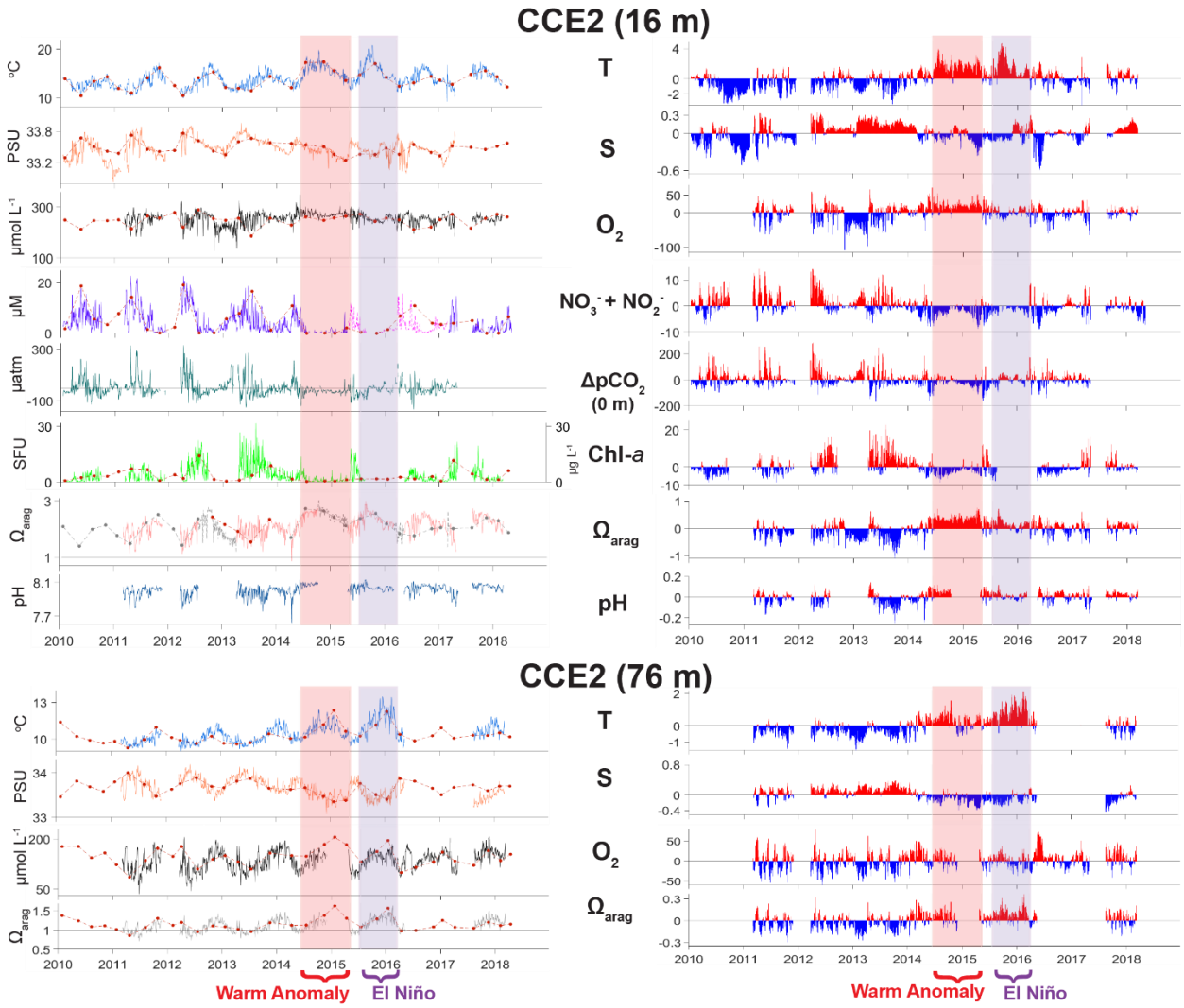

Figure 4.2. Daily-averaged timeseries (*left*) and anomalies (*right*) for the CCE2 mooring at 16 m *(top)* and 76 m *(bottom).* Variables at 16 m are: (*top-bottom*) temperature, salinity, oxygen, nitrate+nitrite, ΔpCO_2, Chl-*a* fluorescence (SFU), omega-aragonite, and pH. Horizontal grey lines for Ω_{arag} at 16 m and 76 m indicate the aragonite saturation horizon ($\Omega = 1$); undersaturation events occur when the timeseries dips below this line. The nitrate timeseries at 16 m includes measured data (purple) and temperature-proxy calculations (magenta). Aragonite saturation timeseries at 16 m and 76 m include proxy calculations from pH-CO_2 (light pink, 16 m only) and temperature-O_2 (grey, 16 m and 76 m) (see Methods 2.4 and Appendices A and B for nitrate and aragonite saturation calculations). The Warm Anomaly and El Niño are shaded by vertical orange and purple bars, respectively. Red dots and dashed lines on left panels are CalCOFI quarterly measurements (not available for pCO_2 or pH; Chl-*a* scale as µg L^{-1}, right axis).

4.3. Results and Discussion

4.3.1. 2014-15 Warm Anomaly: evolution and effects

The 2014-15 Pacific Warm Anomaly produced the longest period of consistently anomalously warm temperatures and near-zero nitrate and chlorophyll-*a* fluorescence at CCE2 since our mooring timeseries began (Fig. 4.2). Nitrate levels were < 1 µM and chlorophyll-*a* was < 1 Standardized Fluorescence Unit (SFU) for the entire period of May 2014-February 2015. Average daily nitrate anomalies at CCE2 at 16 m during the Warm Anomaly were twice the (negative) magnitude of those during El Niño, suggesting that the Warm Anomaly more completely suppressed nitrate inputs to the nearshore region (Fig. 4.3b, red bars). In contrast to CCE2, negative nitrate anomalies at CCE1 only appeared halfway through the Warm Anomaly, and Chl-*a* anomalies increased from moderately negative to positive despite decreasing nitrate levels (Fig. 4.4).

The unusual high nitrate at CCE1 in spring-summer 2014 may have been due to horizontal offshore advection of nutrients from southern-origin waters. To analyze this possible source, we calculated a northern- versus southern-origin water mass index (N/S index), which scales the temperature-salinity properties of a given water mass from -1 (Northern California) to +1 (southern Baja California). At CCE1 at 40 m the N/S index shows predominantly positive values during mid-2012 and 2013-2014, suggesting enhanced subtropical water mass delivery as a source of nitrate (Fig. 4.5a-b). We also computed 30-day backtracked surface water trajectories for particles arriving at CCE1, to further determine the origins of positive N/S index values. Trajectories show that water parcels arriving at CCE1 in mid-2012 and spring 2014 originated predominantly from the nearshore region (black dots in figure 4.5; see Fig. S4.1 for particle tracks separated by year). Particle tracks in mid-2012 show nearshore origins off central

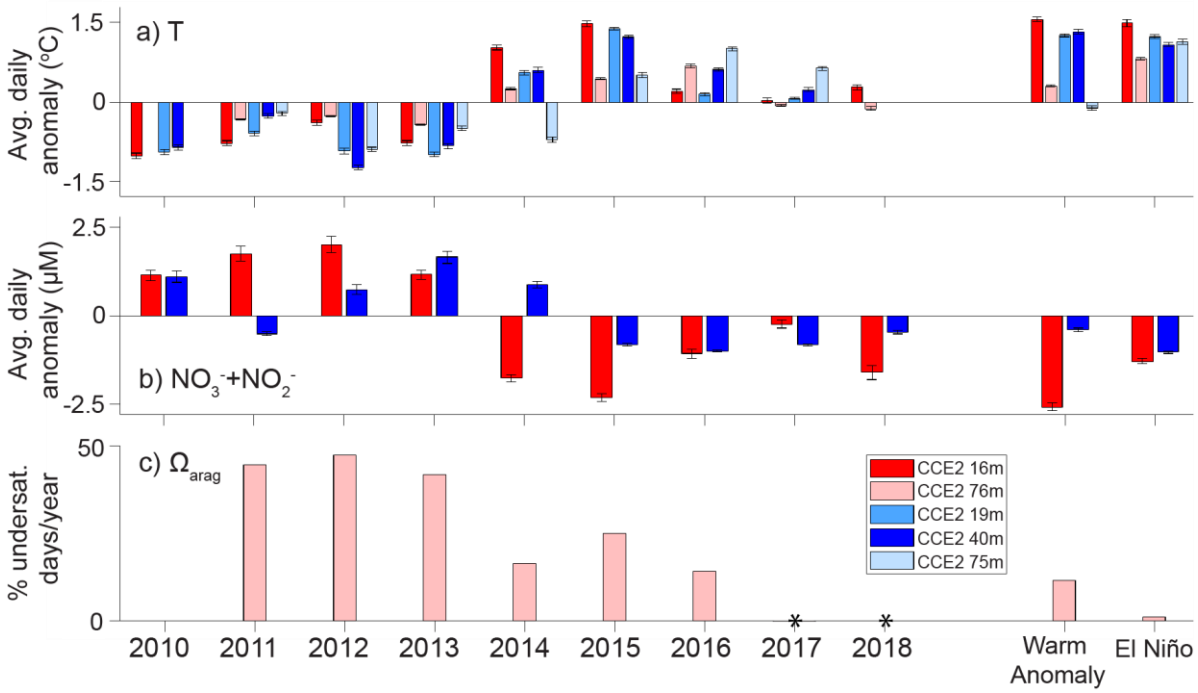

Figure 4.3. Average daily anomalies for a) temperature and b) nitrate+nitrite, both at several depths at CCE1 and CCE2. c) Percent of aragonite undersaturation days per year at CCE2 at 76 m. Average daily anomalies and percentages are calculated for each yearlong period (1 January-31 December) and the Warm Anomaly and El Niño (see Appendix 4C for anomaly start and end dates). Error bars are standard error. Legend in panel c refers to all panels. *symbols in panel c indicate years of insufficient data for calculations.

California (Fig. 4.5c, purple lines; Fig. S4.1 yellow-green lines), suggesting upwelled waters were transported to CCE1 by an offshore-moving filament that also increased nitrate and salinity at CCE2. In contrast, CCE1 tracks in winter 2013-14 appeared to originate from southern waters offshore of the dotted line (Fig. 4.5c; dark grey tracks indicate 2013 and yellow tracks 2014 in southern region. See Fig. S4.1 for within-year seasonal timing). Subsequent minor nitrate inputs to CCE1 in spring 2014 appeared to come from nearshore (yellow tracks and black dots in Fig. 4.5c), suggesting some cross-shore delivery to CCE1 at the beginning of the Warm Anomaly despite significantly reduced nitrate at CCE2.

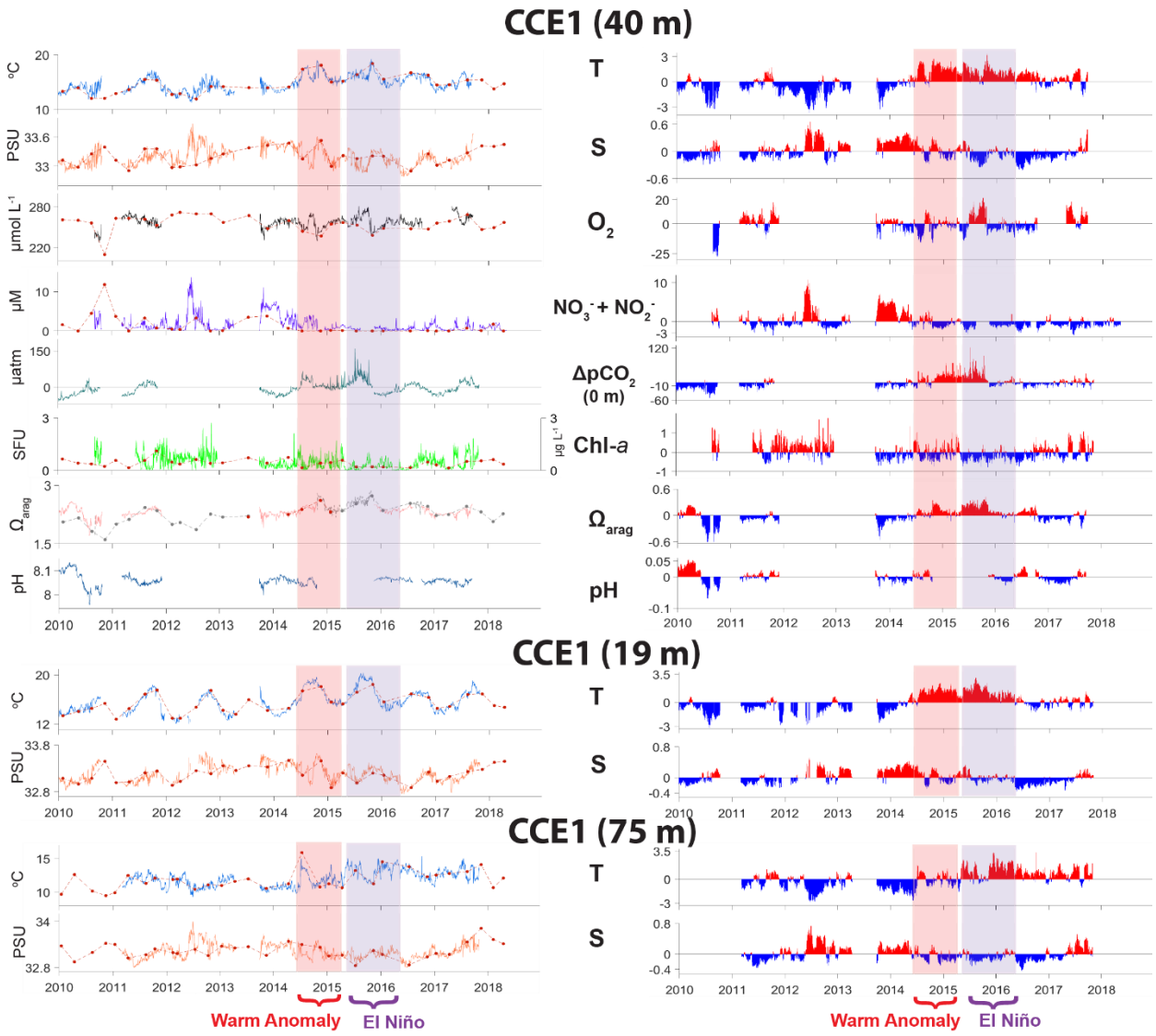

Figure 4.4. As in figure 4.2 but for CCE1 sensors at 40 m (*top row*), 19 m (*middle row*), and 75 m (*bottom row*). Only temperature and salinity are shown for 19 m and 75 m.

Shallow temperature measurements at CCE2 at 16 m (Fig. 4.2) and CCE1 at 19 m and 40 m (Fig. 4.4) indicate concurrent onset of continuous positive temperature anomalies across the region in June 2014. Our timing is consistent with satellite SST measurements by Gentemann et al. (2017), who found that anomalously warm SSTs appeared rapidly across the southern CCS region at the end of June 2014 and subsequently expanded north to connect with offshore North Pacific anomalies. Temperature measurements at CCE2 at 76 m show moderate positive

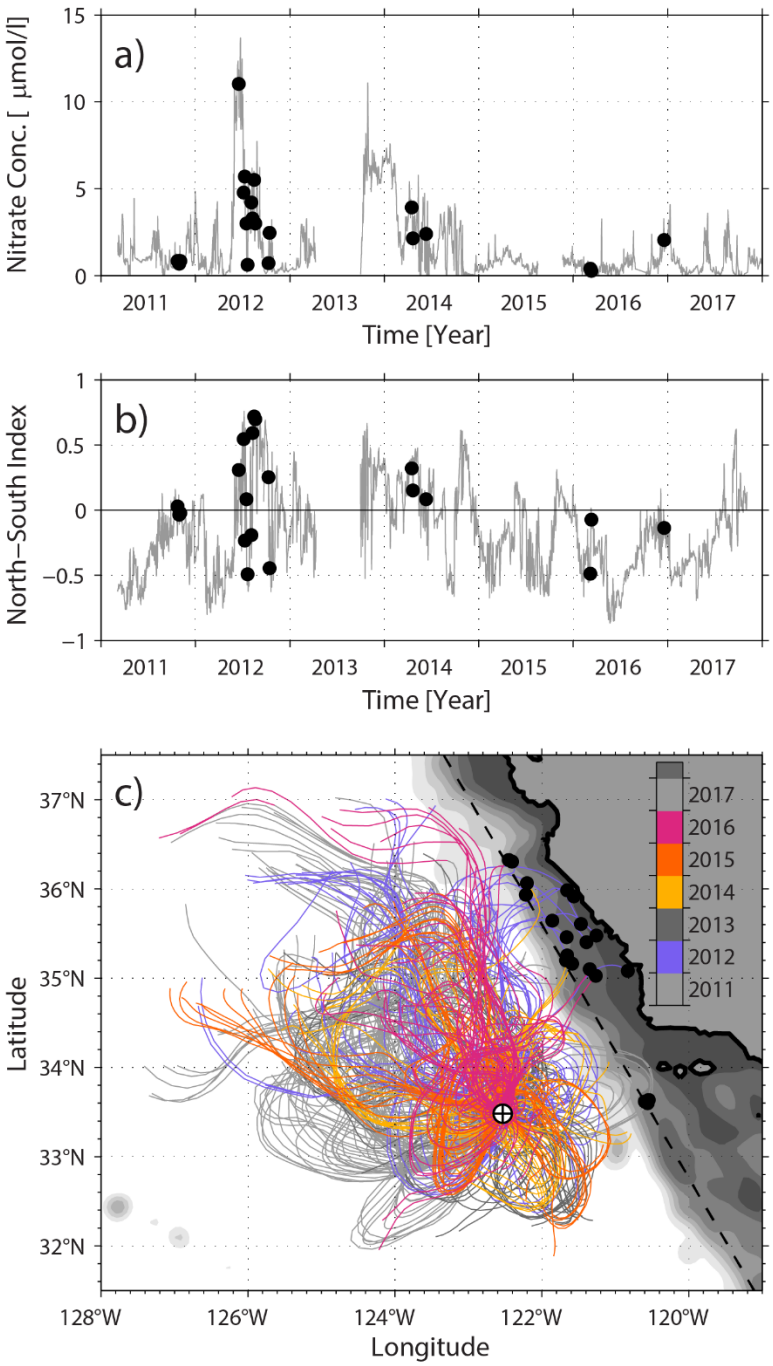

Figure 4.5. Comparison of a) nitrate at CCE1 at 40 m and b) North/South index of water mass origin for waters arriving at CCE1. Positive values indicate southern-origin waters. c) Surface particle trajectories based on altimetry-derived geostrophic velocities. The velocity fields were integrated to find trajectories that end at the CCE1 site (marked). Each trajectory is 30 days in duration (trajectories are shown for every 30-day period of each year). Trajectories with prior excursions in nearshore waters (east of the dashed line) are marked by black dots. Matching black dots in panels a) and b) show the arrival times of these nearshore trajectories to CCE1. See figure S4.1 for particle tracks by individual year.

anomalies during the Warm Anomaly but daily average anomalies only one-fourth of near-surface anomalies, while temperatures at CCE1 at 75 m show slightly negative daily average anomalies during the Warm Anomaly (Fig. 4.3a; CCE2 – red vs. light pink bars; CCE1 – pale blue bars). These findings are consistent with glider observations from Zaba and Rudnick (2016) that the Warm Anomaly was a surface-intensified (< 75 m) phenomenon across the southern CCS.

Spring 2014 showed a 14-fold increase in total pelagic mollusc abundance compared to the 2010-2013 mean. The increase was predominantly driven by unusual presence of *Hyalocylis* spp., which were comprised in 2014 predominantly of the subtropical species *Hyalocylis striata* (Fig. 4.6; L. Sala, pers. comm.). Abundance of family Limacinidae was also moderately elevated in spring 2014. These increases coincided with the onset of elevated aragonite saturation (Ω_{arag}) and pH in spring 2014, likely due to reduced upwelling of high-CO_2, low-O_2 waters (Feely et al., 2016; Feely et al., 2008; Hauri et al., 2013a; Leinweber & Gruber, 2013; McLaughlin et al., 2018). Although our N/S index was developed to assess nutrient delivery, we can also use it as an approximate indicator of advection of southern-origin plankton. As noted above, the N/S index suggests enhanced presence of southern-origin waters in winter-spring 2014. In contrast, favorable aragonite conditions only appeared in spring 2014, coincident with, rather than preceding, increased pelagic mollusc abundance. We therefore conclude that the increase in mollusc abundance in spring 2014 is due to increased advection of subtropical populations into the region rather than in situ population growth.

Offshore elevated nitrate and the marked increase in subtropical molluscs in spring 2014 suggest that the southern CCS received a significant input of southern-origin waters at the

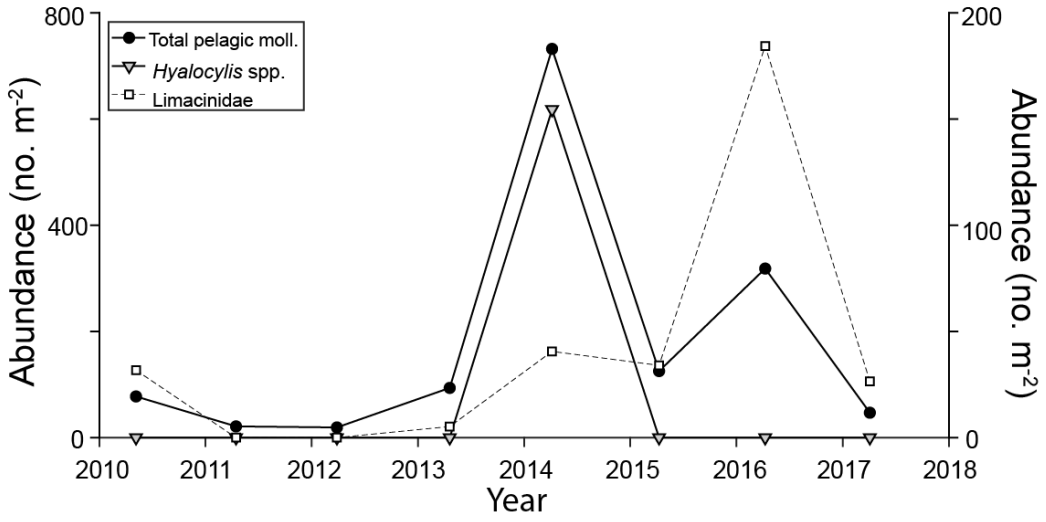

Figure 4.6. Abundance of total pelagic molluscs (solid dots and solid line), *Hyalocylis* spp. (grey triangles and solid line), and family Limacinidae (open squares and dashed line). Symbols represent spring cruise values. Total mollusc and *Hyalocylis* spp. values are shown on the left axis and family Limacinidae values are shown on the right axis.

beginning of the Warm Anomaly. Reduced nitrate at CCE2 during this period may be explained by sub-regional variations in forcing mechanisms. The nearshore region was characterized in spring 2014 by locally increased downward surface heat flux, reduced upwelling winds, high water column static stability, and anomalously deep thermocline, nutricline, and subsurface chlorophyll maximum layers (Bond et al., 2015; Zaba & Rudnick, 2016). A depressed nutricline and reduced vertical mixing would reduce nutrient delivery to surface waters despite possible continued nutrient advection at depth. We note the slightly negative nitrate and Chl-*a* anomalies at CCE2 in spring 2014 as further evidence for a moderately reduced upwelling season preceding region-wide onset of the Warm Anomaly. CCE1, located in the southward-flowing core California Current, measures an ocean environment forced predominantly by horizontal advection and some wind-stress-curl upwelling rather than wind-driven upwelling (Di Lorenzo, 2003; Rykaczewski & Checkley, 2008). Minor differences in response timing and magnitude at CCE1 and CCE2 suggest that some sub-regional nutrient delivery mechanisms acted on CCE1 at

the start of the Warm Anomaly despite region-wide onset of temperature anomalies. Offshore nutrient delivery to CCE1 apparently decreased or reversed partway through the Warm Anomaly, however, as indicated by near-zero nitrate levels. These findings are consistent with observations by Zaba and Rudnick (2016) of onset of downwelling-related onshore flow in 2014-15.

4.3.2. Spring 2015 interlude and 2015-16 El Niño impacts

High nitrate and pCO_2 pulses, increased Chl-*a*, and anomalously cool temperatures at CCE2 were observed from March-June 2015, suggesting that a moderate nearshore upwelling season occurred between the Warm Anomaly and the start of El Niño (Fig. 4.2). Offshore CCE1 temperature anomalies also decreased in spring 2015 but immediately returned to Warm Anomaly levels in summer 2015. Our findings of a direct transition from Warm Anomaly to El Niño temperature conditions offshore are consistent with other studies in the southern CCS and coastal Baja California regions, and again highlight sub-regional differences in event forcing mechanisms (Gentemann et al., 2017; Robinson, 2016).

CCE2 temperature anomalies increased in fall 2015 and produced El Niño daily average values comparable to the Warm Anomaly (Fig. 4.3a, red bars). Nitrate levels at CCE2 decreased in summer 2015 and remained low through the duration of El Niño, although daily average nitrate anomalies were smaller than during the Warm Anomaly (Fig. 4.3b, red bars). We do not have CCE2 Chl-*a* data during El Niño, but quarterly CalCOFI measurements indicate that Chl-*a* remained low from summer 2015-fall 2016 despite moderate nitrate inputs in spring 2016. Sustained negative nitrate and Chl-*a* anomalies at CCE1 only occurred during El Niño, and daily average nitrate anomalies were greater than during the Warm Anomaly (Fig. 4.3b, blue bars).

Persistent low nitrate at CCE1 throughout El Niño is consistent with particle trajectories indicating water mass origins in 2015-16 predominantly in the surrounding and offshore regions that had likely already undergone nutrient drawdown (Fig. 4.5c, orange and magenta tracks).

Deeper (75-76 m) temperature anomalies at both moorings were comparable to near-surface values during El Niño, and daily average anomalies were 2-5 times greater than during the Warm Anomaly (Fig. 4.3a, light pink and light blue bars). El Niño onset in the CCS was attributed partly to coastally trapped waves from the equatorial Pacific (Frischknecht et al., 2017), which may explain anomalous deep temperatures. However, thermocline depth and upwelling winds were anomalously shallow and strong, respectively, in fall-winter 2015-16, more in line with normal CCS upwelling conditions than with past El Niños or the Warm Anomaly (Gentemann et al., 2017; Jacox et al., 2016). Shorter duration and smaller negative daily average nitrate anomalies at CCE2 during El Niño compared to the Warm Anomaly likely reflect this moderate upwelling response in fall-winter 2015-16. Decreases in deep temperatures and aragonite saturation state in May 2016 indicate the abrupt end of the El Niño event, likely due to the appearance of moderate spring upwelling. However, Jacox et al. (2016) predicted that chlorophyll levels off central and southern California would remain low in spring 2016 due to the combined low-nutrient Warm Anomaly-El Niño period. Persistent low Chl-*a* at CCE2 in spring 2016 despite moderate nitrate inputs support this prediction and could reflect phytoplankton community changes or enhanced grazer control.

Total pelagic mollusc abundance declined slightly in spring 2015 relative to 2014 and 2016 but was still higher than other years. Population declines in 2015 may have occurred in response to aragonite undersaturation at CCE2 at 76 m (Fig. 4.2; timeseries dips below horizonal grey line at $\Omega = 1$) or to cessation of anomalous advection. As noted above, our N/S index

indicates northern- and within-region flows to CCE1 throughout 2015, suggesting lower subtropical influxes than in spring 2014 (Fig. 4.5c). Elevated total mollusc abundance in 2015 above non-anomalous springs (2011-2013, 2017) may indicate continued population persistence following 2014, particularly of family Limacinidae. This persistence was likely due to continued moderate in situ reproduction and individual growth. However, the spring 2015 decrease in abundance compared to 2014 and 2016 suggests that a period of separation occurred between the increases in springs 2014 and 2016. Total pelagic mollusc and Limacinidae abundances were again elevated in March-April 2016 (5 and 15 times higher, respectively, than their 2010-13 means) toward the end of the El Niño event, although the subtropical species (*H. striata*) that dominated in spring 2014 was absent. The N/S index and particle tracks suggest lower southern-origin flow in winter-spring 2016 than in 2014, while aragonite saturation conditions remained favorable ($\Omega_{arag} > 1$). We therefore posit that increased mollusc abundances in spring 2016 were due to in situ growth of existing populations (either resident or seeded from the south in 2014) in response to elevated aragonite levels rather than to advection of new populations. Our spring 2016 samples likely captured the height of pelagic mollusc population growth before the return of moderate upwelling conditions and decreased aragonite levels in late spring 2016.

Bednaršek et al. (2018) showed negative pteropod responses in the northern CCS to the 2013-16 combined marine heat wave, El Niño, and enhanced upwelling. Aguilera et al. (2019) similarly observed reductions in growth and egg production in the resident copepod *Acartia tonsa* in the Humboldt Current System under warm, acidic conditions in 2015. Our finding of increased pelagic molluscs in the southern CCS in springs 2014 and 2016 may be explained by several factors. First, subtropical pelagic molluscs were likely advected into the region in spring 2014 and would have contributed to the sudden population increase even if existing cooler-water

species were thermally stressed. Subtropical species likely benefitted from warmer temperature conditions of the Warm Anomaly and El Niño, and may have grown in situ beyond their initial advection, further offsetting decreases in cool-water species. Second, while the southern CCS experienced extreme positive temperature anomalies during 2014-16, Ω_{arag}, pH, and oxygen were all elevated, producing calcifying-favorable conditions that perhaps ameliorated temperature stress. The longest periods of consecutive aragonite undersaturation in our records during the Warm Anomaly and El Niño were significantly shorter than in 2011-2013 (see table 4B1 for values). Bednaršek et al. (2018) note that altered carbonate conditions have a dominant effect on pelagic mollusc health at the cellular level. The favorable carbonate conditions we observed likely provided some offset to thermal stress in 2014 and 2016, while moderate upwelling in spring 2015 produced less favorable carbonate conditions and may have negatively impacted organisms despite cooler temperatures and increased food availability. Third, Bednaršek et al. (2016) note that euthecosome pteropods are omnivores, and many species feed using mucous nets. These feeding strategies may have allowed some molluscs to increase despite overall reduced primary production and smaller phytoplankton sizes during the Warm Anomaly and El Niño, perhaps also offsetting negative effects of thermal stress. Aguilera et al. (2019) observed that *A. tonsa* maintained normal body size despite unfavorable habitat conditions during both the 2015 warm period and general upwelling conditions. The authors attribute this to elevated phytoplankton prey, suggesting food availability may partially offset negative physical oceanographic conditions. Both Bednaršek et al. (2018) and our current study suggest that pelagic mollusc responses vary depending on specific combinations of favorable and unfavorable habitat changes. Subtropical-associated species appear to benefit from El Niño-induced combinations of increased northward advection and in situ elevated aragonite saturation in the

southern CCS, conditions which allow them to temporarily expand their population ranges. Future El Niño-like perturbations therefore need to be evaluated for comprehensive changes in advection, temperature, aragonite, and food availability, in order to predict full effects on pelagic molluscs.

4.3.3. Comparison of 2014-16 Warm Anomaly-El Niño period to 2009-10 El Niño

Our CCE2 timeseries measured the second half of the 2009-10 El Niño, an event of known anomalous forcing in the CCS (Todd et al., 2011) which produced atypical zooplankton community changes relative to other El Niños (Lilly & Ohman, 2018). The 2009-10 El Niño was characterized by direct atmospheric teleconnections from the tropical Pacific to the CCS, with resulting changes in local wind circulation and a lack of oceanic coastally trapped wave propagation (Todd et al., 2011). Nitrate and ΔpCO_2 at CCE2 were elevated in 2010 compared to the 2014-16 period, although lower than 2011-2013, a period encompassing a moderate La Niña and productive CCS conditions (Bjorkstedt et al., 2012; Wells et al., 2013). However, Chl-*a* at CCE2 was anomalously low in 2010, comparable to post-El Niño levels in spring 2016. We have minimal nitrate, ΔpCO_2, and Chl-*a* data at CCE1 from 2010, but CalCOFI measurements suggest that all three variables were slightly elevated in winter-spring 2010 compared to the 2015-16 El Niño, indicating a more minimal offshore impact of the 2009-10 El Niño. Biomass of pelagic molluscs, notably the pteropod family Limacinidae, was also moderately elevated in spring 2010 in conjunction with positive Ω_{arag} anomalies at CCE1 and CCE2. Although the 2009-10 El Niño impacts in the CCS have been attributed to atmospherically-forced local physical changes rather than direct oceanic propagation, the perturbation still produced low Chl-*a* and favorable calcifying conditions at both moorings.

4.4. Conclusions

Temperature data suggest that the 2014-15 Pacific Warm Anomaly developed rapidly region-wide in the southern CCS in spring 2014, although nutrient delivery appeared to show sub-regional differences between offshore and nearshore regions. Coastal waters experienced rapid and sustained onset of upwelling suppression, with likely negative consequences for primary production. Our observations of surface-intensified temperature anomalies during the Warm Anomaly confirm other evidence for a combination of thermocline depression, increased stratification, and reduced wind stress as a cause of reduced upwelling (Zaba & Rudnick, 2016). In contrast, from the outset the 2015-16 El Niño was expressed in subsurface (75 m) as well as surface waters. Offshore nutrient anomalies were much more pronounced during El Niño than during the Warm Anomaly. Neither the Warm Anomaly nor El Niño individually, nor their multi-year combination, appeared to have residual negative impacts on chlorophyll concentration, as evidenced by moderately elevated nitrate and Chl-*a* in 2017-18.

The elevated abundance of pelagic molluscs during both the Warm Anomaly and El Niño suggests that some organisms may have benefited from these anomalous conditions. While increased subtropical pelagic mollusc abundances in spring 2014 were likely due partly to increased northward advection of subtropical species, recurrences in spring 2016 appeared more attributable to in situ growth. Aragonite undersaturation events in the CCS are expected to increase spatially and temporally in the future due to the ocean's absorption of anthropogenic CO_2 (Feely et al., 2016; Feely et al., 2008; Hauri et al., 2013a). More frequent and longer-duration aragonite undersaturation events can have significant negative impacts on calcifying organisms, including reduced growth, shell dissolution, and decreased survival (Bednaršek et al.,

2014; Osborne et al., 2016). However, El Niño events are also predicted to become more extreme in future decades (Cai et al., 2014; Lee & McPhaden, 2010), and such events might create short-term suitable habitat for subtropical calcifiers to increase. We note that northward displacements of subtropical species may temporarily reduce their abundances in their original habitats, but we do not presently know what impacts such biogeographic shifts may have on the original community. Continued high-frequency biogeochemical measurements should be combined with species-level analysis of pelagic mollusc communities to develop a framework for predicting how zooplankton populations in Eastern Boundary Upwelling Systems will vary both short- and long-term in response to ocean changes.

Appendix 4A. Nitrate and Chl-*a* fluorescence sensor calibrations and quality control

Nitrate quality control steps are as follows: First, the raw SUNA data are plotted and a smooth zero baseline is drawn along the lower edge of the timeseries and subtracted from the raw data to obtain baseline-corrected data. This baseline is often nonlinear and non-monotonic and removes sensor drift and zero offset. Second, the baseline-corrected timeseries is compared to in situ nitrate measurements (pre- and post-mooring deployment calibration casts and quarterly CalCOFI nitrate measurements) to check sensor accuracy. Additional baseline offset is applied as needed to match the sensor timeseries to calibration measurements.

Three mooring deployments (CCE1: Sep 2012-May 2013; CCE2: Apr 2015-May 2016, May 2016-Mar 2017) had SUNA sensor failure, so those timeseries were reconstructed using a temperature-nitrate proxy. Temperature and nitrate have an inverse sigmoidal relationship that can be reconstructed using a locally-weighted scatterplot smoothing (LOWESS) non-parametric regression with f=0.1 (where the f parameter balances regression smoothness versus accuracy; see Fig. 4A1a-b). The LOWESS regression equation can then be applied to the mooring temperature timeseries to reconstruct nitrate for the deployment period. To confirm the accuracy of this method, we calculated temperature-reconstructed nitrate timeseries for the entire duration of each mooring and compared those timeseries to corresponding CalCOFI nitrate values and measured nitrate from bottle samples obtained during mooring deployment or recovery (see Fig. 4A1c-d for CCE2 reconstruction; bottle samples not shown; rho = 0.77, $p < 0.01$).

Chlorophyll-*a* fluorescence data undergo a three-step quality control process to calculate Standardized Fluorescence Units (SFU; *cf.* Powell and Ohman (2015)). First, a baseline correction is applied to the raw data as described for nitrate. Second, pre- and post-deployment laboratory calibrations are used to calculate the average slope between fluorometer readings and

known fluorescence values of laboratory-prepared chlorophyll-*a* standards. Laboratory calibrations consist of the following steps: 1) Two sets of chlorophyll-*a* standards are prepared: 12 standards from pure chlorophyll-*a* extracted from *Anacystis nidulans* algae (Sigma-Aldrich C6144) in 90% acetone, in concentrations ranging from 0.0001-0.5 µg/L chlorophyll, and five standards from seawater collected one hour before dawn and diluted to: 100%, 50%, 25%, 12.5%, and 0% raw seawater, with filtered seawater filling the remaining percentage. 2) For each concentration, three replicate fluorometer voltage readings are taken and averaged to get final voltage. The third step involves aligning the timeseries of voltage reading and measured chlorophyll values by scaling them on separate y-axes and then calculating the ratio of max measured Chl-a/max voltage. The daily-averaged voltage timeseries is then multiplied by this ratio to get the SFU timeseries.

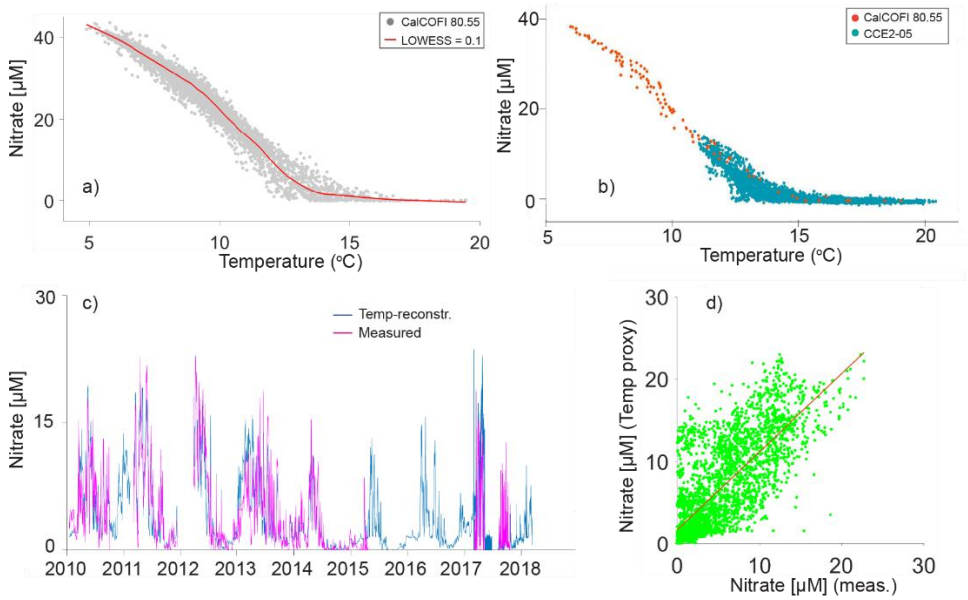

Figure 4.A1. Temperature reconstruction of nitrate. a) Temperature-nitrate relationship for all CalCOFI data collected at CCE2 (Stn. 80.55, 1951-2016), shown as grey dots. Red line is the LOWESS relationship for f=0.1. b) Temperature-nitrate relationship for CCE2-05 deployment data (turquoise dots) and corresponding CalCOFI data at Stn. 80.55 during the same time period (orange dots). c) Timeseries comparison of CCE2 sensor-measured nitrate (pink line) versus temperature-reconstructed nitrate (blue line) for the entire CCE2 mooring timeseries. d) Measured versus temperature-reconstructed nitrate from the data in c (rho = 0.77, $p < 0.01$).

Appendix 4B. Aragonite saturation calculations

We used two methods to calculate aragonite saturation at CCE2 16 m and CCE1 40 m (Method 1: pH-/total alkalinity-derived; Method 2: temperature-O_2 proxy relationship. See Section 4.2.4 in main text for full explanation of calculations). We correlated the timeseries for both methods at CCE2 16 m to determine how closely their estimations matched. The correlation was significant ($rho = 0.90$, $p < 0.01$; not shown), indicating that the two methods produced comparable estimations.

Appendix 4C. Temperature anomaly start/end dates

We determined start and end dates of the Warm Anomaly and El Niño based on periods of continuous positive temperature anomalies with no negative interruptions at the near-surface sensors (CCE1 at 19 m, CCE2 at 16 m; Appendix 4C). The one exception was the CCE1 Warm Anomaly start date, for which we used the CCE1 40 m data. A large positive temperature anomaly occurred at CCE1 at 40 m in June 2014 and was of the same magnitude as subsequent temperature anomalies, so we included that period in the scope of the Warm Anomaly, although we based all other CCE1 dates on the 19 m timeseries. Although moderate positive temperature and negative nitrate and Chl-*a* anomalies occurred intermittently at both moorings in spring 2014, we demarcated 15 Jun 2014 as the start of the 2014-15 Warm Anomaly because that date was the beginning of continuous positive temperature anomalies that lasted through February 2015, and because the temperature anomalies that appeared in June 2014 were significantly greater than temperature anomalies in spring 2014. The mean temperature anomaly at CCE2 during our 2014-15 Warm Anomaly period was 1.57^{o}C, compared to anomalies of < 1.1^{o}C in spring 2014 with only one ten-day period of 1.4^{o}C. The mean Warm Anomaly temperature at CCE1 40 m was 1.44^{o}C, while anomalies in spring 2014 never rose above 0.6^{o}C. The CCE1 timeseries at 19 m never reached negative anomalies between the start of the Warm Anomaly in 2014 and the end of El Niño in 2016. Instead, we used a threshold of anomalies < +1^{o} C in spring 2015 to demarcate the end of the Warm Anomaly and beginning of El Niño, respectively.

We demarcated the Warm Anomaly start date as 15 Jun 2014 at both CCE2 and CCE1, and the end dates as 11 May 2015 at CCE2 and 6 Apr 2015 at CCE1. We demarcated the El Niño start dates as 20 Jul 2015 at CCE2 and 16 May 2015 at CCE1, and the end dates as 27 Mar 2016 at CCE2 and 11 May 2016 at CCE1.

Appendix 4D. Validity of altimetry-derived particle trajectories

To assess how well the altimetry-derived particle trajectories represent reality, we compared altimetry to in situ velocity data from the CCE1 mooring as follows: for most of 2011-2016, the buoy was equipped with a downward-facing ADCP; we integrated ADCP velocities at 30 m depth forward in time for 45 overlapping time windows of 50 days each. This yielded 45 synthetic "trajectories" or progressive vector diagrams (PVDs). If ocean velocities were the same at all locations at any given time, these would be identical to actual particle trajectories. The altimetry-derived surface velocities at the CCE1 location were integrated in an identical fashion. Figure 4D1a shows five comparisons of buoy-derived (solid lines) and altimetry-derived (dashed lines) PVDs. The discrepancies between each pair, and their evolutions over time, are shown in figure 4D1b. The distance from the CCE1 buoy to the nearshore continental rise is approximately 160 km. Figure 4D1b includes the 75^{th} percentile for the ensemble (black line), which reaches 160 km after approximately 30 days of forward integration. We thus posit that the first 30 days of the majority of simulated trajectories will have an associated error less than the distance between the buoy and the nutrient-rich source region discussed in Section 4.3.1. We used this 30-day duration as the cutoff for our confidence in the altimetry-derived trajectories.

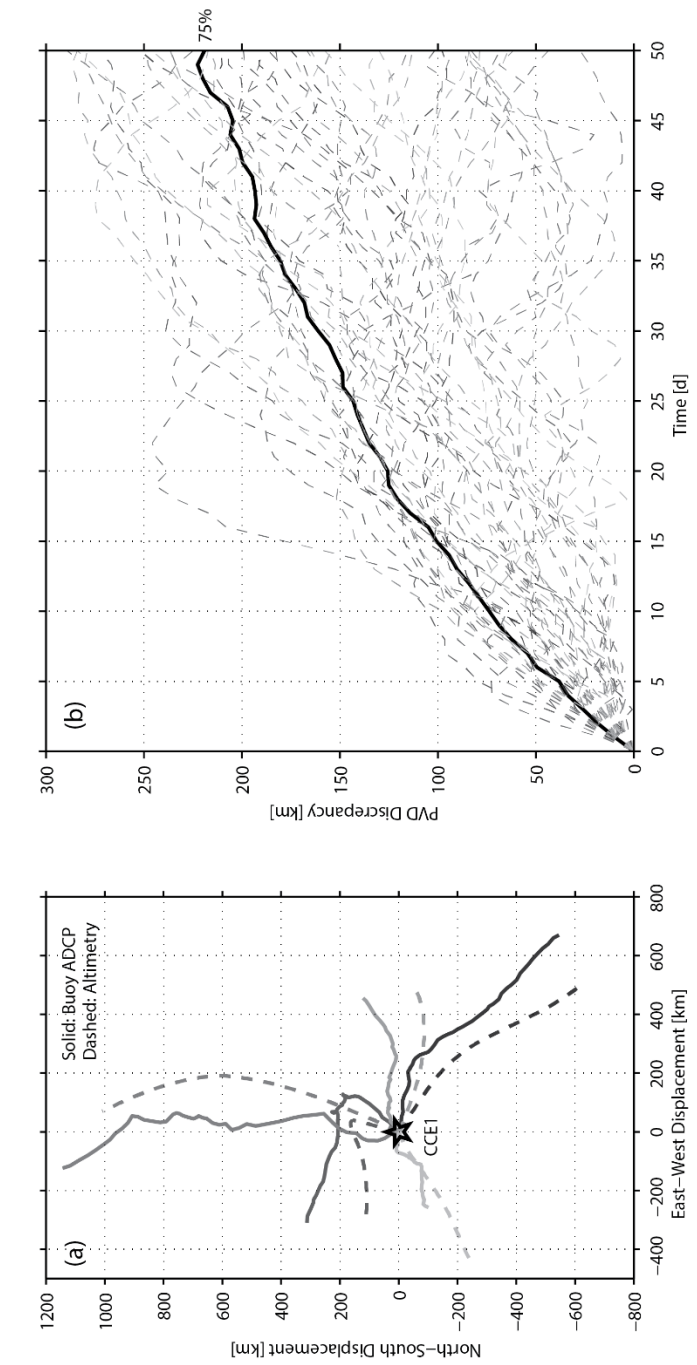

Figure 4.D1. A) Selection of 5 (out of 45) progressive vector diagrams computed by integrating observed in situ velocities from an ADCP (solid lines) and altimetry-derived velocities (dashed lines) at the CCE1 location forward for 30 days. b) Discrepancies between each pair of ADCP-altimetry simulations. Thick black line shows 75th percentile.

Table 4.B1. Aragonite undersaturation day-counts and durations at CCE2 (76 m depth)

Year	No. days Ω < 1 (raw)	Consecutive days (events > 1 day)	Days of data	No. days Ω < 1 (normalized to year-days)
2010	---	---	0	---
2011	119	6, 5, 20, 4, 21, 4, 30, 2, 8, 8, 4, 2, 3	267	0.446
2012	133	6, 12, 2, 13, 5, 37, 21, 28, 5, 3	282	0.472
2013	150	5, 38, 8, 27, 19, 2, 3, 9, 9, 6, 3, 4, 5, 4, 4	361	0.416
2014	52	3, 2, 4, 13, 15, 4, 8	317	0.164
2015	62	16, 42, 3	248	0.250
2016	19	14, 2, 2	134	0.142
2017	1	---	134	0.008
2018	0	---	73	0
Warm Anomaly	20	3, 4, 8, 4	173	0.116
El Niño	3	3	251	0.012

Acknowledgments, Samples, and Data

We thank all contributors to the CCE moorings program, particularly the engineers and technicians in the Send and Martz Labs, C.L. Sabine (University of Hawaii), and the captains and crews of the ships used to deploy the moorings. We thank C. Lowcher, J. Sevadjian, and T. Wirth for data processing and quality control, L. Sala and past managers of the Pelagic Invertebrate Collection for enumerations of CalCOFI zooplankton samples and discussion about mollusc population changes, and P. Franks for discussion. This work was supported by the NOAA Ocean Observing and Monitoring Division and Ocean Acidification Program (NA15OAR4320071), NSF OCE-1614359 and OCE-1637632 to the CCE-LTER site, an NSF Graduate Research Fellowship to L. Lilly, and in-kind support from NOAA NMFS and SWFSC. R. Feely and A. Sutton were supported by the Office of Oceanic and Atmospheric Research of NOAA, US Department of Commerce, including resources from the Ocean Observing and Monitoring Division of the Climate Program Office (fund reference number 100007298) and the Ocean Acidification Program. This is PMEL contribution #4962. CCE moorings are part of the international OceanSITES program. Quality controlled data are available at: ftp://data.ndbc.noaa.gov/data/oceansites/DATA/CCE1/ and ftp://data.ndbc.noaa.gov/data/oceansites/DATA/CCE2/. Surface ocean pCO_2 data are available at https://www.nodc.noaa.gov/ocads/oceans/time_series_moorings.html. The altimetry data study has been conducted using E.U. Copernicus Marine Service Information. The authors declare no competing interests.

Chapter 4, in full, is a reprint of the material as it appears in Journal of Geophysical Research: Oceans, 2019. Lilly, Laura E.; Send, Uwe; Lankhorst, Matthias; Martz, Todd R.;

Feely, Richard A.; Sutton, Adrienne J.; Ohman, Mark D. The dissertation author was the primary investigator and author of this paper.

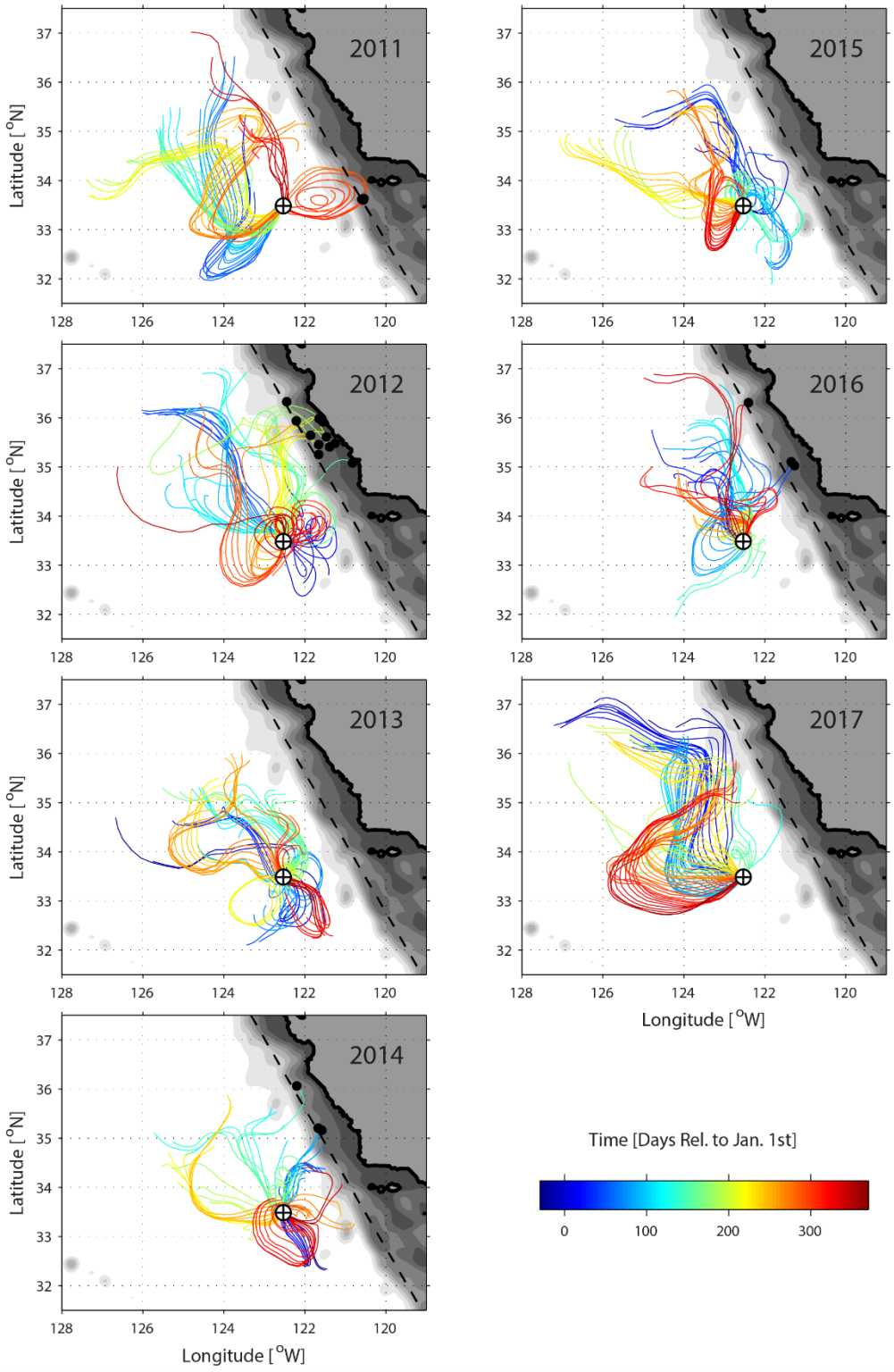

Figure S4.1. As in figure 4.5c, but with particle tracks separated by individual year. Color scale indicates day numbers within each year.

References

Aguilera, V. M., Escribano, R., Vargas, C. A. & González, M. T. (2019). Upwelling modulation of functional traits of a dominant planktonic grazer during "warm-acid" El Niño 2015 in a year-round upwelling area of Humboldt Current. *Plos One, 14*(1). doi:e0209823

Alin, S. R., Feely, R. A., Dickson, A. G., Hernandez-Ayon, J. M., Juranek, L. W., Ohman, M. D. & Goericke, R. (2012). Robust empirical relationships for estimating the carbonate system in the southern California Current System and application to CalCOFI hydrographic cruise data (2005-2011). *Journal of Geophysical Research-Oceans, 117*. doi:Artn C0503310.1029/2011jc007511

Bednaršek, N., Feely, R. A., Beck, M. W., Glippa, O., Kanerva, M. & Engstrom-Ost, J. (2018). El Nino-Related Thermal Stress Coupled With Upwelling-Related Ocean Acidification Negatively Impacts Cellular to Population-Level Responses in Pteropods Along the California Current System With Implications for Increased Bioenergetic Costs. *Frontiers in Marine Science, 5*. doi:UNSP 48610.3389/fmars.2018.00486

Bednaršek, N., Feely, R. A., Reum, J. C. P., Peterson, B., Menkel, J., Alin, S. R. & Hales, B. (2014). Limacina helicina shell dissolution as an indicator of declining habitat suitability owing to ocean acidification in the California Current Ecosystem. *Proc. R. Soc. B, 281*(1785), 20140123.

Bednaršek, N., Feely, R. A., Tolimieri, N., Hermann, A. J., Siedlecki, S. A., Waldbusser, G. G., et al. (2017). Exposure history determines pteropod vulnerability to ocean acidification along the US West Coast. *Scientific Reports, 7*. doi:ARTN 452610.1038/s41598-017-03934-z

Bednaršek, N., Harvey, C. J., Kaplan, I. C., Feely, R. A. & Mozina, J. (2016). Pteropods on the edge: Cumulative effects of ocean acidification, warming, and deoxygenation. *Progress in Oceanography, 145*, 1-24. doi:10.1016/j.pocean.2016.04.002

Bjorkstedt, E. P., Bograd, S. J., Sydeman, W. J., Thompson, S. A., Goericke, R., Durazo, R., et al. (2012). State of the California Current 2011-2012: Ecosystems respond to local forcing as La Niña wavers and wanes. *Reports of California Cooperative Oceanic Fisheries Investigations, 53*, 41-76.

Bograd, S. J., Checkley, D. A. & Wooster, W. S. (2003). CalCOFI: a half century of physical, chemical, and biological research in the California Current System. *Deep-Sea Research Part Ii-Topical Studies in Oceanography, 50*(14-16), 2349-2353. doi:10.1016/S0967-0645(03)00122-X

Bond, N. A., Cronin, M. F., Freeland, H. & Mantua, N. (2015). Causes and impacts of the 2014 warm anomaly in the NE Pacific. *Geophysical Research Letters, 42*(9), 3414-3420. doi:10.1002/2015gl063306

Bresnahan, P. J., Jr., Martz, T. R., Takeshita, Y., Johnson, K. S. & LaShomb, M. (2014). Best practices for autonomous measurement of seawater pH with the Honeywell Durafet. *Methods in Oceanography, 9*, 44-60.

Cai, W. J., Borlace, S., Lengaigne, M., van Rensch, P., Collins, M., Vecchi, G., et al. (2014). Increasing frequency of extreme El Nino events due to greenhouse warming. *Nature Climate Change, 4*(2), 111-116. doi:10.1038/Nclimate2100

Carr, M. E. & Kearns, E. J. (2003). Production regimes in four Eastern Boundary Current systems. *Deep-Sea Research Part Ii-Topical Studies in Oceanography, 50*(22-26), 3199-3221. doi:10.1016/j.dsr2.2003.07.015

Chao, Y., Farrara, J. D., Bjorkstedt, E., Chai, F., Chavez, F., Rudnick, D. L., et al. (2017). The origins of the anomalous warming in the California coastal ocean and San Francisco Bay during 2014-2016. *Journal of Geophysical Research-Oceans, 122*(9), 7537-7557. doi:10.1002/2017jc013120

Chavez, F. P. (1996). Forcing and biological impact of onset of the 1992 El Niño in central California. *Geophysical Research Letters, 23*(3), 265-268.

Chavez, F. P., Pennington, J. T., Castro, C. G., Ryan, J. P., Michisaki, R. P., Schlining, B., et al. (2002). Biological and chemical consequences of the 1997-1998 El Nino in central California waters. *Progress in Oceanography, 54*(1-4), 205-232. doi:Pii S0079-6611(02)00050-2Doi 10.1016/S0079-6611(02)00050-2

Chavez, F. P., Pennington, J. T., Herlien, R., Jannasch, H., Thurmond, G. & Friederich, G. E. (1997). Moorings and drifters for real-time interdisciplinary oceanography. *Journal of Atmospheric and Oceanic Technology, 14*(5), 1199-1211.

Chelton, D. B. (1982). Large-scale response of the California Current to forcing by the wind stress curl. *CalCOFI Rep., 23*, 30-148.

Chelton, D. B., Bernal, P. A. & Mcgowan, J. A. (1982). Large-Scale Interannual Physical and Biological Interaction in the California Current. *Journal of Marine Research, 40*(4), 1095-1125.

Cushing, D. H. (1971). Upwelling and Production on Fish. *Advances in Marine Biology, 9*, 255-&. doi:Doi 10.1016/S0065-2881(08)60344-2

Di Lorenzo, E. (2003). Seasonal dynamics of the surface circulation in the Southern California Current System. *Deep Sea Research Part II: Topical Studies in Oceanography, 50*(14-16), 2371-2388.

Di Lorenzo, E. & Mantua, N. (2016). Multi-year persistence of the 2014/15 North Pacific marine heatwave. *Nature Climate Change, 6*(11), 1042-1047.

Di Lorenzo, E., Schneider, N., Cobb, K. M., Franks, P. J. S., Chhak, K., Miller, A. J., et al. (2008). North Pacific Gyre Oscillation links ocean climate and ecosystem change. *Geophysical Research Letters, 35*(8).

Feely, R. A., Alin, S. R., Carter, B., Bednarsek, N., Hales, B., Chan, F., et al. (2016). Chemical and biological impacts of ocean acidification along the west coast of North America. *Estuarine Coastal and Shelf Science, 183*, 260-270. doi:10.1016/j.ecss.2016.08.043

Feely, R. A., Okazaki, R. R., Cai, W. J., Bednarsek, N., Alin, S. R., Byrne, R. H. & Fassbender, A. (2018). The combined effects of acidification and hypoxia on pH and aragonite saturation in the coastal waters of the California current ecosystem and the northern Gulf of Mexico. *Continental Shelf Research, 152*, 50-60. doi:10.1016/j.csr.2017.11.002

Feely, R. A., Sabine, C. L., Hernandez-Ayon, J. M., Ianson, D. & Hales, B. (2008). Evidence for upwelling of corrosive "acidified" water onto the continental shelf. *Science, 320*(5882), 1490-1492. doi:10.1126/science.1155676

Fiedler, P. C. (1984). Satellite-Observations of the 1982-1983 El-Nino Along the United-States Pacific Coast. *Science, 224*(4654), 1251-1254. doi:DOI 10.1126/science.224.4654.1251

Fiedler, P. C. & Mantua, N. J. (2017). How are warm and cool years in the California Current related to ENSO? *Journal of Geophysical Research-Oceans, 122*(7), 5936-5951. doi:10.1002/2017jc013094

Fisher, J. L., Peterson, W. T. & Rykaczewski, R. R. (2015). The impact of El Niño events on the pelagic food chain in the northern California Current. *Global Change Biology, 21*(12), 4401-4414.

Flament, P. (2002). A state variable for characterizing water masses and their diffusive stability: spiciness. *Progress in Oceanography, 54*(1-4), 493-501. doi:Pii S0079-6611(02)00065-4 Doi 10.1016/S0079-6611(02)00065-4

Frischknecht, M., Munnich, M. & Gruber, N. (2017). Local atmospheric forcing driving an unexpected California Current System response during the 2015-2016 El Nino. *Geophysical Research Letters, 44*(1), 304-311. doi:10.1002/2016gl071316

Frischknecht, M., Münnich, M. & Gruber, N. (2018). Origin, transformation, and fate: The three-dimensional biological pump in the California Current System. *Journal of Geophysical Research: Oceans, 123*. doi:10.1029/2018JC013934

Gentemann, C. L., Fewings, M. R. & Garcia-Reyes, M. (2017). Satellite sea surface temperatures along the West Coast of the United States during the 2014-2016 northeast Pacific marine heat wave. *Geophysical Research Letters, 44*(1), 312-319. doi:10.1002/2016gl071039

Gruber, N., Hauri, C., Lachkar, Z., Loher, D., Frolicher, T. L. & Plattner, G. K. (2012). Rapid Progression of Ocean Acidification in the California Current System. *Science, 337*(6091), 220-223. doi:10.1126/science.1216773

Hartman, S. E., Larkin, K. E., Lampitt, R. S., Lankhorst, M. & Hydes, D. J. (2010). Seasonal and inter-annual biogeochemical variations in the Porcupine Abyssal Plain 2003-2005 associated with winter mixing and surface circulation. *Deep-Sea Research Part Ii-Topical Studies in Oceanography, 57*(15), 1303-1312. doi:10.1016/j.dsr2.2010.01.007

Hauri, C., Gruber, N., McDonnell, A. M. P. & Vogt, M. (2013a). The intensity, duration, and severity of low aragonite saturation state events on the California continental shelf. *Geophysical Research Letters, 40*(13), 3424-3428. doi:10.1002/grl.50618

Hauri, C., Gruber, N., Vogt, M., Doney, S. C., Feely, R. A., Lachkar, Z., et al. (2013b). Spatiotemporal variability and long-term trends of ocean acidification in the California Current System. *Biogeosciences, 10*(1), 193-216. doi:10.5194/bg-10-193-2013

Hu, S. N. & Fedorov, A. V. (2016). Exceptionally strong easterly wind burst stalling El Nino of 2014. *Proceedings of the National Academy of Sciences of the United States of America, 113*(8), 2005-2010. doi:10.1073/pnas.1514182113

Jacox, M. G., Hazen, E. L., Zaba, K. D., Rudnick, D. L., Edwards, C. A., Moore, A. M. & Bograd, S. J. (2016). Impacts of the 2015-2016 El Nino on the California Current System: Early assessment and comparison to past events. *Geophysical Research Letters, 43*(13), 7072-7080. doi:10.1002/2016gl069716

Janssen, A. W., Bush, S. L. & Bednaršek, N. (2019). The shelled pteropods of the northeast Pacific Ocean (Mollusca: Heterobranchia, Pteropoda). *Zoosymposia, 13*(1), 305-346.

Kahru, M. & Mitchell, B. G. (2000). Influence of the 1997-98 El Nino on the surface chlorophyll in the California Current. *Geophysical Research Letters, 27*(18), 2937-2940. doi:Doi 10.1029/2000gl011486

Keiper, C. A., Ainley, D. G., Allen, S. G. & Harvey, J. T. (2005). Marine mammal occurrence and ocean climate off central California, 1986 to 1994 and 1997 to 1999. *Marine Ecology Progress Series, 289*, 285-306. doi:DOI 10.3354/meps289285

Lavaniegos, B. E., Jimenez-Perez, L. C. & Gaxiola-Castro, G. (2002). Plankton response to El Nino 1997-1998 and La Nina 1999 in the southern region of the California Current. *Progress in Oceanography, 54*(1-4), 33-58. doi:Pii S0079-6611(02)00042-3Doi 10.1016/S0079-6611(02)00042-3

Lavaniegos, B. E. & Ohman, M. D. (2007). Coherence of long-term variations of zooplankton in two sectors of the California Current System. *Progress in Oceanography, 75*(1), 42-69.

Lee, D. E., Nur, N. & Sydeman, W. J. (2007). Climate and demography of the planktivorous Cassin's auklet Ptychoramphus aleuticus off northern California: implications for population change. *Journal of Animal Ecology, 76*(2), 337-347. doi:10.1111/j.1365-2656.2007.01198.x

Lee, T. & McPhaden, M. J. (2010). Increasing intensity of El Nino in the central-equatorial Pacific. *Geophysical Research Letters, 37*. doi:Artn L1460310.1029/2010gl044007

Leinweber, A. & Gruber, N. (2013). Variability and trends of ocean acidification in the Southern California Current System: A time series from Santa Monica Bay. *Journal of Geophysical Research-Oceans, 118*(7), 3622-3633. doi:10.1002/jgrc.20259

Li, J. Y., Liu, B. Q., Li, J. D. & Mao, J. Y. (2015). A Comparative Study on the Dominant Factors Responsible for the Weaker-than-expected El Nino Event in 2014. *Advances in Atmospheric Sciences, 32*(10), 1381-1390. doi:10.1007/s00376-015-4269-6

Lilly, L. E. & Ohman, M. D. (2018). CCE IV: El Niño-related zooplankton variability in the southern California Current System. *Deep-Sea Research Part I: Oceanographic Research Papers*.

Locarnini, R. A., Mishonov, A. V., Antonov, J. I., Boyer, T. P., Garcia, H. E., Baranova, O. K., et al. (2013). World Ocean Atlas 2013, Volume 1: Temperature. . In E. S. Levitus & T. E. A. Mishonov (Eds.), *NOAA Atlas NESDIS* (Vol. 73, pp. 40).

Lynn, R. J. & Bograd, S. J. (2002). Dynamic evolution of the 1997-1999 El Nino-La Nina cycle in the southern California Current System. *Progress in Oceanography, 54*(1-4), 59-75. doi:Pii S0079-6611(02)00043-5

Lynn, R. J. & Simpson, J. J. (1987). The California Current System - the Seasonal Variability of Its Physical Characteristics. *Journal of Geophysical Research-Oceans, 92*(C12), 12947-&. doi:DOI 10.1029/JC092iC12p12947

Mantua, N. J., Hare, S. R., Zhang, Y., Wallace, J. M. & Francis, R. C. (1997). A Pacific interdecadal climate oscillation with impacts on salmon production. *Bulletin of the American Meteorological Society, 78*(6), 1069-1079. doi:Doi 10.1175/1520-0477(1997)078<1069:Apicow>2.0.Co;2

McCabe, R. M., Hickey, B. M., Kudela, R. M., Lefebvre, K. A., Adams, N. G., Bill, B. D., et al. (2016). An unprecedented coastwide toxic algal bloom linked to anomalous ocean conditions. *Geophysical Research Letters, 43*(19). doi:10.1002/2016GL070023

McGowan, J. A. (1967). Distributional atlas of pelagic molluscs in the California Current region. *CalCOFI Atlas, 6*.

McLaughlin, K., Nezlin, N. P., Weisberg, S. B., Dickson, A. G., Booth, J. A. T., Cash, C. L., et al. (2018). Seasonal patterns in aragonite saturation state on the southern California

continental shelf. *Continental Shelf Research*. doi:https://doi.org/10.1016/j.csr.2018.07.009

Osborne, E. B., Thunell, R. C., Marshall, B. J., Holm, J. A., Tappa, E. J., Benitez-Nelson, C., et al. (2016). Calcification of the planktonic foraminifera Globigerina bulloides and carbonate ion concentration: Results from the Santa Barbara Basin. *Paleoceanography, 31*(8), 1083-1102. doi:10.1002/2016pa002933

Pennington, J. T. & Chavez, F. P. (2000). Seasonal fluctuations of temperature, salinity, nitrate, chlorophyll and primary production at station H3/M1 over 1989–1996 in Monterey Bay, California. *Deep Sea Research Part II: Topical Studies in Oceanography, 47*(5-6), 947-973.

Peterson, W. T., Fisher, J. L., Strub, P. T., Du, X., Risien, C., Peterson, J. & Shaw, C. T. (2017). The pelagic ecosystem in the Northern California Current off Oregon during the 2014–2016 warm anomalies within the context of the past 20 years. *Journal of Geophysical Research-Oceans, 122*(9), 7267-7290. doi:10.1002/2017JC012952

Peterson, W. T., Robert, M. & Bond, N. A. (2015). *The warm blob continues to dominate the ecosystem of the northern California current*. Retrieved from PICES Press Vol. 23, No. 2: https://search.proquest.com/docview/1705538895/fulltext/BD3F90E0734A43E3PQ/1?accountid=14524

Pickett, M. H. & Paduan, J. D. (2003). Ekman transport and pumping in the California Current based on the U.S. Navy's high-resolution atmospheric model (COAMPS). *Journal of Geophysical Research-Oceans, 108*(C10). doi:Artn 332710.1029/2003jc001902

Powell, J. R. & Ohman, M. D. (2015). Covariability of zooplankton gradients with glider-detected density fronts in the Southern California Current System. *Deep-Sea Research Part Ii-Topical Studies in Oceanography, 112*, 79-90. doi:10.1016/j.dsr2.2014.04.002

Rebstock, G. A. (2001). Long-term stability of species composition in calanoid copepods off southern California. *Marine Ecology Progress Series, 215*, 213-224. doi:DOI 10.3354/meps215213

Robinson, C. J. (2016). Evolution of the 2014–2015 sea surface temperature warming in the central west coast of Baja California, Mexico, recorded by remote sensing. *Geophysical Research Letters, 43*(13), 7066-7071.

Rudnick, D. L., Zaba, K. D., Todd, R. E. & Davis, R. E. (2017). A climatology of the California Current System from a network of underwater gliders. *Progress in Oceanography, 154*, 64-106. doi:10.1016/j.pocean.2017.03.002

Ryan, J. P., Kudela, R. M., Birch, J. M., Blum, M., Bowers, H. A., Chavez, F. P., et al. (2017). Causality of an extreme harmful algal bloom in Monterey Bay, California, during the

2014–2016 northeast Pacific warm anomaly. *Geophysical Research Letters, 44*(11), 5571-5579. doi:10.1002/2017GL072637

Rykaczewski, R. R. & Checkley, D. M. (2008). Influence of ocean winds on the pelagic ecosystem in upwelling regions. *Proceedings of the National Academy of Sciences of the United States of America, 105*(6), 1965-1970. doi:10.1073/pnas.0711777105

Sakamoto, C. M., Johnson, K. S., Coletti, L. J., Maurer, T. L., Massion, G., Pennington, J. T., et al. (2017). HOURLY IN SITU NITRATE ON A COASTAL MOORING A 15-Year Record and Insights into New Production. *Oceanography, 30*(4), 114-127. doi:10.5670/oceanog.2017.428

Simpson, J. J. (1984). El-Nino-Induced Onshore Transport in the California Current during 1982-1983. *Geophysical Research Letters, 11*(3), 241-242.

Sutton, A. J., Sabine, C. L., Feely, R. A., Cai, W. J., Cronin, M. F., McPhaden, M. J., et al. (2016). Using present-day observations to detect when anthropogenic change forces surface ocean carbonate chemistry outside preindustrial bounds. *Biogeosciences, 13*(17), 5065-5083. doi:10.5194/bg-13-5065-2016

Sutton, A. J., Sabine, C. L., Maenner-Jones, S., Lawrence-Slavas, N., Meinig, C., Feely, R. A., et al. (2014). A high-frequency atmospheric and seawater pCO(2) data set from 14 open-ocean sites using a moored autonomous system. *Earth System Science Data, 6*(2), 353-366. doi:10.5194/essd-6-353-2014

Thayer, J. A. & Sydeman, W. J. (2007). Spatio-temporal variability in prey harvest and reproductive ecology of a piscivorous seabird, Cerorhinca monocerata, in an upwelling system. *Marine Ecology Progress Series, 329*, 253-265. doi:DOI 10.3354/meps329253

Todd, R. E., Rudnick, D. L., Davis, R. E. & Ohman, M. D. (2011). Underwater gliders reveal rapid arrival of El Nino effects off California's coast. *Geophysical Research Letters, 38*. doi:Artn L0360910.1029/2010gl046376

Van Heuven, S., Pierrot, D., Rae, J., Lewis, E. & Wallace, D. (2011). MATLAB program developed for CO2 system calculations,. Oak Ridge, Tennessee: Carbon Dioxide Information Analysis Center, Oak Ridge National Laboratory, US Department of Energy.

Wells, B. K., Schroeder, I. D., Santora, J. A., Hazen, E. L., Bograd, S. J., Bjorkstedt, E. P., et al. (2013). State of the California Current 2012–13: no such thing as an “average” year. *California Cooperative Oceanic Fisheries Investigations Reports, 54*(37-71).

Zaba, K. D. & Rudnick, D. L. (2016). The 2014-2015 warming anomaly in the Southern California Current System observed by underwater gliders. *Geophysical Research Letters, 43*(3), 1241-1248. doi:10.1002/2015gl067550

Zweng, M. M., Reagan, J. R., Antonov, J. I., Locarnini, R. A., Mishonov, A. V., Boyer, T. P., et al. (2013). World Ocean Atlas 2013, Volume 2: Salinity. . In E. S. Levitus & T. E. A. Mishonov (Eds.), *NOAA Atlas NESDIS* (Vol. 74, pp. 39).

CONCLUSIONS

Potential El Niño forcing mechanisms on zooplankton

The goals of this thesis were to i) characterize El Niño-related zooplankton community changes in the southern California Current System (CCS) and ii) investigate the dominant forcing mechanisms, specifically the balance of anomalous advection and *in situ* population growth or mortality, that temporarily reshape the zooplankton community. El Niño impacts appear to be felt in the zooplankton community predominantly through changing proportions and spatial distributions of individual species within certain taxa, highlighting the need to improve species-level zooplankton sampling in the CCS. Examination of variability in euphausiid species composition and pteropod population fluctuations between different types of El Niño events indicates that both anomalous advection and altered *in situ* population growth influence these dominant populations to varying degrees.

As shown in Chapters 2 and 3, analysis of the euphausiid community suggests that resident cool-water species are generally negatively impacted by reduced population growth due to unfavorable habitat conditions during El Niño. In major Eastern Pacific (EP) Niños, populations contract into only cool, nearshore upwelling waters. Recent analysis of interannual variability in offshore transport of newly upwelled waters showed that El Niño events are associated with reduced offshore transport; upwelled waters thus stay closer to shore and ‘age’ (decrease in nutrients and primary production) *in situ* (Chabert et al., 2021). Cool-water species likely seek refuge in these narrow nearshore bands of favorable habitat and cannot tolerate warmer, lower-productivity waters offshore. In contrast, subtropical and tropical euphausiid species appear to rely initially on enhanced advection into the southern CCS from either southern

or offshore waters, with varying degrees of *in situ* reproduction during and following some El Niño events. The differential responses of both cool-water and subtropical species to different El Niños, even events within the same category (EP or CP [Central Pacific]), reflect known variability in the dominant physical changes associated with each event.

Chapter 4 drew upon high-resolution (daily) sampling of physical and biogeochemical variables at two moorings off Point Conception to determine the specific timing of arrival and duration of anomalously warm waters and other biogeochemical changes during the 2014-15 Warm Anomaly and 2015-16 El Niño. The high-resolution sampling by the moorings emphasized prolonged, surface-intensified warming throughout the Warm Anomaly period, in contrast to the subsequent El Niño event's deeper warming and greater temporal variability of expression. However, anomalous warming, in combination with higher oxygen and lower pCO_2 levels due to reduced upwelling, contributed to increased (more favorable) levels of aragonite saturation during both the Warm Anomaly and El Niño. The possibly antagonistic combination of negative (elevated temperatures, reduced food availability) and positive (higher aragonite saturation levels) habitat changes during El Niño-like events emphasizes the importance of examining biogeochemical fluctuations at high temporal resolutions and understanding their individual and combined effects on different zooplankton sectors. Chapter 4 focused on the responses of the pteropod community, which is notably negatively impacted by decreases in aragonite saturation (Bednaršek et al., 2014; Bednaršek et al., 2016). Although the dramatic increase in pteropod community biomass in spring 2014 was likely due to anomalous poleward transport of subtropical species (predominantly *Hyalocylis striata*) from southern waters, re-emergence of elevated populations in spring 2016 may have been due to *in situ* population persistence in the southern CCS under favorable conditions of aragonite saturation.

What are the implications of these findings for other components of the zooplankton community? Besides euphausiids, calanoid copepods are the most well-studied taxon in the CCS and an essential prey group for higher trophic levels. Past studies have evaluated potential impacts of certain El Niño events and the Warm Anomaly on copepod communities in both the southern (Mullin, 1995, 1997; Rebstock, 2001) and northern CCS (Hooff & Peterson, 2006; Peterson et al., 2017; Peterson et al., 2002). Chapter 1 found a significant relationship between magnitude of change in calanoid copepod community composition and strength of El Niño signal. This finding suggests that calanoid copepods, similar to euphausiids, are significantly impacted by El Niño, although I did not observe consistent EP/CP Niño distinctions in calanoid community changes. Past studies suggest that dominant species of calanoid copepods in the southern CCS are affected during El Niño events mainly by reduced food availability, which limits recruitment (egg production) (Mullin, 1995, 1997; Nickels & Ohman, 2018). Magnitudes of change in Chl-*a*, a proxy for food availability to calanoids, may not necessarily align with EP and CP distinctions. The above studies also found that El Niño-related decreases in recruitment reversed rapidly with the return of higher Chl-*a* biomass (Mullin, 1995, 1997). However, various warm-water calanoid species increased substantially during different subsets of the El Niño events analyzed in Chapter 1, some from zero presence before El Niño, suggesting at least some contribution of population advection into the southern CCS. The current lack of spatial and habitat reproductive analyses limits my ability to delve further into the dominant advective and reproductive forcing mechanisms that influence species.

Several studies in the northern CCS have hypothesized or tested the importance of anomalous northward and onshore advection in shifting copepod communities between “cool-water” and “warm-water” dominated states (e.g., Keister et al., 2011; Mackas & Galbraith, 2002;

Peterson et al., 2017). The 2014-15 Warm Anomaly produced appearances off Oregon of fourteen copepod species not previously documented in nearshore waters, as well as high abundances of appendicularians and doliolids (Peterson et al., 2017). These observations provide a compelling case for advection of non-resident species with the water mass that arrived off Oregon in fall 2014. Persistence of the community shows some relation to *in situ* conditions: the Warm Anomaly-related community decreased significantly in spring 2015 during moderate upwelling, before both the anomalous warm community and the usual El Niño-related copepod species appeared in fall 2015 (Peterson et al., 2017). Such multiyear persistence of an anomalous copepod community is unprecedented for El Niño events, suggesting that warm-water copepods reach the northern CCS primarily due to anomalous advection from the south or offshore and cannot tolerate subsequent returns to normal conditions.

Although gelatinous zooplankton (e.g., salps, doliolids, pyrosomes) do not show consistent El Niño-related variability in the southern CCS, past studies have attributed appearances of doliolids to advection and temporarily favorable *in situ* conditions. Both Berner (1960) and Blackburn (1979) attributed short-term increases in the warm, offshore species *Doliolum denticulatum* in the southern CCS from fall 1957-spring 1958 primarily to anomalous northward and onshore advection. Blackburn (1979) also noted the association of *D. denticulatum* only with waters >13^{o} C, and population increases at higher Chl-*a* levels, but neither study found evidence for *in situ* reproduction. These habitat associations suggest that, similar to warm-water copepods, subtropical doliolids are transported with favorable habitat waters into the CCS and cannot persist long-term following departure of these waters.

Despite sometimes dramatic decreases in certain sectors of the zooplankton during El Niño, and significant increases in usually uncommon subtropical and tropical species, I found

that both community composition and biomass of CCS zooplankton rebounded to pre-Niño levels within 1-2 years following every El Niño event analyzed (Chapter 1). Such resilience of the system highlights its long-term acclimation to interannual perturbations and its ability to return to a highly productive state with the return of favorable conditions. Lindegren et al. (2018) found that, although the CCS can shift to partial top-down control during periods of weakened bottom-up forcing (i.e., reduced upwelling during El Niño), the system is primarily forced by bottom-up mechanisms which rebound rapidly following El Niño to enhance primary and secondary production. Thus, El Niño events have so far induced only transient changes, rather than regime shifts to subtropical-dominated communities.

Predictions of future habitat changes to the CCS include increasing temperatures and decreasing oxygen by 2100 (Hazen et al., 2013; Rykaczewski & Dunne, 2010; see Chapter 2). However, Chl-*a* concentrations are predicted to increase with enhanced nitrate flux into the nearshore upwelling region (Hazen et al., 2013; Rykaczewski & Dunne, 2010), potentially offsetting negative changes in temperature and oxygen. Predictions of future upwelling changes suggest intensifying upwelling winds and strength, either across the CCS (Bakun et al., 2015) or at its northern edge while southern upwelling weakens (Rykaczewski et al., 2015). El Niño events and decadal variability are predicted to continue to influence the CCS in the coming century (Liguori & Di Lorenzo, 2018), and CP expression will likely form a larger portion of El Niño events (McPhaden, 2012; Yeh et al., 2009).

Despite predictions of moderate warming through Year 2100, my GAM-based predictions of future euphausiid species distributions (Chapter 2) suggest that resident cool-water species will likely maintain high abundances under non-Niño conditions and CP Niño events, likely benefiting from enhanced coastal primary production. These species have already shown

significant long-term population increases since 1951 (see Chapters 1 and 2). However, they are still predicted to compress shoreward and poleward during major EP Niños.

No subtropical euphausiid species currently shows a long-term trend of increase in the southern CCS, although recent analysis of the mesopelagic fish community shows long-term subtropicalization of that trophic level (McClatchie et al., 2018). Subtropical and tropical zooplankton species do show forecasted population increases and poleward and shoreward expansions in Year 2100, particularly during non-Niño and CP Niño periods. Predicted increases may be due to ocean warming to more favorable habitat conditions, which may promote both enhanced survival and increased *in situ* reproduction of subtropical species in the southern CCS. Thus, at some point either El Niño events or warming background conditions may start to induce longer-term 'regime-like' changes toward increased subtropical zooplankton presence. In the near-term, however, and also during major EP Niños that predominantly induce enhanced poleward flow, subtropical and tropical species will likely continue to show only 'transient' presences dependent on anomalous poleward and shoreward advection for significant transport into the southern CCS.

La Niña events

While this thesis focuses on El Niño, the anomalously warm phase of the El Niño-Southern Oscillation (ENSO) cycle, Chapter 1 also evaluated zooplankton changes in the CCS during La Niña events. Unlike El Niño, La Niña events induce cooler temperatures and increased primary production in the CCS (Bograd & Lynn, 2001), often with resulting increases in secondary (zooplankton) production dominated by cool-water species (Lilly & Ohman, 2018). Chapter 1 also highlighted the greater consistency of CCS zooplankton community composition

between La Niña and non-Niña years, and across individual La Niña years, than during and between El Niño years. Thus, while La Niña can induce zooplankton biomass and community changes from non-Niña years, the phenomenon does not show the same EP/CP dichotomy as El Niño does, and changes manifest more as enhancements of the resident cool-water components of the zooplankton rather than intrusions of non-native species. A recent composite analysis by Cordero-Quiros et al. (2019) of El Niño and La Niña physical-biological impacts in the CCS corroborates this interpretation of a consistent La Niña response: anomalies of temperature, pycnocline depth, nitrate, and oxygen were more consistently distinct from the mean state during La Niña than corresponding changes during El Niño events, suggesting a more coherent expression of La Niña events compared to known large variability between El Niños.

Data limitations

The current lack of zooplankton enumerations in the CalCOFI region for seasons other than spring, and thus a lack of intra-annual resolution, limits the ability of this work to fully assess the differential impacts of advection or *in situ* population growth on different groups. For example, a quantitative analysis of the singular influence of winter-to-spring advection on euphausiid populations requires both winter and spring zooplankton samples to provide starting points and end comparisons for hindcasted advection model results. Similarly, consistent winter and spring (at least) zooplankton samples, including multiple developmental stages, would provide a clearer picture of when and how different population stages emerge and respond to *in situ* habitat changes. Chapter 2 notes that while we observed the tropical Pacific euphausiid *Euphausia eximia* in spring samples off Southern California only during El Niño events, prior studies suggest the species experiences regular northward intrusions to Southern California

during the fall period, even in non-Niño years. Higher temporal resolution zooplankton samples would help pinpoint the emergence time and persistence of El Niño-related population changes.

Second, this work would benefit from increased species-level metrics of organismal survival, growth, and reproduction rates across ranges of habitat conditions (e.g., temperature, oxygen, chlorophyll-*a*). Growth rate and reproduction studies have only been conducted for a subset of the euphausiid species examined in this study, and often only at specific temperatures (Gómez-Gutiérrez et al., 2007; Gómez-Gutiérrez & Lavaniegos-Espejo, 1996; Gómez-Gutiérrez & Robinson, 2005; Gomez, 1995; Lavaniegos, 1992; Ross, 1981; Ross et al., 1982). These temperatures do not encompass the full ranges of conditions that euphausiid species appear to inhabit based on my Chapter 2 findings. Acquiring growth measurements for more species and wider habitat ranges would inform expected growth, mortality, and reproduction rates under ranges of CCS conditions; these rates could then be incorporated into individual-based models (IBMs; see Dorman et al., 2011b) to predict population fluctuations with altered temperatures, food availability, and other anomalous conditions.

Impacts of zooplankton shifts for the CCS

Changes in species-level distributions within certain zooplankton taxa can significantly impact foraging patterns of higher trophic levels (fishes, marine mammals, seabirds) that target certain zooplankton species even when other species are more abundant (Ainley & Hyrenbach, 2010; Croll et al., 2005; Lee et al., 2007; Nickels et al., 2018, 2019). Two cool-water euphausiid species (*Euphausia pacifica, Thysanoessa spinifera*) that were shown in Chapter 2 to undergo significant coastal compression and biomass decreases during major EP Niños are preferred prey for various whale and seabird species. Changes in availability of these euphausiids can alter

foraging patterns and timing (Szesciorka et al., 2020), reduce feeding and breeding success of seabirds (Ainley & Hyrenbach, 2010), and even induce prey-switching to non-zooplanktonic populations (Santora et al., 2020). Altered foraging patterns and prey-switching can bring marine mammals into regions of higher human activities such as ship traffic and coastal fishing (Office of Protected Resources, 2018a). Prey-switching by humpback whales (*Megaptera novaeangliae)* during the 2014-15 Warm Anomaly, from *E. pacifica* to northern anchovy (*Engraulis mordax*), brought whale populations into greater contact with crab traps, significantly increasing entanglements (Santora et al., 2020). Improved predictions of changes in spatial distributions of *E. pacifica* and *T. spinifera* during future El Niño or Warm Anomaly-like events may in turn help predict changes in whale and seabird foraging locations so that fisheries and vessel traffic can respond accordingly.

In addition to altering foraging success of higher trophic levels, zooplankton community variability has the potential to significantly impact short- and long-term carbon export throughout the CCS (Stukel et al., 2013). Significant short-term decreases in euphausiid and copepod populations, as observed here for most El Niño events, will reduce their fecal pellet contributions to carbon export, potentially shifting fecal pellets to more amorphous and degraded material and reducing overall export (Morrow et al., 2018). However, long-term increases in zooplankton taxa such as appendicularians (Chapter 1) will likely fuel increased and more efficient carbon export via their mucous feeding ‘houses’. Altered proportions of species within the euphausiid and calanoid taxa require further investigation to determine whether such changes will contribute to altered fecal pellet composition, total carbon fluxes, and biogeochemical cycling.

References

Ainley, D. G. & Hyrenbach, K. D. (2010). Top-down and bottom-up factors affecting seabird population trends in the California current system (1985-2006). *Progress in Oceanography, 84*(3-4), 242-254. doi:10.1016/j.pocean.2009.10.001

Bakun, A., Black, B. A., Bograd, S. J., Garcia-Reyes, M., Miller, A. J., Rykaczewski, R. R. & Sydeman, W. J. (2015). Anticipated Effects of Climate Change on Coastal Upwelling Ecosystems. *Current Climate Change Reports, 1*(2), 85-93. doi:10.1007/s40641-015-0008-4

Bednaršek, N., Feely, R. A., Reum, J. C. P., Peterson, B., Menkel, J., Alin, S. R. & Hales, B. (2014). Limacina helicina shell dissolution as an indicator of declining habitat suitability owing to ocean acidification in the California Current Ecosystem. *Proc. R. Soc. B, 281*(1785), 20140123.

Bednaršek, N., Harvey, C. J., Kaplan, I. C., Feely, R. A. & Mozina, J. (2016). Pteropods on the edge: Cumulative effects of ocean acidification, warming, and deoxygenation. *Progress in Oceanography, 145*, 1-24. doi:10.1016/j.pocean.2016.04.002

Berner, L. D. (1960). Unusual features in the distribution of pelagic tunicates in 1957 and 1958. *CalCOFI Rep., 9*, 247-253.

Blackburn, M. (1979). Thaliacea of the California Current region: relations to temperature, chlorophyll, currents and upwelling. *CalCOFI Rep., 20*, 184-214.

Bograd, S. J. & Lynn, R. J. (2001). Physical-biological coupling in the California Current during the 1997-99 El Niño-La Niña cycle. *Geophysical Research Letters, 28*(2), 275-278.

Chabert, P., d'Ovidio, F., Echevin, V., Stukel, M. R. & Ohman, M. D. (2021). Cross-shore flow and implications for Carbon Export in the California Current Ecosystem: a Lagrangian analysis. *Journal of Geophysical Research: Oceans, e2020JC016611*.

Cordero-Quiros, N., Miller, A. J., Subramanian, A. C., Luo, J. Y. & Capotondi, A. (2019). Composite physical-biological El Nino and La Nina conditions in the California Current System in CESM1-POP2-BEC. *Ocean Modelling, 142*. doi:ARTN 101439 10.1016/j.ocemod.2019.101439

Croll, D. A., Marinovic, B., Benson, S., Chavez, F. P., Black, N., Ternullo, R. & Tershy, B. R. (2005). From wind to whales: trophic links in a coastal upwelling system. *Marine Ecology Progress Series, 289*, 117-130. doi:DOI 10.3354/meps289117

Dorman, J. G., Powell, T. M., Sydeman, W. J. & Bograd, S. J. (2011). Advection and starvation cause krill (Euphausia pacifica) decreases in 2005 Northern California coastal populations: Implications from a model study. *Geophysical Research Letters, 38*. doi:Artn L04605 10.1029/2010gl046245

Gómez-Gutiérrez, J., Feinberg, L. R., Shaw, T. C. & Peterson, W. T. (2007). Interannual and geographical variability of the brood size of the euphausiids Euphausia pacifica and Thysanoessa spinifera along the Oregon coast (1999–2004). *Deep-Sea Research Part I: Oceanographic Research Papers, 54*(12), 2145-2169.

Gómez-Gutiérrez, J. & Lavaniegos-Espejo, B. (1996). Growth production of the euphausiid Nyctiphanessimplex on the coastal shelf off Bahía Magdalena, Baja California Sur, México. *Marine Ecology Progress Series, 138*, 309-314.

Gómez-Gutiérrez, J. & Robinson, C. J. (2005). Embryonic, early larval development time, hatching mechanism and interbrood period of the sac-spawning euphausiid Nyctiphanes simplex Hansen. *Journal of Plankton Research, 27*(3), 279-295.

Gomez, J. G. (1995). Distribution Patterns, Abundance and Population-Dynamics of the Euphausiids Nyctiphanes-Simplex and Euphausia-Eximia Off the West-Coast of Baja-California, Mexico. *Marine Ecology Progress Series, 119*(1-3), 63-76. doi:DOI 10.3354/meps119063

Hazen, E. L., Jorgensen, S., Rykaczewski, R. R., Bograd, S. J., Foley, D. G., Jonsen, I. D., et al. (2013). Predicted habitat shifts of Pacific top predators in a changing climate. *Nature Climate Change, 3*(3), 234-238. doi:10.1038/Nclimate1686

Hooff, R. C. & Peterson, W. T. (2006). Copepod biodiversity as an indicator of changes in ocean and climate conditions of the northern California current ecosystem. *Limnology and Oceanography, 51*(6), 2607-2620. doi:DOI 10.4319/lo.2006.51.6.2607

Keister, J. E., Di Lorenzo, E., Morgan, C. A., Combes, V. & Peterson, W. T. (2011). Zooplankton species composition is linked to ocean transport in the Northern California Current. *Global Change Biology, 17*(7), 2498-2511.

Lavaniegos, B. E. (1992). Growth and larval development of Nyctiphanes simplex in laboratory conditions. *CalCOFI Rep., 33*, 162-171.

Lee, D. E., Nur, N. & Sydeman, W. J. (2007). Climate and demography of the planktivorous Cassin's auklet Ptychoramphus aleuticus off northern California: implications for population change. *Journal of Animal Ecology, 76*(2), 337-347. doi:10.1111/j.1365-2656.2007.01198.x

Liguori, G. & Di Lorenzo, E. (2018). Meridional modes and increasing Pacific decadal variability under anthropogenic forcing. *Geophysical Research Letters, 45*(2), 983-991.

Lilly, L. E. & Ohman, M. D. (2018). CCE IV: El Niño-related zooplankton variability in the southern California Current System. *Deep-Sea Research Part I: Oceanographic Research Papers*.

Lindegren, M., Checkley, D. M., Koslow, J. A., Goericke, R. & Ohman, M. D. (2018). Climate-mediated changes in marine ecosystem regulation during El Nino. *Global Change Biology, 24*(2), 796-809. doi:10.1111/gcb.13993

Mackas, D. L. & Galbraith, M. (2002). Zooplankton community composition along the inner portion of Line P during the 1997-1998 El Nino event. *Progress in Oceanography, 54*(1-4), 423-437. doi:10.1016/S0079-6611(02)00062-9

McClatchie, S., Gao, J., Drenkard, E. J., Thompson, A. R., Watson, W., Ciannelli, L., et al. (2018). Interannual and secular variability of larvae of mesopelagic and forage fishes in the Southern California current system. *Journal of Geophysical Research: Oceans, 123*(9), 6277-6295.

McPhaden, M. J. (2012). A 21st century shift in the relationship between ENSO SST and warm water volume anomalies. *Geophysical Research Letters, 39*(9).

Morrow, R. M., Ohman, M. D., Goericke, R., Kelly, T. B., Stephens, B. M. & Stukel, M. R. (2018). CCE V: Primary production, mesozooplankton grazing, and the biological pump in the California Current Ecosystem: Variability and response to El Nino. *Deep-Sea Research Part I-Oceanographic Research Papers, 140*, 52-62. doi:10.1016/j.dsr.2018.07.012

Mullin, M. M. (1995). The Californian El Niño of 1992 and the fall of Calanus. *CalCOFI Rep., 36*, 175-178.

Mullin, M. M. (1997). The demography of Calanus pacificus during winter-spring Californian El Nino conditions, 1992-1993: Implications for anchovy? *Fisheries Oceanography, 6*(1), 10-18. doi:DOI 10.1046/j.1365-2419.1997.t01-1-00023.x

Nickels, C. F. & Ohman, M. D. (2018). CCEIII: Persistent functional relationships between copepod egg production rates and food concentration through anomalously warm conditions in the California Current Ecosystem. *Deep-Sea Research Part I-Oceanographic Research Papers, 140*, 26-35. doi:10.1016/j.dsr.2018.07.001

Nickels, C. F., Sala, L. M. & Ohman, M. D. (2018). The morphology of euphausiid mandibles used to assess selective predation by blue whales in the southern sector of the California Current System. *Journal of Crustacean Biology, 38*(5), 563-573.

Nickels, C. F., Sala, L. M. & Ohman, M. D. (2019). The euphausiid prey field for blue whales around a steep bathymetric feature in the southern California current system. *Limnology and Oceanography, 64*(1), 390-405. doi:10.1002/lno.11047

Office of Protected Resources, N. (2018). *BLUE WHALE (Balaenoptera musculus musculus): Eastern North Pacific Stock*. Retrieved from https://www.fisheries.noaa.gov/national/marine-mammal-protection/marine-mammal-stock-assessment-reports-species-stock#cetaceans---large-whales

Peterson, W. T., Fisher, J. L., Strub, P. T., Du, X., Risien, C., Peterson, J. & Shaw, C. T. (2017). The pelagic ecosystem in the Northern California Current off Oregon during the 2014–2016 warm anomalies within the context of the past 20 years. *Journal of Geophysical Research-Oceans, 122*(9), 7267-7290. doi:10.1002/2017JC012952

Peterson, W. T., Keister, J. E. & Feinberg, L. R. (2002). The effects of the 1997-99 El Nino/La Nina events on hydrography and zooplankton off the central Oregon coast. *Progress in Oceanography, 54*(1-4), 381-398. doi:Doi 10.1016/S0079-6611(02)00059-9

Rebstock, G. A. (2001). Long-term stability of species composition in calanoid copepods off southern California. *Marine Ecology Progress Series, 215*, 213-224. doi:DOI 10.3354/meps215213

Ross, R. M. (1981). Laboratory Culture and Development of Euphausia-Pacifica. *Limnology and Oceanography, 26*(2), 235-246. doi:DOI 10.4319/lo.1981.26.2.0235

Ross, R. M., Daly, K. L. & English, T. S. (1982). Reproductive-Cycle and Fecundity of Euphausia-Pacifica in Puget Sound, Washington. *Limnology and Oceanography, 27*(2), 304-314. doi:DOI 10.4319/lo.1982.27.2.0304

Rykaczewski, R. R. & Dunne, J. P. (2010). Enhanced nutrient supply to the California Current Ecosystem with global warming and increased stratification in an earth system model. *Geophysical Research Letters, 37*. doi:10.1029/2010gl045019

Rykaczewski, R. R., Dunne, J. P., Sydeman, W. J., Garcia-Reyes, M., Black, B. A. & Bograd, S. J. (2015). Poleward displacement of coastal upwelling-favorable winds in the ocean's eastern boundary currents through the 21st century. *Geophysical Research Letters, 42*(15), 6424-6431. doi:10.1002/2015gl064694

Santora, J. A., Mantua, N. J., Schroeder, I. D., Field, J. C., Hazen, E. L., Bograd, S. J., et al. (2020). Habitat compression and ecosystem shifts as potential links between marine heatwave and record whale entanglements. *Nature Communications, 11*(1). doi:10.1038/s41467-019-14215-w

Stukel, M. R., Ohman, M. D., Benitez-Nelson, C. R. & Landry, M. R. (2013). Contributions of mesozooplankton to vertical carbon export in a coastal upwelling system. *Marine Ecology Progress Series, 491*, 47-+. doi:10.3354/meps10453

Szesciorka, A. R., Ballance, L. T., Širović, A., Rice, A., Ohman, M. D., Hildebrand, J. A. & Franks, P. J. (2020). Timing is everything: Drivers of interannual variability in blue whale migration. *Scientific Reports, 10*(1), 1-9.

Yeh, S. W., Kug, J. S., Dewitte, B., Kwon, M. H., Kirtman, B. P. & Jin, F. F. (2009). El Nino in a changing climate (vol 461, pg 511, 2009). *Nature, 462*(7273). doi:10.1038/nature08546